The Pennsylvania State University

The Graduate School

Eberly College of Science

STUDIES ON THE STABILITY AND REACTIVITY OF 2,4-HEXAHYDROXY-DIPHENOYL(HHDP)-BEARING ELLAGITANNIN MONOMERIC UNIT;

ALLENYL AZIDE CYCLOADDITION CHEMISTRY APPLIED TOWARD THE SYNTHESIS OF ALKALOIDS

A Thesis in

Chemistry

by

Malliga R. Iyer

Submitted in Partial Fulfillment
of the Requirements
for the Degree of

Doctor of Philosophy

May 2007

The thesis of Malliga R. Iyer was reviewed and approved* by the following:

Ken S. Feldman
Professor of Chemistry
Thesis Advisor
Chair of Committee

Raymond L. Funk
Professor of Chemistry

Blake R. Peterson
Associate Professor of Chemistry

Squire J. Booker
Associate Professor of Biochemistry and Molecular Biology

Ayusman Sen
Professor of Chemistry
Head of the Department of Chemistry

*Signatures are on file in the Graduate School

ABSTRACT

The first synthesis of a monomeric 2,4-hexahydroxydiphenoyl (HHDP)-bearing glucopyranose ellagitannin model system was achieved. Attempts to prepare a related model system containing a 1,6-bridge on the glucose core resulted in a strain-driven tautomerization to cyclohexadienone intermediates. This project sought to answer questions relevant to the biosynthesis of geraniin family of natural products as well as address the privileged stability observed in case of 2,4-HHDP-containing natural ellagitannnin, phyllanemblinin B.

A novel cascade cyclization sequence evolving from the thermolysis of allenyl azide was developed. Incorporation of aryl or alkenyl appendages in the allene construct afforded tricyclic and bicyclic products, respectively, following cyanide trapping of the unstable imine intermediate. Azatrimethylenemethane (ATMM) diradicals were speculated to be involved in the cycloaddition/cyclization cascade. A brief survey of electronic influence on the cascade reaction was investigated.

An extension to this novel methodology was achieved by incorporating an aryl residue in the allenyl azide tether. This modification resulted in the synthesis of annealated indoles from (phenylazido)allene substrates. The proposed mechanism invokes the existence of ATMM species in the cyclization. Alternatively, the cyclization was postulated to occur through a conjugated closed shell intermediate. Further application of this methodology in the synthesis of a model system for the natural product (±)-meloscine was attempted with promising results.

TABLE OF CONTENTS

LIST OF FIGURES

LIST OF TABLES

ACKNOWLEDGEMENTS

I would like to express my deepest gratitude to all those who have actively supported me in this endeavor. My greatest acknowledgement goes to my advisor Prof. Ken S. Feldman for his patient guidance throughout the course of this work. His insightful suggestions and hints during apparent *cul de sac* and his ever so 'gentle' push were motivational enough to try my best. The research training I received under his direction is invaluable and will serve me in good stead for a long time. I am especially thankful to Prof. Ray Funk, Prof. Blake Peterson and Prof. Squire Booker for serving on my doctoral committee and for their time and effort. I am also thankful to my past committee member Prof. Tim Glass for his help.

The pleasant atmosphere in the Feldman lab made the endless working hours much more enjoyable. The past and the present group members of the Feldman lab are commendable and their support is much appreciated and acknowledged.

I am indebted to Dr. Lakshmy Ravishankar for her incredible mentoring throughout my undergraduate years. I will always be grateful for her stimulating organic chemistry lessons, her constant encouragement and motivation during those years. Thanks Ma'am you have been an inspiration!!

Over the course of this program at Penn State, I have been fortunate to have made some very good friends. I will always cherish the weekend adventures of Game Club. My friends have been a constant source of lighter moments through testing times. Thanks ye' all for being such a goofy bunch. I especially like to thank Hari (guruji) Prasad for letting me 'fine-tune' my driving skills on his car.

I cannot thank my best ‘friend’ Dr. Devendra Tolani enough. I met him at Penn State and married him while at Penn State. Dev, you have been awesome….

I have to extend my deepest gratitude to my sister Malathi who has been my best critic through years and for her unflinching faith in me. Thanks akka for understanding my choice all along. My niece Rajsri (Chokli) deserves a special mention for her excellent toy handling skills. She is already trained to handle molecular models for future!! Thanks are due to my brother-in-law Raghunath and his family. I am extremely thankful for the prayers and support from Dev’s parents.

Finally, I have to express my indebtedness to those who have been the pillars of my life, my parents. Words cannot express the sacrifices they made to see me reach this stage in my life. I can never thank you enough amma and appa…..

Thanks God!!

Dedicated to my Parents

Chapter 1

Ellagitannin Chemistry: Background of Monomeric Ellagitannin Systems

1.1 Overview

Ellagitannins belong to the hydrolyzable tannin class of polyphenol extractives derived from the secondary metabolism of dicotyledonous species of Angiospermae. The first inroads into ellagitannin constitution were made by Fischer and Freudenberg almost a century ago.[1] Schmidt and Mayer contributed to the structural elucidation of many members of this class.[2] The efforts of Haslam[3], Okuda[4] and Nishioka[5] have enabled the isolation and characterization of over 500 ellagitannins. The burgeoning interest in this class of natural products was fueled by observations that several ellagitannins exhibit promising levels of activities in various anticancer and antiviral assays and hence may serve as potential leads for development of novel therapeutics.[6,7] The defining structural characteristic of all monomeric ellagitannins is the 6,6'-dicarbonyl-2,2',3,3',4,4'-hexahydroxybiphenyl moiety, commonly designated by the trivial name hexahydroxydiphenoyl (HHDP), appended to a pyranose unit.

1.2 Biosynthetic Considerations

A generalized schematic outlining the two main routes to monomeric ellagitannin biosynthesis is shown in Figure 1.[8] All compounds formed are based on cyclization and modification of β-pentagalloylglucopyranose (β-pgg) (**1**) which can be envisioned as

having two distinct conformations, the more stable $^4C_1$ and the less stable $^1C_4$ conformation. Oxidation of **1** promotes biaryl coupling and leads to the formation of a HHDP unit. The orientation of galloyl groups during biaryl bond formation is thought to be dictated by the steric and electronic influence of the glucose ring (Haslam-Schmidt hypothesis).[2,9] This orientational preference leads to stereoselectivity (atropselectivity) upon biaryl bond formation.

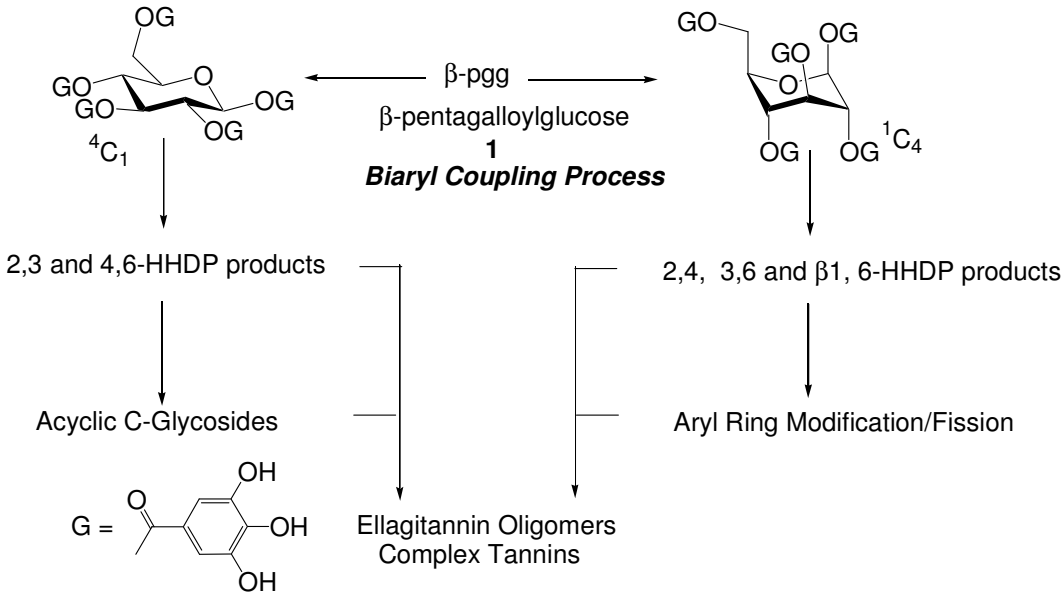

Figure 1: General schematic of ellagitannin biosynthetic pathway.

This hypothesis is best exemplified by examining the structures of two of the simplest ellagitannins, tellimagrandin II (**2**) and punicafolin (**3**) (Figure 2).[8] The galloyl groups are oriented in such a way as to minimize the repulsive forces that would arise by the rings and/or substituents coming too close in space. Hence stereoselective coupling afforded the (*S*)-HHDP structure of **2** and the (*R*)-HHDP of **3**. Further stereoselective couplings

provide more highly condensed structures. Compounds that possess the 4,6- and 2,3-HHDP units result from the oxidative coupling with the D-glucose moiety in the $^4C_1$ conformation and are always found as the *S*-atropisomer. Ellagitannins with 1,6- 3,6- and 2,4-HHDP units are envisioned as resulting from coupling while in $^1C_4$ conformation. The 2,4-HHDP units have an *R*-configuration while the 3,6-HHDP type structures can be found in both forms.

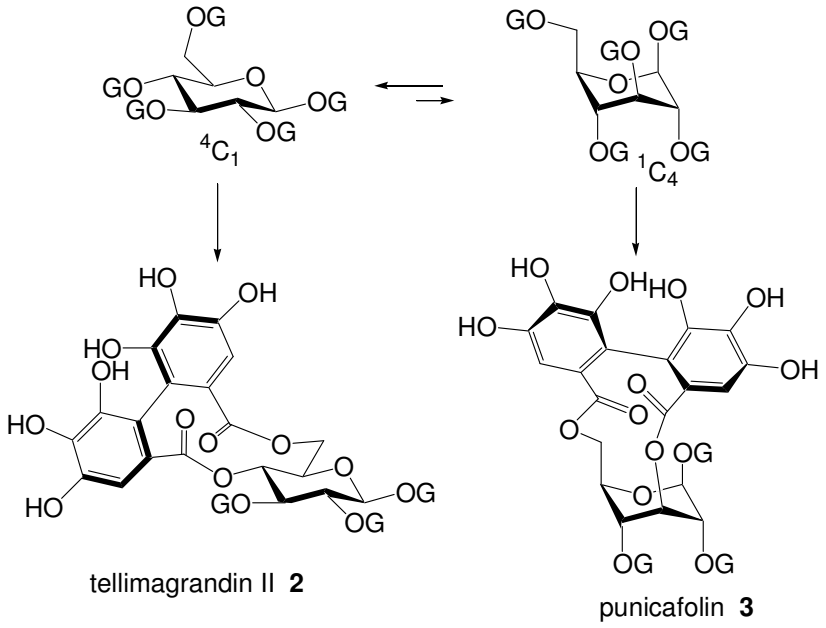

Figure 2: Preferential ring conformation leading to biaryl coupling.

Thus the current understanding in the area of ellagitannin biosynthesis centers on the pivotal role of β-pgg **1** as progenitor for each of the subfamilies via some permutation and/or combination of galloyl coupling. Further complexity can arise from not only C-C biaryl bond formation but also C-O bond formation between galloyl ethers. This biosynthesis speculation has been extended to incorporate a second point of departure,

where tellimagrandin II (**2**) is the precursor for various other ellagitannins based on the $^4C_1$ conformation.[10,11] In this scenario, initial tellimagrandin II synthesis via O(4)/O(6) galloyl coupling within β-pgg **1** is followed by a host of additional coupling processes to afford representative species **4**-**6**. Thus subsequent O(2)/O(3) coupling within **2** might yield casuarictin (**6**)**,** whereas oxidation of the O(6) galloyl group within the HHDP unit of **2** should afford the dehydrohexahydroxydiphenoyl (DDHP) moiety of isoterchebin (**5**) (Figure 3). This biosynthetic speculation carries more weight in light of the fact that **2** is a co-isolate with many of the more complex ellagitannins.[12]

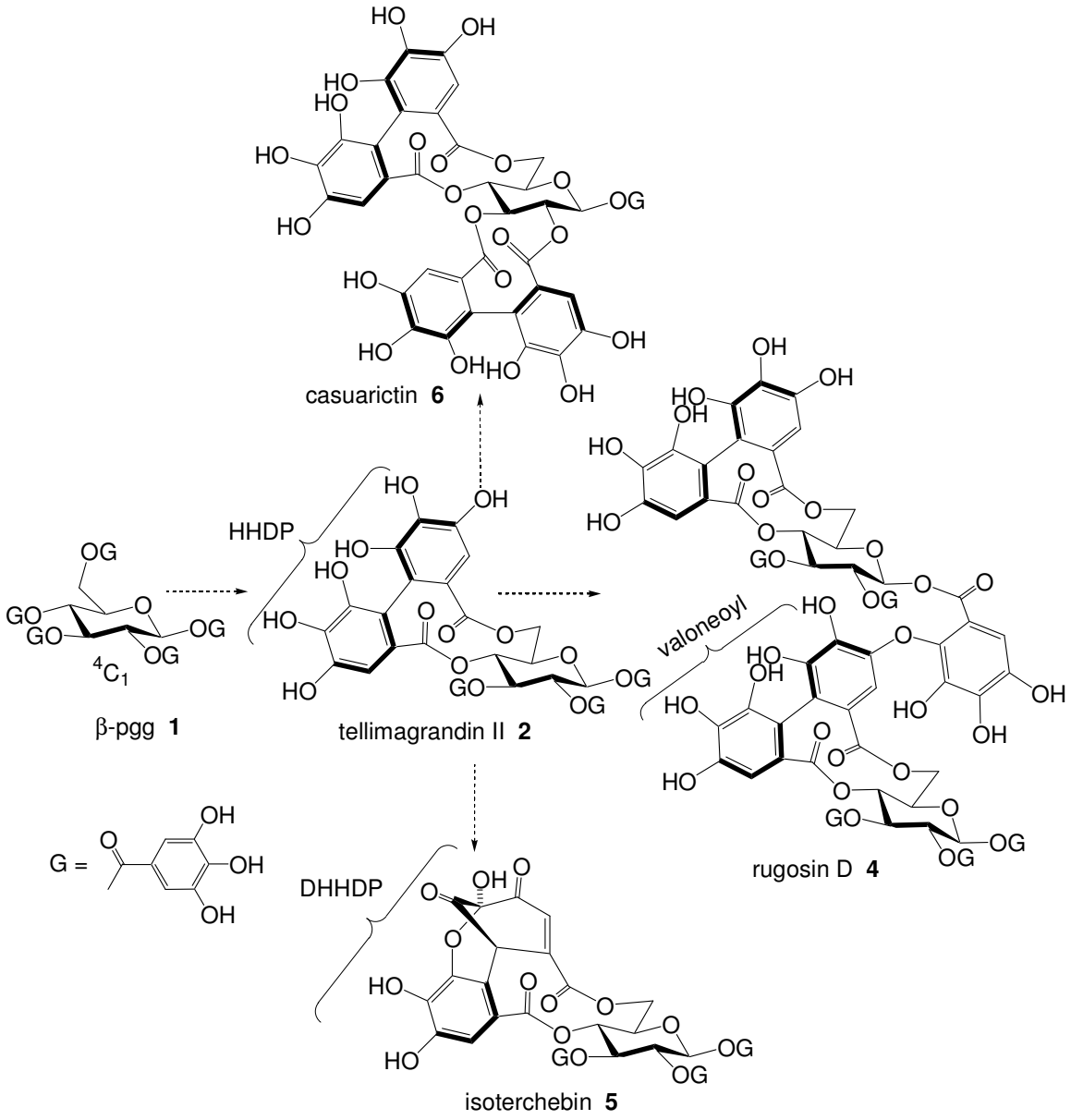

Figure 3: Possible biosynthesis of representative ellagitannins from tellimagrandin II.

The details of the process of oxidative coupling of galloyl esters during ellagitannin biosynthesis to give HHDP units are still unclear. Current hypothesis includes two proposals that are based on the level of oxidation experienced by each galloyl moiety undergoing the coupling.[13] The first proposal involves a two one-electron oxidation resulting in the abstraction of two phenolic hydrogen atoms from **1** to give an intermediate diradical **9**. This diradical can then couple to generate the HHDP. The second hypothesis surmises a two-electron oxidation of one of the galloyl rings to afford an electrophilic ortho-quinone intermediate **7** which then can be immediately trapped by a proximal nucleophilic galloyl ring to furnish the HHDP unit. Protonation can further enhance the electrophilicity of **7** to generate species **7a/7b** (Figure 4). From the synthetic standpoint, entirely different sets of conditions need to be employed to achieve the one or two-electron oxidation processes.

The one-electron oxidation hypothesis seems plausible only in intramolecular couplings or intermolecular homodimerizations. Heterodimerization of discrete ellagitannin monomer radicals may suffer from unacceptable coupling reactions either *in vivo* or *in vitro*. Heteropolar galloyl coupling can be useful synthetically as it does not suffer from this drawback.

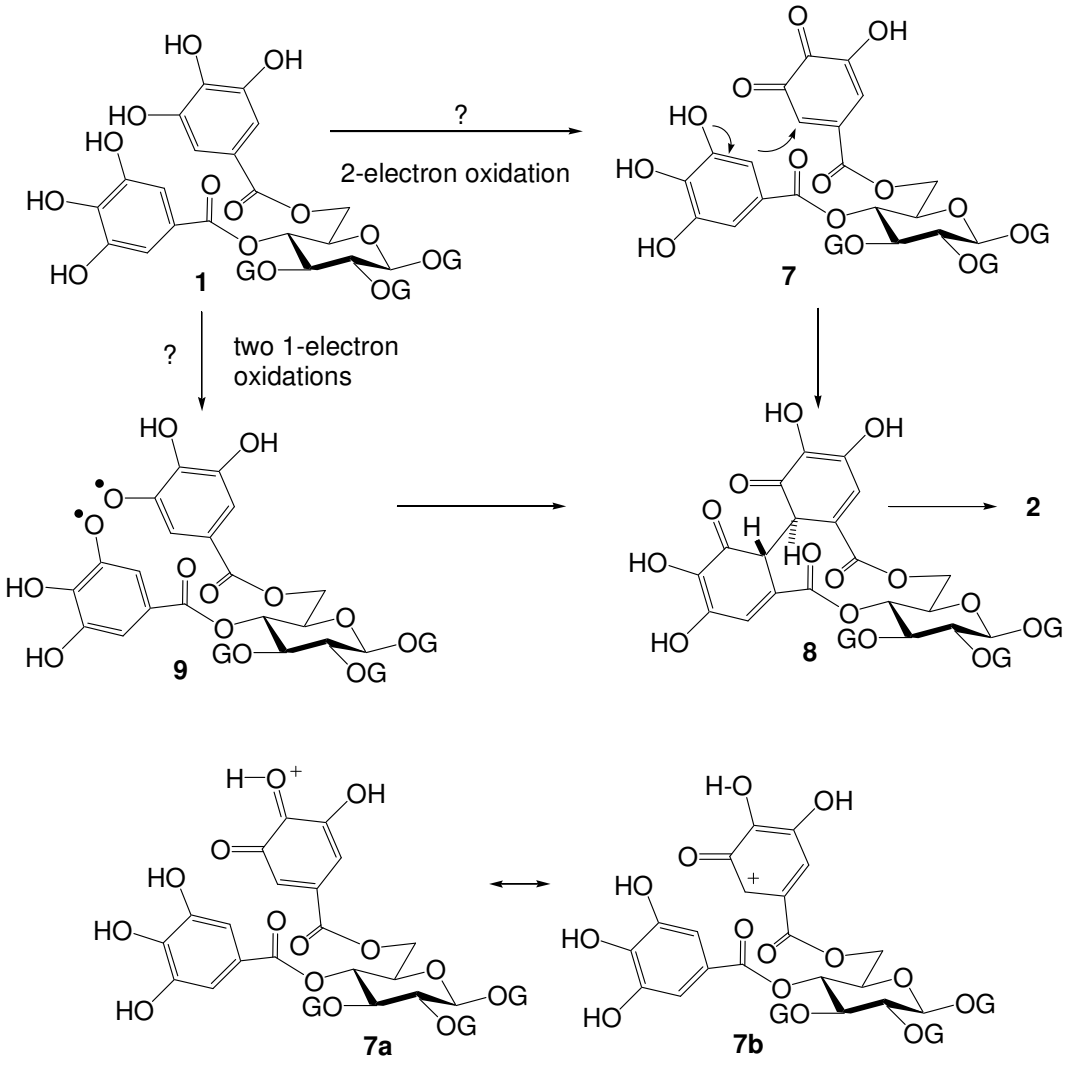

Figure 4: Possible mechanistic sequence for HHDP synthesis via galloyl oxidation.

1.3 HHDP Chemical Synthesis Considerations

1.3.1 Early Attempts at HHDP Synthesis

Successful synthesis of an HHDP unit must address three important concerns: 1) biaryl bond formation, 2) regioselectivity and stereoselectivity (atropselectivity) and 3) avoidance of overoxidation of the HHDP in presence of coupling (oxidizing) agent. Various attempts to couple gallic acid or its derivatives in a biomimetic oxidative process have been documented in the literature. However most of these strategies suffer from low yields. The main drawback has been the formation of overoxidation products and/or hydrolysis of the HHDP unit from the glucose core under coupling conditions.[14,15] The most promising example of an oxidative coupling to yield an HHDP unit was reported by Mayer.[16] According to his strategy, methyl gallate was coupled in the presence of horseradish peroxidase to provide the HHDP derivative **11** in 24% yield (Figure 5). This reaction was however accompanied by formation of substantial amounts of ellagic acid and other side products.

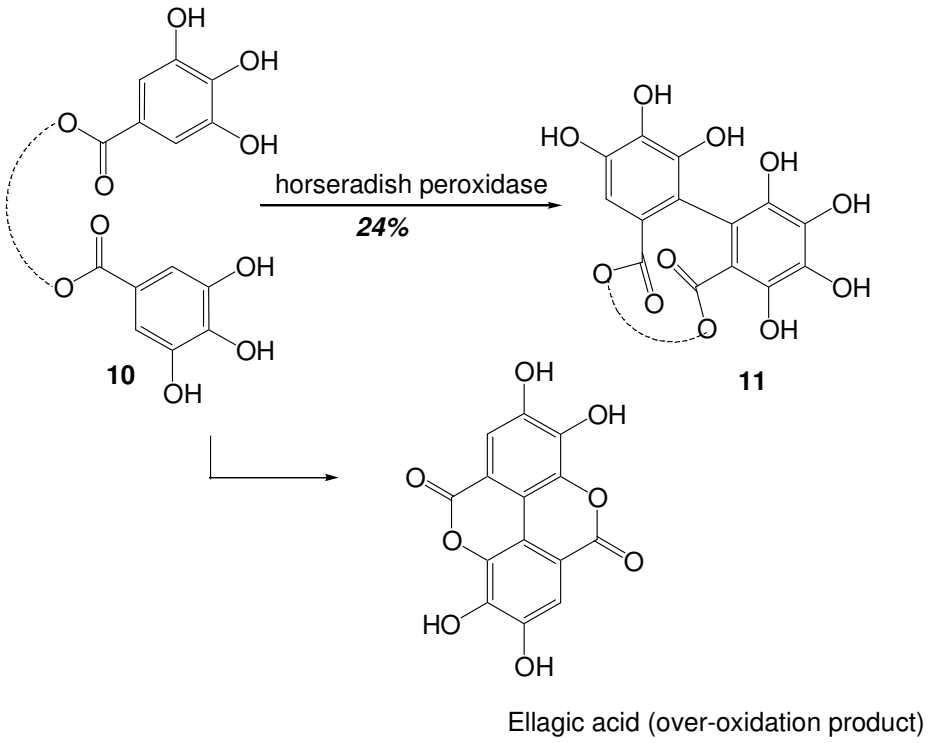

Figure 5: Attempts at HHDP synthesis- Mayer *et al*.

Products arising from overoxidation were avoided by utilizing reductive coupling (Ullmann-type) procedures of suitable galloyl synthons.[17] In a strategy developed by Meyers *et al*., the synthesis of (*S*)-hexamethoxydiphenic acid was achieved by using an intermolecular oxazoline-mediated Ullmann coupling. Synthesis of an ellagitannin can be completed by attaching the acid to an appropriate glucose core (Figure 6). This chiral-auxillary based strategy delivers the biaryl units characteristic of the ellagitannins with complete stereocontrol, although as per-*O*-methyl ethers which are not useful in natural product synthesis.[18]

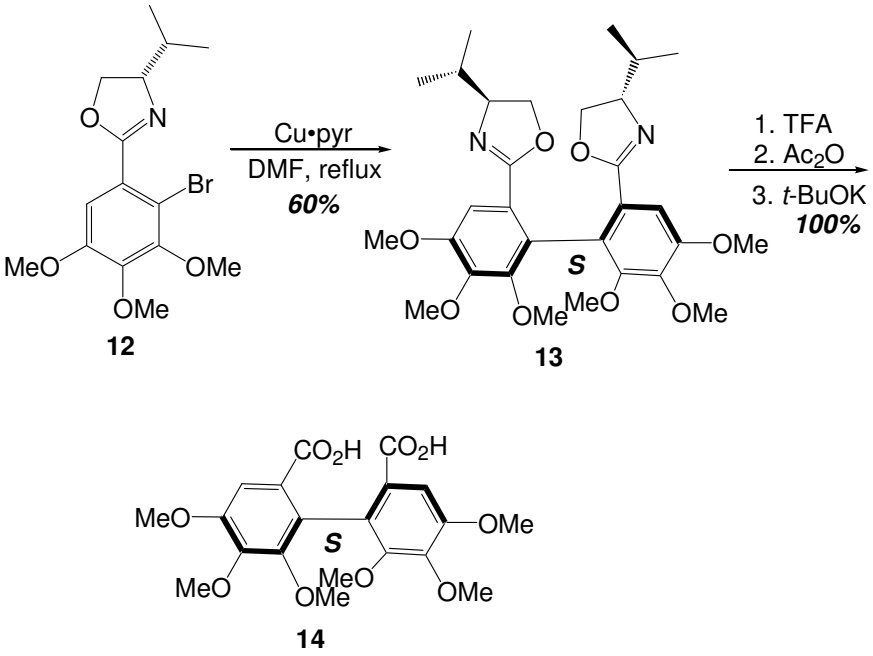

Figure 6: Attempts at HHDP synthesis- Meyers *et al*.

In a related methodology, Lipshutz and coworkers have reported the synthesis of an ellagitannin biaryl unit via an intramolecularly tethered diaryl cuprate. The diaryl cuprate was subsequently oxidized in the presence of oxygen to yield (*S*)-per-*O*-methylated biphenyl unit (Figure **7**). Compound **16** was then converted to (+)-tellimagrandin II, albeit as a per-*O*-methylated derivative.[19]

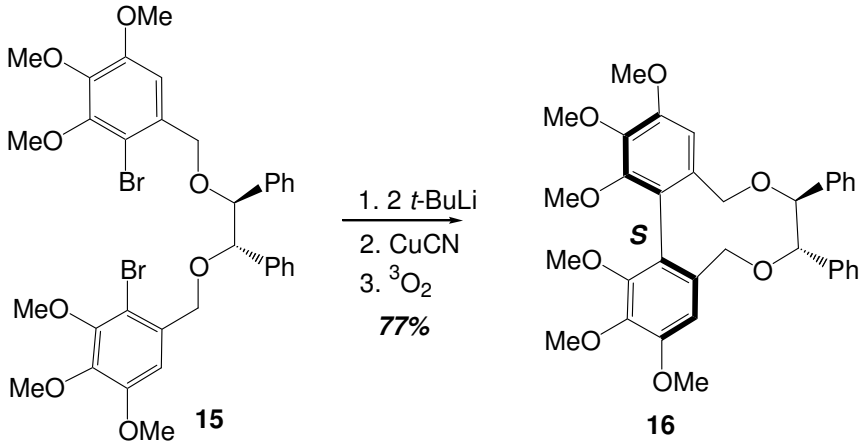

Figure 7: Attempts at HHDP synthesis- Lipshutz *et al*.

1.3.2 Designing an HHDP Synthesis Strategy

Prior to 1993, most approaches to ellagitannin HHDP synthesis failed to exploit the potential of a biomimetic oxidative coupling strategy. These strategies failed to produce a high yielding HHDP synthesis because the protocols utilized lacked a stop-message for the oxidants, thereby leading to overreaction. A useful approach to the oxidative coupling can rely on the capacity of the phenolic hydroxyl substituents to modulate/enhance the electrophilicity of a 2-electron oxidized species **18a** (Figure 8). This strategy is obviously an extension of the biosynthesis speculation indicated in (Figure 4), where reactive electrophilic orthoquinone precursors can be utilized in C-C biaryl bond forming processes. These types of couplings between electrophilic orthoquinones and nucleophilic phenols have been precedented in benzotropolone synthesis.[20] The purported value of "structure/reactivity" approach to HHDP unit can only be realized if a suitable oxidant/substrate pair was available. Thus, the

oxidant/substrate has to be tuned in such a way that it not only orchestrates the sequence of steps outlined in (Figure 8) to deliver the HHDP unit, but also has a built-in stop message to suppress overoxidation. Further, elements of regiocontrol and stereocontrol need to be incorporated in the oxidation protocol.

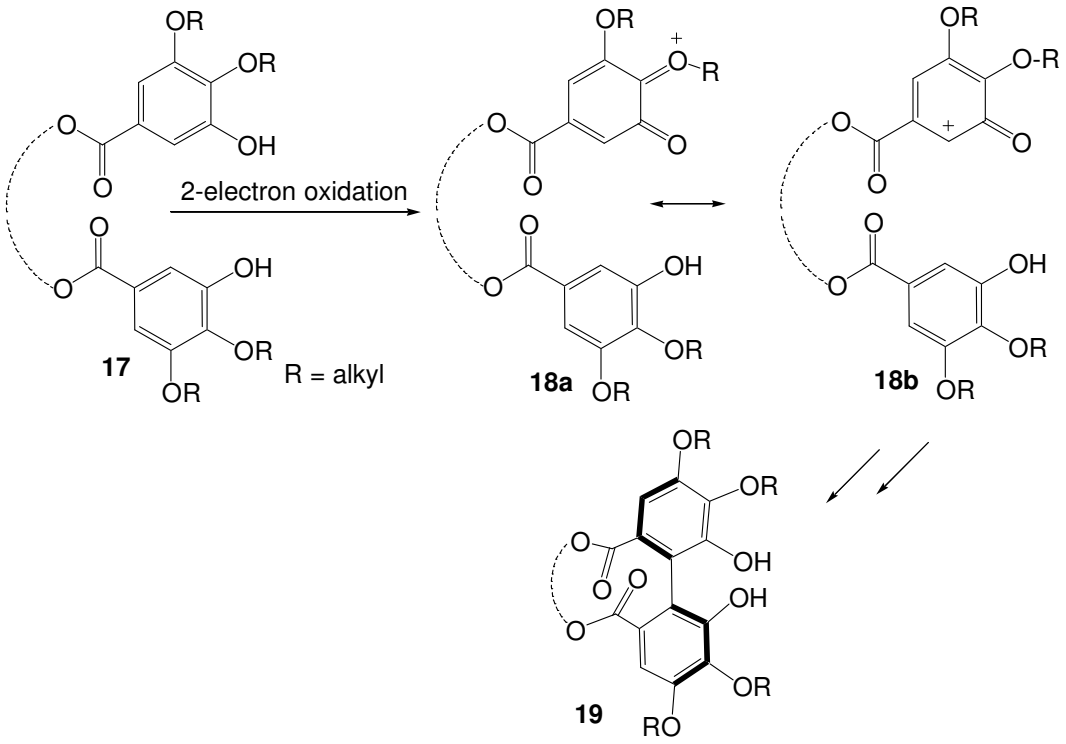

Figure 8: A two-electron oxidation approach to galloyl ester coupling.

1.4 HHDP Synthesis: Synopsis of Earlier Contributions from Feldman's Laboratory

The uncharted territories of ellagitannin synthesis led to the initiation of their total synthesis program in the Feldman laboratory. In the context of HHDP synthesis, a biomimetic oxidative coupling of galloyl esters was used as a strategy of choice. The foundation for such an approach has been laid by Schmidt and Haslam, who postulated that the apparent diastereoselectivity of biaryl bond formation is dictated by the geometrical constraints imposed by the glucopyranose ring.

Synthesis efforts in the Feldman lab were directed towards finding a suitable two-electron phenolic oxidant that would effect biaryl C-C bond formation of a suitably protected galloyl ester in a controlled fashion.

In seminal studies, a roster of mono-, di-, and tri-*O*-methyl galloyl esters attached to the O(4) and O(6) positions of a glucopyranose-derived core was screened against a variety of 2-electron oxidants.[21] However, the intial efforts were discouraging, as overoxidized or intractable product mixtures were obtained. After a series of false starts, it was found that the unsymmetrical tetra-*O*-methylated substrate **20** furnished two characterizable oxidation products upon exposure to lead tetraacetate ($Pb(OAc)_4$, Wessely oxidation).[22] This procedure yielded a major product which was an inseparable mixture of acetate adducts **23a/b** from OAc^- trapping of the putative electrophilic cyclohexadienonyl cation species **21** (Figure 9). The minor product was the much sought after protected (*S*)-HHDP moiety **22**. Isolation of a single tetra-*O*-methyl-(*S*)-HHDP-containing diastereomer was consistent with the Haslam-Schmidt hypothesis and the related MM calculations.[23]

The $Pb(OAc)_4$ mediated oxidation clearly eliminated product overreaction. Mechanistic studies provided evidence that the pivotal C-C bond forming process occurs in an S_N2'-like manner via nucleophilic attack by one galloyl group onto a second galloyl moiety which is quite electrophilic by virtue of formation of an intermediate Ar-$OPb(OAc)_3$ function. Product oxidation would be discouraged in this "anchimeric assistance" mechanistic proposal since it would be exceedingly difficult to juxtapose a third nucleophilic galloyl group alongside a Pb(IV)-activated HHDP, an arrangement which is needed for the C-C bond forming process.[11b,24]

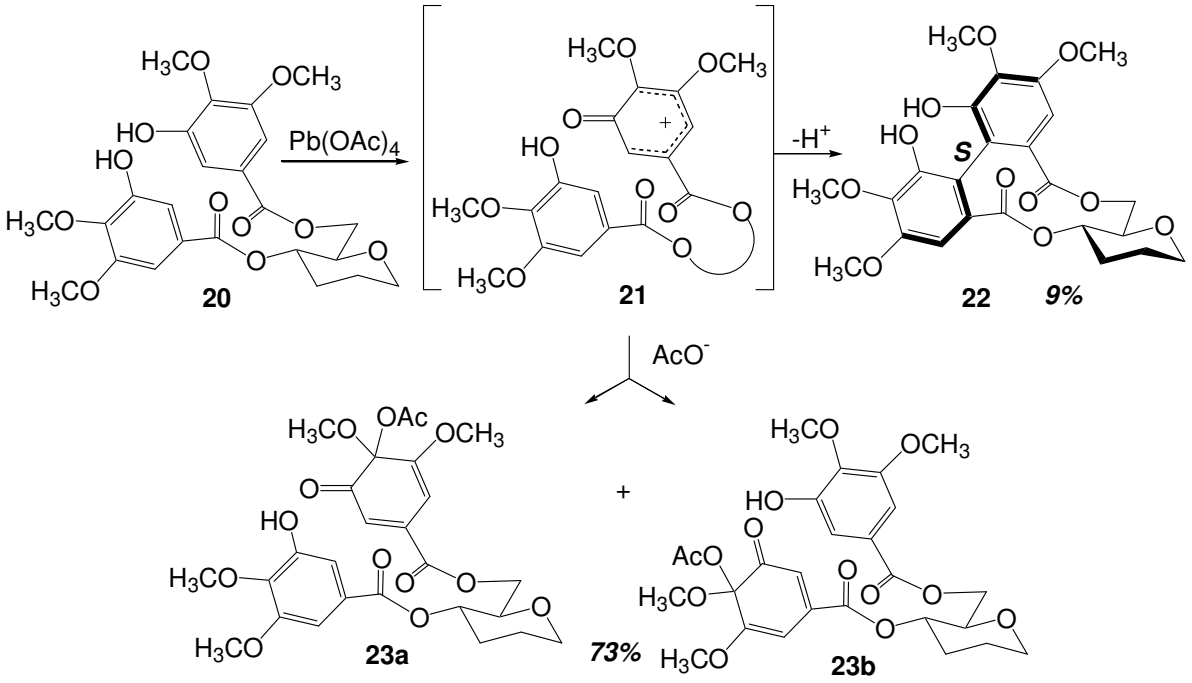

Figure 9: Preliminary success at oxidative galloyl ester coupling.

Although the stereochemical control issues related to HHDP formation were resolved favorably, yield of the desired oxidative coupling product needed an

improvement. Exploitation of different steric environments around the electrophilic atoms of note in **20** provided a solution to this problem. Replacement of the di-*O*-methyl ethers with a diphenyl ketal moiety afforded a bisphenolic substrate whose C(4) aryl carbons are effectively blocked from acetate attack. $Pb(OAc)_4$ oxidation of **24** proceeded smoothly to furnish the biaryl product in good yield as an inconsequential mixture of regioisomers, all bearing the protected (*S*)-HHDP unit.[21] Acetate trapping products were absent in the reaction. An additional advantage conferred by the diphenyl ketal moiety compared to simple methyl ethers is their ease of deprotection under mild hydrogenolytic conditions to provide the free HHDP unit (Figure 10).

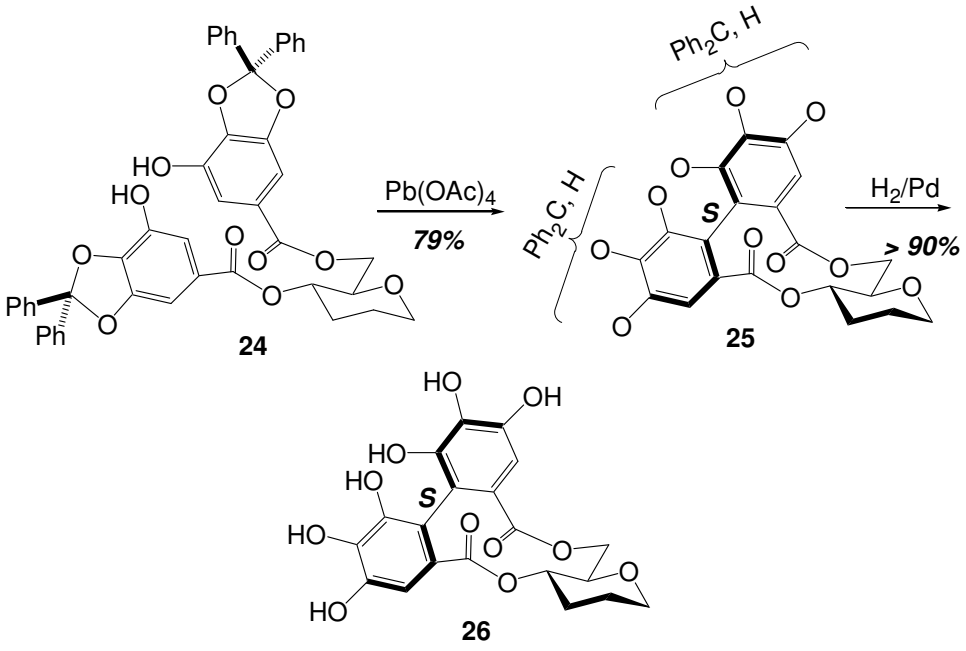

Figure 10: Efficient galloyl ester coupling on a glucopyranose core.

This methodology was extended to the more demanding context of ellagitannin total synthesis. Thus, complete stereoselective and regioselective biomimetic assembly of the monomeric ellagitannin natural products tellimagrandin I (**27**),[25] tellimagrandin II (**2**),[26] sanguiin H-5 (**28**)[27] and pedunculagin (**29**)[28] has been achieved (Figure 11). In all cases the robust $Pb(OAc)_4$-mediated oxidative coupling of diphenyl ketal-protected galloyl esters have been utilized as the key step en route to product. The complex syntheses also utilized a judicious manipulation of protecting groups to achieve a high level of regioselectivity.

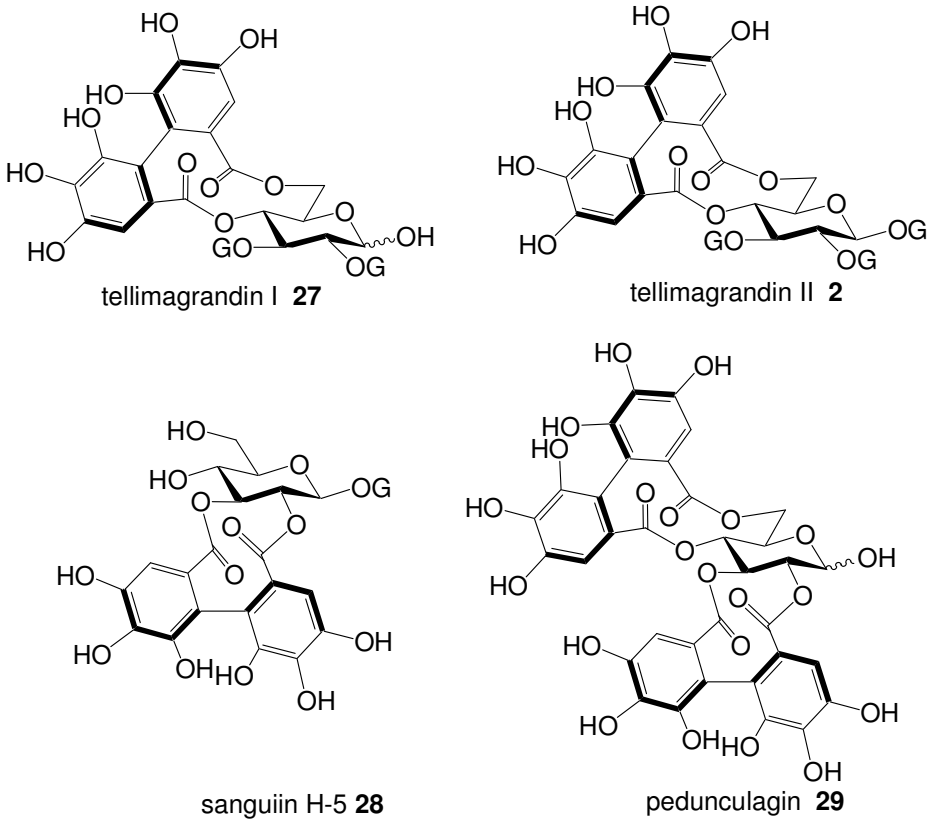

Figure 11: Ellagitannins prepared by $Pb(OAc)_4$-mediated galloyl ester coupling.

1.5 Challenges Ahead

The burgeoning interest in the field of ellagitannin synthesis saw active contributions from various groups with different perspectives and approaches. Khanbabaee and co-workers have prepared several monomeric ellagitannins by glucose diol esterfication of a preformed protected HHDP unit.[29] This strategy is similar to the one proposed earlier by Meyers and Lipshutz wherein chiral auxillaries were used to control the atropselectivity of biaryl bond formation within the HHDP unit.

Within the context of ellagitannin synthesis, the Feldman laboratory has successfully achieved the synthesis of HHDP units built on the $^4C_1$ conformation of the glucopyranose core leading to the total syntheses of aforementioned ellagitannins. What remained to be targeted were the ellagitannins based on $^1C_4$ conformation of the glucose core.

Ellagitannins exemplified by geraniin (**30**), davidiin (**31**), corilagin (**32**) and carpinusin (**33**) have more challenging structures in which (*R*)- and/or (*S*)- HHDP moieties bridge the 1,6- or 3,6- position of the glucopyranose core in the $^1C_4$ conformation (Figure 12).[30,31,32] An additional challenge is the formation of an oxidized (viz., dehydrohexahydroxydiphenoyl, DHHDP) version of the biaryl unit bridging the 2,4-positions of the glucose. The presence of all-axial substituents on these ellagitannins raises the difficulty of any synthetic strategy based on earlier protocols, as these appendages have to be held in a thermodynamically unfavorable position prior to biaryl bond formation.

The challenges mentioned above provided the motivation to devise a synthesis for a geraniin model system. **Chapter 2** presents our work en route to achieving the synthesis of a 2,4-HHDP monomeric ellagitannin unit. It discusses the significance of this work in the light of geraniin biosynthesis.

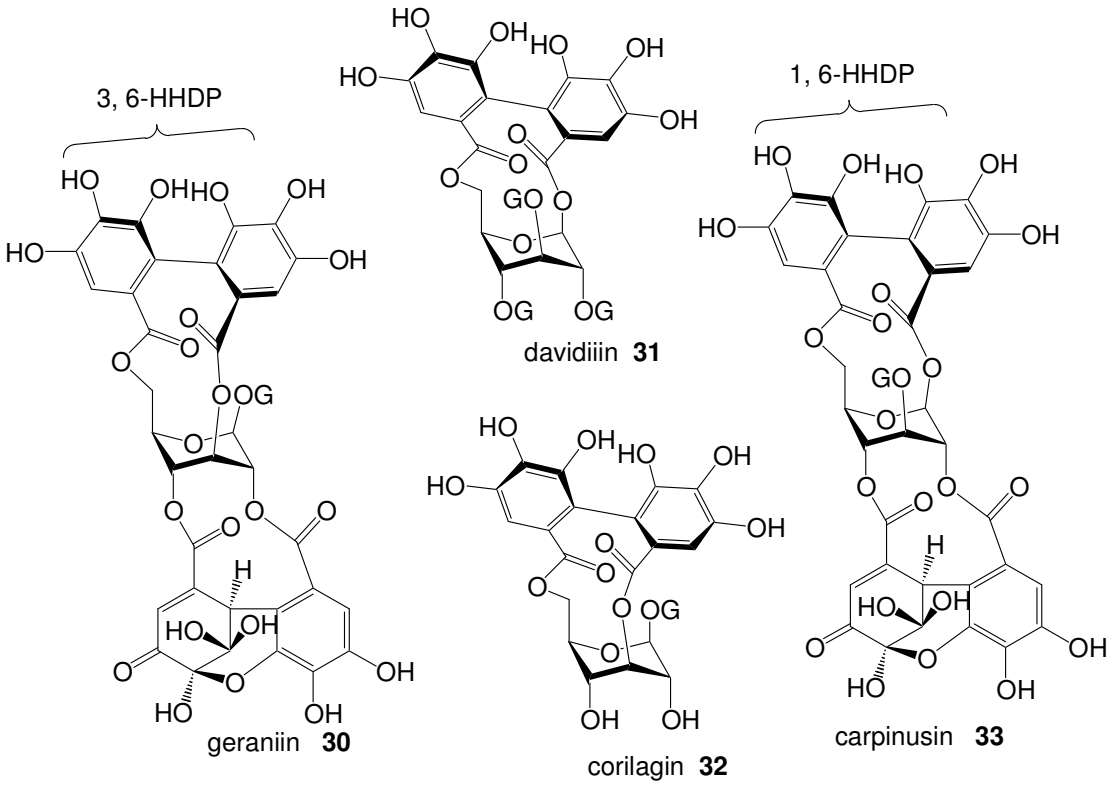

Figure 12: Ellagitannins built upon $^{1}C_{4}$ conformation of glucopyranose core.

Chapter 2

Ellagitannin Chemistry: Studies on the Stability and Reactivity of 2,4-HHDP Containing Ellagitannin Systems

2.1 Overview

One of the challenging aspects in the synthesis of geraniin is the formation of the dehydrohexahydroxydiphenoyl (DDHP) unit. The DHHDP unit can be envisioned to arise via the oxidation of a 2,4-HHDP glucopyranose precursor (Figure 13). Thus the penultimate task in the synthesis of geraniin would be to arrive at a glucose precursor with the requisite 2,4-HHDP unit akin to **34** in place.

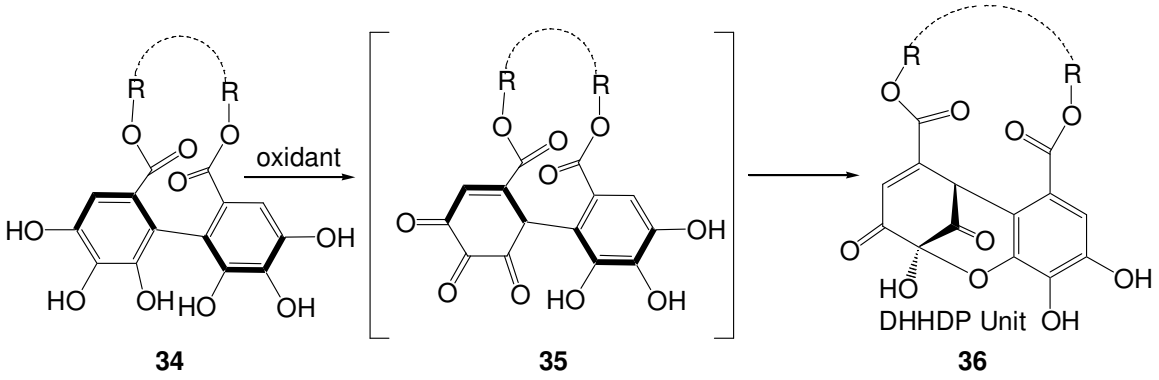

Figure 13: Strategy toward DHHDP synthesis.

The formation of a glucose ring containing a C(2)/C(4)-bridging HHDP system raised some interesting questions in light of the proposed biosynthesis of geraniin (2).[33] Among the 500+ structurally characterized ellagitannins, are species with the HHDP fragment

spanning positions C(1)/C(6), C(3)/C(6), C(4)/C(6), C(2)/C(3), and C(3)/C(4) on glucose.[11] The geraniin family of ellagitannins contains over a dozen structurally related members that all have the C(3)/C(6) (*R*)-HHDP unit and an oxidized/modified HHDP unit spanning the C(2) and C(4) positions of the glucose core.[30] No C(3)/C(6) bridged ellagitannin that includes a simple, unoxidized HHDP group at C(2)/C(4) have been identified, despite the hypothesis that such species are candidates for biosynthesis precursors to the geraniin family.[33] Curiously, there is a single C(2)/C(4)-HHDP-containing ellagitannin, but this natural product, phyllanemblinin B (**38**), does not have the C(3)/C(6) bridge.[34] Instead it has free alcoholic groups at the C(3)/(C(6) position. These observations raise questions about (1) why the 2,4-HHDP-containing ellagitannins like **37** have not been detected in the plants that produce geraniin and related products, and (2) what is so privileged about the 2,4-HHDP-bearing phyllanemblinin B structure (Figure 14).

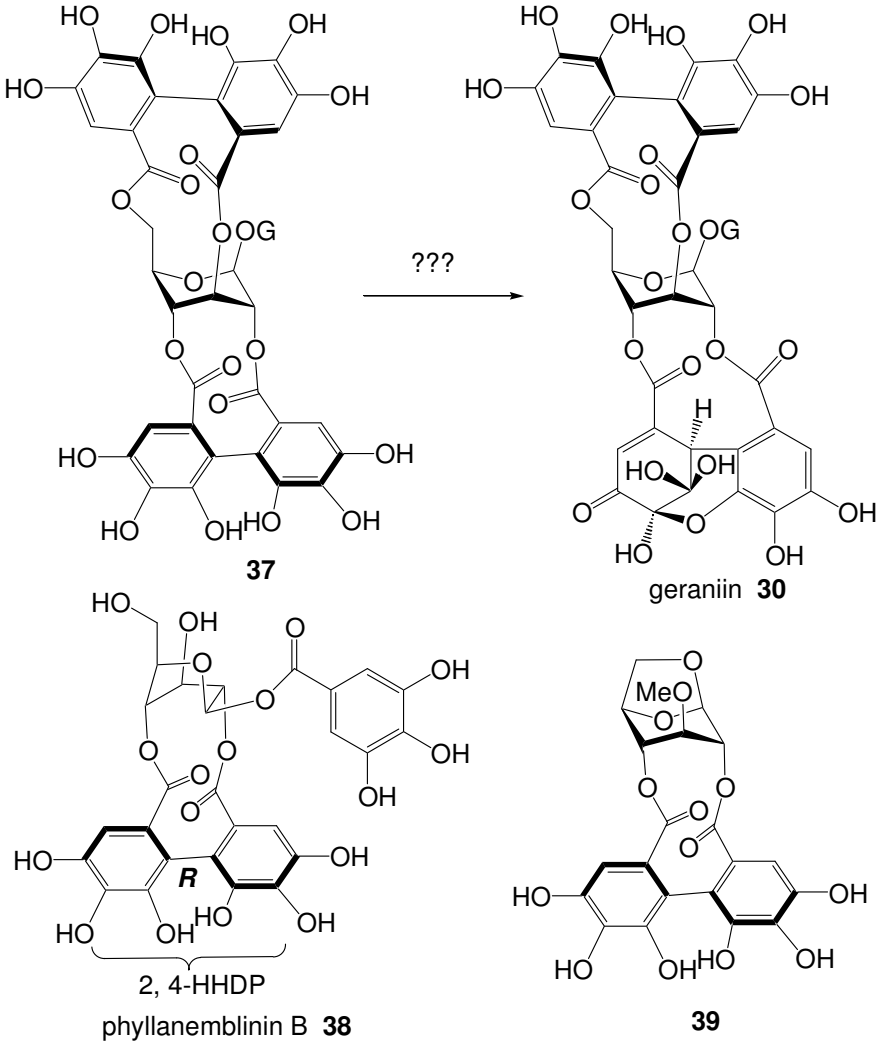

Figure 14: Biosynthetic proposal for geraniin.

2.2 Strategy

The complexity involved in the total synthesis of the unknown species **37** led us to probe the above issues through simple model system transformations. Towards that end, the 2,4-HHDP-containing glucose derivative **39**, with its 1,6-anhydro bridge, was targeted as a related mimic of the rigid C(3)/C(6) HHDP-containing species **30/37**. In both compounds, the glucose ring is held in the $^1C_4$ conformation. It was anticipated that success/failure in synthesizing this model species might be an invaluable exercise in learning the intricacies of geraniin-type ellagitannin biosynthesis.

2.3 Results and Discussion

2.3.1 Initial Attempts Towards 2,4-HHDP Synthesis

The strategy towards the synthesis of the 2,4-HHDP unit **39** required the assembly of key precursors viz., anhydro glucose diol **43** and a suitably protected galloyl coupling partner **47**.

The synthesis of the diol **43** relied upon well-documented carbohydrate manipulation chemistry starting from commercially available 1,6-anhydro-β-D-glucopyranose **40** to assemble the key precursor **43** in 3 steps (Figure 15).[35]

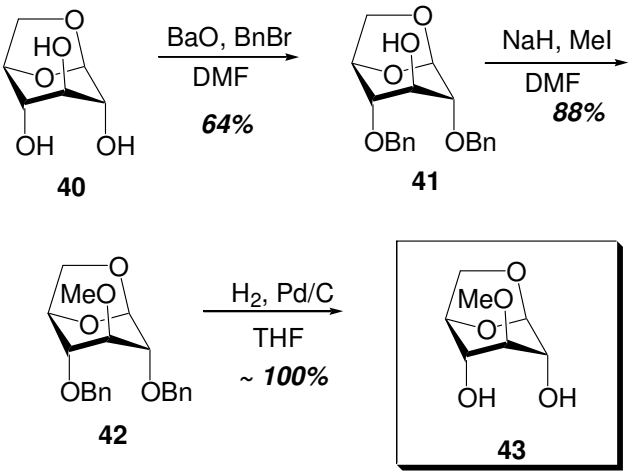

Figure 15: Synthesis of the diol precursor **43**.

The *t*-butyldimethyl silyl (TBS) protected acid **46** was synthesized in four steps starting from methyl gallate utilizing step-wise protection chemistry developed in our laboratory (Figure 16).[21]

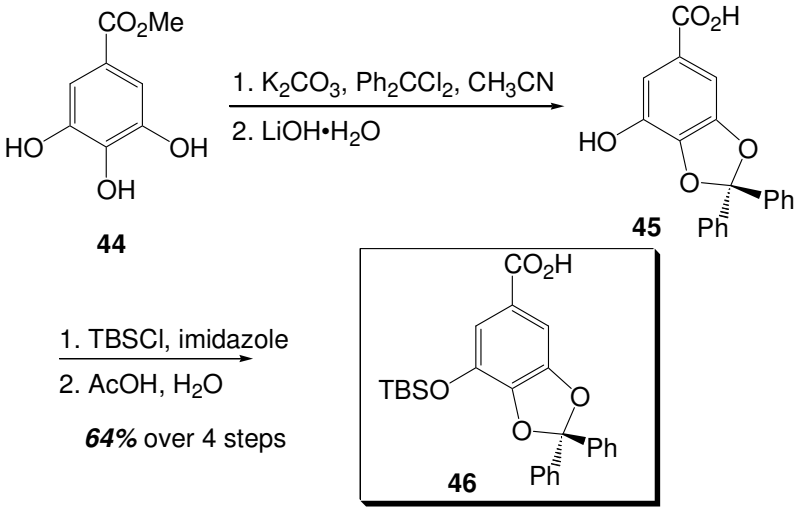

Figure 16: Synthesis of galloyl precursor **46**.

Esterification of **43** with the TBS-protected acid **46** gave the bis-ester **47** in 82% yield. Desilylation of bis-galloyl ester gave the bis-phenol **48** in 85% yield as a white foam. The key Wessely oxidation step discussed earlier effected the C-C biaryl bond formation to afford the protected HHDP product **49** in good yield but as a complex mixture of isomers (Figure 17).

Simple hydrogenolysis led to the removal of diphenylmethylene ketal from **49**. However, it was strangely accompanied by severing of the biphenyl bond. Thus, instead of furnishing the hexahydroxy compound **39**, attempts to remove the ketal led to a quantitative conversion to compound **50** (Figure 18).

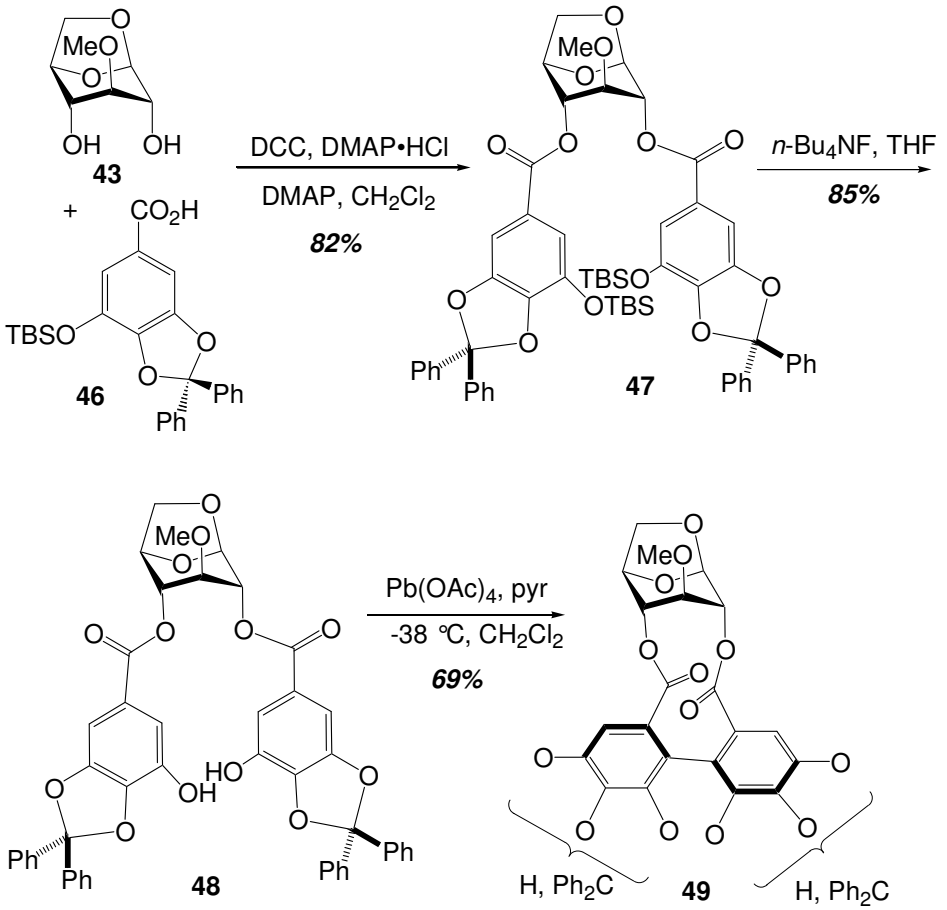

Figure 17: Oxidative coupling of the galloyl ester.

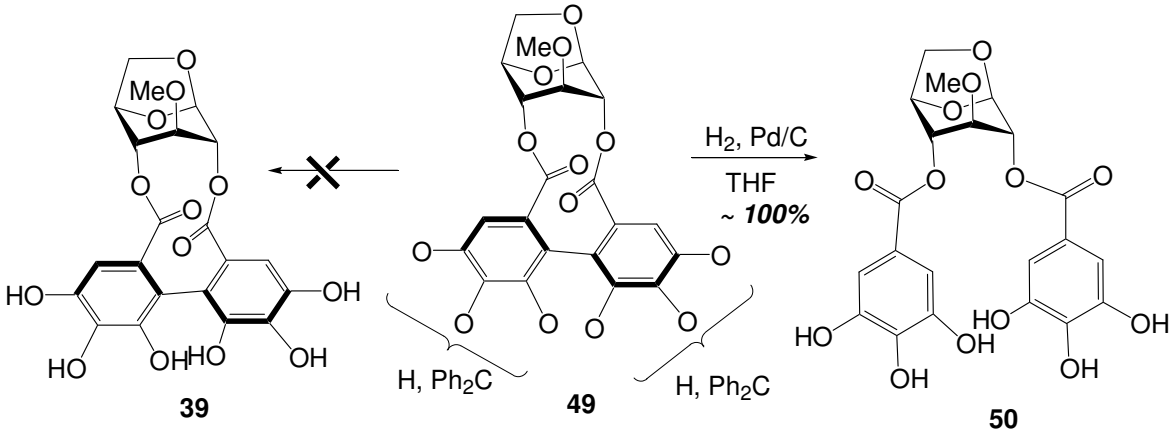

Figure 18: Hydrogenolytic cleavage of diphenylmethylene ketal protecting groups.

This unanticipated development required a more careful examination of the $Pb(OAc)_4$ oxidation product **49**.

The crude oxidation product **49** obtained was purified by flash chromatography and then HPLC to furnish a product that appeared to be a mixture of at least four distinct isomers by ^1H NMR. Circular Dichroism (CD) spectroscopy on this purified product resulted in a signal with minimal elipticity at the characteristic wavelengths for HHDP analysis.[36] This result indicated that the biaryl bond formation did not proceed with expected stereoselectivity as compound **49** was obtained as a mixture of atropisomers in addition to the expected diphenyl ketal regioisomers. Moreover a key feature distinguished this HHDP-containing oxidation product from all previous galloyl derived biaryls prepared by Wessley oxidation: it was bright orange (λ_{max} = 386 nm). All other HHDP derivatives prepared previously by Wessely oxidation were white or off-white solids, whereas the bright orange color of **8** was more reminiscent of the cyclohexadienone products (cf. **52**, Figure 19) prepared from Wessely oxidation of simple monophenolic galloyl methyl ethers.[21] In addition, the ^{13}C NMR spectrum presented a surprise: two signals at δ 191.5 and 190.7 along with the expected cluster of eight differentiated ester signals (four individual compounds) at δ 164-163. This unexpected observation from the UV/vis coupled with CD and ^{13}C NMR spectroscopic data acquired for **49** prompted the mechanistic speculation shown in Figure 19.

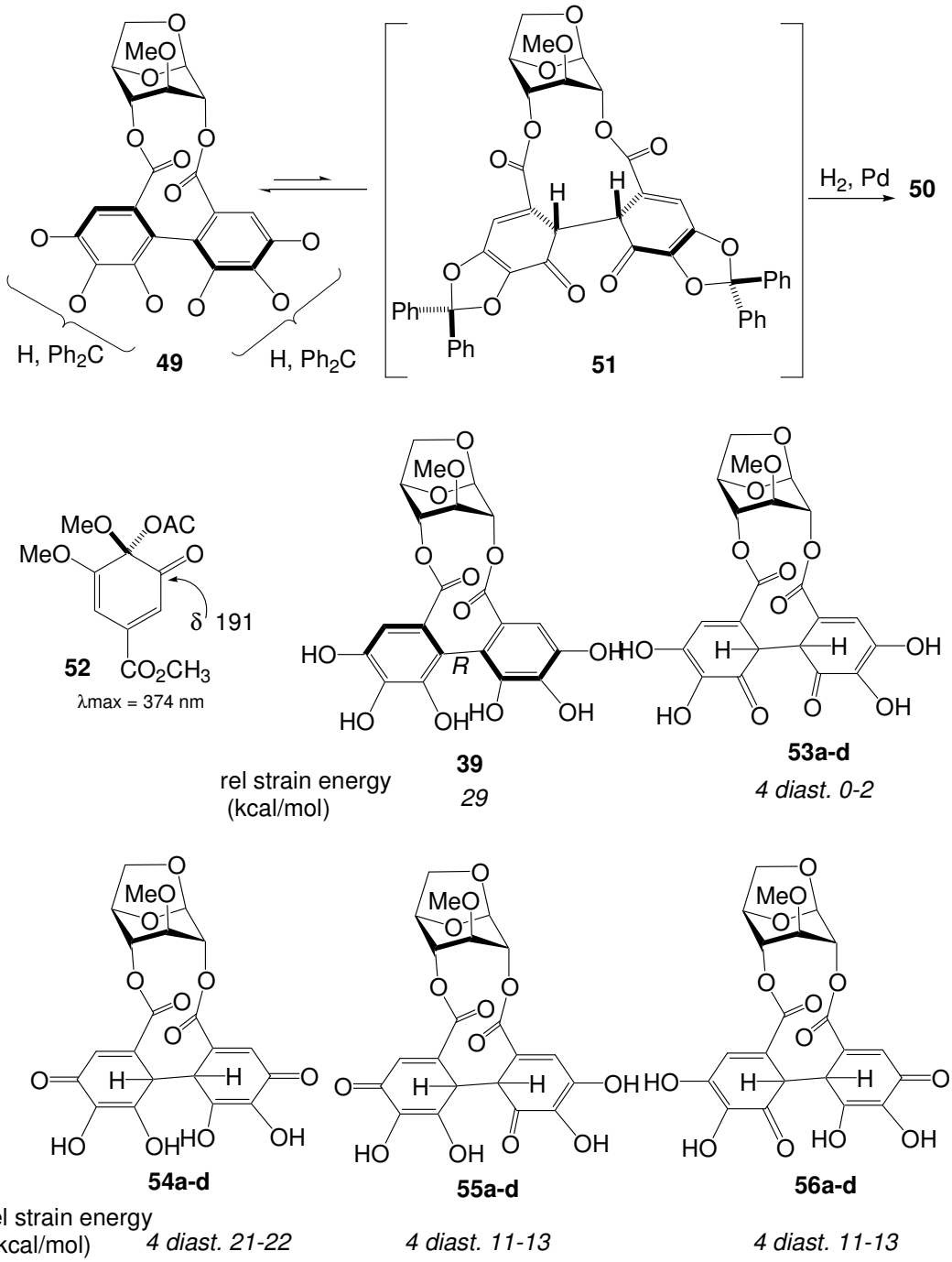

Figure 19: Mechanistic analysis.

The assumption that the relatively high strain energy amassed upon oxidative biaryl bond formation within **49** could be released by two tautomerizations was supported by molecular mechanics (MM) calculations[23,37] on model systems lacking the diphenyl ketal units; **39, 53-56**. When a tautomerization process converts **49** into a dienone, the calculated relative strain energies of model dienone systems **53-56** suggested that all of the 16 isomers possible were substantially less strained than the HHDP-containing species **39**, although limitations about the failure of MM calculations to completely address issues of tautomerization need to be noted.[38] Thus, it is not unfair to suppose that detectable amounts of a bis cyclohexadienone, e.g., **51** might be present in equilibrium with **49**. The involvement of such a species would explain the orange color observed for **49**, the downfield carbonyl peaks in the ^{13}C NMR (cf. **52**), and possibly the strange behavior upon attempted hydrogenolysis of the diphenylketal groups. It can be proposed that simple addition of hydrogen to one of the ketones in **51** could trigger a retro-Michael reaction that cleaves the two rings and furnishes **50** after tautomerization and diphenyl ketal hydrogenolytic scission. This mechanistic speculation can be extended to the geraniin series of ellagitannins, where an unobserved biscyclohexadienone product in equilibrium with **30** might provide a platform for the subsequent oxidation/nucleophilic addition processes which characterize this family of metabolites. Although it is not realistic to use the MM derived structure-energy data to draw any conclusions about the precise tautomers/diastereomers present, it is clear that any member of this set could serve the dual roles of (1) relieving the strain inherent in **39/49**, and (2) preceding formation of **50**.

These preliminary results on the constrained $^1C_4$ glucopyranose framework provided the motivation for studies on the complementary question of why phyllanemblinin B **38** is *unusually* stable.

2.3.2 Revised Route to 2,4-HHDP Unit

A reasonable supposition is that the scission of the C(6)/C(1) bridge in **49** might result in a glucopyranose species which would be flexible enough to adopt a less strained glucopyranose conformation. This structural adjustment might then permit the C(2)/C(4) HHDP unit to survive without the complications of tautomeric equilibria suffered by compound **49**.

In practice, this supposition was put to test by first protecting the free phenols in compound **49**. Silylation of **49** within the mixture gave a *white* solid **57**. The formation of a *white* solid clearly indicated the suppression of the equilibrium **49** → **51**. Examination of the ^{1}H NMR spectrum of this mixture revealed the presence of at least four discrete isomers. Careful chromatography of this mixture led to the isolation of two major pure isomers designated as **57a** (ca. 40% of the crude mixture of isomers) and **57b** (ca. 36% of the crude mixture of isomers (Figure 20). The former compound displayed the characteristic CD spectrum of an (*R*)-HHDP-containing ellagitannin, whereas **57b**'s CD spectrum revealed an (*S*)-HHDP-containing ellagitannin (**57a**: (MeOH) λ_{max} ($\Delta\varepsilon$) 238 (-4.4), 263 (+2.2), 290 (-4.9); **57b**: (MeOH) λ_{max} ($\Delta\varepsilon$) 238 (+1.9), 263 (-4.1), 290 (+5.8) (compare (*R*)-phyllanemblinin B (**38**), (EtOH) λ_{max} ($\Delta\varepsilon$) 230 (-22.8), 267 (+19.1), 295 (-

16.5))). Thus, it was concluded that the Wessely oxidation/silylation sequence provided approximately equal amounts of (*R*)- and (*S*)-HHDP-containing products.

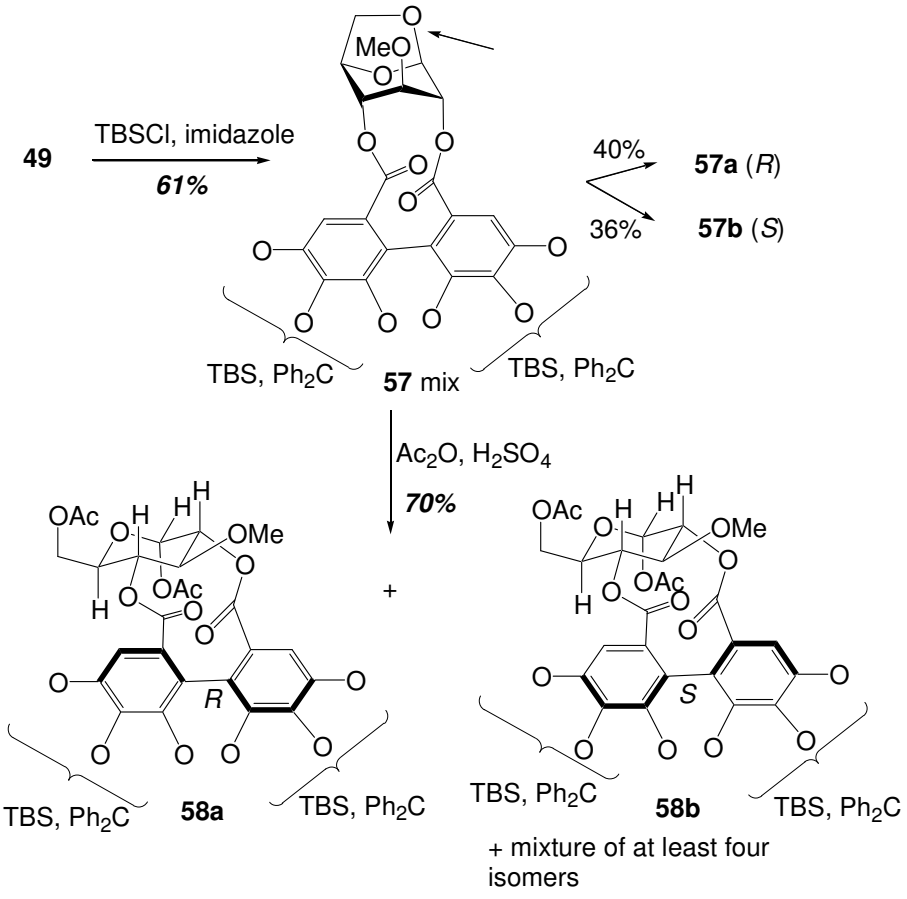

Figure 20: Revised route to 2,4-HHDP unit.

There is not enough data to decide if this lack of atropselectivity resulted from kinetic (i.e., nonselective Pb-mediated coupling) or thermodynamic (i.e., equilibration via diones such as **51**) factors. The silyl ether mixture **57** was then treated with Ac_2O/H_2SO_4 to afford a good yield of the ring-opened white diacetates **58** as a mixture of at least six compounds (Figure 20). Two pure isomers, designated as **58a** and **58b**, respectively,

could be isolated from this mixture following careful prep-plate chromatography. Isomer **58a** corresponded to the major component of the mixture (ca. 36% by ^{1}H NMR integration of the methoxy proton signals within the mixture). The CD spectrum of this species displayed the clear signature of an (*R*)-HHDP unit ((MeOH) λ_{max} ($\Delta\varepsilon$) 237 (-8.5), 263 (+1.1), 290 (+1.0)), whereas the other pure compound **58b**, only a minor component of the overall mixture (ca. 12%), produced a characteristic CD spectrum for an (*S*)-HHDP unit ((MeOH) λ_{max} ($\Delta\varepsilon$) 238 (+30.7), 263 (-6.4), 290 (-12.0)). Similar reaction of pure **57a** with Ac_2O/H_2SO_4 led to formation of a 1:1 mixture of **58a** and a second isomer, whereas pure **57b** furnished a 1:1 mixture of **58b** and a new isomer. Unfortunately, not enough material could be isolated from these experiments to characterize the other isomers formed. The tentative assignments of anomeric stereochemistry for **58a** and **58b** rest on an analysis of the glucopyranose ring's proton-proton coupling constants (see **Chapter 6**). In particular, the large $J_{2,3}$, $J_{3,4}$, and $J_{4,5}$ values are consistent only with the near diaxial disposition of these protons in a chairlike conformation. The small $J_{1,2}$ coupling for both **58a** and **58b** (ca. 3.6 Hz) is consistent with a near 90° dihedral between these protons, a geometry best accommodated by assigning the anomeric acetate functions to the axial locations shown. It was important to note that isomers **58a** and **58b** did not equilibrate at room temperature.

Desilylation of the silyl ethers within this mixture **58** resulted yet again in a complex mixture **59** of at least six isomers, from which two pure, white compounds **59a** (35%) and **59b** (27%) could be isolated by careful prep plate chromatography. Pure silyl ether **58a** was desilylated independently to furnish two new species (55:45), neither of which was identical to **59a** or **59b**. Similarly, pure isomer **58b** was converted to two

species (70:30), the major one of which was identical to **59b**. In a notable departure from the chemistry observed with **58a/58b**, the isomers **59a/59b** equilibrated over the course of 48 h in acetone-d_6 solution. The CD spectra of both mixtures derived from **58a** and **58b**, respectively, and the **59a/59b** equilibrated mixture (45:55) displayed very little elipticity at the key HHDP wavelengths. However, both **59a** and **59b** survived as discrete species long enough to acquire adequate characterization data, including CD spectra, that supported the atropisomer and anomeric stereochemistry assignments shown in Figure 21 (see **Chapter 6**). The mechanism of the HHDP isomerization is still unclear although, neither a direct Ar-Ar bond rotation nor a tautomerization-based process (cf. **49** → **51**) can be ruled out.

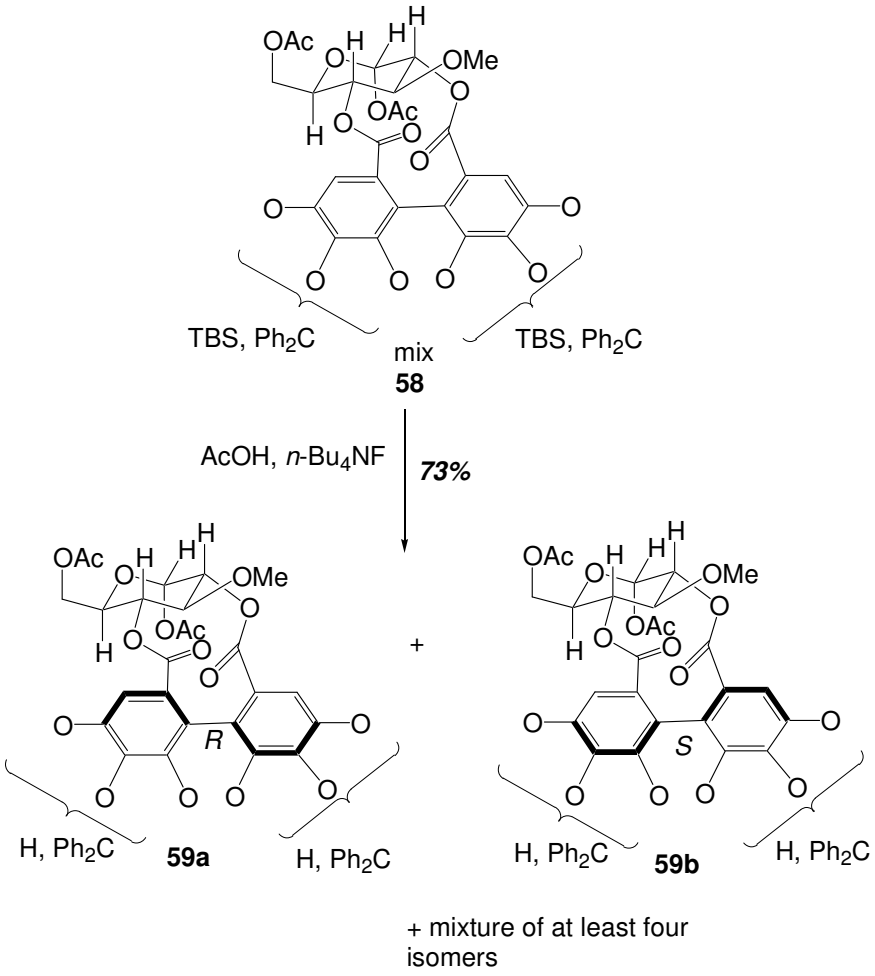

Figure 21: Desilylation of precursors en route to 2,4-HHDP unit.

2.3.3 Securing the 2,4-HHDP Ellagitannin Monomeric Unit

The final test of the proposed hypothesis came when deprotection of the ketal groups was attempted. Hydrogenolytic removal of the diphenyl ketals within the individual atropisomers proceeded uneventfully i.e., (*R*)-atropisomer **59a** delivered a single pale yellow hexaphenol isomer **60a** and similar treatment of the pure (*S*)-

atropisomer **59b** yielded a hexaphenolic product distinct from **60a**, designated as **60b**. Circular dichroism measurements for both **60a** and **60b** confirmed that the HHDP units retained their (*R*) and (*S*) absolute configurations throughout (**60a**: (MeOH) λ_{max} ($\Delta\varepsilon$) 238 (-2.0), 263 (+1.0), 290 (-4.8); **60b**: (MeOH) λ_{max} ($\Delta\varepsilon$) 238 (+0.9), 263 (-0.5), 290 (-0.8)). These hexaphenols, much like their ketal predecessors, underwent facile atropisomerization (**60a** ↔ **60b** equilibration) over 24 h. No evidence for any Ar-Ar cleavage products could be discerned. The complete mixture of isomers **59** from the desilylation reaction was exposed to H_2/Pd/C as described for the pure isomers, and a ca. 1:1 mixture of **60a** and **60b** resulted (Figure 22). Some minor and uncharacterized species were present as well (ca. 10%), but overall it appears that the acid-mediated ring opening **57** → **58** proceeded with largely inversion of stereochemistry at C(1) to furnish axial acetate-containing products. MM-based analysis of **60**, in comparison with the bridged precursor **39**, supports the contention that cleavage of the tricyclic framework results in a substantial reduction (ca. 10 kcal/ mol) in molecular strain. Thus, it appears that the stability of the C(2)/C(4) HHDP unit in **60a/60b**, and by inference in phyllanemblinin B (**38**) as well, can be attributed to the decrease in strain energy that accompanies removal of a rigidifying bridge on the β-face of the glucopyranose ring. Incorporation of such a constraint (**49** or geraniin (**30**)) leads to strain-driven rearrangement of the HHDP moiety to a reactive cyclohexadienone-containing species, which, in the natural product series, might serve as a precursor to the geraniin-based family of C(2)/C(4) HHDP-derived addition /oxidation products mentioned earlier.[38]

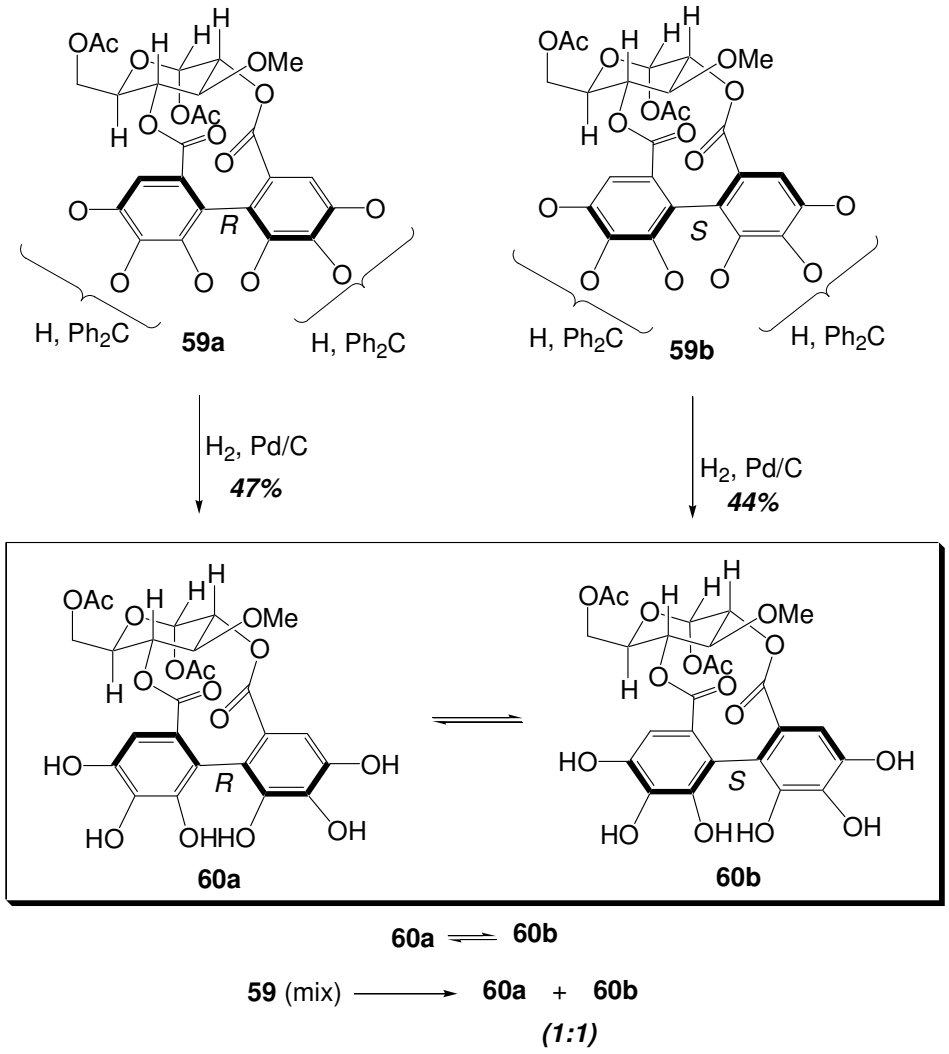

Figure 22: Securing the monomeric ellagitannin 2,4-HHDP unit.

2.3.4 Conclusions and Summary

The first synthesis of an ellagitannin monomeric unit with the HHDP group spanning the C(2)/C(4) positions of the glucose core was achieved. Along the way, pertinent questions related to geraniin biosynthesis and the mystifying stability of a related natural product phyllanemblinin was addressed.

The assembly of a variety of naturally occurring ellagitannins (see **Chapter 1**) and more specifically, in this particular context the preparation of a C(2)/C(4)-HHDP-bearing ellagitannin monomeric unit in the Feldman laboratory, unarguably show that numerous challenges in the ellagitannin synthesis have been successfully addressed. The synthesis of an ellagitannin DHHDP unit, though, has been elusive. Simple systems bearing these units have been prepared with much ease. The overarching goal of converting species **60a/b** to the geraniin DHHP unit was met with failure. This approach requires the need to curb the likely product overoxidation to achieve further progress. The great diversity of ellagitannin architectures still present many problems to be solved. Development of new chemistry to address these challenges will be necessary.

Chapter 3

1,3-Diradical Cyclization Chemistry

3.1 Overview

1,3-Diradical cycloaddition/cyclization chemistry has had a long and interesting history since its genesis.[39] Trimethylenemethane 1,3-diyls (TMMs) have been exploited in a variety of trapping reactions leading to an efficient assembly of polycylic skeleta of natural products.[39c,d] Over the years, the trimethylenemethane diyl has been demonstrated to undergo cycloadditions to suitable diylophiles either in an intramolecular or intermolecular fashion.

Continuing chemical development of these processes, and expansion into new 1,3-diyl-based areas of cycloaddition/rearrangement chemistry, led to the emergence of a heretofore unexplored version of 1,3-diradical cyclization based on the trapping of nitrogen containing TMM viz., azatrimethylenemethane diyl (ATMM).[40] This strategy towards polycyclic nitrogen-containing compounds feature an intramolecular cycloaddition of an azide to an allene followed by N_2 extrusion from the triazoline intermediate and alkene trapping of the derived N-containing 1,3-diyl (ATMM). Azide/allene cycloadditions[41,42] and azatrimethylenemethane intermediates[40] have been scarcely reported in the literature. The work detailed in both **Chapter 4** and **Chapter 5** clearly suggests that this area was ripe for development.

3.2 TMM Chemistry

It is not unfair to assume that ATMM chemistry can be designed to parallel the related TMM diyl cyclization chemistry. Hence a brief history of TMM helps set the stage for the subsequent commentary on ATMM chemistry. Diradicals as such were postulated as reactive intermediates in unimolecular thermal reactions of alicyclic compounds as long ago as 1934. Chambers and Kistiakowsky invoked trimethylene **62** in the thermolytic conversion of cyclopropane to propylene. These diradicals were of interest from a theoretical perspective (Figure 23).[43] Efforts to capture them practically have been discouraging as a consequence of the inability of a capture reagent to compete kinetically with their intramolecular ring closure. Structural modifications applied to the trimethylene diradical have proved to be useful in understanding its reactivity and has led to new reactions with broad applications.

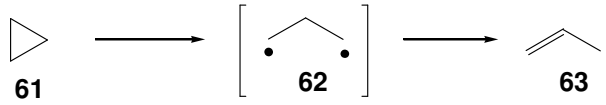

Figure 23: Early reports of 1,3-diradicals.

TMMs had been widely discussed as putative intermediates in thermolytic rearrangements of methylenecyclopropanes (Figure 24) since 1949.[44] However it was not until 1966 that these diradicals were shown to have unusual stability by the late Paul Dowd (Figure 25). He generated the TMM species **68** at 77K by irradiation of 4-methylenepyrazoline **67** and was able to characterize this species using ESR

spectroscopy.[45] The spectral signature of this TMM was consistent with the theoretical prediction of a triplet, and evidence suggested that the triplet corresponds to its ground state.

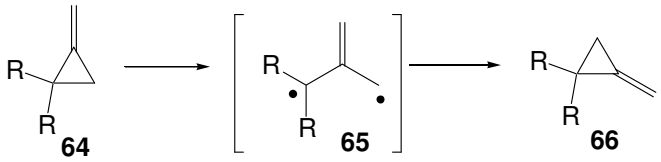

Figure 24: Initial structural modifications to access 1,3-diyl intermediates.

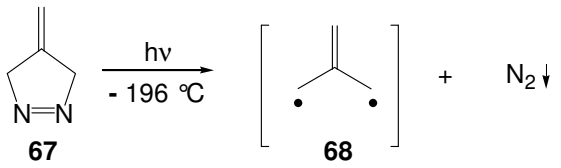

Figure 25: First example of a successful TMM detection.

Sporadic sightings of the intermolecular reactions of TMMs appeared in the literature in the 1960s. However, the yields of the products were usually low, and it was not clear in most instances whether the relative species was actually the free TMM.[46]

The foundation for much of the work in 1,3-diyl trapping reactions were laid by Berson and coworkers.[39b] They introduced the TMM series of 2-alkylidenecyclopentane-1,3-diyls in the hope of retarding the self-cyclization in the parent trimethylenemethane species. The critical assumption of the strategy is that the strain in the ring closure

products will increase the barrier to ring closure, thereby prolonging the lifetime of the diradical and increasing the chance to intercept it intermolecularly.

In 1971, Berson reported that 2-isopropylidenecyclopentane-1,3-diyls can be generated by the pyrolysis of the bicyclic diazene **69.**[47] This process resulted in the formation of four hydrocarbon dimeric products (Figure 26).

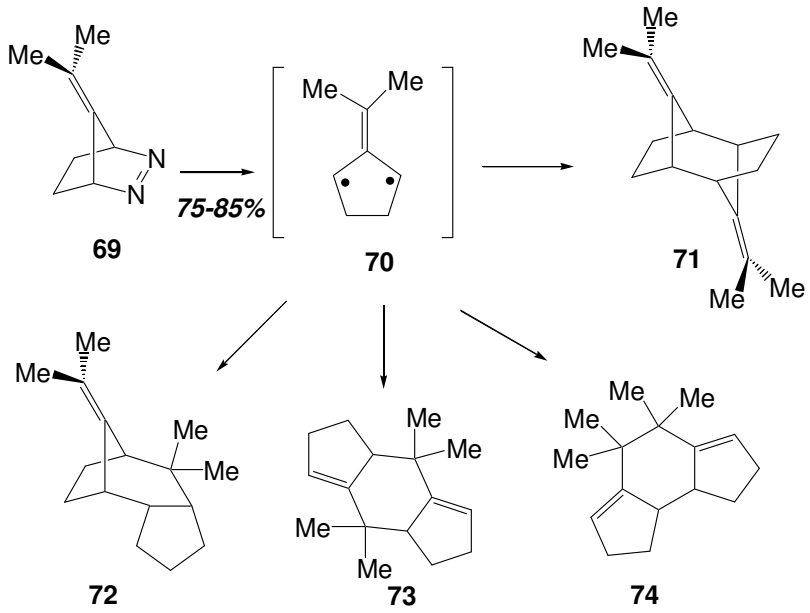

Figure 26: 2-Alkylidenecyclopentane 1,3-diyls, strain protected TMMs.

Photochemical treatment of the diazene **69** at 77K resulted in a triplet spectrum attributable to the species **70**. Question still remained about whether the common intermediate(s) implied by the dimerization results involve the same entity as seen in the triplet spectrum. In principle, dimerization may involve the combination of two triplets, two singlets or a singlet and a triplet. Kinetic evidence strongly suggested that the dimers arise from the union of two triplet diradicals. When the reaction was carried out in the

preheated probe of NMR spectrometer, the proton signals of the dimers all appear in emission within the first 1-2 min. These chemically induced dynamic nuclear polarization (CIDNP) emission signals in the ^{1}H NMR spectrum soon fade away and are replaced by the normal absorption spectrum.[47] In an accompanying paper, Closs described the radical pair theory of CIDNP and inferred that the process involves either a singlet (S) plus triplet (T) or a T plus T combination.[48] Direct evidence that the bulk of dimerization involves the combination of two triplets, was provided by the kinetics of the decline of the triplet ESR signal, which was a second order reaction and was too fast to be a singlet –plus-triplet process.[49] It was seen that in the absence of trapping agents, the yield of the dimers **71-74** from diazene **69** was quantitative, as opposed to that of 4-methylpyrazoline **67** which gives mainly methylenecyclopropane **75** and only small amounts of the dimer **76** upon thermal[50] or photochemical deazetation (Figure 27).[51] This difference in reactivity points to the strain barrier in the diradical **70** which retards its closure.

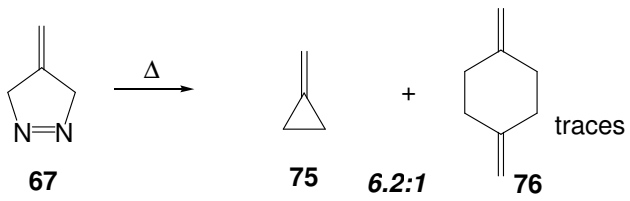

Figure 27: Deazetation of 4-methylenepyrazoline.

3.3 The Cascade Mechanism in Diyl Trapping Reaction

The isoproylidene diyl **70** can be intercepted by a variety of trapping reagents called diylophiles. As in a cycloaddition reaction the diyl acts as an electron-rich system (diene) and undergoes addition to electron deficient trapping agents (dienophile) to furnish fused and/or bridged adducts. The diyl trapping reaction can be utilized in either an intermolecular chemistry or the more efficient intramolecular trapping. This strategy served as a key element in designing succinct routes to natural products bearing five-membered rings.[39c,d]

Much of the work carried out in 1,3-diyl cyclization chemistry owes it success to the pioneering mechanistic studies done by the Berson group.[39b] In what is deemed as the "cascade mechanism", they have shown that the first trappable intermediate in the thermal or photochemical deazetation of diazene **69** is a singlet species **70S**, which at any temperature above -60 °C reversibly interconverts with housane **77**. If no trapping agent is present, **70S** undergoes intersystem crossing (ISC) to the triplet diradical **70T** which ultimately undergoes dimerization (Figure 28). In the presence of olefinic trapping agents, dimer formation is suppressed and cycloadducts of the fused- **79** and bridged type **80** appear in high yields.

The cascade mechanism with two sequentially formed intermediates predicts that as long as the concentration of reactive trapping reagents is high and it is very reactive, then the singlet diyl **70S** can be trapped selectively to afford fused adducts. Dilution of the reaction mixtures decreases the yield of cycloadducts formed from the singlet relative to that formed from the triplet. The triplet diyl **70T**, like triplet nitrenes and carbenes,[52] is

not very discriminating and affords both fused and bridged adducts. The triplet processes are essentially stereorandom and regiorandom.

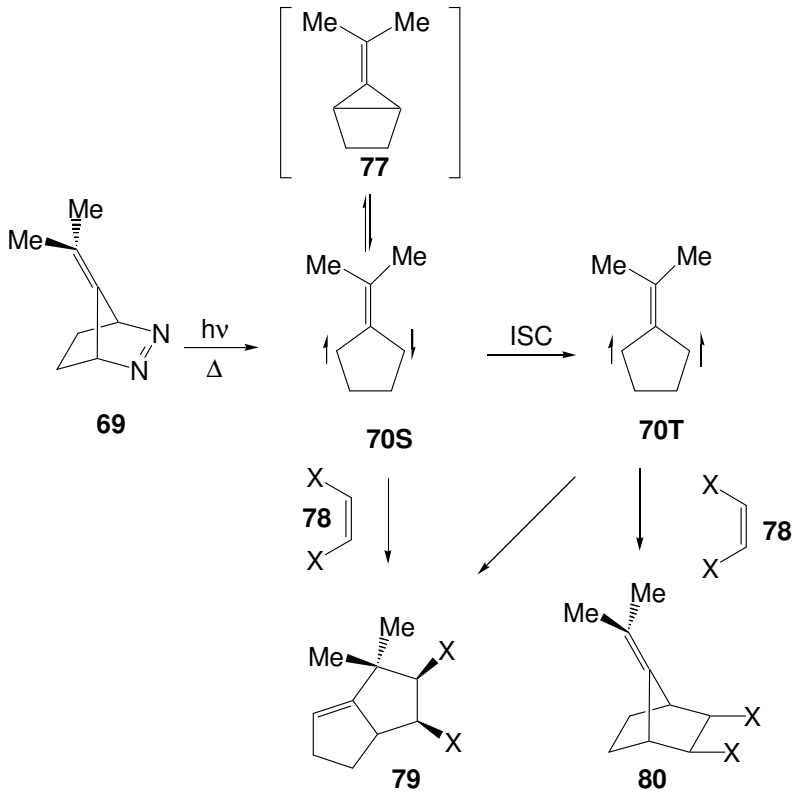

Figure 28: Cascade mechanism in deazetation of diazene **69**.

Berson and co-workers have shown that the triplet diyl reacts with molecular oxygen, and this process can be used to suppress the formation of triplet-derived cycloadducts (Figure 29).[53]

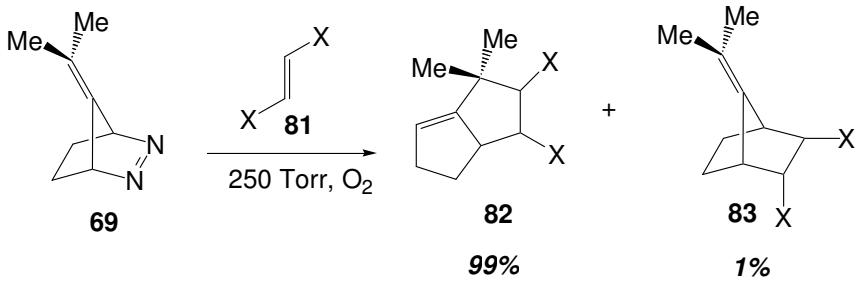

Figure 29: Quenching the triplet diyl with molecular oxygen.

Additionally, Little and co-workers have used this chemistry to afford the enone **86** from diazene **84** (Figure 30).[54]

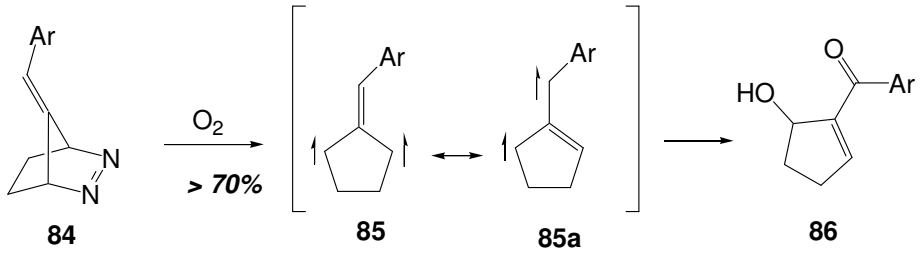

Figure 30: Quenching of triplet diyl from aryl diazene.

3.4 Diyl Trapping Reactions en Route to Natural Products

In practice, diyls are generated easily under either thermal or photochemical conditions from bicyclic azo compounds such as **69**. The temperature required for extrusion of nitrogen varies as a function of the substituents on the alkene termini. Replacement of the methyl groups in compound **69** with methoxy groups results in a very labile system. Here, the loss of nitrogen occurs readily even at -20 ℃.[55] Most systems are usually easy to handle, requiring heating at reflux to facilitate formation of the diyl. A

variety of solvents can be used, most commonly acetonitrile or THF. Photogeneration of the diyl is also readily accomplished using a light filter which allows irradiation of the low-intensity UV maximum which appears near 340 nm.

The foundation in TMM chemistry laid by Dowd and Berson was utilized in many natural product synthesis strategies by Little and coworkers.[39c,d]

3.4.1 Entry to the Linearly Fused Tricyclopentanoids

Little demonstrated that heating a benzene solution of dimethyl diazene **69** to 70-75 ℃ in the presence of an excess cyclopentenone afforded a 90-98% yield of cycloadducts **87-89**.[56] However, the process displayed essentially no stereoselectivity or regioselectivity (Figure 31).

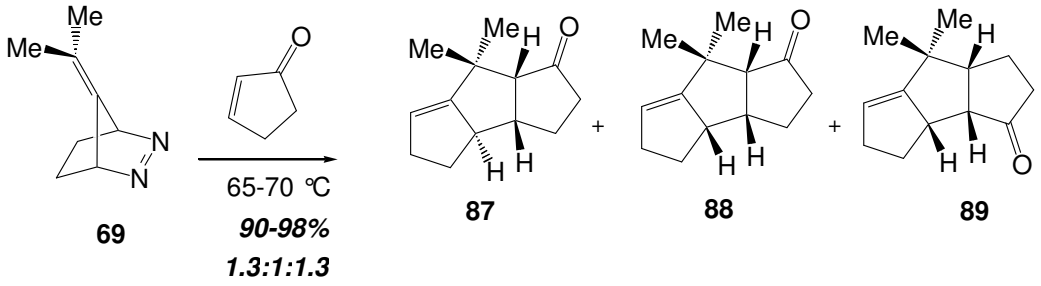

Figure 31: Intermolecular diyl trapping reaction.

It soon became clear that many of the problems encountered during intermolecular diyl trapping reaction could be solved using an intramolecular variant. Thus, as shown in Figure 32 the relationship between B- and C-ring substituents in

tricyclopentanoids is determined by their relationship to one another on the tether and diylophile.

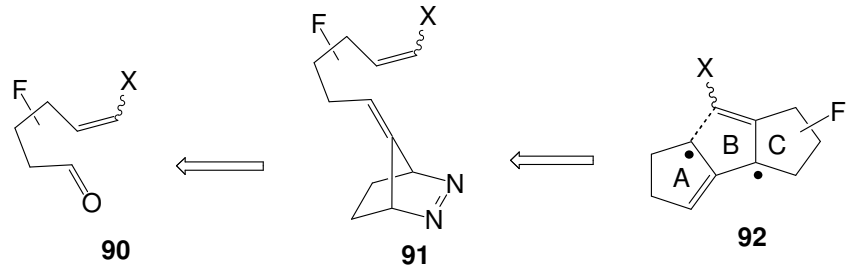

Figure 32: Approach to cyclopentanoid core

Following the general route for bicyclic diazenes the major task in an intramolecular diyl trapping is the construction of the functionalized unit **91**. The intramolecular diyl trapping reaction can be then generalized to give access to the carbon framework shown in Figure 33.

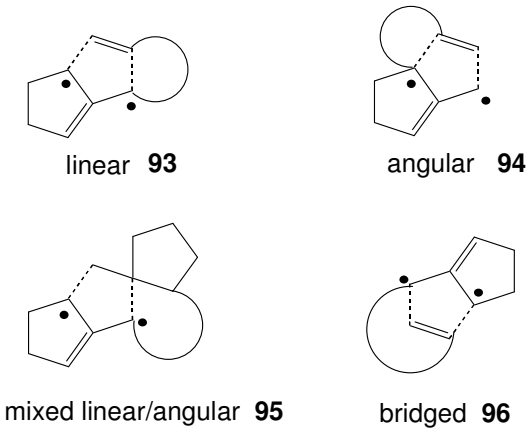

Figure 33: Intramolecular diyl trapping possibilities.

In an intramolecular diyl trapping reaction, it was shown that diazene **97** bearing a *Z*-substituted diylophile upon reflux in acetonitrile solution gave cycloadducts **98** and **99** in 87:13 ratio in a combined yield >85% (Figure 34).[57] This paved the way for an expanded utility of this cascade cyclization, as evidenced by the work done by Little and co-workers.[39c,d]

In retrospect, what is worth considering is that the work done by Dowd, Berson and Little showed that the short-lived highly reactive 1,3-diradicals can serve as useful intermediates in organic synthesis.

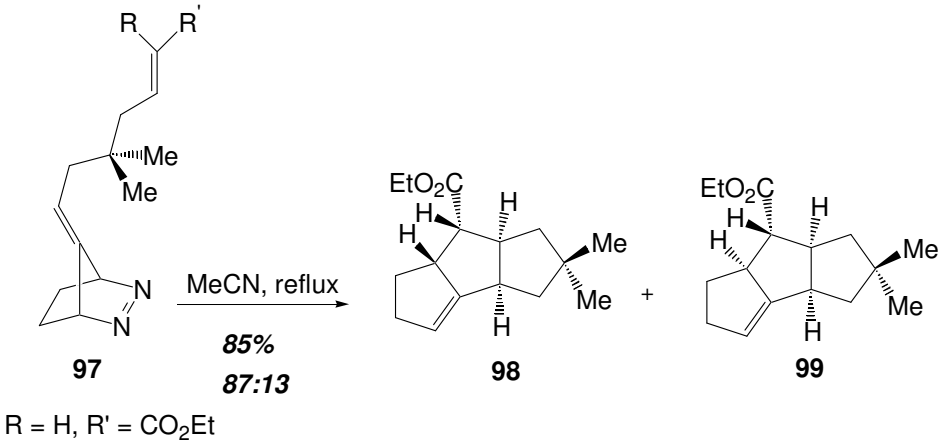

Figure 34: Intramolecular diyl trapping reaction.

The diyl trapping reactions have been successfully utilized in the synthesis of a variety of cyclopentanoid natural products exemplified by coriolin (**100**),[58] hypnophillin (**101**),[58] capnellene (**102**)[59] and hirsutene (**103**) (Figure 35).[60]

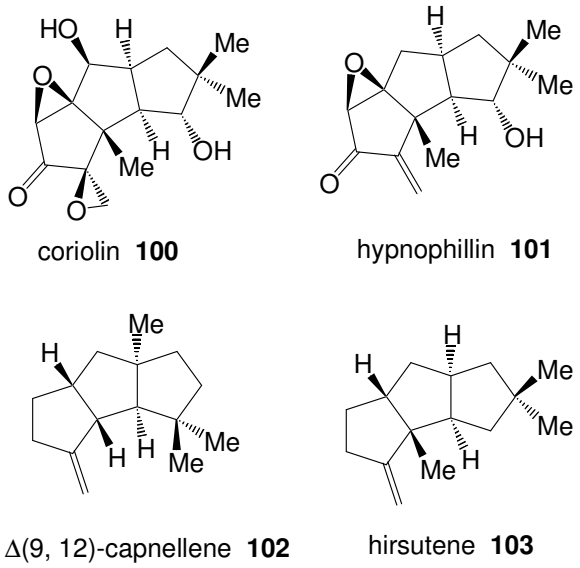

Figure 35: Natural product candidates accessed from diyl trapping reactions.

3.5 1,3-Diyl Cyclizations from Feldman's Laboratory

The cascade bicyclization reaction triggered by the addition of the lithium anion of dienyltosylamide **104** to alkynyliodonium salt **105** is a transformation which merges alkylidene carbene chemistry with TMM chemistry. Feldman and co-workers have shown that the efficient conversion of simple materials into bicyclic adduct proceeds sequentially through the alkylidene carbene **106**, the strained methylenecyclopropane **107** and the orthogonal diyl **108** (Figure 36).[61]

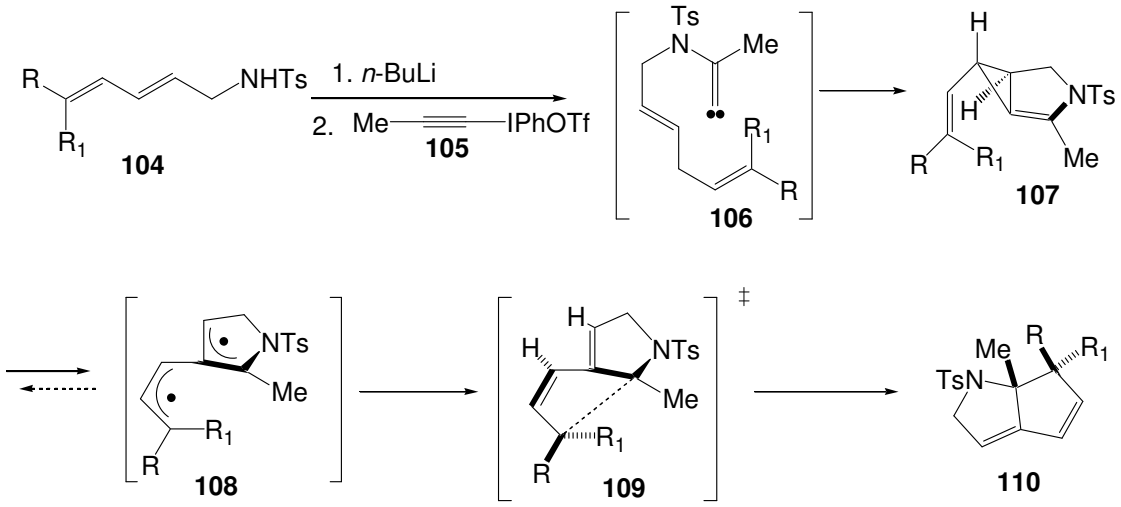

Figure 36: Merger of alkylidene carbene chemistry with 1,3-diyl cyclization cascade.

A second example of alkylidenecarbene and diyl chemistry can be found in the cascade sequence which converts the alkynylstannane **111** to oxygenated cyclopentanoid compounds **115** and **116** (Figure 37).[62] While this work was in progress, Lee and Kim revealed a similar reaction sequence starting from oxiranyl hydrazone alkylidenecarbene precursors (Figure 38).[63]

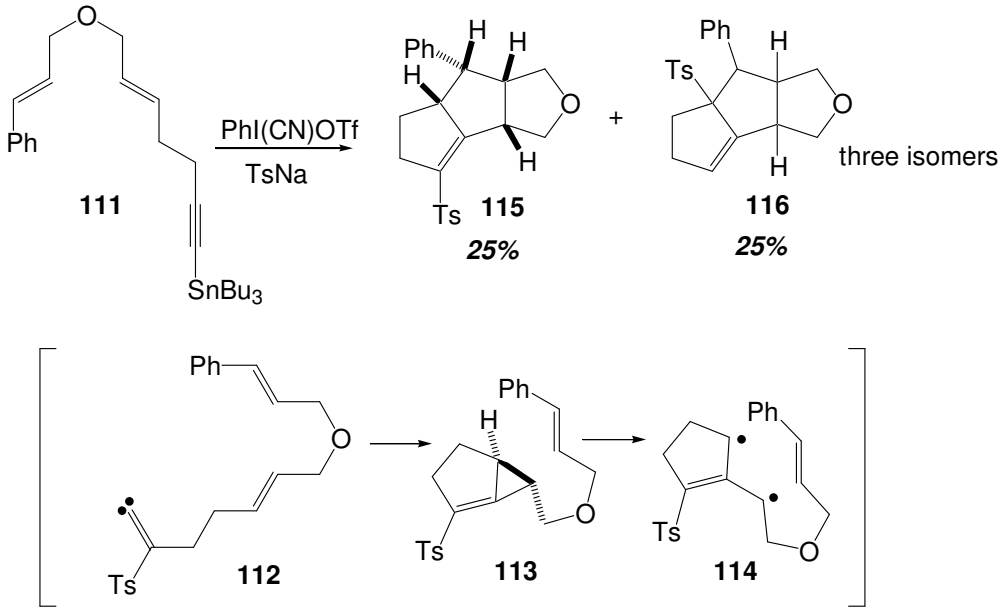

Figure 37: Alkylidene carbene chemistry combined with 1,3-diyl cyclization cascade.

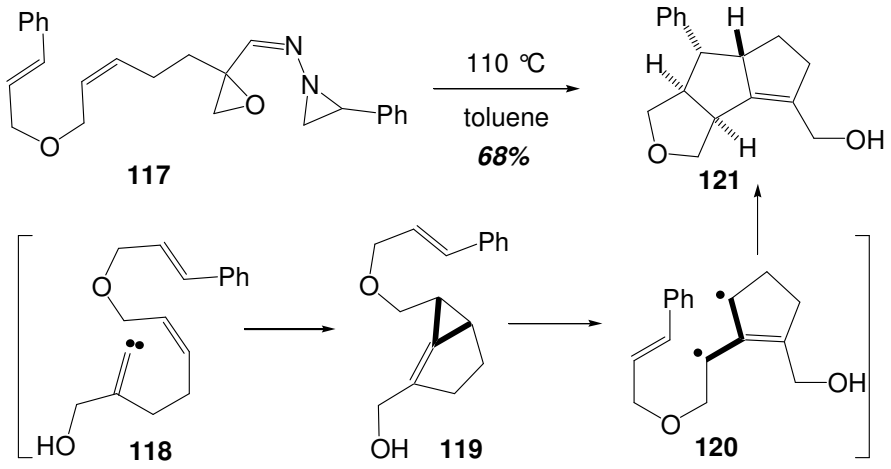

Figure 38: Alkylidene carbene chemistry/1,3-diyl cyclization cascade- Lee *et al*.

3.6 Motivation and Summary

The cycloaddition strategies involving the parent TMM diyl have been exploited possibly to its fullest potential. Unique opportunities still exist in the under-explored area of hetero TMMs, more specifically the azatrimethylenemethane-based cycloaddition/cyclizations.

Thus, prospects for introducing considerable efficiencies into the syntheses of certain polycyclic pyrrolidine-bearing alkaloid architectures encouraged plans to explore intramolecular allene/azide cycloadditions as a route to ATMM diyl trapping.

Chapter 4

Allenyl Azide Cycloaddition Chemistry

4.1 History of Allenyl Azide Cycloaddition Chemistry

Olefins react with organic azides to give triazolines **122**, aziridines **123** and imines **124**.[64] The aziridines and imines usually are generated from the decomposition of the triazolines or from the reaction of the olefins with nitrenes derived from decomposition of the azides (Figure 39). Correspondingly, it can be expected that organic azides would react with allenes to give alkylidenetriazoles **126**, which can be decomposed to aziridinyl enamines **127**, their isomeric cyclopropanonimines **128**, or related isomers (Figure 40).[65]

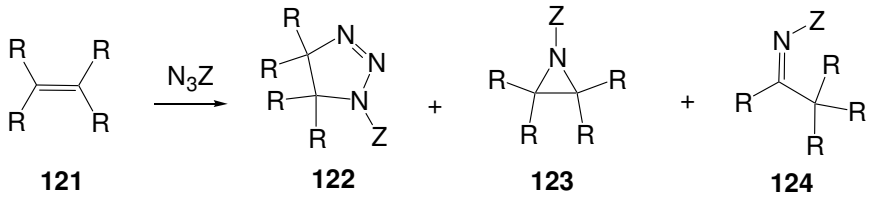

Figure 39: Reaction of azides with olefins.

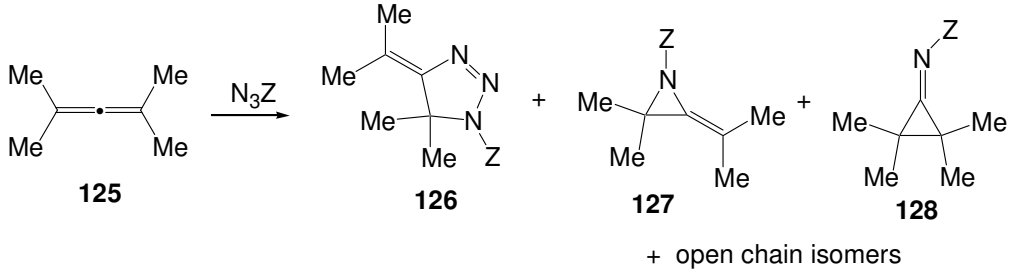

Figure 40: Reaction of azides with allenes.

An investigative look into the reaction of an allene with an organic azide was published by Blieholder and Shechter in 1968.[41a] They reported that the thermolysis of ethyl azidoformate with tetramethylallene yields ethyl 4-isopropylidene-5,5-dimethyl-Δ^2-1,2,3-triazoline-1-carboxylate **130** (38%) and 2-ethoxy-4-isopropylidene-5,5-dimethyl-2-oxazoline **131** in 29% yield (Figure 41).

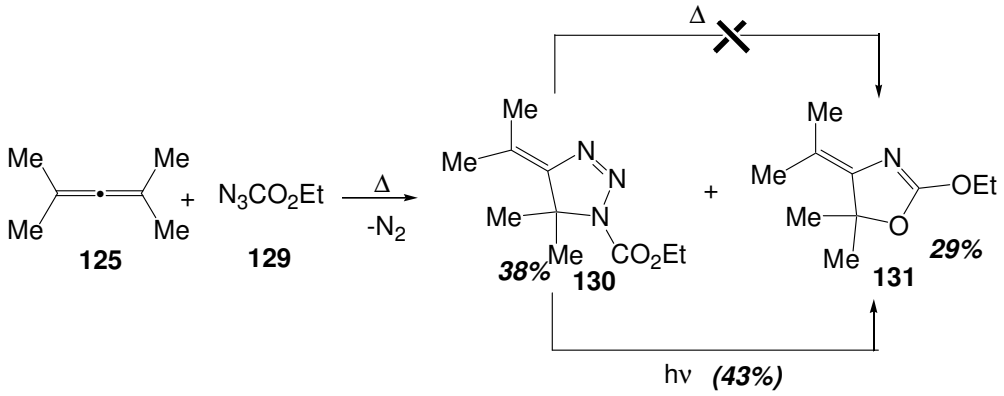

Figure 41: Reaction of tetramethyl allene with ethyl azido formate.

The triazoline **130** clearly appeared to be formed from the 1,3-cycloaddition of ethyl azidoformate to the allene **125**. What was interesting and unprecedented was the formation of the oxazoline derivative **131** from the reaction. It was clear that the triazoline **130** was not an intermediate towards the formation of **131**, as refluxing the triazoline in chlorobenzene for 40 h resulted in clean recovery of starting material. However photolysis of the triazoline at 25-30 ℃ in hexane led to the oxazoline **131** in 43% yield. Although, the exact mechanism of the formation of the oxazoline was not known at that time, it was proposed that it could result from the 1,3-dipolar addition of carbethoxy nitrene to allene **125** or by 1,1-addition of the nitrene to yield aziridinyl

enamine **132** which then rearranges to the oxazoline (Figure 42). Consequently the mechanism of the photolytic conversion of triazoline **130** to the oxazoline may be the result of the loss of nitrogen followed by rearrangement of the intermediate aziridinyl enamine. It was interesting to note that the enamine **132** was never isolated from the tetramethyl allene reaction.

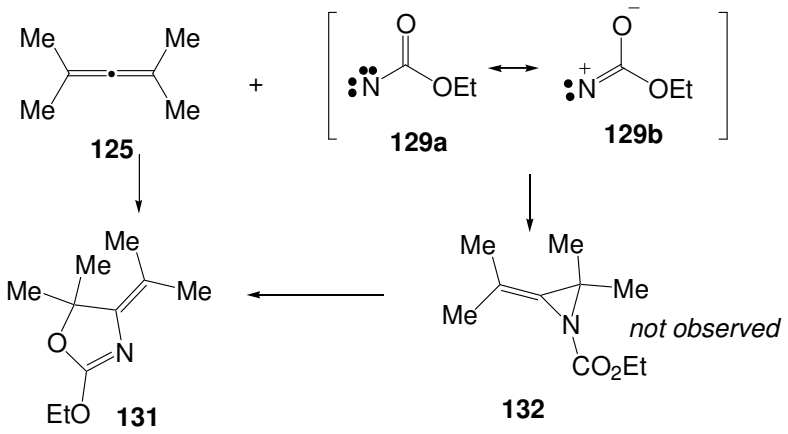

Figure 42: Addition of nitrenes to allenes.

In 1974, Bingham and Gilbert[42a] re-investigated the reaction by studying the reaction of triplet carbethoxynitrene with allenes. They suggested that the triplet nitrene is radical-like in character and its addition to C-2 of the allenic moiety would potentially provide an entry into triplet hetero-trimethylenemethanes (Figure 43).[66]

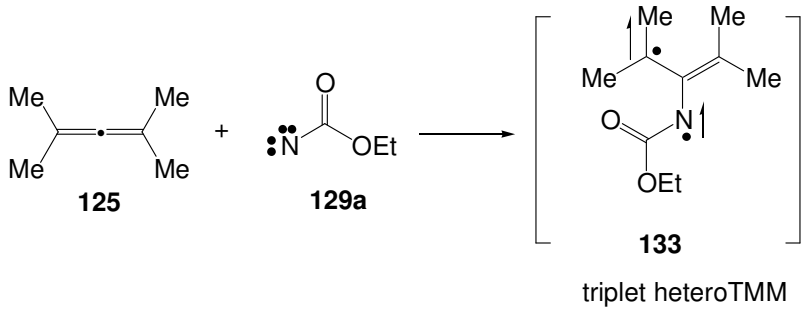

Figure 43: First suggestion of a hetero-trimethylenemethane diyl.

In an interesting set of experiments (Figure 44) involving the addition of carbethoxynitrene to allene **134a**, 1,1-dimethyl allene **134b** and tetramethylene allene **125**, they showed that 2-methylene-*N*-carbethoxyaziridine **135a**, alkylideneaziridine **135b** and starting allene were obtained respectively as products. The product **135a** was surmised to be the result of 1,2-cycloaddition mode reminiscent of the reaction of allenes and carbenes. Mechanistically it was rationalized that the addition of triplet nitrene can produce diradical **136** or **136a**, which would then undergo spin relaxation to furnish the product. In the case of 1,1-dimethyl allene, the authors suggest that the triplet nitrene preferentially adds to the less encumbered position of the allene to give the diradical **136**, which gets converted to product **135b**. According to Bingham and Gilbert, the steric hindrance faced by the nitrene upon addition to tetramethyl allene explains the recovery of starting material in that particular case. This publication was the first to invoke the possibility of a hetero TMM.

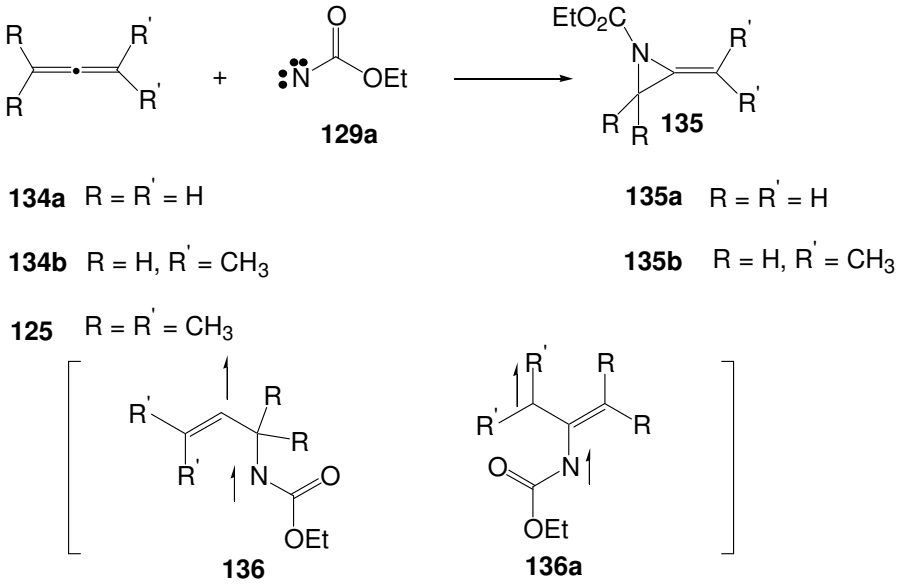

Figure 44: Investigative addition of nitrenes to allenes.

4.2 Evidence for ATMM: Quast's Contribution

Quast followed up on the efforts of Shechter and Gilbert with a thorough investigation into the generation, structural properties and reaction chemistry of aza-, diaza- and triazatrimethylenemethane species.[40] The most persuasive evidence for an ATMM intermediate was found in the conversion of the triazoline **137** into cyclopropylimine **139** (Figure 45).

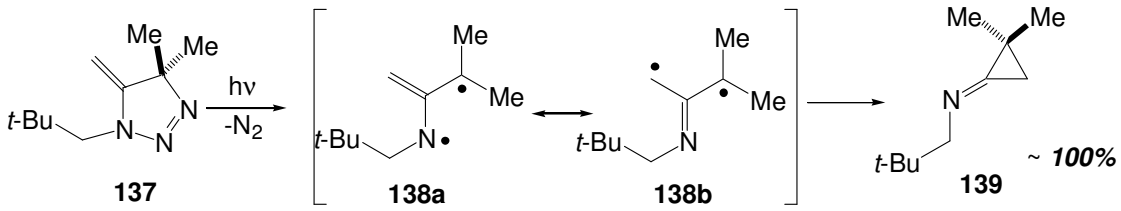

Figure 45: Quast's triazoline conversion to cyclopropylimine.

It was observed that the photochemical or thermal extrusion of molecular nitrogen from 1,4,4-trialkyl-5methylene-1,2,3-triazoline **137** occurred readily to yield stereoselectively *E*-propenamine **139**. This process undeniably has to pass through the diyl intermediate **138a/138b**. Quast proposed that the products of nitrogen extrusion from **137** originate on the least-motion path.[40c,g] Not even traces of methyleneaziridines **141** were detected (Figure 46). The cyclization regioselectivity of this diradical intermediate apparently, is determined by product stability. The assumption of diastereomeric ATMMs as intermediates led to the following mechanistic scenario for the photolysis of **137** to give cyclopropanimine **139**: Rupture of the NN bond that is the shear point of **137** generates the diazenylazaallyl diradical **140**. After loss of molecular nitrogen from **140** to afford the mono-orthogonal ATMM diyl **139c**, conversion to the bis-orthogonal ATMM **138d** occurs en route to product **139**.

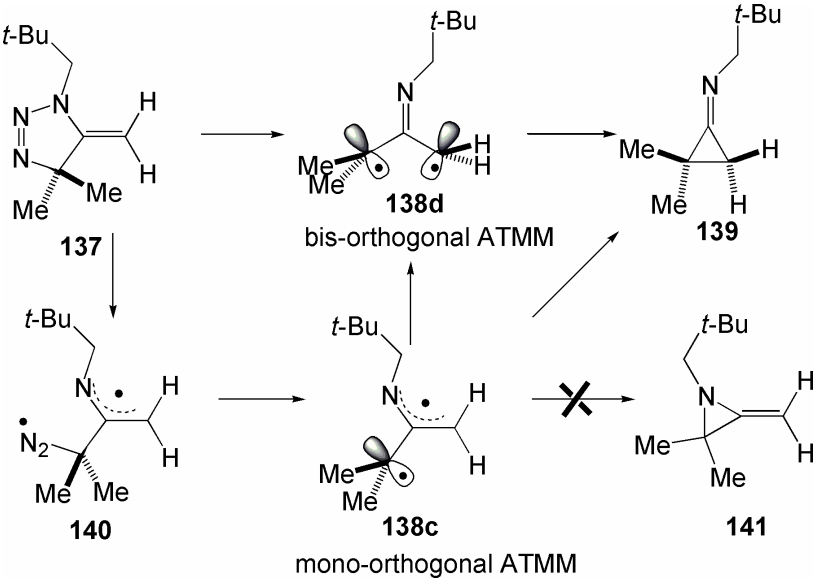

Figure 46: Extrusion of dinitrogen from triazoline derivative **137**.

It should also be mentioned that organometallic equivalents of ATMM e.g **142**, [67] have been prepared and structurally characterized. However, their reaction chemistries are far too different from the uncoordinated species (Figure 47).

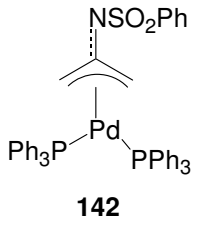

Figure 47: Metal co-ordinated ATMM.

Finally, an intriguing bit of information was gleaned from the work of Bertozzi and Bednarski,[68] where they report that the allenyl azide **143** prepared in the study of

carbohydrates, decomposed slowly to uncharacterized products (Figure 48). In this context, it is not unfair to speculate that an intramolecular allenyl azide cycloaddition might have lead to the formation of a triazoline derivative which might have collapsed overtime via diyl formation.

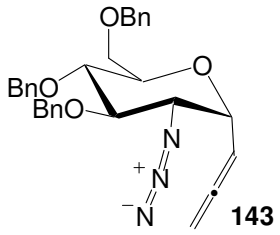

143

Figure 48: Allenyl azide built on carbohydrate template.

Further studies provided both indirect as well as direct evidence for the analogous diazatrimethylenemethane (diATMM).[40h] Interestingly, it was observed that the cyclohexenyl tetrazole **144** is an isolable and characterizable species, whereas the cyclopentenyl analogue **147** is apparently too strained to handle at ambient temperatures (Figure 49). Triplet diATMM **149** was isolated and characterized by ESR spectroscopy from the tetrazole **148** (Figure 50). The strain-induced reactivity (**144** vs. **147**) should offer ample room for exploitation.

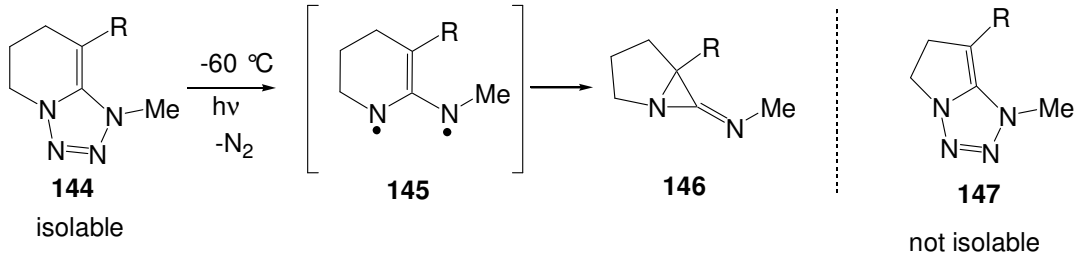

Figure 49: Diazatrimethylenemethane.

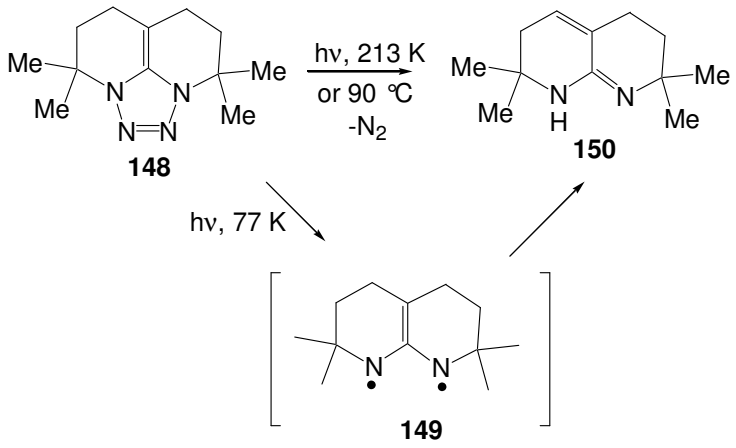

Figure 50: DiATMM ground state triplet.

Substantial evidence for triazatrimethylenemethane (triATMM) was obtained from the matrix photolysis of tetrazolinimine **151** at 80 K. ESR spectroscopy showed the generation of a triplet trisiminomethane or triATMM **152** en route to diaziridinimines **153** (Figure 51).

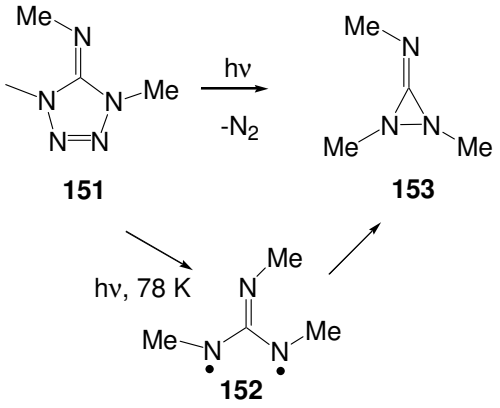

Figure 51: Triazatrimethylenemethane.

4.3 Challenges Toward Realizing ATMM Chemistry

The seminal investigations done by Quast clearly supported the notion that triazolines of the type **137** should be competent precursors for ATMM diyls. In addition, the earlier precedents also revealed that (1) direct, intermolecular azide/allene cycloaddition was not a viable route to triazolines due to incompatible reaction regiochemistry, and (2) facile ATMM closure to iminocyclopropanes of the type **139** may render the diyl capture problematic. Successful approaches to employing ATMM diyls in cyclization chemistry must simultaneously address the issue of suppressing its facile tendency for ring closure (i.e., **137** → **139**) while providing a proximal or built-in diyl trap to capture the reactive species before the intrusion of undesired side reactions.

Relying on an intramolecular allenyl azide cyloaddition to form cyclopentenyl-fused triazoles can be a solution well-suited to solve both the above cited problems (Figure 52). It can be expected that direct closure of **156b** to furnish an

iminocyclopropane (**156d**) as per Quast's studies is less likely as it would be energetically penalizing.[61]

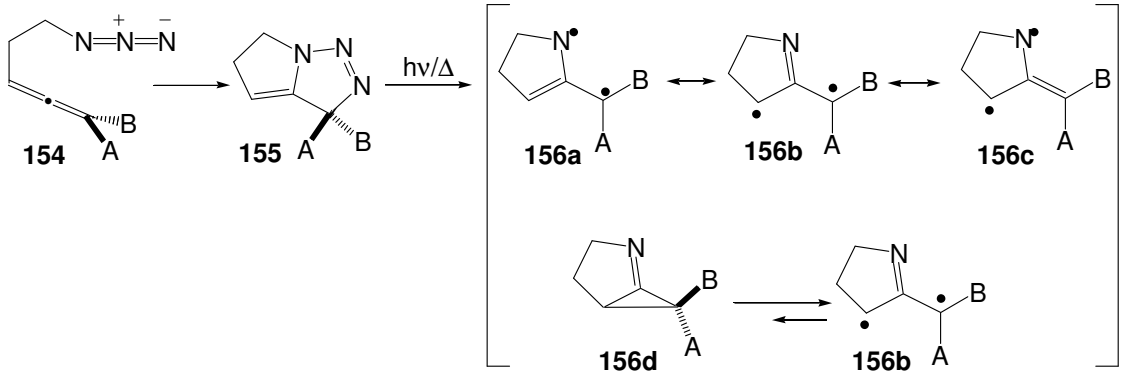

Figure 52: Intramolecular allenyl azide cycloaddition.

Further, tethering the reactive components together should overcome the inherent and undesired regiochemical bias for this cycloaddition, as suggested by the recent work from Mukai.[69] The Mukai study documented that intramolecular allenyl azide cycloadditions on **157** do proceed with favorable regiochemistry for the synthesis of triazolines related to **137**, although subsequent alkene migration afforded aromatized triazole product **158** which do not support ATMM generation (Figure 53). The use of a terminally disubstituted allene might thwart the alkene isomerization/aromatization pathway and open up the possibility of utilizing Quast chemistry to presumably generate the ATMM diyl.

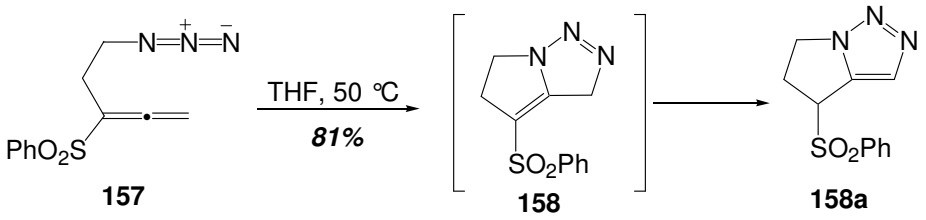

Figure 53: Intramolecular azide/allene cycloaddition - Mukai *et al*.

4.4 Contributions from Feldman Laboratory

4.4.1 Basic Idea

1-Aryl- and/or 1-vinyl-substituted 5-azidoallene substrates **159** and **161** might be candidates that could be utilized in an intramolecular azide/allene cycloaddition (Figure 54). Allenes **159** and **161** have a built-in reactive alkene tether which can serve as a suitable diyl trap. Additionally, the terminal disubstitution pattern on these allenes disallow the triazoline alkene isomerization/aromatization pathway,[69] further paving the path for the ATMM generation.

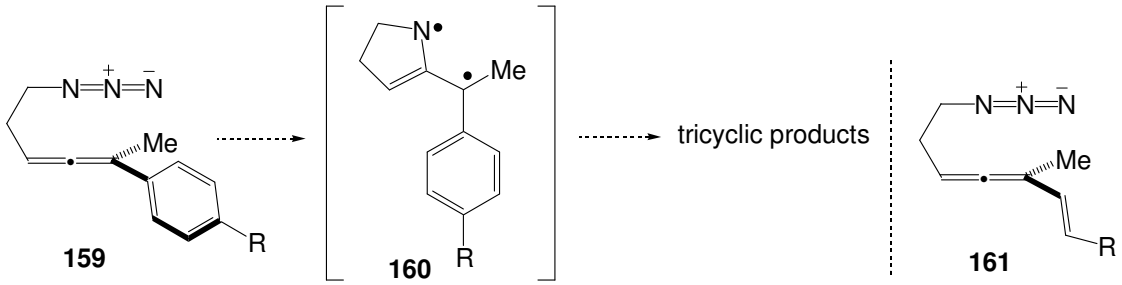

Figure 54: Basic idea on ATMM trapping via intramolecular azide/allene cycoaddition.

4.4.2 Results and Discussion

4.4.2.1 Azidoallene Substrate Synthesis

The feasibility of an intramolecular allenyl azide cycloaddition cascade based ATMM trapping depended on an efficient synthesis of 5-azidoallenes. The synthesis of the cycloaddition precursor **159a** posed little problem and was achieved in 5 steps starting from simple materials. Commerically available acrolein was converted to 2-azidopropionaldehyde using a known procedure.[70] Treatment of the aldehyde **162** with 1-propynylmagnesium bromide followed by protection of the alcohol as a mesylate gave compound **163** in 38% overall yield over two steps (Figure 55). Upon treatment of the mesylate **163** with phenyl zincate (generated from phenylmagnesium bromide and $ZnCl_2$) and catalytic palladium tetrakis(triphenylphosphine) ($Pd(PPh_3)_4$), allene **159a** was obtained as a clear oil in 85% yield.[71]

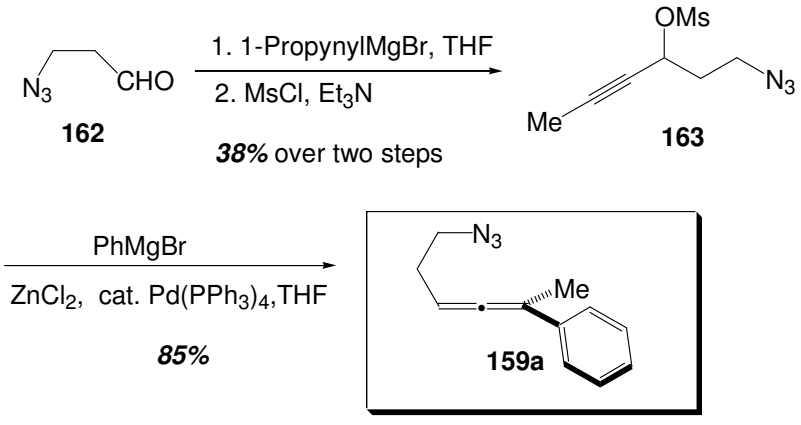

Figure 55: Scheme for synthesis of a phenyl-substituted allenyl azide.

4.4.2.2 Thermolysis of Allenyl Azide 169a

After scouting a number of different solvents and reaction temperatures, it was found that a toluene-d_8 solution (0.07 M) of allenyl azide **159a** in a sealed-tube was transformed to a new product at 100 ℃. Isolation of this product turned out to be an impossible task as exposing the crude reaction mixture to air resulted in conversion to a new product. After analysis and characterization, it was found that this new product was the keto-lactam **165**. Neverthless, analysis of the crude thermolysis solution by ^{13}C NMR prior to air exposure revealed a peak at δ 183 characteristic of an imine carbon. It was thought that if the allenyl azide did indeed convert to the imine **164a** under thermolytic conditions, then it should be possible to intercept the imine with a nucleophile in the absence of air. This plan could be implemented by the addition of the crude imine solution to an excess of TMS-CN. This step gave a new isolable product whose spectral data pointed to the cyanoamine **166a** (Figure 56). The stereochemistry of this product was established by dnOe studies.

The formation of the keto-lactam **164a** can be rationalized by citing a formal addition of molecular oxygen to the enamine **167** in a step-wise or concerted manner to give the oxetane derivative **169**. *Apriori* attempts to trap the enamine tautomer by acylation went unrewarded. Compound **169** would then spontaneously collapses in a retro [2+2] cycloaddition to furnish **165**.

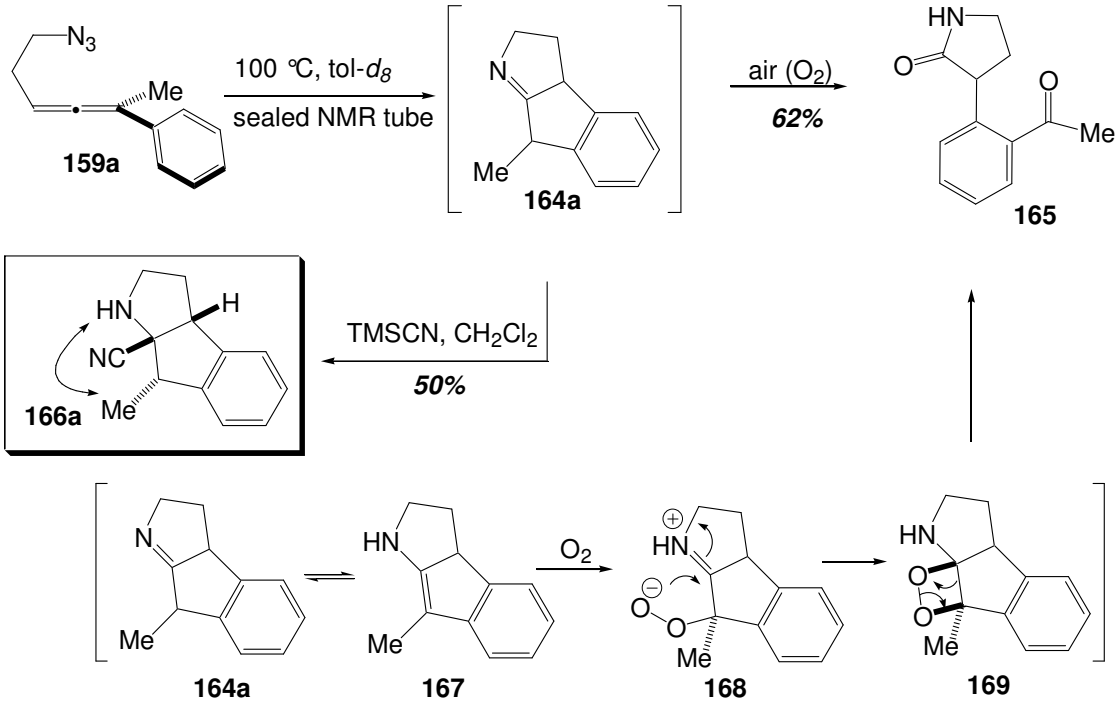

Figure 56: Thermolysis of allenyl azide **159a**.

4.4.2.3 Mechanistic Rationale for Tricyle Formation

The formation of the cyanoamine tricycle **166a** is consistent with the ATMM-based reaction cascade proposed in Figure 57. Mechanistic speculation about this reaction sequence commences with an initial intramolecular allene azide cycloaddition, which generates the regiochemically desired triazoline **170**. Lability of this triazoline **170** prevented its isolation, and spontaneous expulsion of N_2 as per the Quast work delivers the key ATMM diyl intermediate **171**, whose cyclization chemistry finds precedent in earlier work.[61,72] In principle, this ATMM diyl intermediate could cyclize through resonance form **171a** (e.g., at nitrogen) to furnish a pyrrolizidine-type product **174**. That

cyclization through the imine resonance form **171b** is favored might be a reflection of both the stability of the imine function in **171b**, and the greater spin density at carbon in the ATMM diyl construct. Density functional calculations (Spartan, pPB86/DN**) on the parent triplet species **176** suggests that the total spin density is greater on carbon than nitrogen (38% of the total spin density on each carbon, 24% on nitrogen). A zwitterionic resonance form **171c**[73] may also contribute to the structure and chemistry of the putative ATMM intermediate derived from **159a**. This dipolar representation of an ATMM has been invoked to rationalize the [4+3] cycloaddition results obtained by treating either an α-chloroenamine with silver salts, or a methyleneaziridine with a Lewis acid, in the presence of a diene.[74] Calculations on the analogous oxallyl system support the view that **171** is primarily a singlet diradicaloid (on carbon) species with only minor zwitterionic character.[74] An alternate pathway involving a [3,3]-sigmatropic shift on a key closed-shell species **175** can be proposed too, although it seems unlikely by analogy to Quast's observations.[40d] Irrespective of the mechanistic intricacies, this encouraging result prompted further exploration of the scope of this process.

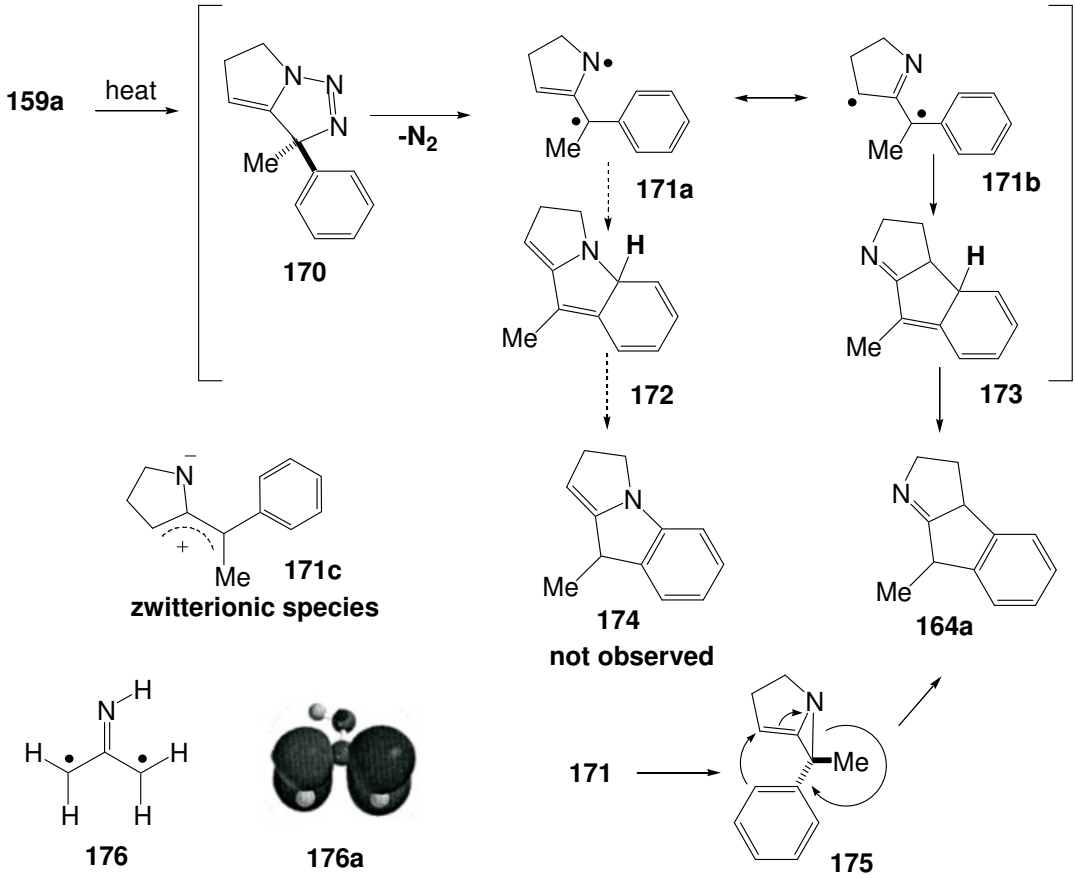

Figure 57: Mechanistic proposal for the formation of tricycle.

4.4.2.4 Exploring Electronic Effects on the Cyclization Reaction Yield

In order to probe the influence of electronic effects on the overall efficiency of this cascade process, aryl-substituted substrates **159b**-**e** were prepared. The allenyl azides **159b-e** were synthesized from the mesylate derivative **163** using commercially available Grignard reagents. Both relatively electron-rich (**159b** and **159c**) and relatively electron-deficient (**159d** and **159e**) aryl rings were examined. The yields for the allene forming step is shown in Table 1.

Table 1: Synthesis of aryl-substitued 5-azidoallenes.

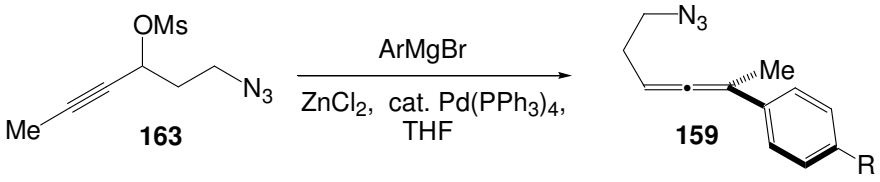

R		Yield(%) of allene
OMe	**159b**	67
Me	**159c**	81
Cl	**159d**	77
CO_2Et	**159e**	63

Thermolysis of the allenes was achieved under previously established reaction conditions, followed by TMS-CN treatment of the crude thermosylate. In all cases the desired pyrrolidinyl cyanide products **166b**-**e** were formed in moderate yield (Table 2). Analysis of the crude thermolysates by ^{1}H NMR spectroscopy revealed that seemingly a single stereoisomer of the imine product was present (5% detection limit) in almost all cases. Some decomposition of the allene under thermolytic conditions was also seen. In the case of allene **159c,** a second stereoisomer was isolated in very minor amounts (9% overall yield). Allene **159b** also showed traces of minor stereoisomer in the crude thermoslyate, however, it escaped isolation post purification. The stereochemical assignments of the major stereoisomers followed from comparison of their ^{1}H and ^{13}C NMR spectral data with those of **166a**, whose stereochemistry was secured by dnOe

spectroscopy, and with those of **166d**, whose structure was assigned unambiguously on the basis of single-crystal X-ray analysis (see **Chapter 6**).

Evaluation of this limited data set suggested that electron rich aryl rings provide product with marginally higher yields. Though it is difficult to pinpoint where the electronic effects play their role in the complex reaction cascade, it can be surmised that formation of the presumably electron-deficient ATMM diyl intermediate **171b** is favored when the attached aryl ring can better satisfy the diyl's electron demand. This hypothesis can also be applied to species **171c** with a contribution of zwitterionic character to the ATMM intermediate (Figure 58).

Table 2: Thermolysis of aryl-substitued 5-azidoallenes.

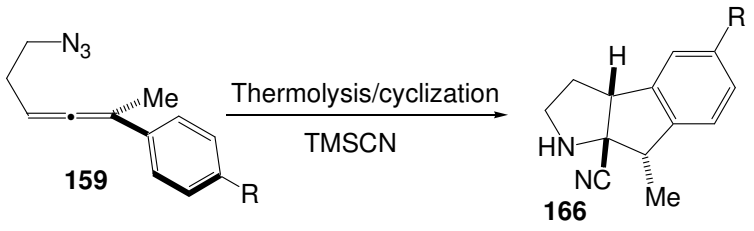

azidoallene **159** R		pyrrolidinyl nitrile **166** yield (%)	
-H	**159a**	50	**166a**
-OMe	**159b**	52	**166b**
-Me	**159c**	63	**166c**
-Cl	**159d**	47	**166d**
-CO_2Et	**159e**	38	**166e**

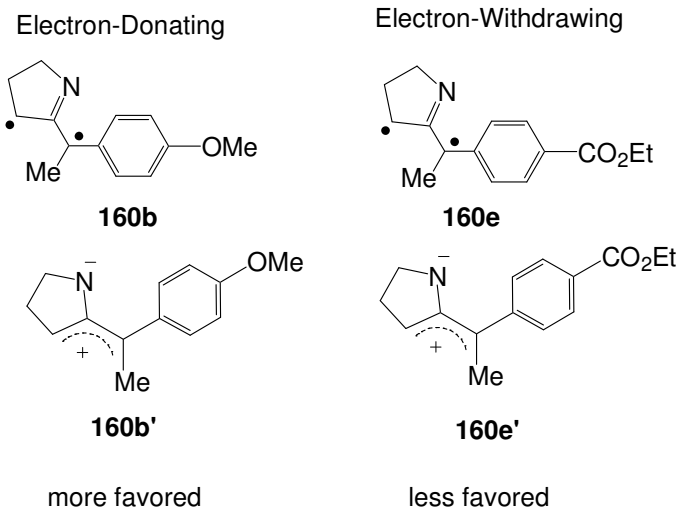

Figure 58: Electronic effects on the diyl formation.

Replacement of the phenyl group with a furanyl group at the allene termini gave the azido allene **177** in modest yield. This substrate underwent the cyclization cascade and TMSCN trapping to give the tricycle **178**, albeit in low yield (Figure 59)**.** This result clearly demonstrated that heteroaromatic groups can also act as suitable traps for the putative ATMM diyl.

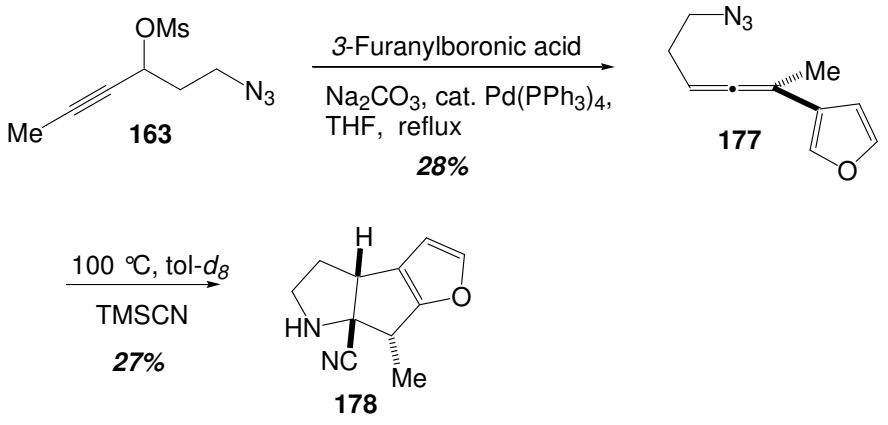

Figure 59: Thermolysis of furanyl-substituted 5-azidoallene.

4.4.2.5 Vinyl Substrates

Strongly encouraged by these results, similar thermolysis studies were performed on the vinyl-substituted allenyl azide substrates **161a-c**. Synthesis of allenylazide **161a** was achieved by applying the standard protocol on mesylate **163**, but now using $ZnCl_2$ and vinyl magnesium bromide as the Grignard reagent of choice. Synthesis of substrate **161b** required a slight modification of the standard protocol. Replacing the alkenic Grignard reagent with *trans*-phenylethenyl boronic acid under $Pd^{(0)}$ catalyzed conditions gave the *E*-allenyl azide **161b** bearing a styryl appendage.[75] Synthesis of vinyl ester allenyl azide **161c** proved to be a little tricky. The *E*-allenyl azide was obtained in low yields from the palladium catalyzed reaction of the mesylate **163** with vinyl ester zincate **179** (Figure 60).[75,76]

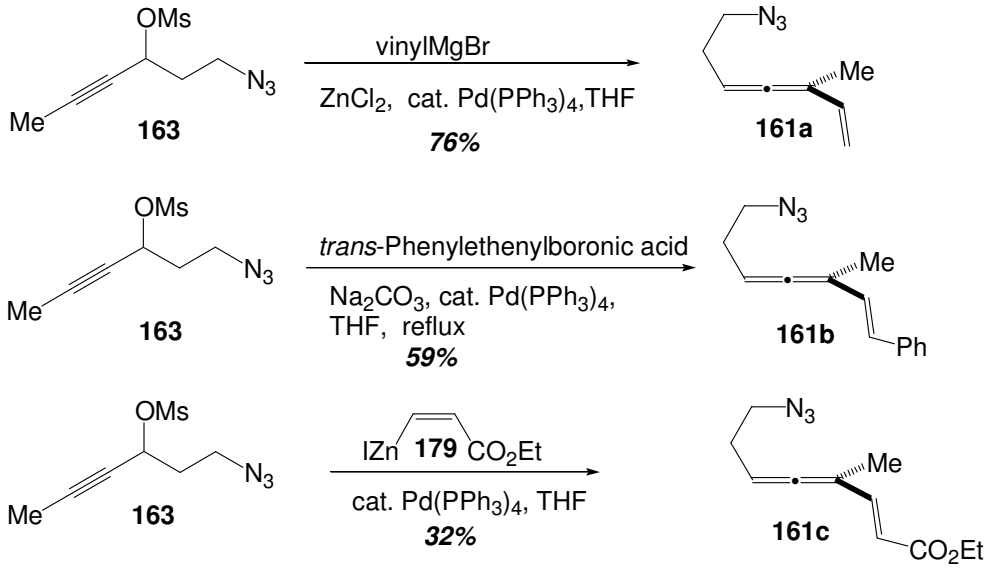

Figure 60: Synthesis of vinyl-substituted 5-azidoallenes.

With the three vinyl allenyl azides with different substituent pattern in hand, the themolysis was attempted as per the conditions previously developed. In this instance, cycloaddition/N_2 extrusion/cyclization furnished high yields of bicyclic products **180a-c**, respectively, with the alkene positioned adjacent to the cyanoamine center, as opposed to the alkene-isomerized versions of the aryl-substituted series (Table 3). This extends the transformation to generation of non-aromatic products. The newly formed secondary stereogenic centers in **180b** and **180c** emerged as single epimers. The assignment as *syn* to the adjacent ring fusion hydrogen was based upon key difference nOe measurements.

Table 3: Thermolysis of vinyl-substituted 5-azidoallenes.

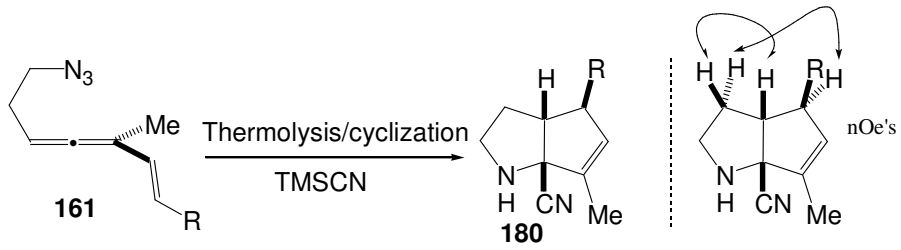

azidoallene **161** R		pyrrolidinyl nitrile **180** yield (%)	
-H	**161a**	96	**180a**
-Ph	**161b**	84	**180b**
-CO_2Et	**161c**	90	**180c**

A model for the evolution of *syn* stereochemistry upon 1,5-pentenediyl closure in a related system has been advanced earlier .[61,77] According to Cohen, stereochemical integrity is largely maintained upon diyl formation and cyclization, indicating that the closure of the bis allylic radical is faster than its equilibriation to the diradical **181b**. Formation of both **180b** and **180c** is in accord with the expectations of that model (Figure 61).

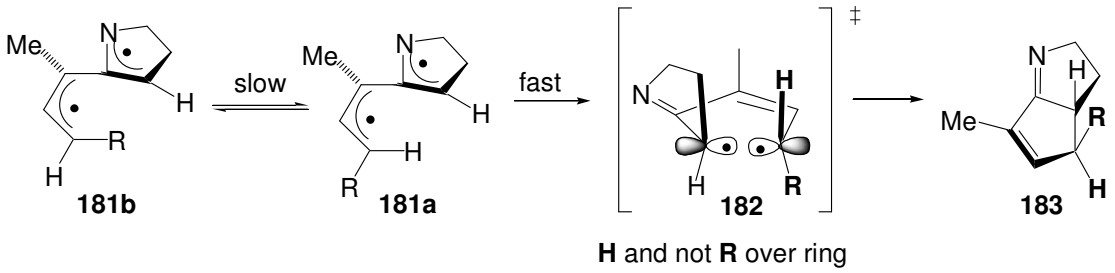

Figure 61: Model to explain the observed stereochemistry.

In summary, a heretofore unexplored cascade cyclization sequence evolving from the thermolyses of allenyl azides has been developed. Incorporation of aryl rings or alkenyl appendages leads to tricyclic or bicyclic pyrrolidine products, respectively, following cyanide trapping of an unstable imine.[78]

4.5 Extension of the Allenyl Azide Cyclization Chemistry

The success of the first intramolecular allenyl azide casacade trapping strategy, based possibly on the intermediacy of ATMM, can open up whole new extensions. C(2)-C(3)-Annelated indoles were thought to represent one potential target class for this chemistry, and given the success of the **159** conversion, wherein only cyclization through the imine species **171b** was observed, it seemed plausible to expect that incorporation of an aryl residue in the allene-azide tether of **161** would lead by analogy to the C(2)-C(3) cyclopentannelated indole products **185** (Figure 62).

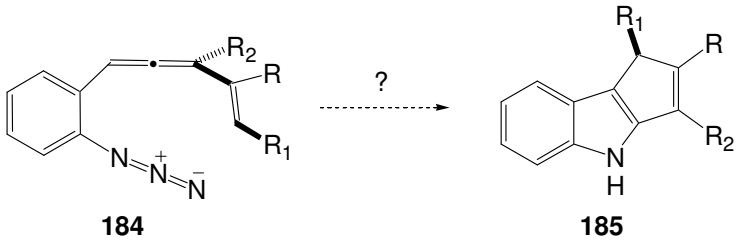

Figure 62: Extension of allenyl azide cyclization chemistry.

This goal was achieved in practice. However, the unanticipated intervention of subtle electronic effects, presumably as a consequence of the electronic connectivity provided by the intervening aryl ring, served to divert some of the reactive intermediate(s) down alternative pathways, leading to N-C(2) annelated products also (Figure 63). A description of the scope of this process for cyclopentannelated indole synthesis with alkenyl- 2-(azidophenyl)allenes will be discussed below.

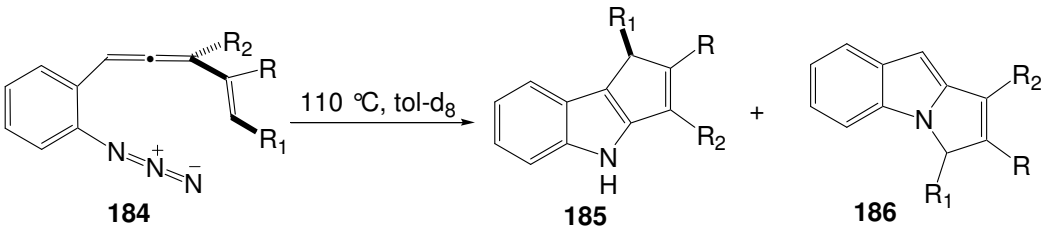

Figure 63: Thermolysis of 2-azidophenyl allenes.

4.6 Results and Discussion

4.6.1 Synthesis of 2-(Azidophenyl)allene substrates

The syntheses of suitable 2-(azidophenyl) allenes of the type **184** were accomplished by straightforward chemistry using Konno's procedure for palladium-mediated (alkenyl)zinc addition to propargylic acetates **188**,[71] or the cuprate-based alternative procedure of Palenzuela.[79] The propargylic acetates were synthesized from 2-azidobenzaldehyde by the step-wise treatment with a Grignard reagent or an alkynyl lithium (**188d-j**) followed by acetate protection of the alcohol (Figure 64).

The azide function attached to the phenyl ring survived exposure to the organometallic reagents without any detectable decomposition. All the allenes synthesized were cleanly isolable and characterizable compounds.

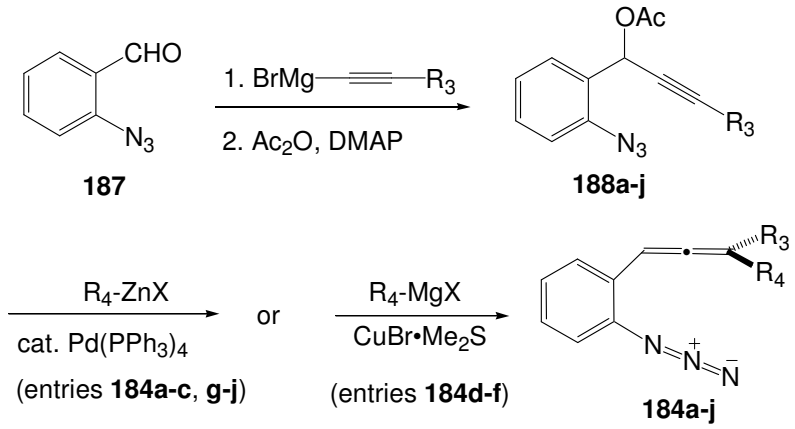

Figure 64: Synthesis of 2-azidophenyl allenes.

The yields of the 2-azidophenyl allenes from corresponding acetates are summarized in (Table 4).

Table 4: Yields for propynyl acetates and 2- azidophenyl allenes.

entry	R_3	R_4	(%) yield **188** (acetate)	(%) yield **184** (allene)
a	Me	H_2C=CH-	48	58
b	Me	H_2C=C(Ph)-	48	67
c	Me	H_2C=C(CH_3)-	48	59
d	PhCH=CH-	Me	47	34
e	1-cyclohexenyl	Me	31	37
f	1-cyclopentenyl	Me	49	30
g	CH_2OTBS	H_2C=CH-	91	55
h	CH_2CH_2OTBS	H_2C=CH-	73	57
i	*t*-Bu	H_2C=CH-	78	63
j	trimethylsilyl	H_2C=CH-	88	21

4.6.2 Thermolysis of 2-(Azidophenyl)allene Substrates

The thermolysis/cyclization studies of allene substrates **184a-j** commenced with the prototype substrate **184a** bearing a methyl group and an unadorned vinyl group. Heating a 0.1 M solution of **184a** in toluene-d_8 led cleanly to the formation of two products. Spectral data clearly suggested the formation of tricyclic products in both cases.

Further chromatographic purification of the crude thermolysate furnished two pure compounds, and their spectroscopic data were completely consistent with those

expected for the anticipated C(2)-C(3) annelated indole **185a** and, surprisingly, the unanticipated pyrrole **189a**. The more polar compound **185a** exhibited the characteristic N-H resonance of an indole (δ 8.03 (s)) as well as signals for an alkene-bound CH_3 (δ 2.22, d, J =1.6 Hz) and for a single alkenyl proton (δ 6.22, m). The faster eluting species displayed spectral data that were comparable to those reported for the characterized reference compound des methyl **189a**,[80] allowing ready assignment of **189a** as a pyrrole. X-ray crystallographic analysis of **189a** also confirmed the structural assignment (see **Chapter 6**). Interestingly, examination of the crude reaction product by ^{1}H NMR prior to purification indicated the presence of only **185a** and compound **186a**; pyrrole **189a** was not formed until exposure of the crude thermolysate to SiO_2. The ratio of isolated **185** to isolated **189** mostly tallied with the **185/186** ratio (Table 5). The ^{1}H NMR-based examination of the crude thermolysate immediately after reaction allowed identification of signals consistent with the indole species **186a**, but these signals disappeared over the course of a few hours as the spectroscopic signature for the pyrrole **189a** grew in.

All the other allenes synthesized in this series were subjected to cyclization under these thermolytic conditions. The ^{1}H NMR-based examination of the crude thermolysate immediately after reaction gave the ratios of the products reported in Table 5**.** The actual ratios of the products **185/189**, obtained after silica-gel or alumina chromatography was occasionally at variance to the observed ratio of products **185/186**. This disconnect could be attributed to the differential stability of products on a silica/alumina gel column. Thus the ratio of **185/186** can be considered as a seemingly accurate picture of the reaction profile (Table 5).

Table 5: Thermolysis of 2-azidophenyl allenes.

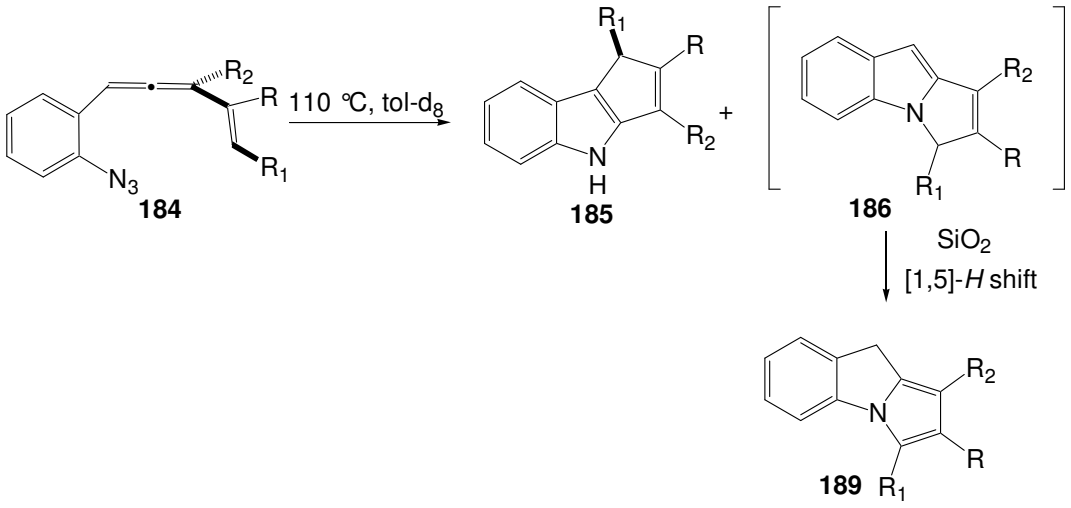

entry	R	R_1	R_2	(%) yield **185**	(%) yield **189**	ratio **185**/**186**
a	H	H	Me	40	56	1:1.2
b	Ph	H	Me	40	30	1:1.2
c	CH_3	H	Me	36	36	1:1.3
d	H	Ph	Me	-	35 (**186d**)	1:1.1
e	$-(CH_2)_4-$		Me	36	51	1:1.4
f	$-(CH_2)_3-$		Me	-	40 (**186f**)	1:1.5
g	H	H	CH_2OTBS	22	29	1.2:1
h	H	H	CH_2CH_2OTBS	52	43	1.5:1
i	H	H	*t*-Bu	57	20	2.7:1
j	H	H	TMS	-	-	-

In only a few allene cases (**184d**, **184i**) was the N-C(2) cyclopentannelated indole isolable, but even in those instances, isomerization into the pyrrole followed after a few more hours at room temperature. The entries (**184b**,**c**) test the effect of a substituent at the internal (R) position of the alkene. For both substrates, the reaction proceeded similarly to the simpler (**184a**, R=H) cases to afford nearly equal mixtures of the indole **185b/185c** and pyrrole **189b/189c** products. The Ph-bearing substrate **184d** introduces at the alkene terminus a group that might confer both electronically favorable (i.e., radical stabilizing) and sterically unfavorable characteristics, and the tradeoff between these possibly opposing effects appears to favor the latter. The C(2)-C(3) cyclized indole product in this case did not survive attempted chromatographic purification, and the regioisomeric N-C(2) indole **186d** was the only identifiable species isolated. However, the indole **185d** was detected in the crude thermolysate admixed with **186d** permitting the measurement of the product ratio. Hydrogenation of **186d** (Figure 65) furnished the *cis*-disposed indole product whose structure was secured by single-crystal X-ray analysis.

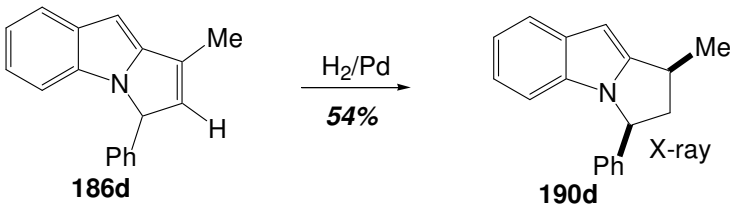

Figure 65: Hydrogenation of **186d**.

The next two examples, **184e** and **184f**, probed the capability of this cascade cyclization sequence to deliver tetracyclic material. The cyclohexenyl case **184e**

proceeded uneventfully to deliver a slightly biased mixture of the pyrrole **189e** and the indole product **185e** in excellent overall yield. The cyclopentyl lower homologue **184f**, in contrast, yielded only a moderate amount of the N-C(2) cyclized indole product **186f** as the only tetracyclic material to survive chromatography. The corresponding C(3)-cyclized material **185f** was observed in the crude thermolysate's ^{1}H NMR spectrum, at the ratio reported in Table 5, but it decomposed upon attempted purification. In all the above examples with R_2 = methyl, the cyclization proceeded with a slight bias toward the N-C cyclized indole product **189**.

Examples **184g-j** involved the testing of allenes where R_2 is sterically more demanding than methyl. The results demonstrated that both silyl ethers (**184g**, **h**) and steric bulk (**184i**) at the R_2 position are tolerated in the transformation with little impact on yield. Interestingly, comparing entries **g-i** reveals that the ratio of C/N cyclization is responsive to the size of the R_2 substituent, with the bulkiest entry (**184i**, R_2 = *t*-butyl) leading to the greatest selectivity for the desired C-C cyclization regioisomer **185**. The R substituent resides at a position that apparently exerts little steric or electronic influence on the course of the reaction, as both the R = Me and R = Ph cases proceed to product(s) in very similar yields/selectivities.[81]

The allene substrate bearing the TMS group (**184j)** was unique in that it did not yield either the C(2)-C(3) indole product or the pyrrole product analogous to **185** or **186** Instead a compound bearing an unreacted vinyl appendage was obtained. Spectral analysis showed that the silyl group was no longer part of the product and further analysis pointed to the formation of the triazole **192**. Formation of the triazole from the allene can be rationalized as proceeding through a protodesilylation intiated by adventitious acid.

Loss of the TMS group precedes the extrusion of nitrogen and hence the expected ATMM chemistry is not expressed (Figure 66).

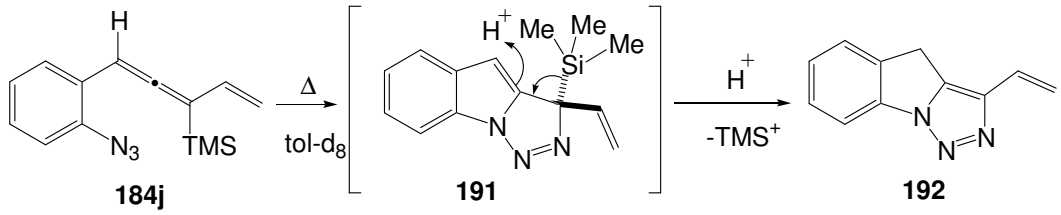

Figure 66: Rationalization for the formation of product **192** from allene **184j**.

4.6.3 Mechanistic Insights

A mechanistic outline similar to the conversion of **159** to **166** can be proposed here (Figure 67). The reaction sequence begins with an intramolecular [3+2] cycloaddition of the azide to the allene to form the triazoline **193**, followed by the expulsion of nitrogen to possibly give an ATMM diyl, which cyclizes into the appending alkene. However, the formation of two products in roughly equal ratios points to a possible divergence in the mechanistic progression. In light of the similarities and the differences between the reactions of the diyls derived from **159/161** and **184**, it is fitting to consider the conceivable roles that the different candidate diradicals or closed shell species might play in product formation.

Interesting and unanticipated results emerged from the computational studies performed by collaborators López and Faza[82] in considering the possible pathways for the formation of the indole products **185** and **186** from the triazoline **193**. Three possible mechanistic courses were envisioned:

(1) Single C-N or N-N bond scission to furnish intermediate diazo radicals **194** and **194a** respectively, followed by loss of nitrogen to deliver the singlet diyl **195**. This diyl could cyclize directly via either a clockwise rotation to give C-C bonded product **185** or in a counterclockwise direction to furnish the C-N bonded product **186**.

(2) Rotation of bond *a* within **195** but sans bond formation would momentarily convert the diyl into closed shell indolidenes (*E*)-**196** and (*Z*)-**196**, which then might electrocyclize to the observed products **185** and **186**, respectively.

(3) Concerted elimination of dinitrogen from **193** to afford the indolidenes (*E*)-**196** and (*Z*)-**196** directly, en route to **185** and **186.**

Transition states for C-N bond cleavage from **193** and concerted loss of N_2 from this same substrate were located by CASSCF (complete active space self-consistent field) calculations. Attempts to identify a transition state corresponding to N-N cleavage with **193** led instead to the same concerted transition state found above. The computational results indicate a strong bias towards concerted loss of N_2 from **193**. $\Delta G^{\ddagger}$ = 17.4 kcal/mol for direct **193** → **196** conversion, and $\Delta G^{\ddagger}$ = 25.0 kcal/mol for **193** → **194**.

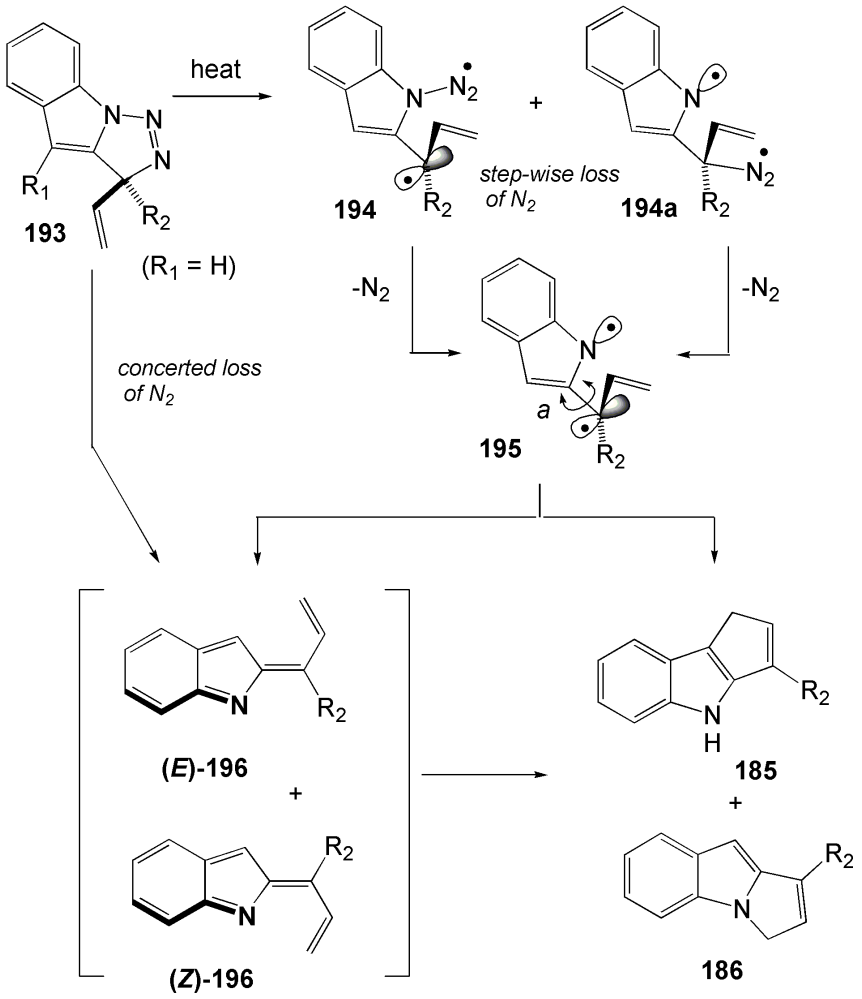

Figure 67: Mechanistic proposal for cyclization of 2-azidophenyl allenes .

The relatively lower activation barrier for concerted loss of N_2 from **193a** was somewhat surprising, given that this transformation should correspond to a formally disallowed [10π + 2π] thermal, suprafacial pericyclic retrocycloaddition in the Woodward-Hoffman designation. The key to understanding this apparent divergence from the time-tested Woodward-Hoffman rules lies in appreciating the orthogonal disposition of the scissile C-N and N-N bonds with the remaining π system in **193a**.

Calculations obtained from the computational techniques ACID (anisotropy of the current *i*nduced density) and NICS (nucleus independent chemical shift) for the concerted elimination of N_2 from**193a** indicate there is virtually no electron density "flowing" between the N=N fragment and the remainder of the (orthogonal) π system.[83] Thus, these calculations suggest that there is no electronic communication between the two halves (N_2 and indole fragment) as the C-N bond cleaves in a concerted manner. This result is in complete contrast to the results of a similar calculation performed on a stereotypical Diels Alder reaction. The cycloaddition between butadiene and ethylene reveal a constant "flow" of electronic communication between the reacting partners. For the present case, it can be assumed that, as the transition state is surmounted, rotation of bond *a* within **193a** can occur, bringing the two electronic halves into conjugation. This "non-least-motion" type of mechanistic pathway, seen in the chemistry of carbenes, then can deliver the closed shell species (*E*)-**196** and (*Z*)-**196**, and finally the observed products **185** and **186**. Clearly, the lack of electronic communication between the two unsaturated fragments at the transition state for bond cleavage places the present case outside of the Woodward-Hoffman realm.

4.6.4 Effect of Steric Bulk on the Cyclization Ratio

The thermolysis of 2-azidophenyl allenes resulted in cyclization products obtained from C-C as well as N-C bond formation. Interesting trends emerged from the roster of allenes examined. In the cases where R_2 = Me, the cyclization products favored the ratio for N-C bond formation resulting in **186** over C-C bond formation giving **185**.

The N-C/C-C product formation ratio was reversed when R_2 was an alkyl group other than a methyl group. This trend can be rationalized as shown in Figure 68. The transition state of the cyclization cascade shows a key steric interaction between groups R_1 and R_2 in structure **195a**. It can be expected that with R_1 = H, as the size of R_2 increases the formation of **(*E*)-196** which places R_1 and R_2 farther away from each other should be preferred over **(*Z*)-196**. This is consistent with the observed results for the allenes examined in Table 5. The selectivity for the C-C /N-C product formation was the greatest (2.7:1) when R_2 = *t*-butyl. It remains to be seen if this steric interaction can be further exploited to induce much better selectivities in the future.

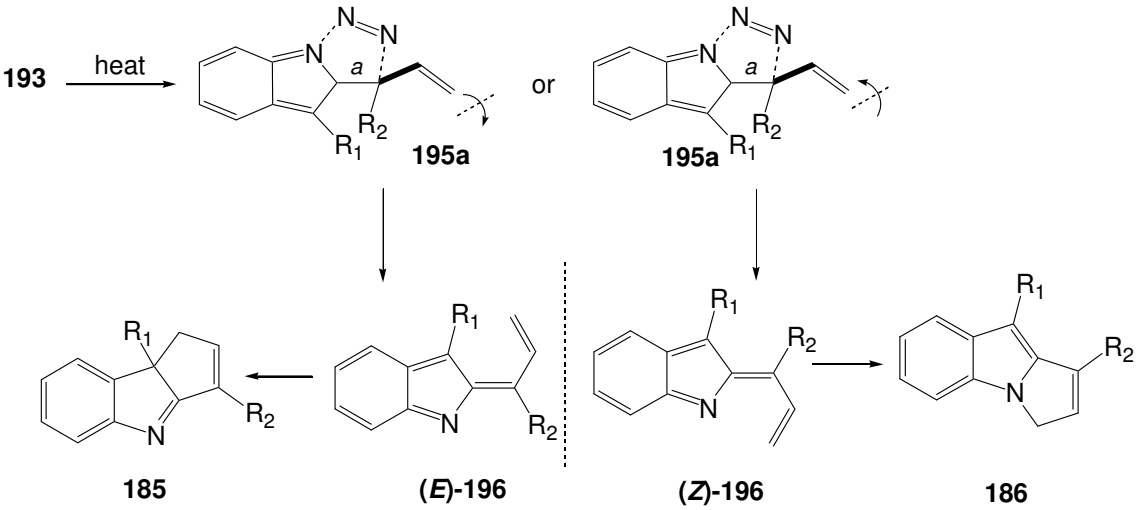

Observed Results

R_1	R_2	C-C/N-C ratio
H	Me	1:1.2
H	CH_2CH_2OTBS	1.5:1
H	*t*-Bu	2.7:1

Figure 68: Effect of steric bulk on the cyclization ratio.

4.7 Summary and Conclusions

Allenyl azides bearing aryl or alkenyl appendages have been utilized in the synthesis of bicyclic and tricyclic compounds. These polycyclic compounds are proposed to result from a reaction cascade that initiates with an intramolecular [3+2] dipolar cycloaddition of the azide to the allene. This cycloaddition is followed by the formation of a putative azatrimethylenemethane (ATMM) diradical, which subsequently cyclizes through the alkene/aryl unit. All substrates delivered a pyrrolidinyl nitrile after TMSCN trapping of the first-formed imine, in moderate yields. An array of electronically differing substituents on the phenyl ring was examined. It was observed that the cyclization yields were typically higher for electron rich groups on the phenyl ring. The cyclization/cascade was demonstrated to work successfully even in a heteroaromatic (furan) bearing allenyl azide. Further, replacement of the aromatic groups with vinyl appendages afforded entry into bicyclic 5-5 ring systems, this time in excellent yields for the substrates tested. In an extension of this strategy, introduction of an aryl ring between azide and allene gave access to indole products under similar thermolytic conditions. This strategy also resulted in the formation of pyrrolo-indole products. A roster of azido-phenyl allenes was synthesized to study the effect of sterics on the cyclization cascade. Of the substrates tested, it was observed that sterically demanding groups on the allene terminus favored the formation of C-C cyclopentannelated products over the pyrrolo-indole N-C cyclized products. The cyclization cascade of the azido-phenyl allenes proceeded in good yields and the overall yields of the cyclization remained largely unaffected by the substituents' steric bulk.

The above mentioned cyclization cascasdes are the first examples of productive utilization of putative ATMMs in synthesis. At this point, no direct experimental support is available to sort out the various intermediates proposed in the mechanistic hypothesis. However calculations performed by López et al., have provided a theoretical framework to rationalize the product formation.

As it stands, future work and results should help understand these conversions in a better light. Nevertheless, the cycloaddition/cyclization cascade protocols developed are expected to be of high value in the construction of nitrogen-containing natural product architectures. This area of research abounds with opportunities for further development.

Chapter 5

Allenyl Azide Cycloaddition Chemistry: Approach Towards a Model System for (±)-Meloscine

5.1 Overview

Intramolecular allenyl azide cycloaddition chemistry offers opportunities for the rapid construction of bicyclic and tricyclic nitrogen-bearing compounds. This trait can be especially useful in the synthesis of alkaloids. The natural product (±)-meloscine might be a good candidate to explore the potential of the allenyl azide cyclization cascade in this context. Towards that end, a route for the total synthesis of meloscine was designed. The present **Chapter** details the various approaches towards a model system for the target natural product.

5.2 Isolation Studies on Meloscine

The isolation of meloscine was first reported by Weiss et al in 1969[85]. The Apocynaceae *Melodinus scadens* Forst yielded three new alkaloids (+)-meloscine (**197**), (+)-epimeloscine (**198**) and (+)- Scandine (**199**) (Figure 69).[85] These alkaloids were reported to be structurally related to the *Aspideosperma* alkaloids. A characteristic of the genus Melodinus of the Apocynaceae family is the presence of a rare type of indole alkaloids, where the ring B has expanded to become six membered with a concomitant

contraction of the ring C, meloscine being the prototype.[86] Studies on the biological activity of meloscine have not been reported to date.

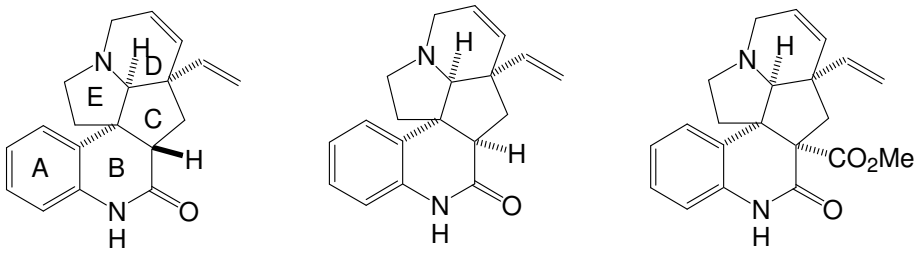

(+)-meloscine **197** (+)-epimeloscine **198** (+)-scandine **199**

Figure 69: Alkaloids from *Melodinus scadens*.

5.3 Synthetic Approaches to Meloscine

The only total synthesis of meloscine (as the racemate) was reported by Overman and co-workers in 1991.[87] An asymmetric approach to the core structure of *Melodinus* alkaloids was reported by Schultz and co-workers.[88] A laboratory success of the proposed biosynthetic pathway to (+)-meloscine from the related alkaloid tabersonine (ca. 2% yield) has also been reported.[89]

5.3.1 Biomimetic Synthesis

The tetrahydroquinolone *Melodinus* alkaloid meloscine (**197**) was proposed to result from an oxidative rearrangement of Δ^{18}-tabersonine (**200**) (Figure 70).[85] This proposal had no successful *in vitro* correlation until the laboratory conversion attempted by Lévy and co-workers. Prior to the work by Lévy, Palmisano[86] had published a partial

synthesis of tetrahydromeloscine **205** through the rearrangement of the **201**, which was obtained from vincadifformine (Figure 71).[90]

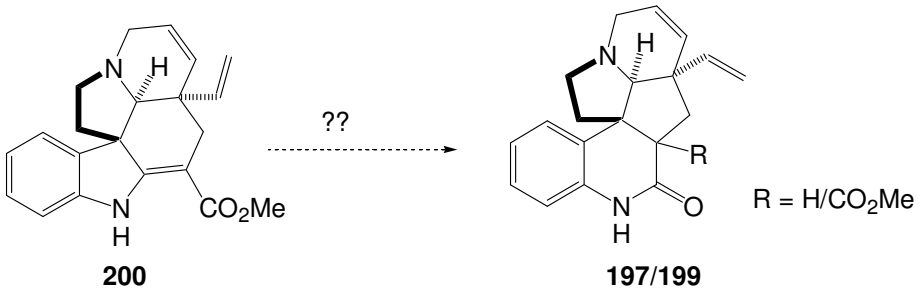

Figure 70: Biosynthetic proposal for meloscine.

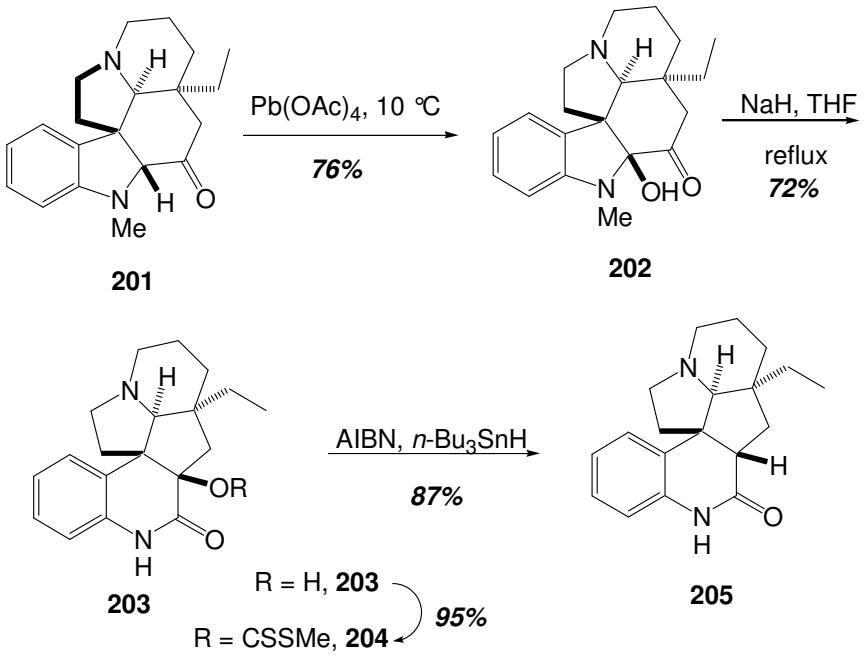

Figure 71: Palmisano's attempt at meloscine biosynthesis.

In their route, Lévy *et al*., began the synthesis from **200**, which was obtained from vindoline (Figure 72).[91] Δ^{18}-tabersonine (**200**) was first oxidized to the unstable 16-chloroindolenine **206**, which was then reduced using $NaBH_3CN$ to the aziridine **207**.[92] Flow thermolysis of **207** was conducted in MeOH-PhMe (2:1) with a ca. 500 ℃ heated glass fitted column.[93] This procedure allowed recovery of **207**, regeneration of **200** and isolation of imine **208**. Selective oxidation of imine **208** was achieved by using Jones reagent at -10 ℃ for 30 min, which allowed a 35% conversion to scandine (**199**). Decarbomethoxylation gave meloscine (**197**), identical to the reference material.

This synthesis of meloscine and scandine from Δ^{18}-tabersonine (**200**) was thought to mimic the biotransformations of the *Aspidosperma* precursors.

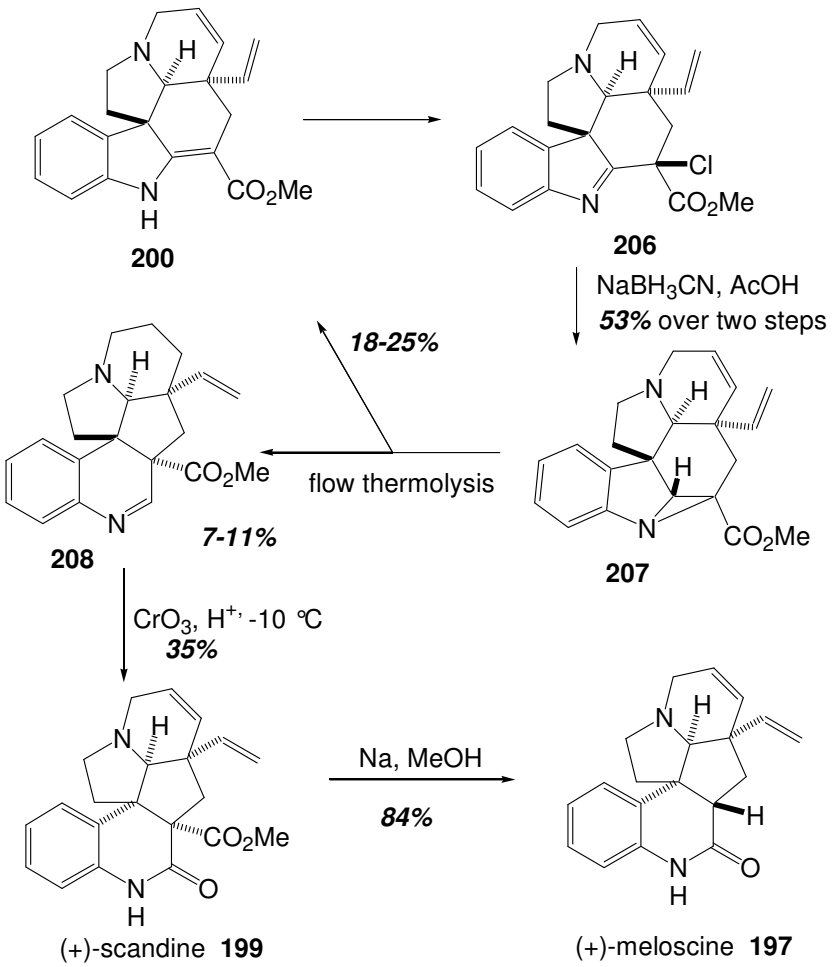

Figure 72: Biomimetic synthesis of meloscine by Lévy *et al*.

5.3.2 Total Synthesis of (±)-Meloscine: Overman *et al*.

The basic strategy developed by Overman is presented in the retrosynthetic format in Figure 73. Overman visualized a Wolff-ring contraction of **210** to access the melodinus ring system. The key 9a-arylhydrolilolidine intermediate **210** was envisaged to

arise by tandem cationic aza-cope rearrangement-Mannich cyclization of formaldiminium ion intermediate **211**.[87]

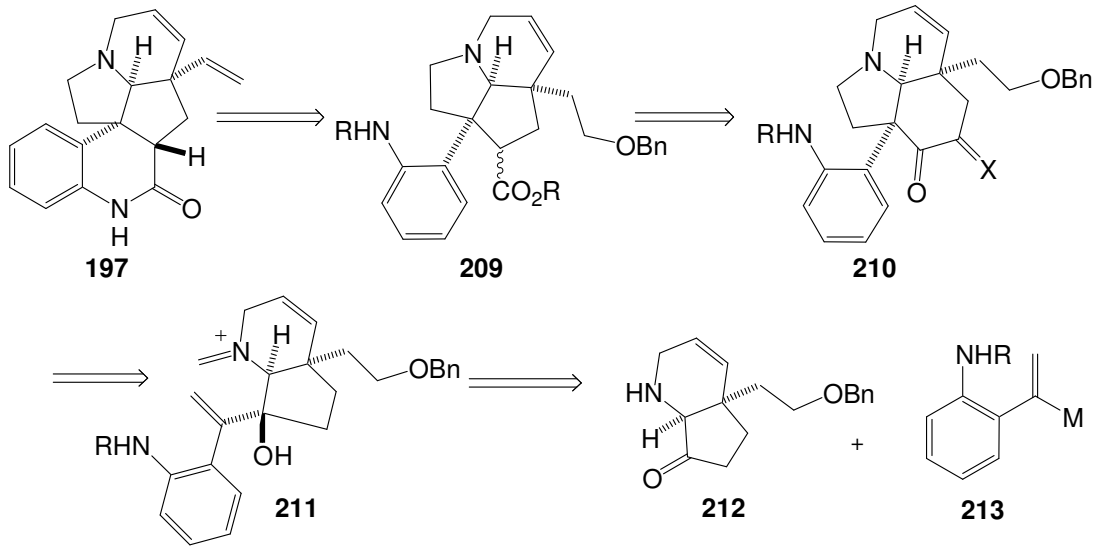

Figure 73: Retrosynthetic strategy for meloscine by Overman et al.

The allylic alcohol functionality of the key intermediate **211** was developed by combining a bicyclic ketone and a styrenyl nucleophile. Thus, the *cis*-hexahydro-*7H*-1-pyridin-7-one **214** was assembled on a preparative scale in 13 steps and 11% overall yield from readily available ethyl 2-oxocyclopentaneacetate.[94] Coupling of **214** with the dianion of trimethylsilyl cyanohydrin **215**[95] under carefully controlled conditions provided the desired tricyclic carbamate **216** as a single stereoisomer. Olefination of **216** followed by selective hydrolysis of the cyclic carbamate gave the desired aza-Cope rearrangement precursor **218** in 78% yield (Figure 74). Treatment of pyrindinol **218** with paraformaldehyde and camphorsulfonic acid in refluxing benzene for 3-5 h facilitated the aza-Cope-Mannich rearrangement to afford the crucial tricyclic ketone **219** in 82% yield.

The ring contraction was effected using the α-diazo ketone **220** under photolytic conditions to afford two epimeric esters in a ratio of 4:1 and in excellent overall yield. Treatment of either of the esters **221** with a large excess of KOH in EtOH/H_2O (6:l) at 0 ℃ followed by slow warming to 150 ℃ over a 24 h period gave the desired pentacyclic amides **222** in 95% yield and a ratio of ca. l0:1, respective1y for the favored isomer.

Elaboration of the major pentacyclic amide **222** to (±)-meloscine **197** was straightforward. Debenzylation of **222** followed by tosylation of the resultant alcohol (16 h) afforded the primary tosylate **223** in 96%. Formation of the selenide **224** was effected in 58% which was followed by oxidation and addition of Me_2S and Et_3N and warming to room temperature provided (±)-meloscine in 81% yield as a colorless solid.

This synthesis by Overman and co-workers although lengthy (24 steps 3-4% overall yield), showcased the utility of tandem cationic aza-Cope rearrangement-Mannich cyclization reactions as key elements of alkaloid synthesis design.

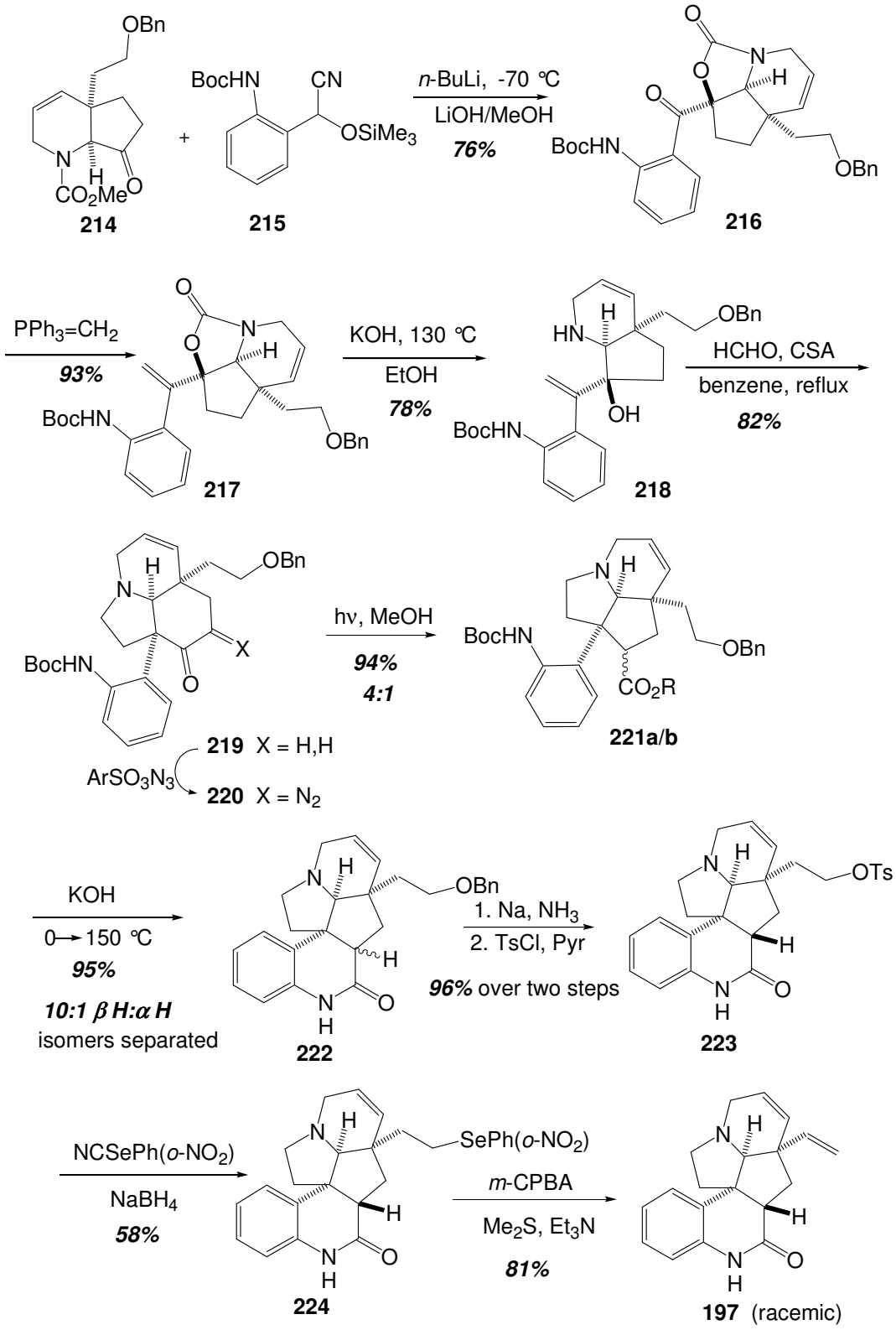

Figure 74: Synthesis of meloscine-Overman *et al*.

5.3.3 Asymmetric Synthesis of (+)-Meloscine Core Structure: Schultz *et al*.

Schultz and co-workers [88]described an asymmetric synthesis of the meloscine core structure **242** by utilization of the asymmetric Birch reduction-alkylation **225** → **226** to establish absolute configuration at C(20) of the alkaloid and the Mannich cyclization **232** → **233** to provide the *cis*-pyrindin-6-one ring system.[96] An important strategic element of this approach was an early incorporation of the aromatic ring in **197** as the 5-benzyl substituent in **225**.

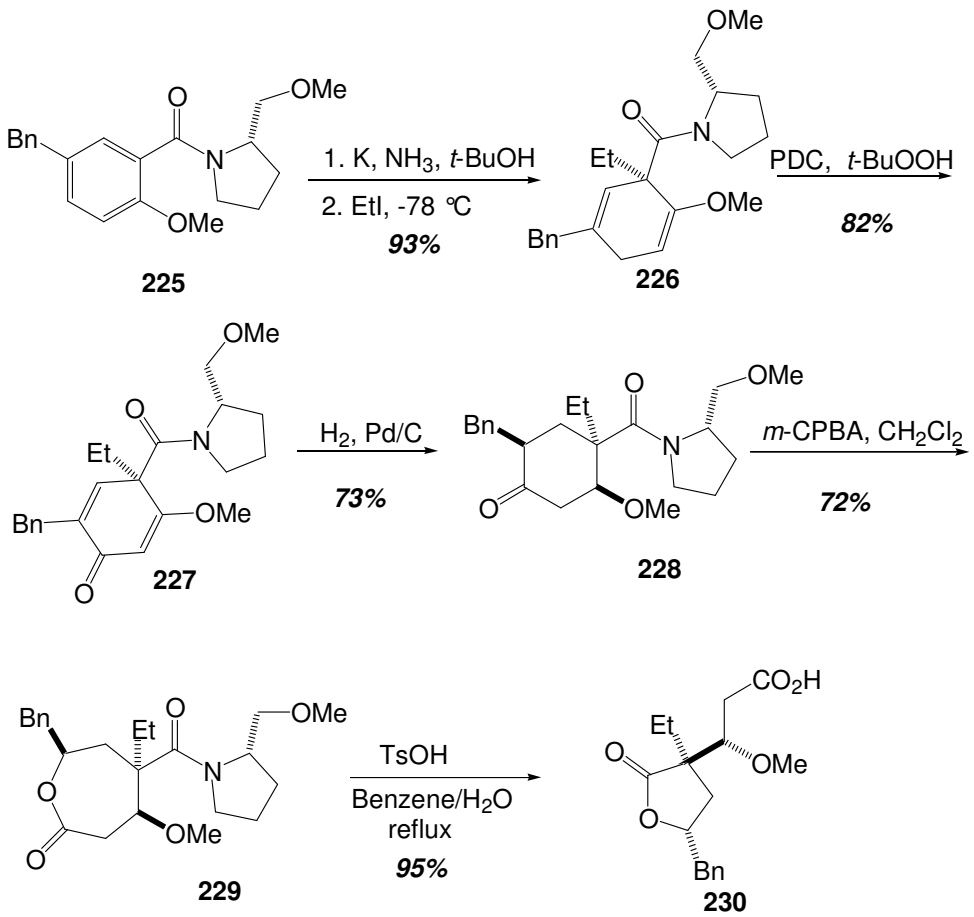

Figure 75: Schultz route towards meloscine core.

The synthesis commenced with the reduction of the chiral benzamide.[97] with potassium in NH_3, at -78 °C followed by consumption of excess metal by the addition of piperylene, and then alkylation of the amide enolate with EtI gave the 1,4-cyclohexadiene 3 in 93% yield (Figure 75). Bis-allylic oxidation of **226** provided the 2-benzyl-5-methoxy-2,5-cyclohexadien-l-one **227**, which was efficiently converted to butyrolactone **230** as shown in Figure 75.

Conversion of the carboxylic acid group in **230** to the amide **231** was achieved by coupling with allyl amine. This was followed by reduction of the lactone in **231** to the corresponding diol with LiBH4; Swern oxidation of the diol gave the key Mannich cyclization substrate **232.** Treatment of **232** with triflic acid afforded the *cis*-pyrindin-6-one **233** in 72% yield. Oxidative cleavage of the N-allyl group in **233** gave the keto aldehyde **234**. Acid-catalyzed cyclization of **234** gave **235** as an inconsequential mixture of alcohol diastereomers in 66% overall yield. Deoxygenation of the hydroxyl group in **235** was accomplished by reduction of the intermediate (thiocarbonyl)imidazolide[98] with *n*-Bu_3SnH in refluxing benzene to give the core structure of the *Melodinus* alkaloid in 70% overall yield from **235** (Figure 76). (+)-Meloscine was expected to be available by utilization of a derivative of **225** containing a modified 5-benzyl substituent.

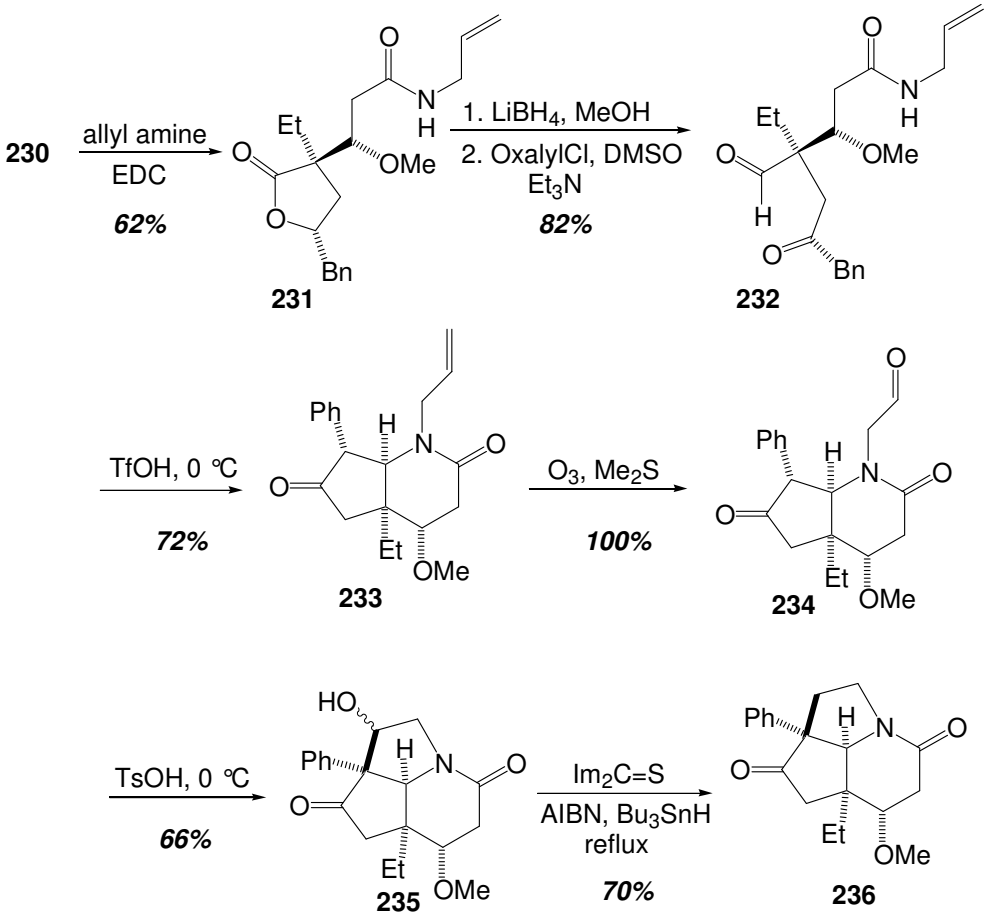

Figure 76: Completion of meloscine core-Schultz *et al*.

5.4 Contributions from Feldman's Laboratory

The successful development of an ATMM-based intramolecular allenyl azide cascade cyclization methodology led to synthetic efforts toward (±)-meloscine. It was thought that the core 5-5 fused ring system can be accessed via the allenyl azide transformation chemistry. Herein, the detailed approaches toward a model system for (±)-meloscine are discussed.

5.4.1 Retrosynthetic Analysis

The basic strategy is outlined in a retrosynthetic fashion in Figure 77. The heart of the synthetic plan is the stereocontrolled assembly of the functionalized compound **239** based on the allenyl azide cycloaddition protocol developed earlier. It was envisaged that the tricyclic structure **239** can arise from the thermolysis of the allene **240**, which in turn can be generated from 2-nitrobenzaldehyde **242** using known chemistry. Further manipulation of the tricyclic key precursor to deliver meloscine would depend on the alkyl substituent on the allene terminus. To test the feasibility of the approach, the proposed synthetic plan was to be tested using a simple methyl group at the allene terminus.

The cyclohexane of meloscine was planned for attachment via a palladium mediated Heck-Coupling of the tetracyclic precursor **237**. The lactam formation in **238** was to be achieved by the reduction of the nitro group followed by amide bond formation (Figure 77).

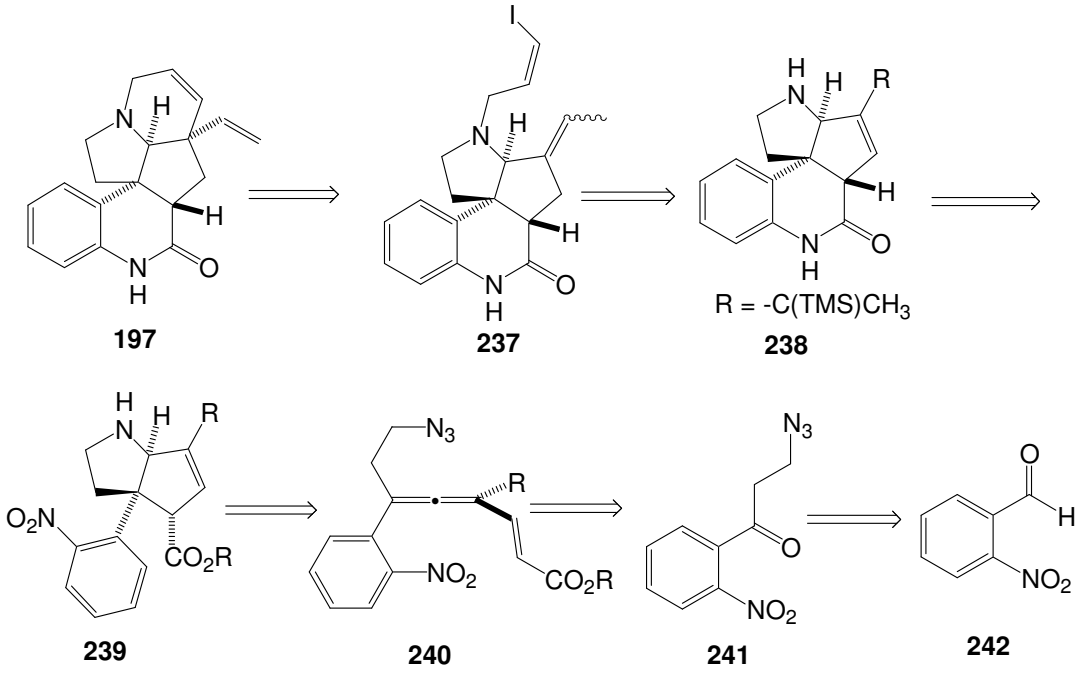

Figure 77: Retrosynthetic strategy towards meloscine.

5.4.2 Results and Discussion

5.4.2.1 Synthesis of Key Substrate

The synthesis commenced with the initial goal of testing the cyclization on the simpler vinyl allene **245** before proceeding to the vinyl ester allene **240**. Toward that end, 2-nitrobenzaldehyde was converted to the known vinyl ketone **243** by a step-wise addition of vinyl magnesium bromide and oxidation of the obtained secondary alcohol.[99] Conjugate addition of sodium azide to **243** afforded the azido ketone **241**. Addition of 1-propynyl magnesium bromide followed by treatment of the alcohol with Ac_2O/DMAP yielded the acetate **244** as a brown viscous oil. Conversion of the acetate **244** to the allene

cyclization precursor was achieved by using vinyl magnesium bromide, $ZnCl_2$ and catalytic $Pd(PPh_3)_4$. However allene **245** proved to an unstable entity and was susceptible to decomposition within minutes at room temperature (Figure 78). The fleeting nature of the allene permitted acquisition of only limited characterization data. Attempts to carry out the cycloaddition/cyclization on this allene either as a pure compound or on crude material were unsuccessful and led only to decomposition products. It is unclear at present why the presence of the nitro foiled this chemistry. Perhaps its proximity to the allene led to unwanted cyclization reactions not involving the azide formation (Figure 79).

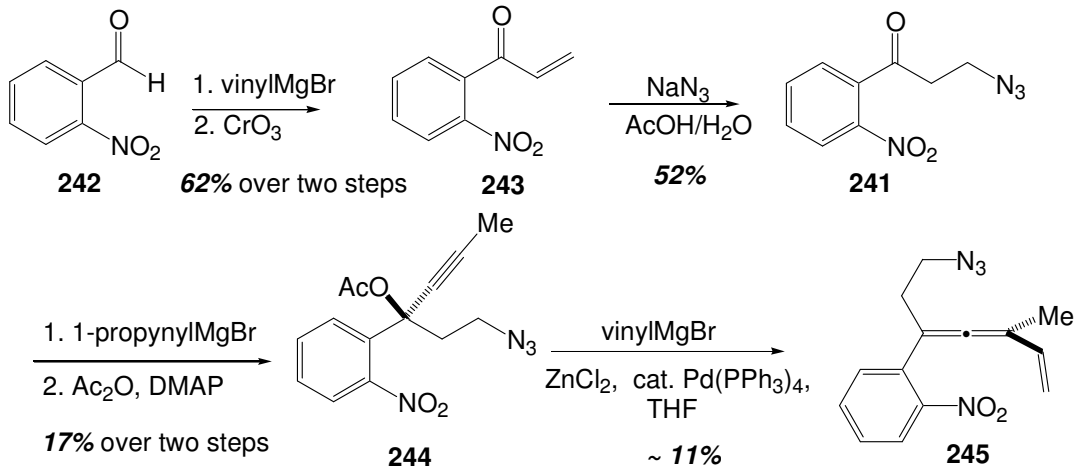

Figure 78: Synthesis of nitro-allene **245**.

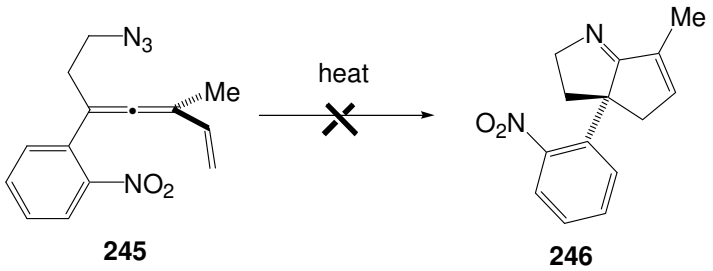

Figure 79: Cyclization attempt on nitro-allene **245**.

5.4.2.2 Modification of the Allene Substrate

In an effort to tune the stability and/or reactivity of the nitrogen substituted allene precursor, substrates with protected amino groups, **248** and **249**, were investigated as cyclization precursors.

Intial investigations on the diBoc-protected amino starting material **248** and **249** revealed the lability of the Boc-group to survive acidic manipulations (Figure 80). Various manipulations of the alcohol substrate **249** resulted in the loss of one of the Boc

protecting group (see **Chapter 6**). As a result of this development, the allene substrate **253** bearing a mono Boc-protected amino group was targeted for synthesis and subsequent cyclization.

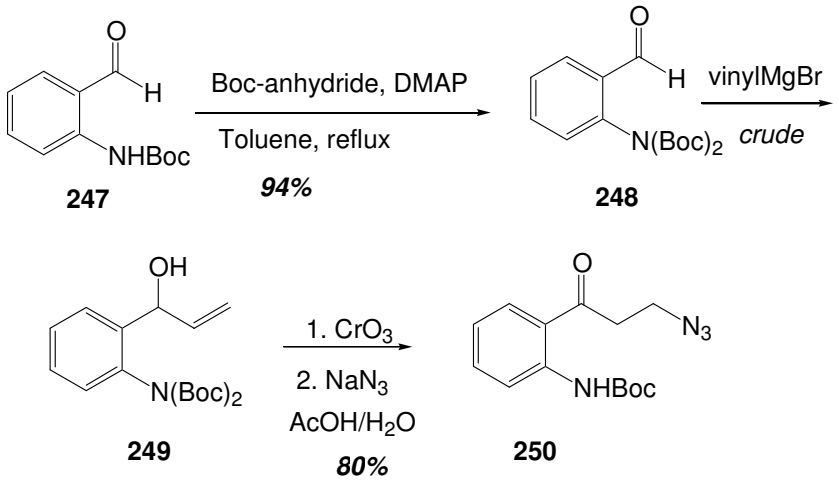

Figure 80: Di-Boc protected precursors.

Synthesis of the cyclization precursor followed along the same lines as the precursor bearing the nitro group. The known aldehyde **247**[100] was converted first to the vinyl alcohol, which was then oxidized to furnish the ketone **251**. Addition of sodium azide to **251** under acidic conditions furnished the azido ketone **250**. Treatment of the ketone **250** with 1-propynyl magnesium bromide followed by acetate protection of the alcohol product afforded the alkyne **252**, which was processed on to the allene **253** by simple treatment with vinyl magnesium bromide/$ZnCl_2$ under catalytic Pd $^{(0)}$ to furnish the key allene in moderate yield (Figure 81).

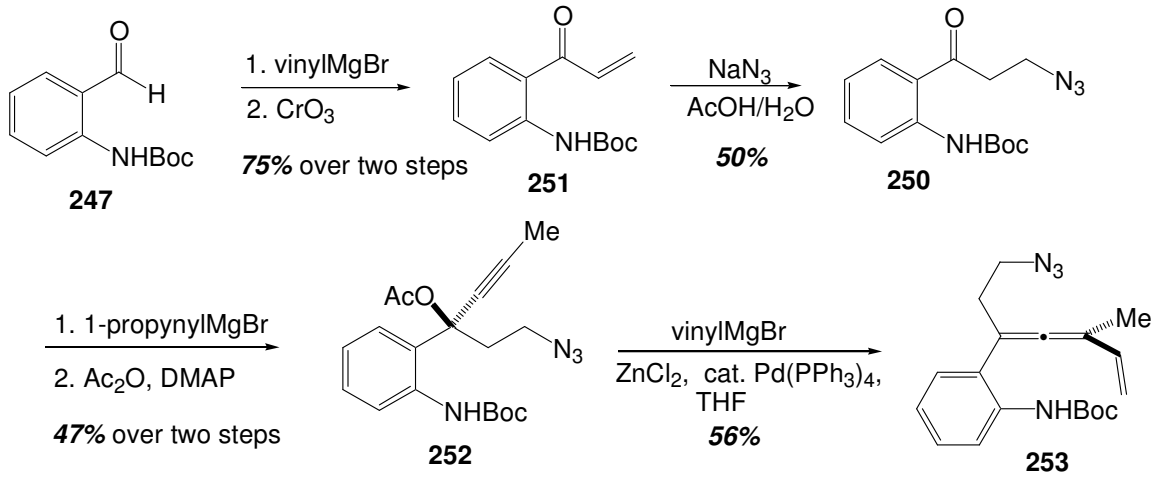

Figure 81: Synthesis of mono-Boc protected amino allene.

5.4.2.3 Cyclization of the Allene Substrate 259

Cycloaddition/cyclization of the allene **253** under thermolytic conditions (110 °C, tol-d_8) failed to yield the cyclization product **254** and resulted in decomposition of the allenyl azide. Lower thermolysis temperature (benzene-d_6, 80 °C) did not affect the outcome of the cyclization. Cyclization attempted under photolytic conditions (254 nm, CD_3CN,) for 25 min also resulted in decomposition (Table 6).

Table 6: Thermolytic cyclization attempts on allene **253**.

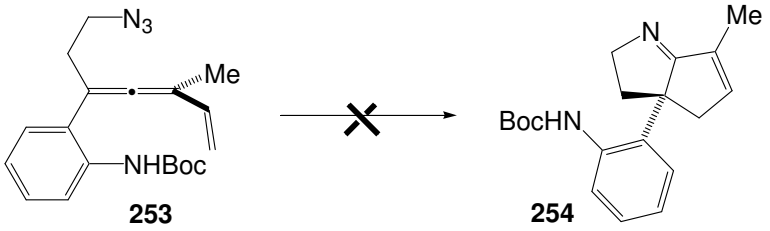

Cyclization Attempts	Result
Toluene-d_8, 110 °C	Decomposition
Benzene-d_6, 80 °C	Slow decomposition
Microwave 90 °C	Unidentified products
Photochem 254 nm	Decomposition

5.4.2.4 Further Revision of the Allene Precursor

Due to the unexpected failure of the allenyl azides **245** and **253** to cyclize, a bromo group was chosen next as the substituent on the phenyl appendage of the allene. It was anticipated that if such a bromo-allene bearing an ester group similar to **240** can be obtained and cyclized, then post-cyclization manipulations of the ester group could provide a bromo amide. This type of species is known to undergo lactam-forming cyclization under conditions reported by Buchwald and Hartwig.[101]

The synthesis of the bromo-bearing allenyl azide **259** is shown in Figure 82. The first generation route involved synthesizing allene **259** bearing an un-functionalized vinyl group. A simple methyl group on the allene terminus was chosen for this model system.

The synthesis of the allenyl azide proceeded utilizing the chemistry developed for the nitro- and amino-bearing allenes. Starting from the known vinyl ketone **256**,[102] conversion to the keto azide **257** was achieved under acidic conditions using sodium azide in 74% yield. Propynyl lithium addition to the ketone **257** at room temperature followed by acetate protection of the desired alcohol provided compound **258** in 46% yield over two steps. The acetate **258** was uneventfully converted to the stable allene **259** in 55% yield, thus enabling clean spectral characterization of the allene (Figure 82).

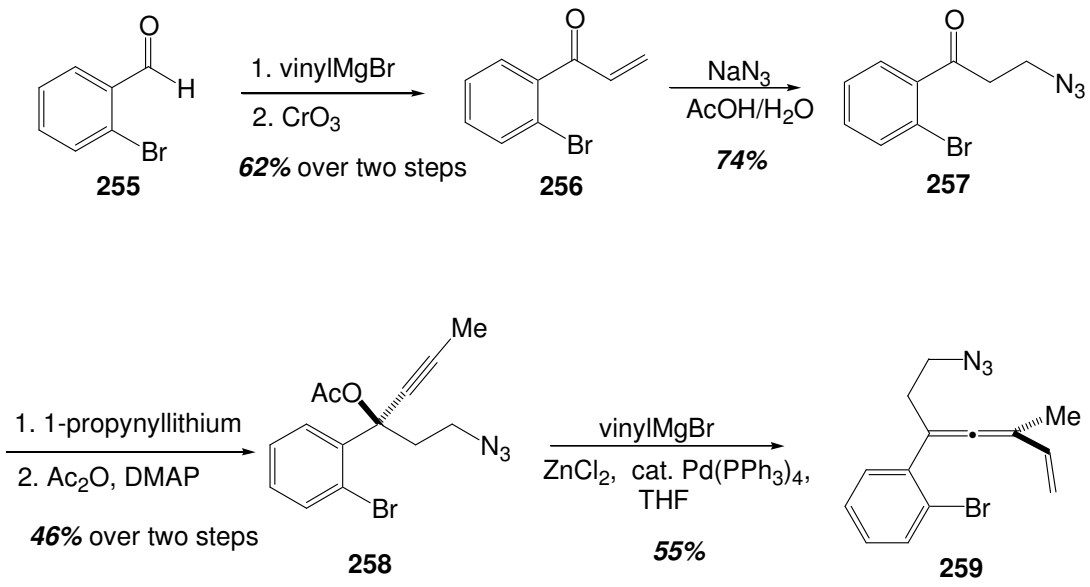

Figure 82: Synthesis of bromo-allene **259**.

5.4.2.5 Cyclization of the Bromo-Allenyl Azide Substrate

Allene **259** was subjected to cycloaddition/cyclization at 110 °C in tol-d_8 under air-free conditions. Clean conversion to a new product was obtained within 20 min of reaction time. Opening the product to air/O_2 did not affect the crude ^{1}H NMR spectrum of

the product attesting to its stability to molecular oxygen. SiO_2 purification of the compound resulted in the isolation of a pale yellow solid whose spectral characteristics pointed to **266** (Figure 83). This assignment was further supported by X-ray analysis of **260** (see **Chapter 6**). This result indicated that the bromo-group is robust under the cyclization conditions and is probably the right choice for further manipulations.

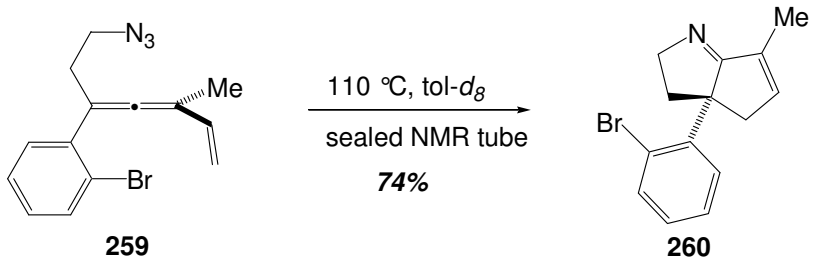

259 **260**

Figure 83: Thermolytic cyclization of bromo-allene **259**.

5.4.2.6 Attempts at the Synthesis of Vinyl Ester Allenyl Azide

The successful cyclization of the simple vinyl allene **259** to deliver the 5-5 fused ring **260** resembling the meloscine core stimulated the synthesis of an additional model, this time bearing the requisite functionality viz., ester/amido group for post-cyclization coupling with the bromo substituent on the phenyl ring.

Toward that end, acetate **258** was subjected to a $Pd^{(0)}$ catalyzed reaction with vinyl ester zincate **179**.[76] Initial unsuccessful attempts led to increase in the catalyst loading from 5 mol% to 10 mol%. This change resulted in formation of the required allene **261** amidst a lot of side products. The scheme for the vinyl ester allene synthesis is shown in (Figure 84).

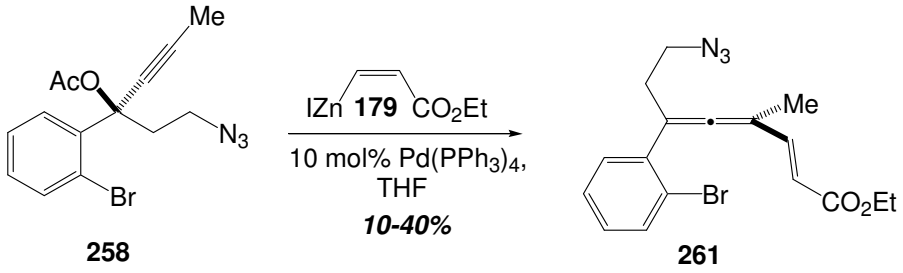

Figure 84: Synthesis of vinyl ester allene **261**.

5.4.2.7 Cyclization of the Bromo-Allenyl Azide Substrate 261

Bromo-allene **261** was subjected to cycloaddition/cyclization at 110 °C, in tol-d_8 (0.1 M) under air-free conditions. Conversion to a new product was observed, again within 20 min of reaction time. Exposing the product to air/O_2 did not affect the crude ^{1}H NMR spectrum of the product, attesting to its stability to molecular oxygen similar to the des ester species **261**. SiO_2 purification of the compound resulted in the isolation of a sole compound whose spectral characteristics pointed to **262** (Figure 85). Some decomposition of the product was seen on exposure to SiO_2 or air over a period of time. The stereochemistry of **262** was secured by multiple 2D-NMR (COSY, HMQC and NOESY) experiments.

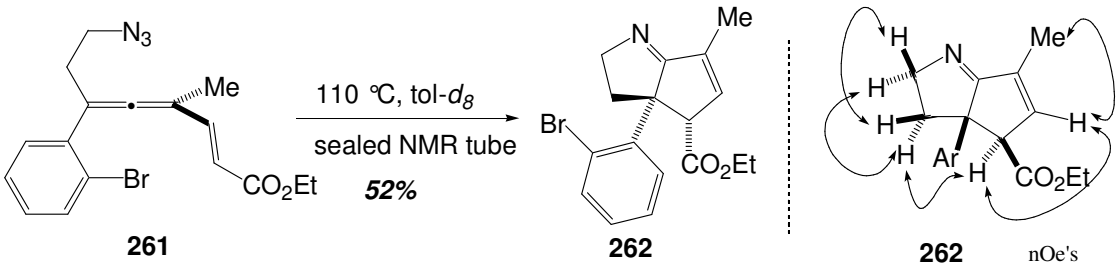

Figure 85: Thermolytic cyclization of vinyl ester allene **261**.

5.4.2.8 Synthesis of Vinyl Ester Allenyl Azide: Alternate Route

A route to vinyl ester allene **261** can also be envisioned via the allene **265**. This approach would require the prior installation of the susbstituted alkenyl group followed by introduction of the terminal alkyl group as an alkyl cuprate. This strategy was successfully employed in the synthesis of allene **265** from ketone **257** and OTBS protected 2-penten-4yn-1-ol **263**. Acetate protection of the alcohol and methyl cuprate addition to **264** gave the allene **265** without any complications (Figure 86).

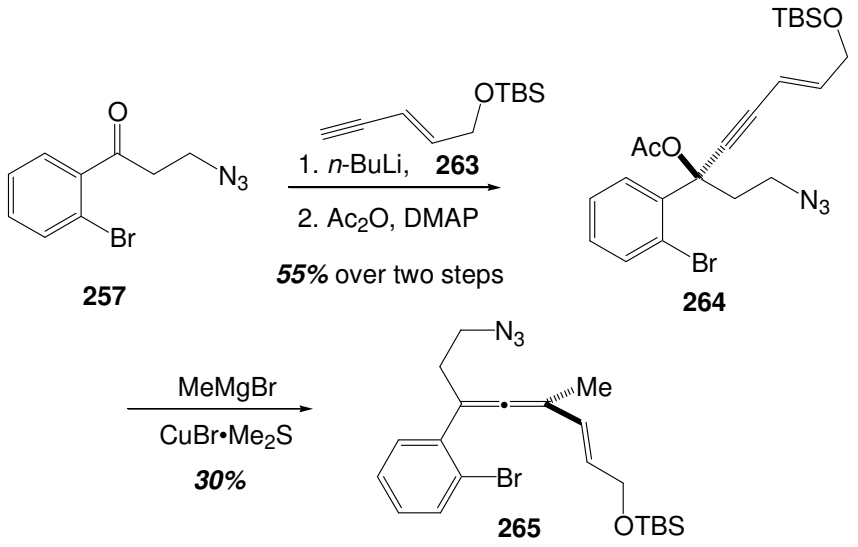

Figure 86: Alternate route to vinyl ester allene via allene **265**.

5.4.2.9 Cyclization of the Allenyl Azide Substrate 265

Bromo-allene **265** was subjected to cycloaddition/cyclization at 110 °C, in tol-d_8 (0.1 M). Conversion to a new product was obtained within 20 min of reaction time. Opening the product to air/O_2 did not affect the crude ^{1}H NMR spectrum of the product clearly indicating its stability to molecular oxygen. SiO_2 purification of the compound resulted in the isolation of a pale yellow compound whose spectral characteristics confirmed the product to be **266** (Figure 87). Stereochemistry of **266** was secured by dnOe studies. Compound **266** can be converted to **262** via deprotection of TBS group, oxidation of the alcohol to carboxylic acid followed by esterification. Formation of the amide derivative required for the meloscine core can be achieved directly from the carboxylic acid. These steps were not attempted in practice. The conversion of allene **265**

to cyclization product **266** clearly shows the availability of an alternate route to **262**, or its amide derivative, should the need arise.

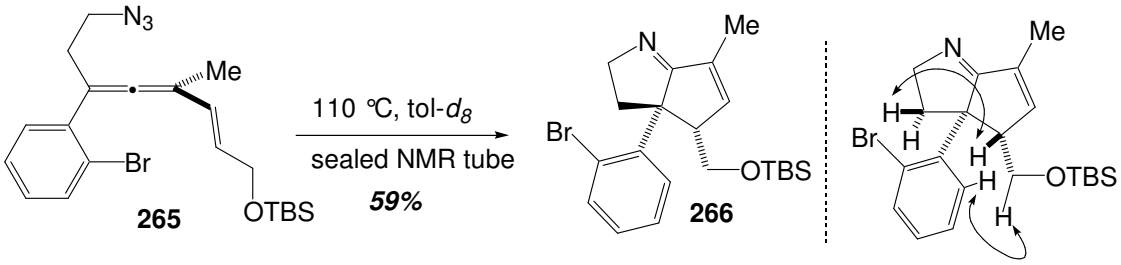

Figure 87: Thermolytic cyclization of allene **265**.

5.4.3 Reductive Alkylation of Substrate 260

With the advanced intermediate **262** in hand, further progress required the reduction of the imine function. Compound **260** was chosen as the model for investigation of the imine reduction. A one-pot reduction of the imine function in **260**, as well as the introduction of the allyl function was achieved using silver perchlorate/allyl iodide/$NaBH_4$ in acetonitrile. This concoction gave the product **267** as shown in Figure 88. Various modifications of the above conditions failed to preserve the alkenic bond conjugated to the imine functionality.

A roster of reductants was tried in hope of reducing the imine functionality while preserving the ring unsaturation. However, the conditions attempted resulted in either recovery of starting material or reduction of the ring double bond (Table 7).

Further progress toward the meloscine model system requires the development of reductive conditions tolerable to the ester group in **262**.

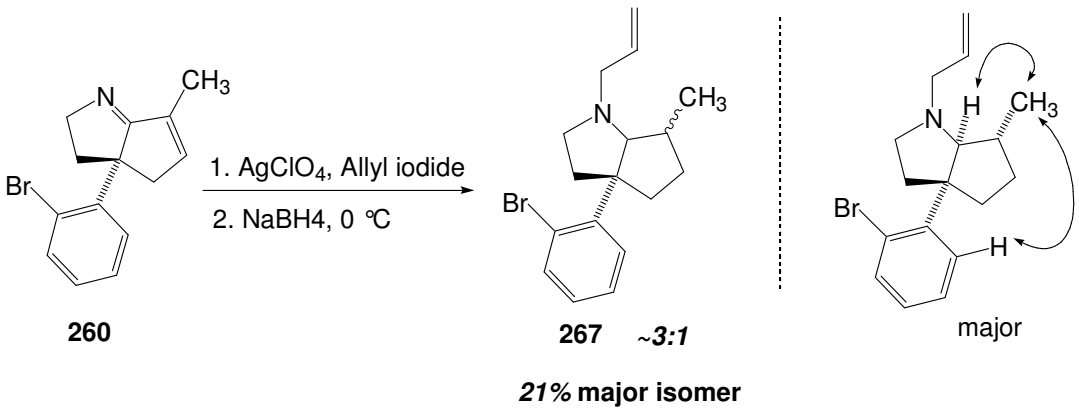

Figure 88: Reductive allylation of **260**.

Table 7: Attempts at reduction of imine **260**.

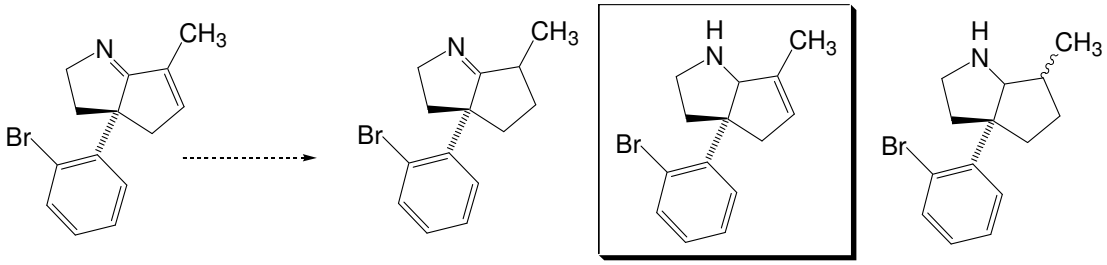

260 **268** **269** **270**

Conditions	Results				
	Sm	**268**	**269**	**270**	**unknown**
$NaBH_4$ (1.5 eq), AcOH, MeOH, -78 °C, 24 h	major	traces	-	-	-
$NaBH_4$ (1.5 eq), $CeCl_3$, MeOH, -78 °C, 24 h	90%	~10%	-	-	-
$NaBH_4$ (1.0 eq), HCl, 0 °C, 7 h	-	30%	-	??	~60%
BH_3-THF (1.2 eq), succinic acid, -25 °C, 3 h	recovery	25%	-	-	~10%
BH_3-THF (1.2 eq), succinic acid, -78 °C, 4 h	40%	25%	-	-	~10%
$SiHCl_3$, DMF, CH_2Cl_2, rt, 24 h	recovery	-	-	-	-
DibalH (1.5 eq), THF, -78 °C, 24 h	recovery	-	-	-	-
DibalH (1.5 eq), 0 °C	-	traces	-	??	~90%
$NaBH_3CN$ (1.5 eq), THF, HCl, 0 °C	-	traces	-	~80% mix of stereoisomers	-

5.5 Conclusions and Summary

The idea of showcasing intramolecular allenyl azide cascade-cyclization chemistry in the total synthesis of meloscine is closer to success. It was shown that through model-system chemistry, an advanced intermediate resembling the meloscine core with three stereogenic centers could be prepared easily in a little more than half dozen steps. With appropriate modifications to the alkyl group in the allene system **261**, the actual synthesis of the target natural product can commence.

In summary, through the work described in **Chapter 4** and in **Chapter 5**, it is clear that ATMM-based intramolecular allenyl azide cycloaddition chemistry can be a very useful tool for construction of alkaloid architectures. Presently, this is just tip of the iceberg, and this protocol is ready to be fully exploited in the years to come.

Chapter 6

Experimental

6.1 General Experimental

Moisture and oxygen sensitive reactions were carried out in flame-dried Schlenk glassware under an argon atmosphere. Toluene was distilled from sodium fluorenone ketyl under argon prior to use. Tetrahydrofuran (THF) was distilled from sodium benzophenone ketyl under an argon atmosphere immediately before use. All organic reagents were used as purchased. Purification of products via flash chromatography[103] was performed with 32-63 μm silica gel and the solvent systems indicated. Hexanes, CH_2Cl_2, EtOAc and Et_2O used in flash chromatography were distilled from CaH_2 prior to use. All reactions run after July 2004 utilized solvents (THF, ether, CH_2Cl_2, acetonitrile, benzene, toluene, methanol) obtained from a purification column (conditioned alumina resin) available from Glass Contours (http://www.glasscontour.com/). Melting points are uncorrected. Low- and high resolution mass spectra were obtained according to the specified technique and were performed at the Pennsylvania State University, University Park, PA. X-Ray data was obtained at the small molecule crystallography facility in the Pennsylvania State University, University Park, PA.

6.2 Ellagitannin Chemistry: Studies on the Stability and Reactivity of 2,4-HHDP Containing Ellagitannin Systems

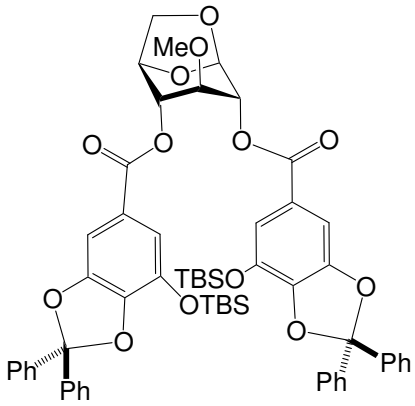

3-*O*-Methyl 2,4-bis((3,4-diphenylmethylene)dioxy)-5-*t*-butyldimethylsilyloxy-benzoyl)-1,6-anhydro-β-D-glucopyranoside (47).

A solution of diol **43**[35] (0.88 g, 5.0 mmol), acid **46** [21] (4.5 g, 10 mmol), 4-(dimethylamino)pyridine (DMAP) (0.31 g, 2.5 mmol), DMAP.HCl (0.40 g, 2.5 mmol) and 1,3 dicyclohexylcarbodiimide (2.5 g, 12 mmol) in dry CH_2Cl_2 (100 mL) was purged with argon and stirred at room temperature for 14 h. The emulsion was then filtered through Celite, the filter cake was washed three times with 10 mL of CH_2Cl_2 and the filtrate was concentrated *in vacuo*. Purification of the resulting pale yellow solid by silica gel chromatography using 30% ether in hexanes as eluent afforded 4.26 g (82 %) of the diester product **47** as a frothy white solid. IR (KBr) 1714 cm^{-1}; ^1H NMR (C_3D_6O, 300 MHz) δ 7.64-7.29 (m, 24 H), 5.59 (brs, 1H), 4.97 (s, 1H), 4.83 (brs, 2H), 4.80 (d, *J* = 5.0 Hz, 1H), 4.20 (d, *J* = 7.3 Hz, 1H), 3.77 (t, *J* = 7.2 Hz, 1H), 3.65 (s, 1H), 3.56 (s, 3H) 0.98 (s, 18H), 0.20 (s, 3H), 0.19 (s, 3H), 0.18 (s, 3H), 0.17 (s, 3H); ^{13}C NMR (C_3D_6O, 90 MHz) δ 164.8, 164.7, 149.2, 149.1, 142.0, 140.1, 139.2, 129.9, 129.8, 129.7, 129.5, 128.9, 128.8, 126.5, 126.4, 124.5, 124.4, 118.9, 118.8, 118.7, 104.1, 100.0, 78.5, 74.5,

72.0, 70.9, 65.5, 58.4, 25.7, 25.4, 24.7, 18.4, -4.4, -4.7; APCIMS *m/z* relative intensity 1037 (MH^+, 100); HRMS (+APCI) Calcd for $C_{59}H_{64}O_{13}Si_2$: 1037.3963, Found: 1037.3917.

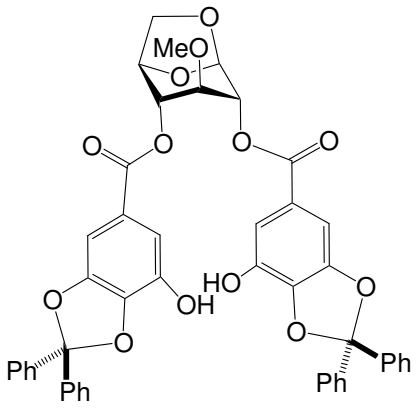

3-*O*-Methyl 2,4-bis((3,4-diphenylmethylene)dioxy)-5-hydroxybenzoyl)-1,6-anhydro-β-D-glucopyranoside (48).

A solution of digallolylated glucose derivative **47** (4.2 g, 4.0 mmol) in dry THF (100 mL) was cooled to 0 °C and purged with argon. A solution of tetrabutylammonium fluoride (1.0 M in THF, 12 mmol, 12 mL) was added and the reaction mixture was stirred at room temperature for 1.5 h. The reaction solution was then carefully diluted with ice-cold 1 M H_3PO_4 and the product was extracted into ethyl acetate. The organic extract was washed with brine, dried over anhydrous Na_2SO_4 and the solvent was evaporated to give an off-white solid. The crude compound was purified by flash chromatography using 90% ether in hexanes as the eluent to yield 2.76 g (85%) of the bisphenol **48** as a white foam. Mp 274-276 °C (dec); IR (KBr) 3322, 1711 cm^{-1}; ^1H NMR (C_3D_6O, 300 MHz) δ 9.1 (brs, 1H), 7.6-7.3 (m, 22 H aromatic), 7.22 (d, *J* = 1.5, 1H), 7.19 (s, *J* = 1.5, 1H), 5.56 (brs, 1H), 5.00 (brs, 1H), 4.83 (brs, 1H), 4.79 (d, *J* = 5.8 Hz, 1H), 4.22 (d, *J* = 7.5 Hz,

1H), 3.79 (dd, J = 7.1, 6.0, Hz, 1H), 3.54 (brs, 4H); ^{13}C NMR (C_3D_6O, 75 MHz) δ 164.8, 164.7, 150.0, 148.9, 141.2, 141.1, 140.5, 140.4, 140.3, 138.9, 129.7, 129.6, 128.7, 128.7, 126.5, 126.4, 124.5, 124.4, 118.4, 114.5, 102.6, 99.8, 78.5, 74.2, 71.9, 69.9, 65.2, 58.2; IR (KBr) 3322, 1711 cm^{-1}; APCIMS *m/z* relative intensity 809 (MH^+, 100); HRMS (+APCI) Calcd for $C_{47}H_{36}O_{13}$809: 2234, Found: 809.2229.

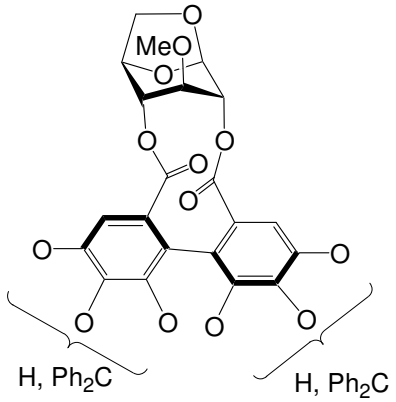

Lead Tetraacetate Oxidation of 3-*O*-Methyl 2,4-bis((3,4-diphenylmethylene)-dioxy)-5-hydroxybenzoyl)-1,6-anhydro-β-D-glucopyranoside (49).

A solution of $Pb(OAc)_4$ (1.6 g, 3.6 mmol) in dry CH_2Cl_2 (5 mL) was added drop-wise to a deoxygenated solution of bisphenol **48** (2.6 g, 3.3 mmol) in dry CH_2Cl_2 (100 mL) and pyridine (1.1 mL, 13 mmol) at -38 °C. The dark orange solution was stirred at -38 °C for 2 h. The solution was diluted with aqueous $NaHCO_3$ and extracted into CH_2Cl_2. The organic extract was washed with water and saturated $CuSO_4$ solution to remove traces of pyridine, dried over Na_2SO_4 and evaporated *in vacuo* to yield an orange-brown solid which upon flash chromatography using 65% ether in hexanes, afforded 1.8 g (69%) of **49** a bright orange solid: mp 222-228 °C; ^{1}H NMR (C_3D_6O, 300 MHz) (mixture of isomers): δ 7.8-7.2 (m, 20 H), 7.0-6.6 (2H), 5.7-5.5 (m, 1H), 5.1-4.6, (m, 3H), 4.3-4.2 (m, 1H), 3.75 (m, 1H), 3.6-3.3 (m, 4H); ^{13}C NMR (C_3D_6O, 75 MHz) δ 191.5, 190.7,

163.9, 163.8, 163.7, 163.5, 163.3, 163.1 158.5, 158.4, 158.2, 158.1, 149.1, 146.4, 144.0, 141.0, 140.7, 140.0, 139.8, 139.5, 139.4, 139.3, 137.2, 137.1, 137.0, 136.9, 129.9, 129.5, 128.9, 128.8, 128.7, 128.4, 126.7, 126.6, 126.5, 126.3, 126.2, 124.1,124.0, 123.8, 122.9, 120.9, 120.7, 119.8, 119.5, 118.2, 107.2, 107.1, 105.4, 100.5, 99.5, 99.1, 98.9, 98.3, 96.1, 95.9, 94.1, 94.0, 77.2, 77.1, 77.0, 74.0, 73.6, 73.5, 73.4, 72.6, 70.8, 70.4, 70.2, 69.2, 69.0, 68.9, 67.9, 65.3, 65.2, 64.7, 58.0, 57.9; IR (KBr) 3410, 1714, cm^{-1}; APCIMS *m/z* relative intensity 807 (MH^+, 48); HRMS (+APCI) Calcd for $C_{47}H_{34}O_{13}$: 807.2077, Found: 807.2041.

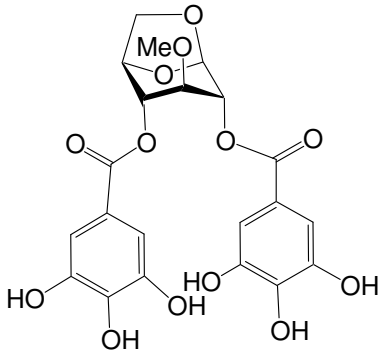

Hydrogenolysis of Compound 49.

A deoxygenated solution of compound **49** (60 mg, 0.07 mmol) and 30 mg of 10% Pd on C in dry THF (10 mL) was stirred at room temperature under H_2 at 1 atm for 14 h. At that time, the flask was purged with argon and the reaction mixture was filtered through Celite. The filtrate was concentrated *in vacuo* to give 35 mg (~100%) of **50** as a pale brown film. IR (CH_2Cl_2) 3375, 1717, cm^{-1}; ^1H NMR (C_3D_6O, 300 MHz) δ 7.24 (s, 2 H), 7.21 (s, 2H), 5.53 (brs, 1H), 4.94 (brs, 1H), 4.81 (brs, 1H), 4.76 (d, *J* = 7.2 Hz, 1H), 4.20 (d, *J* = 7.2 Hz, 1H), 3.77 (t, *J* = 7.0 Hz, 1H), 3.54 (s, 3H); 3.52 (s, 1H); ^{13}C NMR

(C_3D_6O, 75 MHz) δ 165.6, 165.4, 145.5, 138.8, 128.8, 126.6, 120.8, 120.6, 109.8, 100.1, 78.9, 74.5, 71.2, 70.2, 65.5, 58.2. APCIMS *m/z* relative intensity 481 (MH^+, 67).

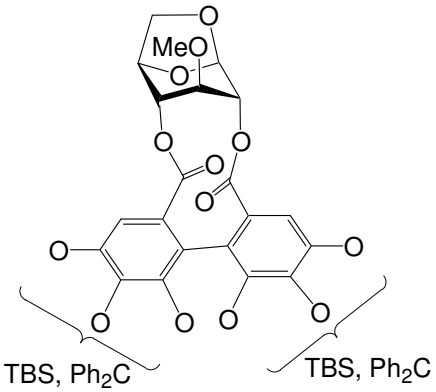

3-*O*-Methyl 2,4-((3,4, 3',4'-diphenylmethylene)dioxy)-5, 5'-*tert*-butyldimethylsilyldiphenoyl)-1,6-anhydro-β-D-glucopyranoside (57).

A solution of compound **49** (0.10 g, 0.12 mmol) in dry CH_2Cl_2 (10 mL), imidazole (34 mg, 0.48 mmol) and TBSCl (74 mg, 0.48 mmol) was stirred at room temperature for 30 h. The reaction solution was poured into ice-cold 1.0 M H_3PO_4 and the product was extracted into CH_2Cl_2. The organic layer was washed with brine, dried over Na_2SO_4 and the solvent was evaporated to yield a yellow solid. Purification of the crude compound by flash chromatography using 60% ether in hexanes as eluent yielded 80 mg (63%) of **57** as a white solid. Further chromatography on a prep-plate with 45% ethyl acetate in hexanes as the mobile phase furnished two major isomers that were labeled and characterized as **57a** and **57b**.

Isomer 57a: ^{1}H NMR (C_3D_6O, 400 MHz) δ 7.6-7.4 (m, 20 H), 7.03, (s, 1H), 6.66 (s, 1H), 5.42 (s, 1H), 4.76 (brs, 1H), 4.66 (brs, 1H), 4.52 (s, 1H), 4.13 (d, *J* = 7.3 Hz, 1H), 3.70 (t, *J* = 7.0 Hz, 1H), 3.44 (s, 1H); 3.04 (s, 3H), 0.65 (s, 9H), 0.63 (s, 9H) 0.31 (s, 3H),

0.28 (s, 3H), -0.13 (s, 3H), -0.14 (s, 3H); ^{13}C NMR (C_3D_6O, 75 MHz) δ 168.6, 164.4, 148.6, 148.1, 140.8, 140.2, 140.0, 139.9, 139.3, 138.5, 137.5, 130.0, 129.9, 129.7, 129.6, 128.9, 128.8, 128.7, 128.0, 126.6, 126.5, 126.4, 124.6, 122.6, 118.8, 118.0, 100.4, 99.6, 98.8, 74.5, 72.5, 72.2, 69.9, 65.2, 58.1, 25.1, 25.0, 18.1, 18.0, -4.1, -4.2, -5.5, -5.6; CD (CH_3OH) 238 nm, -4.4; 263 nm, +2.2; 290 nm, -4.9.

Isomer 57b: ^{1}H NMR (C_3D_6O, 400 MHz) δ 7.6-7.4 (m, 20 H), 7.04, (s, 1H), 6.65 (s, 1H), 5.48 (s, 1H), 4.73 (brs, 1H), 4.65 (m, 1H), 4.52 (s, 1H), 4.20 (d, *J* = 7.2 Hz, 1H), 3.64 (t, *J* = 7.1 Hz, 1H), 3.44 (s, 1H); 3.05 (s, 3H), 0.65 (s, 9H), 0.62 (s, 9H) 0.31 (s, 3H), 0.27 (s, 3H), -0.13 (s, 3H), -0.14 (s, 3H); ^{13}C NMR (C_3D_6O, 75 MHz) δ 168.5, 164.7, 148.7, 148.1, 140.8, 140.3, 140.0, 139.9, 139.7, 139.3, 138.6, 137.6, 130.0, 129.9, 129.8, 129.6, 129.0, 128.9, 128.8, 128.7, 128.0, 127.0, 126.6, 126.5, 126.4, 124.6, 122.7, 118.9, 118.1, 99.4, 98.9, 98.7, 75.5, 75.4, 72.4, 68.8, 64.2, 58.1, 25.1, 25.0, 18.1, 18.0, -4.1, -4.2, -5.5, -5.6; CD (CH_3OH) 238 nm, +1.9; 263 nm, -4.1; 290 nm, 5.8.

Isomers 57a-b: IR (KBr) 1734 cm^{-1}; APCIMS *m/z* relative intensity 1035 (MH^+, 100); HRMS (+APCI) Calcd for $C_{59}H_{62}O_{13}Si_2$: 1035.3807, Found: 1035.3891.

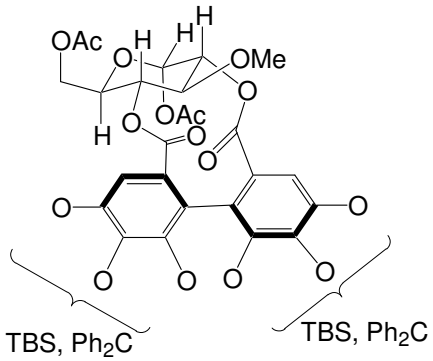

3-*O*-Methyl 1,6-di-*O*-acetyl 2,4-((3,4, 3',4'-diphenylmethylene)dioxy)-5, 5'-*tert*-butyldimethylsilyldiphenoyl)- β-D-glucopyranoside (58).

To a suspension of the mixture **57** (80 mg, 0.08 mmol) in Ac_2O (2.0 mL) was added conc. H_2SO_4 (3 drops). After 4 min at 40 °C the now homogeneous mixture was poured into water and stirred overnight. The mixture was extracted with CH_2Cl_2 and the organic phase was washed successively with water and saturated $NaHCO_3$ solution, dried with Na_2SO_4 and concentrated to give a white solid. Flash chromatography of the crude reaction product using 85% ether in hexanes afforded a white foamy solid in 70% yield (61 mg). Two isomers were separated from this mixture and designated as **58a** and **58b**.

Isomer 58a: ^{1}H NMR (C_3D_6O, 400 MHz) δ 7.6-7.4 (m, 20 H), 7.25 (s, 1H), 7.21 (s, 1H), 6.08 (d, *J* = 3.7 Hz, 1H), 5.05 (t, *J* = 9.5 Hz, 1H), 4.84 (dd, *J* = 10.1, 3.7 Hz 1H), 4.12 (dd, *J* = 11.9, 4.2 Hz, 1H), 4.06 (m, 1H), 4.01 (dd, *J* = 12.1, 2.3 Hz, 1H), 3.90 (t, *J* = 9.7 Hz), 1H), 3.46 (s, 3H), 2.13 (s, 3H), 2.10 (s, 3H); ^{13}C NMR (C_3D_6O, 75 MHz) δ 170.2, 169.8, 168.9, 164.5, 140.8, 140.7, 140.3, 140.0, 139.9, 137.5, 137.3, 129.8, 129.7, 129.6, 129.5, 128.9, 128.8, 128.7, 126.8, 126.5, 126.4, 118.7, 118.5, 103.9, 103.8, 88.9, 78.7, 71.1, 70.1, 69.7, 62.1, 59.9, 25.2, 20.3, 20.1, 18.1, 18.0, -4.1, -4.8, -4.9; CD (CH_3OH) 238 nm, -8.5; 263 nm, +1.1; 290 nm, +1.0.

Isomer 58b: ^{1}H NMR (C_3D_6O, 400 MHz) δ 7.66-7.44 (m, 21 H), 7.30 (s, 1H), 6.11 (d, *J* = 3.6 Hz, 1H), 5.06 (dd, *J* = 10.2, 9.2 Hz, 1H), 4.74 (dd, *J* = 10.1, 3.6 Hz 1H), 3.84 (dd, *J* = 12.2, 4.6 Hz, 1H), 3.67 (dd, *J* = 12.2, 1.9 Hz, 1H), 3.58 (t, *J* = 9.6 Hz, 1H), 3.41 (ddd, *J* = 10.4, 4.4, 2.2 Hz, 1H), 3.29 (s, 3H), 2.01 (s, 3H), 1.94 (s, 3H); ^{13}C NMR (C_3D_6O, 75 MHz) δ 169.9, 169.8, 168.9, 165.2, 147.6, 140.6, 140.4, 140.0 139.7, 137.5, 137.2, 137.0, 130.1, 129.8, 129.7, 129.6, 129.0, 128.8, 128.7, 126.7, 126.5, 126.4, 124.3, 119.0, 118.8, 103.9, 103.8, 88.9, 78.1, 71.8, 69.9, 69.4, 61.8, 60.1, 25.4, 25.0, 20.1, 20.0, 19.9, 18.2, -3.8, -4.1, -4.7; CD (CH_3OH) 238 nm, +30.7; 263 nm, -6.4; 290 nm, -12.0.

Isomers 58a-b: IR (KBr) 1746 cm^{-1}; APCIMS *m/z* relative intensity 1137 (MH^+, 100); HRMS (+APCI) Calcd for $C_{63}H_{68}O_{16}Si_2$: 1137.4124, Found: 1137.4093.

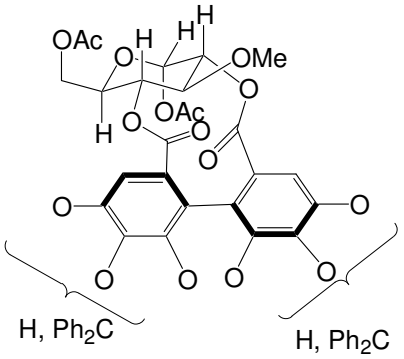

3-*O*-Methyl 1,6-di-O-acetyl 2,4-((3,4, 3',4'-diphenylmethylene)dioxy)-5, 5'-hydroxy diphenoyl)- β-D-glucopyranoside (59).

A solution of the silyl ether mixture **58** (60 mg, 0.05 mmol) in dry THF (7.0 mL) was cooled to 0 °C and treated with acetic acid (13 μL, 0.21 mmol). A solution of tetrabutylammonium fluoride (1.0 M in THF, 0.21 mmol, 0.21 mL) was added and the reaction mixture was stirred at room temperature for 1.5 h. The reaction solution was then

carefully diluted with ice-cold 1 M H_3PO_4 and the product was extracted into ethyl acetate. The organic extract was washed with brine, dried over anhydrous Na_2SO_4 and the solvent was evaporated to give a pale yellow solid. The crude mixture was purified on a preparative silica-gel plate using 70% ethyl acetate in hexanes as eluent to yield 35 mg (73%) of bisphenol **59** as a pale white solid. Two isomers isolated in pure form were characterized as **59a** and **59b.**

Isomer 59a: ^{1}H NMR (C_3D_6O, 400 MHz) δ 7.70-7.43 (m, 20 H), 7.34 (s, 1H), 7.33 (s, 1H), 6.09 (d, *J* = 3.5 Hz, 1H), 5.04 (t, *J* = 10.2 Hz, 1H), 4.74 (dd, *J* = 10.1, 3.6 Hz 1H), 3.89 (dd, *J* = 12.5, 4.7 Hz, 1H), 3.85 (dd, J = 12.3, 2.3 Hz, 1H), 3.75 (ddd, J = 10.3, 4.6, 2.4 Hz, 1H), 3.26 (s, 3H), 3.20 (t, *J* = 10.2 Hz, 1H) 2.03 (s, 3H), 1.94 (s, 3H); ^{13}C NMR (C_3D_6O, 125 MHz) δ 172.8, 172.4, 171.6, 167.6, 150.0, 149.9, 143.5, 143.4, 143.0, 141.8, 141.7, 141.3, 132.6, 132.5, 132.4, 132.2, 132.1, 131.6, 131.4, 131.3, 129.4, 129.2, 129.0, 128.9, 128.8, 120.2, 120.1, 106.6, 105.6, 91.6, 80.8, 75.5, 72.6, 72.1, 64.6, 63.1, 22.9, 22.8; CD (CH_3OH) 238 nm, -5.0; 263 nm, +1.0; 290 nm, -2.0.

Isomer 59b: ^{1}HNMR (C_3D_6O, 400 MHz) δ 7.69-7.42 (m, 20 H), 7.40 (s, 1H), 7.25 (s, 1H), 6.14 (d, *J* = 3.6 Hz, 1H), 5.05 (t, *J* = 10.2 Hz, 1H), 4.74 (dd, *J* = 10.1, 3.6 Hz 1H), 3.82 (dd, *J* = 12.6, 4.5 Hz, 1H), 3.72 (dd, *J* = 12.5, 2.0 Hz, 1H), 3.48 (t, *J* = 10.0 Hz, 1H), 3.31 (ddd, *J* = 10.5, 4.6, 2.0 Hz, 1H), 3.28 (s, 3H), 2.03 (s, 3H), 2.01 (s, 3H); ^{13}C NMR (C_3D_6O, 90 MHz) δ 170.1, 169.8, 169.0, 165.4, 147.4, 140.9, 140.8, 140.5, 140.1, 138.9, 138.0, 130.0, 129.8, 129.6, 128.9, 128.8, 126.8, 126.6, 126.5, 126.4, 124.0, 123.8, 118.5, 118.2, 103.6, 103.1, 89.1, 78.8, 71.8, 70.3, 69.6, 61.9, 60.3, 20.2, 20.4; CD (CH_3OH) 238 nm, +16.0; 263 nm, -5.0; 288 nm, -6.0.

Isomers 59a-b: IR (KBr) 3310, 1746, cm^{-1}; APCIMS *m/z* relative intensity 909 (MH^+, 95); HRMS (+APCI) Calcd for $C_{51}H_{40}O_{16}$: 909.2394, Found: 909.2431.

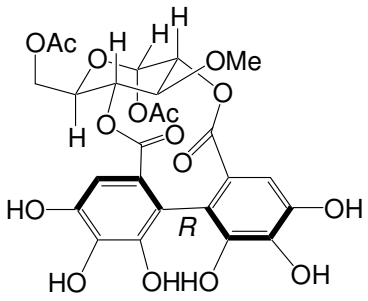

Hexaphenol (60a).

A deoxygenated solution of compound **59a** (15 mg, 0.01 mmol) and 10% Pd on carbon (10 mg) in dry THF (6 mL) was stirred at room temperature under H_2 at 1 atm for 20 h. The resultant mixture was filtered through Celite and concentrated *in vacuo* to give a yellow-brown film. Purification on a prep-plate using 1:3:1 hexane:ethyl acetate:acetic acid as the mobile phase gave 4.5 mg (47%) compound **60a** as a pale-brown film.

^1H NMR (C_3D_6O, 400 MHz) δ 8.1 (s, 1H), 7.28 (d, 2H), 6.10 (d, *J* = 3.6 Hz, 1H), 4.99 (t, *J* = 9.9 Hz, 1H), 4.72 (dd, *J* = 10.2, 3.7 Hz 1H), 3.81 (m, 2H), 3.52 (m, 1H), 3.34 (s, 3H), 3.26 (t, *J* = 10.2 Hz, 1H), 2.02 (s, 3H), 1.97 (s, 3H); CD (CH_3OH) 238 nm, -2.0; 263 nm, +1.0; 290 nm, -4.0.

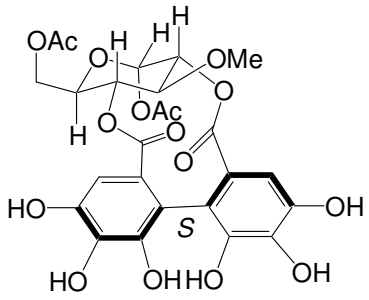

Hexaphenol (60b).

A deoxygenated solution of compound **59b** (15 mg, 0.01 mmol) and 10% Pd on carbon (10 mg) in dry THF (6 mL) was stirred at room temperature under H_2 at 1 atm for 20 h. The resultant mixture was filtered through Celite and concentrated *in vacuo* to give a yellow-brown film. Purification on a prep-plate using 1:3:1 hexane:ethyl acetate:acetic acid as the mobile phase gave 4.2 mg (44%) compound **60b** as a pale-brown film**.** ^{1}H NMR (C_3D_6O, 400 MHz) δ 8.1(s, 1H), 7.37 (s, 1H), 7.25 (s, 1H), 6.09 (d, *J* = 3.5 Hz, 1H), 5.02 (t, *J* = 9.4 Hz, 1H), 4.71 (dd, *J* = 10.0, 3.6 Hz 1H), 3.92 (dd, *J* = 12.3, 2.2 Hz, 1H), 3.87 (dd, *J* = 12.5, 4.6 Hz, 1H), 3.34 (m, 1H), 3.31 (t, *J* = 9.8 Hz, 1H) 3.26 (s, 3H), 2.02 (s, 3H), 1.98 (s, 3H); CD (CH_3OH) 238 nm, +0.9; 263 nm, -0.5; 290 nm, -0.8.

^{13}C NMR of **60a** and **60b** (C_3D_6O, 75 MHz) δ 170.3, 169.9, 169.4, 167.6, 165.9, 162.5, 144.3, 144.2, 143.8, 137.9, 137.2, 128.8, 126.4 122.3, 122.0, 121.2, 120.8, 119.4, 119.1, 118.5, 111.6, 111.3, 110.7, 110.4, 89.0, 88.9, 78.3, 72.0, 71.9, 70.2, 70.1, 69.2, 69.1, 62.3, 61.9, 61.0, 60.7, 60.3, 20.5, 20.4, 20.2, 20.1.

Isomers 60a-b: IR (CH_2Cl_2) 1747 cm^{-1}; APCIMS *m/z* relative intensity 581 (MH^+, 100); HRMS (+APCI) Calcd for $C_{25}H_{24}O_{16}$: 581.1143, Found: 581.1153.

6.3 Intramolecular Allenyl Azide Cyclization Chemistry

6.3.1 General Procedure 1. Allenyl Azide Synthesis

To a solution of $ZnCl_2$ (3.3 equiv) in THF (0.33 M solution) was added the appropriate Grignard reagent RMgBr (3.3 equiv) and the mixture was stirred at room temperature for 30 min. The reaction mixture was cooled to -50 °C and $Pd(PPh_3)_4$ (5 mol%) in 2 mL of THF and the propargylic azidomesylate **163** (1.0 equiv) in THF (0.18 M solution) were added sequentially. The reaction mixture was allowed to warm to room temperature over the course of 10 h. After addition of an equal volume of a saturated NH_4Cl solution, the organic layer was extracted into Et_2O and washed with water and brine. Drying the organic phase over Na_2SO_4 and removal of solvent under reduced pressure resulted in a yellow oil. This crude product was purified by chromatography using 5% Et_2O in hexane as the eluent.

6.3.2 General Procedure 2. Cyclization and Trapping with TMSCN

A deoxygenated solution of allenylazide in toluene-d_8 (0.06 M) was refluxed in a flame-dried Schlenk flask for 5h, after which time the reaction mixture was cooled to room temperature and cannulated into a flask containing a deoxygenated 0 ^oC solution of TMSCN (2.0 equiv) in CH_2Cl_2 (0.05 M). After stirring the mixture for 12 h at room temperature, water was added and the mixture was extracted with an equal volume of CH_2Cl_2, washed with brine and dried over Na_2SO_4. Evaporation of the organic phase in

vacuo gave a brown oil. Purification of this crude material by flash chromatography (1:1 hexanes/Et_2O) furnished the cyanopyrrolidine product **166** as a pale yellow film.

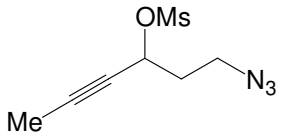

1-Azido-hex-4-yn-3-yl Methanesulfonate (163).

To an ice-cold solution of 3-azidopropionaldehyde[70] (1.1 g, 12 mmol) in 20 mL of THF, 1-propynyl magnesium bromide (0.50 M in THF, 24 mL, 12 mmol) was added dropwise under a nitrogen atmosphere. The reaction mixture was held at 0 °C for 1.5 h and then slowly warmed to room temperature over an additional 1 h. The reaction mixture was poured into 30 mL of saturated NH_4Cl solution and the organic layer was extracted into Et_2O, washed with water and then brine. Drying the organic phase over Na_2SO_4, followed by evaporation of the solvent in vacuo, gave a yellow oil. Purification of this crude material through a small silica gel plug with Et_2O as the eluent gave the product as a pale yellow oil (1.1 g, 65%). IR (neat): 3390, 2099 cm^{-1}; ^1H NMR (400 MHz, $CDCl_3$) δ 4.46 (bs, 1H), 3.52-3.42 (m, 2H), 2.64 (d, J = 4.4 Hz, 1H), 1.94-1.86 (m, 2H), 1.84 (d, J = 2.1 Hz, 3H); ^{13}C NMR (100 MHz, $CDCl_3$) δ 82.3, 79.6, 60.3, 48.2, 37.1, 3.9. APCIMS *m/z* relative intensity 140 (MH^+ 55); HRMS (+ESI) Calcd for $C_6H_{10}N_3O$: 140.0824 , Found: 140.0828.

Methanesulfonyl chloride (1.2 mL, 16 mmol) and triethylamine (2.8 mL, 20 mmol) were added to a solution of 1-azido-hex-4-yn-3-ol (1.1 g, 7.9 mmol) in 40 mL of CH_2Cl_2 at -50 °C, and the mixture was stirred for 2.5 h at that temperature. The reaction

mixture was poured into 30 mL of saturated $NaHCO_3$ solution. The mixture was then extracted with 30 mL of CH_2Cl_2 and the organic layer was then washed with water and brine, dried over Na_2SO_4 and concentrated in vacuo. This crude material was purified by column chromatography (1:1 hexane/Et_2O) to give the azidopropargylic mesylate **163** as a pale yellow oil (1.0 g, 58%). IR (neat): 2099 cm^{-1}; ^1H NMR (400 MHz, $CDCl_3$) δ 5.24 (m, 1H), 3.49 (t, *J* = 6.6 Hz, 2H), 3.1 (s, 3H), 2.14-2.00 (m, 2H), 1.89 (d, *J* = 2.1 Hz, 3H); ^{13}C NMR (100 MHz, $CDCl_3$) δ 87.0, 74.4, 69.9, 47.3, 39.5, 35.6, 4.0. ESIMS *m/z* relative intensity 140 (MH^+ -N_2); HRMS (+ESI) Calcd for $C_7H_{12}NO_3S$: 190.0538, Found: 190.0536.

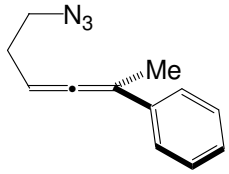

1-Azido-5-(phenyl)hexa-3,4-diene (159a).

Following General Procedure 1, azidomesylate **163** (200 mg, 0.92 mmol) and phenyl magnesium bromide (3.0 M, 1.0 mL) were converted into azidoallene **159a** (155 mg, 85%). IR (neat): 2096, 1950 cm^{-1}; ^1H NMR (400 MHz, $CDCl_3$) δ 7.44 (d, *J* = 7.4 Hz, 2H), 7.36 (t, *J* = 7.5, 2H), 7.23 (t, *J* = 7.2 Hz, 1H), 5.5 (m, 1H), 3.42 (t, *J* = 7.1 Hz, 2H), 2.42 (q, *J* = 6.7 Hz, 2H), 2.14 (d, *J* = 3.0 Hz, 3H); ^{13}C NMR (75 MHz, $CDCl_3$) δ 205.2, 137.4, 128.8, 127.2, 126.1, 102.2, 89.8, 51.2, 29.0, 17.5; APCIMS *m/z* relative intensity 172 (MH^+-N_2 50); HRMS (+ESI) Calcd for $C_{12}H_{13}N_3Na$: 222.0998, Found: 222.1007.

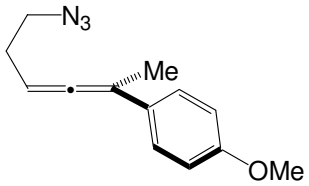

1-Azido-5-(4'-methoxyphenyl)hexa-3,4-diene (159b).

Following General Procedure 1, azidomesylate **163** (0.20 g, 0.92 mmol) and (4-methoxy)phenyl magnesium bromide (0.50 M, 6.0 mL) was converted into azidoallene **159b** (140 mg, 67%). IR (neat): 2094, 1960 cm^{-1}; ^1H NMR (300 MHz, $CDCl_3$) δ 7.35 (d, *J* = 8.8 Hz, 2H), 6.88 (d, *J* = 8.9 Hz, 2H), 5.47 (m, 1H), 3.82, (s, 3H), 3.41 (t, *J* = 6.9 Hz, 2H), 2.40 (q, *J* = 6.6 Hz, 2H), 2.11 (d, *J* = 2.9 Hz, 3H); ^{13}C NMR (75 MHz, $CDCl_3$) δ 204.6, 159.0, 129.6, 127.2, 114.2, 101.7, 89.6, 55.7, 51.2, 29.1, 17.6; APCIMS *m/z* relative intensity 202 (MH^+-N_2 45); HRMS (+ESI) Calcd for $C_{13}H_{16}NO$: 202.1232, Found: 202.1219.

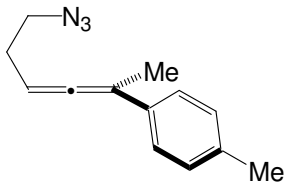

1-Azido-5-(4'-methylphenyl)hexa-3,4-diene (159c).

Following General Procedure 1, azidomesylate **163** (0.50 g, 2.3 mmol) and (*p*-tolyl) magnesium bromide (1.0 M, 7.6 mL) were converted into azidoallene **159c** (400 mg, 81%). IR (neat): 2095 1951 cm^{-1}; ^1H NMR (360 MHz, $CDCl_3$) δ 7.21 (d, *J* = 8.2 Hz, 2H), 7.05 (d, *J* = 8.0 Hz, 2H), 5.4 (m, 1H), 3.3 (t, *J* = 6.9 Hz, 2H), 2.32-2.27 (m, 2H), 2.25 (s, 3H), 2.02 (d, *J* = 2.9 Hz, 3H); ^{13}C NMR (90 MHz, $CDCl_3$) δ 204.9, 136.8, 134.4, 129.5, 126.0, 102.1, 89.5, 51.2, 29.0, 21.5, 17.5; APCIMS *m/z* relative intensity 186 (MH^+-N_2 100); HRMS (+ESI) Calcd for $C_{13}H_{16}N$: 186.1283, Found: 186.1286.

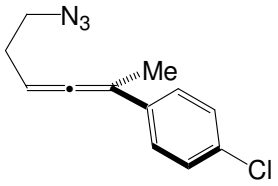

1-Azido-5-(4'-chlorophenyl)hexa-3,4-diene (159d).

Following General Procedure 1, azidomesylate **163** (0.20 g, 0.92 mmol) and (4-chloro)phenyl magnesium bromide (1.0 M, 3.0 mL) was converted into azidoallene **159d** (165 mg, 77%). IR (neat): 2096, 1952 cm^{-1}; ^1H NMR (400 MHz, $CDCl_3$) δ 7.36-7.20 (m, 4H), 5.55-5.48 (m, 1H), 3.42 (t, *J* = 6.8 Hz, 2H), 2.44-2.38 (q, *J* = 6.6 Hz, 2H), 2.12 (d, *J* = 2.9 Hz, 3H); ^{13}C NMR (100 MHz, $CDCl_3$) δ 205.2, 135.9, 132.8, 128.8, 127.4, 101.4, 90.2, 51.1, 28.9, 17.4; APCIMS *m/z* relative intensity 206 (MH^+-N_2 100); HRMS (+APPI) Calcd for $C_{12}H_{13}ClN$: 206.0737, Found: 206.0743.

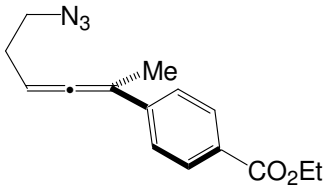

1-Azido-5-(4'-carbethoxyphenyl)hexa-3,4-diene (159e).

A solution of propargyl azidomesylate **163** (200 mg, 0.92 mmol) and $Pd(PPh_3)_4$ (53 mg, 0.05, 5 mol%) in 15 mL of THF was cooled to -50 °C. Commercially available 4-(ethoxycarbonylphenyl) zinc iodide (0.50 M in THF, 5.6 mL, 2.8 mmol) was added to the reaction mixture dropwise and the solution was allowed to warm to room temperature over the course of 12 h. The reaction mixture was then poured into 20 mL of saturated NH_4Cl solution and extracted with 30 mL of Et_2O. The organic phase was then washed with water and brine and dried over Na_2SO_4, and the solvent was removed in vacuo. Purification of the crude oil by column chromatography using 5% Et_2O in hexane

resulted in **159e** as a pale yellow oil (154 mg, 61%). IR (neat): 2099, 1950 cm^{-1}; ^1H NMR (400 MHz, $CDCl_3$) δ 8.01 (d, *J* = 8.6 Hz, 2H), 7.47 (d, *J* = 8.4 Hz, 2H), 5.5 (m, 1H), 4.40 (q, *J* = 7.1 Hz, 2H), 3.43 (t, *J* = 6.8 Hz, 2H), 2.42 (q, *J* = 6.2 Hz, 2H), 2.15 (d, *J* = 2.9 Hz, 3H), 1.41 (t, *J* = 7.1 Hz, 3H); ^{13}C NMR (75 MHz, $CDCl_3$) δ 206.1, 166.9, 142.2, 130.0, 128.0, 125.9, 101.9, 90.2, 61.3, 51.1, 28.8, 17.3, 14.7; APCIMS *m/z* relative intensity 244 (MH^+-N_2 100); HRMS (+APPI) Calcd for $C_{15}H_{18}NO_2$: 244.1338, Found: 244.1353.

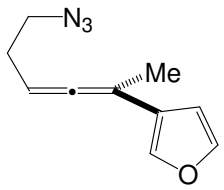

1-Azido-5-(furanyl)hexa-3,4-diene (177).

To a solution of propargyl azidomesylate **163** (0.14 g, 0.65 mmol) and $Pd(PPh_3)_4$ (36 mg, 0.03 mmol, 5 mol%) in 10 mL of THF was added commercially available 3-furanyl boronic acid (0.17g, 1.5 mmol) and sodium carbonate (95 mg, 0.9 mmol). After the reaction mixture was refluxed for 4 h, the solution was poured into water and the mixture was extracted with 15 mL of Et_2O. Drying over Na_2SO_4, followed by evaporation of solvent and chromatography on silica gel using 5% Et_2O in hexane afforded **177** as a pale yellow oil (35 mg, 28%). IR (neat): 2098, 1948 cm^{-1}; ^1H NMR (400 MHz, $CDCl_3$) δ 7.38 (t, *J* = 1.8 Hz, 1H), 7.37 (s, 1H), 6.4(d, *J* = 1.73 Hz, 1H), 5.42 (m, 1H), 3.40 (t, *J* = 6.9 Hz, 2H), 2.37 (q, *J* = 6.6 Hz, 2H), 2.01 (d, *J* = 2.9 Hz, 3H); ^{13}C NMR (75 MHz, $CDCl_3$) δ 204.4, 143.7, 138.8, 124.9, 109.4, 95.3, 89.3, 51.1, 29.0, 17.6; TOFMSES *m/z* relative intensity (MH^+ 20); HRMS (+ESMS) Calcd for $C_{10}H_{12}N_3O$: 190.0980 , Found: 190.0987.

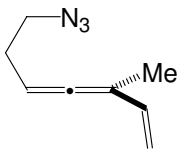

1-Azido-6-methylhepta-3,4,7-triene (161a).

Following General Procedure 1, azidomesylate **163** (0.20 g, 0.92 mmol) and vinyl magnesium bromide (1.0 M, 3.0 mL) was converted into azidoallene **161a** (105 mg, 76%). IR (neat): 2097, 1948 cm^{-1}; ^1H NMR (360 MHz, $CDCl_3$) δ 6.25 (dd, *J* = 17.4, 10.6 Hz, 1H) 5.16 (m, 1H), 5.04 (d, *J* = 17.4 Hz, 1H), 4.96 (d, *J* = 10.6 Hz, 1H), 3.26 (t, *J* = 6.9 Hz, 2H), 2.22 (q, *J* = 6.7 Hz, 2H), 1.75 (d, *J* = 2.7 Hz, 3H); ^{13}C NMR (90 MHz, $CDCl_3$) δ 207.9, 136.0, 113.0, 101.9, 87.2, 51.0, 28.8, 15.1; APCIMS *m/z* relative intensity 244 (MH^+-N_2 100); HRMS (+ESI) Calcd for $C_{16}H_{23}N_6$ (M_2H^+): 299.1984, Found: 299.1976.

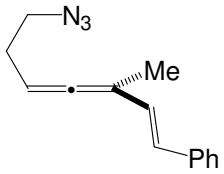

(*E*)-1-Azido-6-methyl-8-(phenyl)octa-3,4,7-triene (161b).

To a solution of propargyl azidomesylate **163** (55 mg, 0.25 mmol) and $Pd(PPh_3)_4$ (15 mg, 0.01 mmol, 5 mol%) in 10 mL of THF was added commercially available *trans*-2-phenylvinylboronic acid (67 mg, 0.45 mmol) and sodium carbonate (95 mg, 0.9 mmol). After the reaction mixture was refluxed for 4 h, the solution was poured into water and the mixture was extracted with 15 mL of Et_2O. Drying over Na_2SO_4, followed by

evaporation of solvent and chromatography on silica gel using 5% Et_2O in hexane afforded **161b** as a pale yellow oil (33 mg, 59%). IR (neat): 2096, 1942 cm^{-1}; ^1H NMR (360 MHz, $CDCl_3$) δ 7.11-7.38 (m, 5H), 6.68 (d, *J* = 16.1 Hz, 1H), 6.35 (d, *J* = 16.4 Hz, 1H), 5.24 (bs, 1H), 3.29 (t, *J* = 6.7 Hz, 2H), 2.76 (q, *J* = 6.7 Hz, 2H), 1.87 (d, *J* = 2.1 Hz, 3H); ^{13}C NMR (90 MHz, $CDCl_3$) δ 208.9, 137.9, 129.0, 128.1, 128.0, 127.7, 126.7, 102.3, 87.4, 51.3, 29.0, 15.9; APCIMS *m/z* relative intensity 198 (MH^+-N_2 100); HRMS (+ESI) Calcd for $C_{14}H_{16}N$: 198.1283, Found: 198.1292.

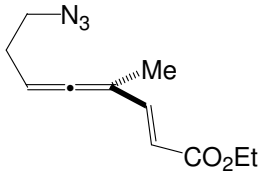

Ethyl (*E*)-1-Azido-4-(methyl)oct-2,4,5-trienoate (161c).

To a solution of propargyl azidomesylate **163** (0.12 g, 0.50 mmol) and $Pd(PPh_3)_4$ (30 mg, 0.02, 5 mol%) in 10 mL of THF was added (*Z*)-ethoxycarbonylethenylzinc **179** iodide[76] (1.5 mmol), and the mixture was heated at 50 °C for 3 h. At this time, the reaction solution was cooled to room temperature, water was added and the mixture was extracted with 15 mL of Et_2O. The organic layer was dried over Na_2SO_4 and solvent was evaporated in vacuo. The crude product was purified by chromatography using 8% Et_2O in hexane as the eluent to give **161c** as a yellow oil (35 mg, 32%). IR (neat): 2099, 1941 cm^{-1}; ^1H NMR (400 MHz, $CDCl_3$) δ 7.32 (d, *J* = 15.7 Hz, 1H), 5.83 (d, *J* = 15.7 Hz, 1H), 5.38 (bs, 1H), 4.22 (q, *J* = 7.2 Hz, 2H), 3.38 (t, *J* = 6.7 Hz, 2H), 2.37 (q, *J* = 6.7 Hz, 2H), 1.87 (d, *J* = 2.6 Hz, 3H), 1.37 (t, *J* = 7.2 Hz, 3H) ; ^{13}C NMR (100 MHz, $CDCl_3$) δ 211.3, 167.1, 144.9, 118.2, 101.2, 87.8, 60.7, 50.9, 28.4, 15.4, 14.7; APCIMS *m/z* relative

intensity 194 (MH^+-N_2 100); HRMS (+ESI) Calcd for $C_{11}H_{16}NO_2$: 194.1181, Found: 194.1179.

Thermolysis/Cyclization of Allene Substrates.

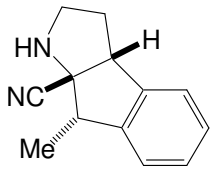

Phenyl Substrate (166a).

Following General Procedure 2, azidoallene **159a** (45 mg, 0.23 mmol) was converted into cyanopyrrolidine **166a** (23 mg, 50%). IR (neat): 3342, 2097 cm^{-1}; ^1H NMR (400 MHz, $CDCl_3$) δ 7.29-7.27 (m, 2H), 7.14-7.19 (m, 2H), 4.05 (dd, *J* = 8.7, 2.7 Hz, 1H), 3.64 (q, *J* = 7.2 Hz, 1H), 3.24 (apparent q, *J* = 7.3 Hz, 1H), 3.12-3.07 (m, 1H), 2.56-2.48 (m, 1H), 2.15-2.07 (m 1H), 1.51 (d, *J* = 7.1 Hz, 3H); ^{13}C NMR (75 MHz, $CDCl_3$) δ 144.0, 143.2, 128.2, 128.1, 124.4, 124.0, 123.2, 68.3, 55.5, 47.5, 46.7, 31.3, 12.5; APCIMS *m/z* relative intensity 199 (MH^+ 100); HRMS (+APCI) Calcd for $C_{13}H_{14}N_2$: 199.1241, Found: 199.1229.

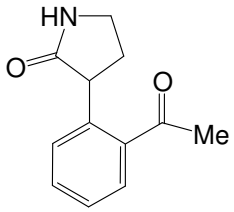

3-(2-Acetyl-phenyl)-pyrrolidin-2-one (165)

A deoxygenated solution of allenylazide **159a** (30 mg, 0.15 mmol) in toluene-d_8, (2 mL) was heated in a sealed tube at 100 °C for 5 h. The reaction mixture was cooled to room temperature and solvent evaporated to give a brown film. Purification of this crude oil by flash chromatography (9:1 EtOAc/Et_3N) resulted in **165** as a yellow film (19 mg, 62 %). IR (neat): 3297, 1684 cm^{-1}; ^1H NMR (400 MHz, $CDCl_3$) δ 7.73 (d, *J* = 7.7 Hz, 1H) 7.49 (t, *J* = 6.4 Hz, 1H), 7.36 (q, J = 7.7 Hz, 2H), 4.31 (t, *J* = 9.4 Hz, 1H), 3.49 (dd, *J* = 8.9, 4.8 Hz, 2H), 2.77 (m, 1H), 2.63 (s, 3H) 2.22 (m 1H); ^{13}C NMR (75 MHz, $CDCl_3$) δ 202.6, 179.1, 139.2, 139.0, 132.5, 130.3, 129.6, 127.3, 45.6, 40.8, 32.0, 30.0; APCIMS *m/z* relative intensity 204 (MH^+40); HRMS (+APCI) Calcd for $C_{12}H_{14}NO_2$: 204.1025, Found: 204.1033.

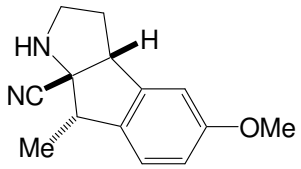

Methoxyphenyl Substrate (166b).

Following General Procedure 2, azidoallene **159b** (70 mg, 0.31 mmol) was converted into cyanopyrrolidine **166b** (36 mg, 52%). IR (neat): 3441, 2220 cm^{-1}; ^1H NMR (400 MHz, $CDCl_3$) δ 7.04 (d, *J* = 8.3 Hz, 1H), 6.81 (dd, *J* = 8.9, 1.9 Hz, 1H), 6.70 (s, 1H), 3.99 (dd, *J* = 6.7, 2.2 Hz, 1H), 3.81 (s, 3H), 3.59 (q, *J* = 7.1, 1H), 3.24 (apparent q, *J* = 9.2 Hz, 1H), 3.12 (ddd, *J* =8.3, 8.3, 4.3 Hz, 1H), 2.53-2.45 (m, 1H), 2.13-2.06 (m, 1H), 1.76 (bs, 1H), 1.47 (d, 7.1 Hz, 3H); ^{13}C NMR (75 MHz, $CDCl_3$) δ 160.3, 145.5, 135.3, 124.6, 123.2, 113.8, 110.0, 68.5, 55.9, 55.4, 46.8, 31.1, 12.8; APCIMS *m/z* relative

intensity 229 (MH^+ 100); HRMS (+APCI) Calcd for $C_{14}H_{17}N_2O$: 229.1335, Found: 229.1335.

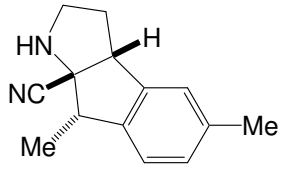

Methylphenyl Substrate (166c).

Following General Procedure 2, azidoallene **159c** (35 mg, 0.16 mmol) was converted into cyanopyrrolidine **166c** (22 mg, 63%) and **166c'** (4 mg, 9%). IR (neat): 3337, 2220 cm^{-1}; ^1H NMR (400 MHz, $CDCl_3$) δ 7.09 (d, *J* = 7.7 Hz, 1H), 7.02 (d, *J* = 7.7 Hz, 1H), 6.98 (s, 1H), 4.01 (dd, *J* = 8.7, 2.4 Hz, 1H), 3.60 (q, *J* = 7.0 Hz, 1H), 3.25 (apparent q, *J* = 8.5 Hz, 1H), 3.10 (ddd, *J* = 8.0, 8.0, 3.6 Hz, 1H), 2.53-2.45 (m, 1H), 2.36 (s, 3H), 2.13-2.06 (m, 1H), 1.85 (bs, 1H), 1.48 (d, *J* = 7.1 Hz, 3H); ^{13}C NMR (75 MHz, $CDCl_3$) δ 144.1, 140.2, 138.1, 128.9, 125.1, 123.7, 123.9, 68.4, 55.4, 47.1, 46.7, 31.1, 21.7, 12.6; APCIMS *m/z* relative intensity 213 (MH^+ 100); HRMS (+APCI) Calcd for $C_{14}H_{17}N_2$: 213.1381, Found: 213.1386.

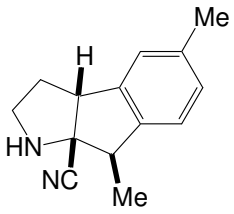

(166c').

^1H NMR (400 MHz, $CDCl_3$) δ 7.10 (m, 2H), 6.99 (s, 1H), 6.98 (s, 1H), 4.08 (dd, *J* = 10.0, 2.5 Hz, 1H), 3.31 (q, *J* = 7.1 Hz, 1H), 3.22 (m, 1H), 3.11 (m, 1H), 2.53 (m, 1H),

2.36 (s, 3H), 2.02 (m, 1H), 1.82 (bs, 1H), 1.44 (d, *J* = 7.3 Hz, 3H); ^{13}C NMR (75 MHz, $CDCl_3$) δ 141.6, 140.5, 136.8, 127.7, 124.0, 123.3, 120.6, 70.0, 53.8, 47.4, 45.5, 29.9, 20.3, 19.3.

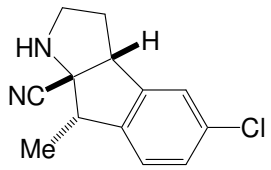

Chlorophenyl Substrate (166d).

Following General Procedure 2, azidoallene **159d** (35 mg, 0.15 mmol) was converted into cyanopyrrolidine **166d** (16 mg, 47%). Crystals suitable for X-ray crystallographic analysis were obtained by slow evaporation of an Et_2O solution of **166d** over a period of 48 h at 25 °C. Mp: 92-98 °C; IR (neat): 3338, 2220 cm^{-1}; ^{1}H NMR (400 MHz, $CDCl_3$) δ 7.24 (dd, *J* = 8.1, 1.3 Hz, 1H), 7.15 (s, 1H), 7.06 (d, *J* = 8.1 Hz, 1H), 4.01 (dd, *J* = 8.9, 2.7 Hz, 1H), 3.58 (q, *J* = 7.0 Hz, 1H), 3.24 (apparent q, *J* = 8.3 Hz, 1H), 3.12 (ddd, *J* = 8.1, 8.1, 4.3 Hz, 1H), 2.55-2.47 (m, 1H), 2.12-2.04 (m, 1H), 1.88 (bs, 1H), 1.48 (d, *J* = 7.1 Hz, 3H); ^{13}C NMR (75 MHz, $CDCl_3$) δ 146.0, 141.7, 133.9, 128.4, 125.2, 124.8, 122.8, 68.4, 55.1, 47.1, 46.6, 31.1, 12.5; APCIMS *m/z* relative intensity 233 (MH^+ 100); HRMS (+APCI) Calcd for $C_{13}H_{14}N_2Cl$: 233.0845, Found: 233.0840.

X-Ray Analysis (166d).

A clear plate shaped crystal of **166d** ($C_{13}H_{13}ClN_2$) with approximate dimensions 0.1 x 0.17 x 0.25 mm was used for the X-ray crystallographic analysis. The X-ray intensity data were measured at 98(2) K, cooled by Rigaku-MSC X-Stream 2000, on a

Bruker SMART APEX CCD area detector system equipped with a graphite monochromator and a MoKα fine-focus sealed tube (λ = 0.71073Å) operated at 1600 watts power (50 kV, 32 mA). The detector was placed at a distance of 5.8 cm from the crystal.

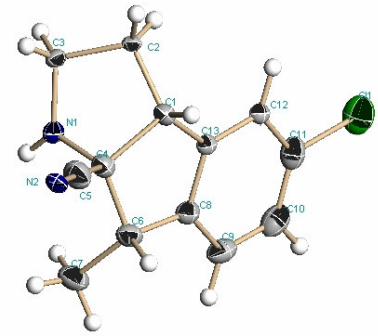

A total of 1850 frames were collected with a scan width of 0.3º in ω and an exposure time of 5 seconds/frame. The total data collection time was about 4 hours. The frames were integrated with the Bruker SAINT software package using a narrow-frame integration algorithm. The integration of the data using a Monoclinic unit cell yielded a total of 7319 reflections to a maximum θ angle of 28.29θ (0.90 Å resolution), of which 2783 were independent, completeness = 95.5 %, R_{int} = 0.0290, R_{sig} = 0.0322 and 2483 were greater than 2θ (I). The final cell constants: a = 9.6258(16)Å, b = 7.7123(13)Å, c = 16.200(3)Å, α = 90°, β = 103.750(3)°, γ = 90°, volume = 1168.2(3)$Å^3$, are based upon the refinement of the XYZ-centroids of 4472 reflections above 20θ (I) with 2.588° <θ <28.289° . Analysis of the data showed negligible decay during data collection. Data were corrected for absorption effects using the multiscan technique (SADABS). The ratio of minimum to maximum apparent transmission was 0.927354.

The structure was solved and refined using the Bruker SHELXTL (Version 6.1)

Software Package, using the space group P2(1)/c, with Z = 4 for the formula unit, $C_{13}H_{13}ClN_2$. The final anisotropic full-matrix least-squares refinement on F^2 with 146 variables converged at R1 = 5.03 %, for the observed data and wR2 = 12.77 % for all data. The goodness-of-fit was 1.079. The largest peak on the final difference map was 0.690 $e^-/Å^3$ and the largest hole was -0.677 $e^-/Å^3$. Based on the final model, the calculated density of the crystal is 1.323 g/cm^3 and F(000) amounts to 488 electrons.

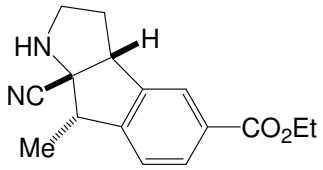

Phenylester Substrate (166e).

Following General Procedure 2, azidoallene **159e** (30 mg, 0.11 mmol) was converted into cyanopyrrolidine **166e** (11 mg, 37%). IR (neat): 3339, 2225, 1714 cm^{-1}; ^1H NMR (400 MHz, $CDCl_3$) δ 7.98 (d, *J* = 7.9 Hz, 1H), 7.85 (s, 1H), 7.20 (d, *J* = 7.9 Hz, 1H), 4.38 (q, *J* = 7.1 Hz, 2H), 4.06 (dd, *J* = 8.7, 2.5 Hz, 1H), 3.65 (q, *J* = 6.9 Hz, 1H), 3.27 (apparent q, *J* = 8.5 Hz, 1H), 3.14-3.07 (m, 1H), 2.60-2.51 (m, 1H), 2.20-2.12 (m, 1H), 1.69 (bs, 1H), 1.52 (d, *J* = 7.1 Hz, 3H), 1.41 (t, *J* = 7.1 Hz, 3H); ^{13}C NMR (75 MHz, $CDCl_3$) δ 166.8, 148.5, 144.5, 130.8, 129.9, 125.8, 123.9, 122.8, 68.3, 61.5, 55.1, 47.6, 46.6, 31.1, 14.8, 12.5; APCIMS *m/z* relative intensity 271 (MH^+ 100); HRMS (+APCI) Calcd for $C_{16}H_{19}N_2O_4$: 271.1423, Found: 271.1441.

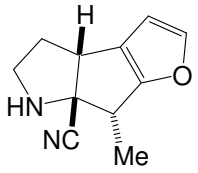

Furanyl Substrate (178).

Following General Procedure 2, azidoallene **177** (30 mg, 0.16 mmol) was converted into cyanopyrrolidine **178** (8 mg, 27%). IR (neat): 3346, 2098 cm^{-1}; ^1H NMR (400 MHz, $CDCl_3$) δ 7.34 (d, *J* = 1.0 Hz, 1H), 6.2 (d, *J* = 1.8 Hz, 1H), 3.97 (dd, *J* = 8.4, 4.0 Hz, 1H), 3.46 (q, *J* = 7.1, 1H), 3.22 (m, 1H), 3.11-3.18 (m, 1H), 2.16-2.24 (m, 1H), 1.93-2.04 (m, 1H), 1.34 (d, 7.1 Hz, 3H); ^{13}C NMR (75 MHz, $CDCl_3$) δ 157.3, 147.6, 127.0, 123.0, 107.6, 72.6, 50.7, 48.0, 41.6, 29.2, 13.6; TOFMSES *m/z* relative intensity 189 (MH^+ 100); HRMS (+ES) Calcd for $C_{11}H_{13}N_2O$: 189.1028, Found: 189.1019.

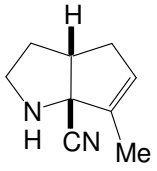

Vinyl Substrate (180a).

Following General Procedure 2, azidoallene **161a** (20 mg, 0.10 mmol) was converted into cyanopyrrolidine **180a** (19 mg, 96 %). IR (neat): 3426, 2097 cm^{-1}; ^1H NMR (400 MHz, $CDCl_3$) δ 5.5 (d, *J* = 1.3 Hz, 1H), 3.20 (dddd, *J* = 11.5, 8.7, 5.9, 2.7 Hz, 1H), 3.07 (dt, *J* = 10.4, 6.3, 6.3 Hz, 1H), 2.92 (dt, *J* = 10.4, 6.2, 6.2 Hz, 1H), 2.76 (dddd, *J* = 11.2, 8.8,4.9, 2.5 Hz, 1H), 2.22-2.16 (m, 1H), 2.16-2.09 (m, 1H), 1.85 (bs, 1H) 1.54 (d, *J*= 7.3 Hz, 3H), 1.57-1.49 (m, 1H); ^{13}C NMR (100 MHz, $CDCl_3$) δ 137.2, 129.8,

122.5, 72.8, 49.0, 47.3, 38.5, 36.0, 12.9; APCIMS *m/z* relative intensity 149 (MH^+ 100); HRMS (+APCI) Calcd for $C_9H_{13}N_2$: 149.1075, Found: 149.1073.

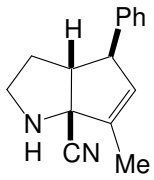

(*E*)-Styryl Substrate (180b).

Following General Procedure 2, azidoallene **161b** (18 mg, 0.08 mmol) was converted into cyanopyrrolidine **180b** (15 mg, 84%). IR (neat): 3331, 2098 cm^{-1}; ^1H NMR (400 MHz, $CDCl_3$) δ 7.37-7.17 (m, 5H), 5.59 (s, 1H), 3.6 (s, 1H), 3.17-3.14 (m, 2H), 3.04-2.98 (m, 1H), 2.28-2.20 (m, 1H), 1.96 (d, *J* = 1.27 Hz, 3H), 1.89-1.78 (m, 1H); ^{13}C NMR (100 MHz, $CDCl_3$) δ 144.1, 138.3, 133.5, 129.3, 127.6, 127.3, 122.3, 72.8, 59.1, 58.4, 47.2, 35.4, 13.1; APCIMS *m/z* relative intensity 225 (MH^+ 100); HRMS (+APCI) Calcd for $C_{15}H_{17}N_2$: 225.1390, Found: 225.1386.

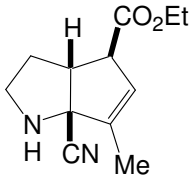

(*E*)-Acryloyl Substrate (180c).

Following General Procedure 2, azidoallene **161c** (18 mg, 0.08 mmol) was converted into cyanopyrrolidine **180c** (16 mg, 90 %). IR (neat): 3250, 2090, 1731 cm^{-1}; ^1H NMR (300 MHz, $CDCl_3$) δ 5.57(s, 1H), 4.19 (q, *J* = 7.1 Hz, 2H) 3.53 (m, 1H), 3.30 (d, *J* = 2.3 Hz, 1H), 3.17-3.09 (m, 1H), 2.96-2.88 (m, 1H), 2.31-2.19 (m, 1H), 1.89 (t, *J* =

1.6 Hz, 3H), 1.89-1.58 (m, 1H) 1.30 (t, J = 7.2 Hz, 3H); ^{13}C NMR (75 MHz, $CDCl_3$) δ 172.7, 140.7, 127.5, 121.5, 72.4, 61.8, 57.0, 51.8, 47.2, 34.8, 14.6, 13.1; APCIMS *m/z* relative intensity 225 (MH^+ 100); HRMS (+ESI) Calcd for $C_{12}H_{17}N_2O_2$: 221.1289, Found: 221.1284

6.4 Extension of the Intramolecular Allenyl Azide Cyclization Chemistry to Cyclopentannelated Indoles

6.4.1 General Procedure 3. Allenyl Azide Synthesis

To a solution of $ZnCl_2$ (2.5 equiv) in THF (0.30 M solution) was added the appropriate Grignard reagent RMgBr (2.5 equiv) and the mixture was stirred at room temperature for 1 h. $Pd(PPh_3)_4$ (5 mol%) in 2 mL of THF and the propargylic acetate **188** (1 equiv) in THF (5 mL) were added sequentially. The reaction mixture was allowed to stir at room temperature for 20 min. After addition of an equal volume of a saturated NH_4Cl solution, the organic layer was extracted into Et_2O and washed with water and brine. Drying the organic phase over Na_2SO_4 and removal of solvent under reduced pressure resulted in a dark oil. This crude product was purified by chromatography using pure hexane as the eluent.

6.4.2 General Procedure 4. Allenyl Azide Synthesis

To a solution of CuBr•Me_2S (12 equiv) in 20 mL of THF at -40 °C was added MeMgBr (12 equiv) and the mixture was stirred for 1 h, after which propargyl alkenyl acetate **188** (1.0 equiv) in 5 mL of THF was cannulated into the reaction mixture at -40 °C. The reaction mixture was warmed to room temperature over a period of 8 h to allow complete consumption of starting material. The excess cuprate was then destroyed with drop-wise addition of saturated NH_4Cl solution. The organic layer was extracted with 3x50 mL of Et_2O and washed with water and brine. Drying the combined organic extracts

over Na_2SO_4 and removal of solvent under reduced pressure resulted in a brown oil. This crude product was purified by column chromatography using pure hexanes as the eluent.

6.4.3 General Procedure 5. Azidophenyl Alkynyl Alcohol Synthesis

A solution of the appropriate alkyne (1.0 equiv) in THF (20 mL) was cooled to -78 °C and *n*-butyllithium (2.3 M in hexanes, 1.0 equiv) was added. The reaction mixture was stirred at -78 °C for 30 min. 2-Azidobenzaldehyde (**187**) (1.0 equiv) in 5 mL of THF was cannulated into the reaction mixture and the solution was warmed to room temperature over a period of 2 h. The reaction mixture was poured into an equal amount of saturated NH_4Cl solution and extracted with 3x30 mL of Et_2O. The combined organic layers were washed with water and brine, dried over Na_2SO_4 and the solvent was evaporated. The crude alcohol was purified by flash chromatography using 40% Et_2O in hexanes to give the alkynyl alcohols.

6.4.4 General procedure 6. Azidophenyl Alkynyl Acetate Synthesis

Acetic anhydride (1.2 equiv) and DMAP (1.2 equiv) were added to an ice-cold solution of an appropriate 1-(2-azidophenyl)propargyl alcohol (1.0 equiv) in 40 mL of CH_2Cl_2, and the mixture was stirred for 24 h with warming to room temperature. The reaction mixture was poured into 30 mL of saturated $NaHCO_3$ solution. The mixture was then extracted with 3x30 mL of CH_2Cl_2 and the combined organic layers were washed

with water and brine, dried over Na_2SO_4 and concentrated *in vacuo*. The crude material was purified by column chromatography (25% Et_2O in hexanes) to give the acetates.

6.4.5 General Procedure 7. Cyclization

A deoxygenated solution of allenylazide **184** in toluene-d_8, (0.10 M) was heated in a clean, sealed tube for 15 min, after which the reaction mixture was cooled to room temperature. Evaporation of the solvent *in vacuo* gave a brown oil. The ratio of the products **185/186** was determined at this stage by ^{1}H NMR analysis. Purification of this crude oil using an alumina column resulted in two products; **185** (80% Et_2O in hexanes) and **189** (10% Et_2O in hexanes).

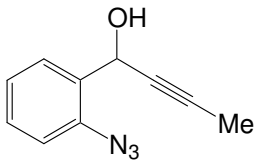

1-(2-Azidophenyl)but-2-yn-1-ol.

To a solution of 2-azidobenzaldehyde (**187**) (2.0 g, 14 mmol) in 20 mL of THF at -20 °C was added 1-propynylmagnesium bromide (0.50 M, 30 mL, 15 mmol) and the mixture was stirred for 2 h. The reaction mixture was warmed to room temperature over an additional hour and poured into 20 mL of saturated NH_4Cl solution. The organic layer was extracted with 3x30 mL of Et_2O and the combined organic extracts were washed with water and brine, dried over Na_2SO_4 and the solvent was evaporated to yield a brown oil. The crude material was carried over to the next step. A small batch was purified by

column chromatography (40% Et_2O in hexanes) to give a white solid: mp 49 - 50 °C; IR (neat): 3400, 2125 cm^{-1}; ^1H NMR (300 MHz, C_6D_6) δ 7.69 (m, 1H), 6.86 (m, 2H), 6.61 (m, 1H), 5.67 (d, *J* = 2.1 Hz, 1H), 3.07 (br s, 1H), 1.47 (d, *J* = 2.2 Hz, 3H); ^{13}C NMR (75 MHz, $CDCl_3$) δ 137.0, 131.9, 129.4, 128.1, 124.9, 118.0, 82.9, 78.2, 60.3, 3.6; TOFESMS *m/z* relative intensity 210.1 (MNa^+ 100%); HRMS (+ES) Calcd for $C_{10}H_9N_3ONa$: 210.0643, Found: 210.0639.

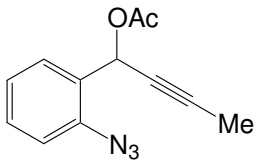

1-Acetoxy-1(2-azidophenyl)but-2-yne (188a).

Following General Procedure 6, 1-(2-azidophenyl)but-2-yn-1-ol (2.0 g, 11 mmol) was converted to acetate **188a** (1.5 g, 61%): mp 49-50 °C; IR (neat): 2140, 1736 cm^{-1}; ^1H NMR (360 MHz, C_6D_6) δ 7.75 (dd, *J* = 7.5, 1.8 Hz, 1H), 6.91 (m, 3H), 6.64 (dd, *J* = 7.6, 1.4 Hz, 1H), 1.66 (s, 3H), 1.45 (d, *J* = 2.3 Hz, 3H); ^{13}C NMR (90 MHz, C_6D_6) δ 168.9, 138.1, 130.2, 129.5, 129.3, 124.9, 118.4, 83.6, 76.4, 61.3, 20.4, 3.3; TOFESMS *m/z* (relative intensity) 252.0 (MNa^+, 100%), 284.0 ($MMeOH^+$,70%); HRMS Calcd for $C_{12}H_{11}N_3O_2Na$: 252.0749, Found: 252.0762.

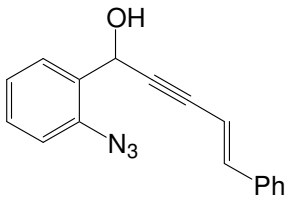

1-(2-Azidophenyl)5-phenylpent-4-en-2-yn-ol.

Following General Procedure 5, 2-azidobenzaldehyde (**187**) (0.46 g, 3.1 mmol) was treated with 4-phenylbut-3-en-1-ynyllithium (1.0 equiv, 3.1 mmol) to give 1-(2-azidophenyl)5-phenylpent-4-en-2-yn-ol as a bright yellow oil (460 mg, 54%). IR (neat): 3396, 2126 cm^{-1}; ^{1}H NMR (400 MHz, $CDCl_3$) δ 7.71 (dd, *J* = 8.1, 1.3 Hz, 1H), 7.44-7.23 (m, 8H), 7.02 (d, *J* = 16.3 Hz, 1H), 6.24 (dd, *J* = 16.3, 1.9 Hz, 1H), 5.84 (m, 1H), 2.75 (bs, 1H) ; ^{13}C NMR (75 MHz, $CDCl_3$) δ 142.6, 137.8, 136.5, 132.2, 130.2,129.3, 129.2, 128.9, 126.8, 125.6, 118.8, 107.8, 90.7, 86.1, 61.5; TOFESMS *m/z* relative intensity 276 (MH^+ 30); HRMS (+ES) Calcd for $C_{13}H_{15}N_3O$: 276.1137, Found: 276.1123.

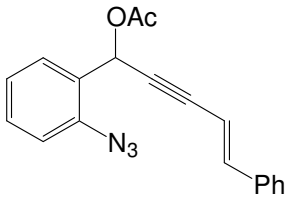

1-Acetoxy-1-(2-azidophenyl) 5-phenylpent-4en-2-yne (188d).

Following General Procedure 6, 1-(2-azidophenyl)5-phenylpent-4-en-2-yn-ol (0.40 g, 1.6 mmol) was converted to acetate **188d** (460 mg, 91%). IR (neat): 2127, 1742 cm^{-1}; ^{1}H NMR (400 MHz, $CDCl_3$) δ 7.78 (dd, *J* = 7.8, 1.3 Hz, 1H), 7.44-7.20 (m, 8H), 7.04 (d, *J* = 16.3 Hz, 1H), 6.87 (d, *J* = 1.8 Hz, 1H) 6.22 (dd, *J* = 16.3, 2.0 Hz, 1H), 2.16 (s, 3H); ^{13}C NMR (75 MHz, $CDCl_3$) δ 170.0, 143.2, 138.3, 136.3, 130.8, 129.8, 129.4, 129.2, 128.6, 126.8, 125.5, 118.8, 107.5, 87.5, 86.7, 61.9, 21.4; TOFESMS *m/z* relative intensity 318 (MH^+ 68); HRMS (+ES) Calcd for $C_{19}H_{16}N_3O_2$: 318.1243, Found: 318.1261.

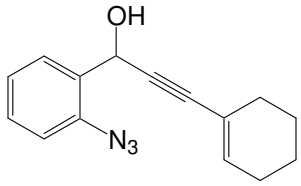

1-(2-Azidophenyl)3-cyclohex-1-enylprop-2-yn-1-ol.

Following General Procedure 5, 2-azidobenzaldehyde (**187**) (0.50 g, 3.4 mmol) was treated with 1-cyclohexenylethynyllithium (0.85 equiv, 2.9 mmol) to give 1-(2-azidophenyl)3-cyclohex-1-enylprop-2-yn-1-ol as a yellow oil (280 mg, 38%). IR (neat): 3390, 2126 cm^{-1}; ^{1}H NMR (300 MHz, $CDCl_3$) δ 7.67 (d, *J* = 7.7 Hz, 1H), 7.36 (m, 1H), 7.19-7.11 (m, 2H), 6.16 (m,1H), 5.76 (d, *J* = 4.6 Hz, 1H), 3.23 (d, *J* = 5.3 Hz, 1H), 2.15-2.09 (m, 4H), 1.64-1.58 (m, 4H); ^{13}C NMR (75 MHz, $CDCl_3$) δ 137.7, 136.1, 132.5, 130.0, 128.9,125.5, 120.5, 118.7, 88.7, 85.9, 61.1 29.5, 26.1, 22.7, 21.9; TOFESMS *m/z* relative intensity 254 (MH^+ 75); HRMS (+ES) Calcd for $C_{15}H_{16}N_3O$: 254.1293, Found: 254.1302.

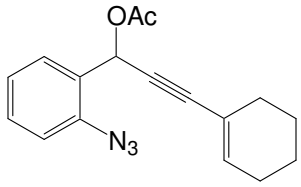

1-Acetoxy-1-(2-azidophenyl) 3-cyclohex-1-enylprop-2-yne (188e).

Following General Procedure 6, 1-(2-azidophenyl)3-cyclohex-1-enylprop-2-yn-1-ol (0.28 g, 1.1 mmol) was converted to acetate **188e** (260 mg, 80%). IR (neat): 2127, 1742 cm^{-1}; ^{1}H NMR (400 MHz, $CDCl_3$) δ 7.72 (dd, *J* = 7.5, 1.3 Hz, 1H), 7.42 (dd, *J* = 7.2, 1.5 Hz, 1H), 7.18-7.22 (m, 2H), 6.76 (m, 1H) 6.20 (m, 1H), 2.11 (s, 3H), 2.16-2.10 (m, 4H), 1.67-1.55 (m, 4H); ^{13}C NMR (75 MHz, $CDCl_3$) δ 169.9, 138.2, 137.0, 130.6, 129.8, 128.9, 125.4, 120.2, 118.7, 89.3, 82.7, 61.7, 29.3, 26.0, 22.6, 21.8, 21.5;

TOFESMS *m/z* relative intensity 318 (MNa^+ 100); HRMS (+ES) Calcd for $C_{17}H_{17}N_3O_2Na$: 318.1203, Found: 318.1218.

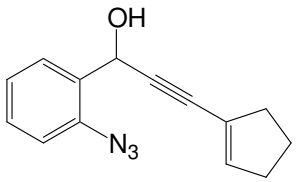

1-(2-Azidophenyl)3-cyclopent-1-enylprop-2-yn-1-ol.

Following General Procedure 5, 2-azidobenzaldehyde (**187**) (0.35 g, 2.4 mmol) was treated with 1-cyclopentenylethynyllithium (1.3 equiv, 3.2 mmol) to give 1-(2-azidophenyl)3-cyclopent-1-enylprop-2-yn-1-ol as a yellow oil (330 mg, 54%). IR (neat): 3354, 2126 cm^{-1}; ^1H NMR (400 MHz, $CDCl_3$) δ 7.67 (dd, *J* = 8.2, 1.6 Hz, 1H), 7.43 (m, 1H), 7.22-7.15 (m, 2H), 6.12 (t, *J* = 2.4 Hz, 1H), 5.80 (d, *J* = 6.2 Hz 1H), 2.61 (d, *J* = 6.1 Hz, 1H), 2.51-2.42 (m, 4H), 1.96-1.89 (m, 2H); ^{13}C NMR (75 MHz, $CDCl_3$) δ 139.0, 137.4, 131.7, 129.8, 128.5, 125.1, 123.8, 118.3, 88.9, 84.1, 61.2 36.3, 33.3, 23.3; TOFESMS *m/z* relative intensity 240 (MH^+ 30); HRMS (+ES) Calcd for $C_{14}H_{14}N_3O$: 240.1127, Found: 240.1137.

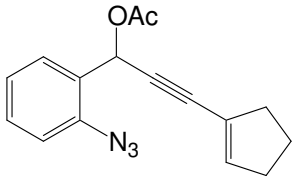

1-Acetoxy-1(2-azidophenyl) 3-cyclopent-1-enylprop-2-yne (188f).

Following General Procedure 6, 1-(2-azidophenyl)3-cyclopent-1-enylprop-2-yn-1-ol (0.33 g, 1.3 mmol) was converted to acetate **188f** (330 mg, 88%). IR (neat): 2126,

1746 cm^{-1}; ^1H NMR (400 MHz, $CDCl_3$) δ 7.71 (d, *J* = 8.6 Hz, 1H), 7.42 (d, *J* = 7.7 Hz, 1H), 7.25-7.18 (m, 2H), 6.79 (m, 1H), 6.22 (m, 1H), 2.62-2.45 (m, 4H), 2.12 (s, 3H), 1.96-1.88 (m, 2H); ^{13}C NMR (75 MHz, $CDCl_3$) δ 169.9, 140.1, 138.3, 130.6, 129.8, 128.7, 125.4, 124.0, 118.7, 86.4, 84.8, 61.9, 36.6, 33.7, 23.7, 21.5; TOFESMS *m/z* relative intensity 282 (MH^+ 30); HRMS (+ES) Calcd for $C_{16}H_{16}N_3O_2$: 282.1243, Found: 282.1229.

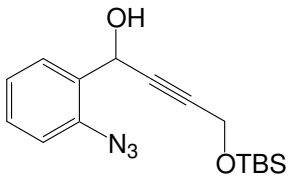

1-*t*-Butyldimethylsilyloxy-4-(2-azidophenyl)but-2-yn-4-ol.

Following General Procedure 5, 2-azidobenzaldehyde (**187**) (0.59 g, 4.0 mmol) was treated with 1-*t*-butyldimethylsilyloxybuy-2-ynyllithium (1.0 equiv, 4.0 mmol) to give 1-*t*-butyldimethylsilyloxy-5-(2-azidophenyl)but-2-yn-4-ol as a yellow oil (1.2 g, 96%). IR (neat): 3404, 2127 cm^{-1}; ^1H NMR (400 MHz, $CDCl_3$) δ 7.64 (d, *J* = 7.8 Hz, 1H), 7.39 (t, *J* = 7.6 Hz, 1H), 7.19 (d, *J* = 7.3 Hz, 2H), 5.68 (m, 1H), 4.44 (s, 2H), 0.91 (s, 9H), 0.12 (s, 6H); ^{13}C NMR (75 MHz, $CDCl_3$) δ 137.7, 131.5, 130.1, 128.8, 125.5, 118.7, 85.7, 84.0, 61.1, 52.2, 26.2, 18.7, -4.8; TOFESMS *m/z* relative intensity 318 (MH^+ 30); HRMS (+ES) Calcd for $C_{16}H_{24}N_3O_2Si$: 318.1638, Found: 318.1636.

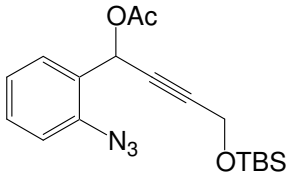

1-*t*-Butyldimethylsilyloxy-4-acetoxy-4-(2-azidophenyl)but-2-yne (188g).

Following General Procedure 6, 1-*t*-butyldimethylsilyloxy-4-(2-azidophenyl)but-2-yn-4-ol (1.3 g, 3.9 mmol) was converted to acetate **188g** (1.3 g, 92%). IR (neat): 2127, 1745 cm^{-1}; ^1H NMR (400 MHz, $CDCl_3$) δ 7.69 (d, *J* = 7.6 Hz, 1H), 7.40 (t, *J* = 7.6 Hz, 1H), 7.18 (d, *J* = 7.8 Hz, 2H), 6.68 (m,1H), 4.44 (d, *J* = 1.8 Hz, 2H), 2.11 (s, 3H), 0.91 (s, 9H), 0.11 (s, 3H), 0.10 (s, 3H); ^{13}C NMR (75 MHz, $CDCl_3$) δ 169.8, 138.2, 130.7, 129.7, 128.3, 125.3, 118.6, 86.3, 81.2, 61.2, 52.2, 26.1, 21.3, 18.6, -4.8; TOFESMS *m/z* relative intensity 360 (MH^+ 80); HRMS (+ES) Calcd for $C_{18}H_{26}N_3O_3Si$: 360.1743, Found: 360.1731.

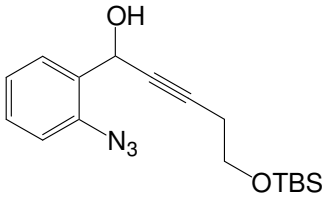

1-*t*-butyldimethylsilyloxy-5-(2-azidophenyl)pent-3-yn-5-ol.

Following General Procedure 5, 2-azidobenzaldehyde (**187**) (0.66 g, 4.4 mmol) was treated with 1-*t*-butyldimethylsilyloxypent-3-ynyllithium (1.0 equiv, 4.4 mmol) to give 1-*t*-butyldimethylsilyloxy-5-(2-azidophenyl)pent-3-yn-5-ol as a yellow oil (1.3 g, 96%). IR (neat): 3423, 2110 cm^{-1}; ^1H NMR (400 MHz, $CDCl_3$) δ 7.68 (d, *J* = 7.5 Hz, 1H), 7.37 (t, *J* = 7.2 Hz, 1H), 7.18 (t, *J* = 7.3 Hz, 2H), 5.64 (m,1H), 3.76 (t, *J* = 7.1 Hz, 2H), 2.50 (dt, *J* = 7.0, 1.8 Hz, 2H), 0.91 (s, 9H), 0.08 (s, 6H); ^{13}C NMR (75 MHz,

$CDCl_3$) δ 137.8, 132.3, 130.1, 128.9, 125.5, 118.7, 85.0, 80.4, 62.1, 61.2, 26.3, 23.7, 18.7, -4.9 (2C); TOFESMS *m/z* relative intensity 332 (MH^+ 40); HRMS (+ES) Calcd for $C_{17}H_{26}N_3O_2Si$: 332.1794, Found: 332.1780.

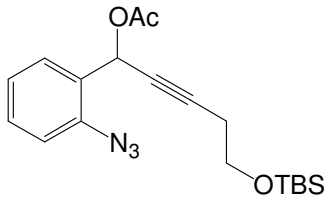

1-*t*-Butyldimethylsilyloxy-5-acetoxy-5-(2-azidophenyl)pent-3-yne (188h).

Following General Procedure 6, 1-*t*-butyldimethylsilyloxy-5-(2-azidophenyl)pent-3-yn-5-ol (1.3g, 3.9 mmol) was converted to acetate **188h** (1.2 g, 82%). IR (neat): 2129, 1747 cm^{-1}; ^1H NMR (400 MHz, $CDCl_3$) δ 7.71 (d, *J* = 7.7 Hz, 1H), 7.41 (dt, *J* = 7.7, 1.5 Hz, 1H), 7.19 (t, *J* = 7.7 Hz, 2H), 6.64 (t, *J* = 2.0 Hz, 1H), 3.75 (t, *J* = 6.9 Hz, 2H), 2.49 (dt, *J* = 6.9, 2.1 Hz, 1H), 2.11 (s, 3H), 0.89 (s, 9H), 0.07 (s, 6H); ^{13}C NMR (75 MHz, $CDCl_3$) δ 169.9, 138.2, 130.6, 129.9, 128.9, 125.4, 118.7, 85.7.3, 82.2, 61.9 61.5, 26.3, 23.7, 21.4, 18.7, -4.9 (2C); TOFESMS *m/z* relative intensity 396 (MNa^+ 65); HRMS (+ES) Calcd for $C_{19}H_{27}N_3O_3SiNa$: 396.1719, Found: 396.1716.

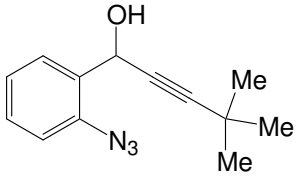

1-(2-Azidophenyl)4,4-dimethylpent-2-yn-1-ol.

Following General Procedure 5, 2-azidobenzaldehyde (**187**) (0.60 g, 4.0 mmol) was treated with 3,3-dimethylbutynyllithium (1.0 equiv, 4.0 mmol) to give 1-(2-

azidophenyl)4,4-dimethylpent-2-yn-1-ol as a yellow oil (800 mg, 87%). IR (neat): 3375, 2128 cm^{-1}; ^1H NMR (400 MHz, $CDCl_3$) δ 7.69 (d, *J* = 7.6 Hz, 1H), 7.37 (t, *J* = 7.5 Hz, 1H), 7.17-7.28 (m, 2H), 5.67 (s,1H), 2.53 (bs, 1H) 1.28 (s, 9H); ^{13}C NMR (75 MHz, $CDCl_3$) δ 137.9, 132.6, 130.0, 128.9, 125.4, 118.7, 96.4, 77.7, 60.1, 31.3 27.9; TOFESMS *m/z* relative intensity 230 (MH^+ 80); HRMS (+ES) Calcd for $C_{13}H_{16}N_3O$: 230.1293, Found: 230.1280.

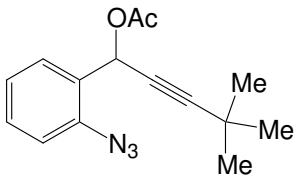

1-Acetoxy-1-(2-azidophenyl)4,4-dimethylpent-2-yne (188i).

Following General Procedure 6, 1-(2-azidophenyl)4,4-dimethylpent-2-yn-1-ol (0.80 g, 3.5 mmol) was converted to acetate **188i** (850 mg, 90%). IR (neat): 2127, 1745 cm^{-1}; ^1H NMR (400 MHz, $CDCl_3$) δ 7.72 (d, *J* = 7.8 Hz, 1H), 7.39 (t, *J* = 7.7 Hz, 1H), 7.20 (t, *J* = 8.3 Hz, 2H), 6.64 (s,1H), 2.10 (s, 3H), 1.26 (s, 9H); ^{13}C NMR (75 MHz, $CDCl_3$) δ 169.9, 138.4, 130.5, 130.0, 129.1, 125.3, 118.7, 96.7, 74.9 61.6, 31.2, 27.9, 21.5; TOFESMS *m/z* relative intensity 272 (MH^+ 32); HRMS (+MSES) Calcd for $C_{15}H_{18}N_3O_2$: 272.1399, Found: 272.1392.

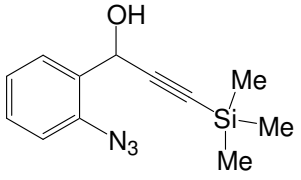

1-(Trimethylsilyl)3-(2-azidophenyl)-prop-1-yn-3-ol.

Following General Procedure 5, 2-azidobenzaldehyde (**188**) (0.44 g, 3.0 mmol) was treated with trimethylsilylethynyllithium (1.0 equiv, 3.0 mmol) to give as a 1-(trimethylsilyl)3-(2-azidophenyl)-prop-3-yn-1-ol yellow oil (582 mg, 79%). IR (neat): 3392, 2128 cm^{-1}; ^1H NMR (400 MHz, $CDCl_3$) δ 7.69 (dd, *J* = 7.4, 1.5 Hz, 1H), 7.39 (dt, *J* = 7.7, 1.6 Hz, 1H), 7.20 (t, *J* = 7.8, Hz, 1H), 5.67 (s,1H), 2.72 (bs, 1H), 0.22 (s, 9H); ^{13}C NMR (75 MHz, $CDCl_3$) δ 137.9, 131.7, 130.2, 128.9, 125.5, 118.7, 104.4, 92.1, 77.7, 61.3, 0.2; TOFESMS *m/z* relative intensity 230 (MH^+ 100); HRMS (+ES) Calcd for $C_{12}H_{16}N_3OSi$: 246.1063, Found: 246.1064.

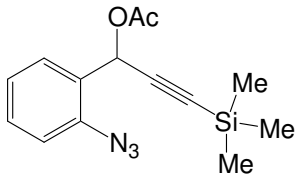

1-(Trimethylsilyl)3-acetoxy-3-(2-azidophenyl)-propyne (188j).

Following General Procedure 6, 1-(trimethylsilyl)3-(2-azidophenyl)-prop-1-yn-3-ol (0.53 g, 2.2 mmol) was converted to acetate **188j** (550 mg, 88%). IR (neat): 2127, 1747 cm^{-1}; ^1H NMR (400 MHz, $CDCl_3$) δ 7.72 (dd, *J* = 7.7, 1.4 Hz, 1H), 7.42 (dt, *J* = 7.7, 1.5 Hz, 1H), 7.20 (t, *J* = 8.3 Hz, 2H), 6.66 (s,1H), 2.10 (s, 3H), 0.2 (s, 9H); ^{13}C NMR (75 MHz, $CDCl_3$) δ 169.7, 138.4, 130.7, 130.0, 129.9, 128.3, 125.3, 118.7, 101.2, 92.8, 74.9 61.5, 21.4, 0.1; TOFESMS *m/z* relative intensity 287 (MH^+ 40); HRMS (+MSES) Calcd for $C_{14}H_{17}N_3O_2Si$: 288.1168, Found: 288.1166.

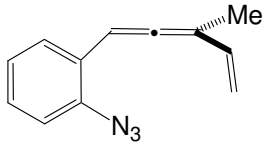

1-(2-Azidophenyl)3-methylpent-1,2,4-triene (184a).

Following General Procedure 3, **188a** (0.23 g, 1.0 mmol) and vinyl magnesium bromide (1.0 M, 3.0 mL) were converted to **184a** (114 mg, 58%). IR (neat): 2120, 1930 cm^{-1}; ^{1}H NMR (400 MHz, $CDCl_3$) δ 7.36 (d, *J* = 7.4 Hz, 1H), 7.27 (d, *J* = 7.4, 1H), 7.16 (d, *J* = 7.3 Hz, 1H), 7.10 (t, *J* = 7.3 Hz, 1H), 6.54 (m, 1H), 6.42 (dd, *J* = 17.4, 10.5 Hz, 1H), 5.25 (d, *J* = 17.4 Hz, 1H), 5.15 (d, *J* = 10.5 Hz, 1H), 1.97 (d, *J* = 2.8 Hz, 3H); ^{13}C NMR (75 MHz, $CDCl_3$) δ 210.3, 136.8, 135.0, 128.9, 128.4, 126.3, 125.3, 118.9, 114.0, 104.6, 89.1, 14.9; TOFESMS *m/z* relative intensity 170 (MH^+-N_2 100); HRMS (+ES) Calcd for $C_{12}H_{12}N$: 170.0970, Found: 170.0977.

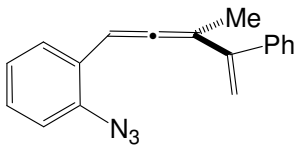

1-(2-Azidophenyl)3-methyl-5phenylpent-1,2,4-triene (184b).

Following General Procedure 3, acetate **188a** (0.20 g, 0.88 mmol) and 1-phenyl vinyl zinc bromide (0.50 M, 5.3 mL) were converted to **184b** (160 mg, 67%). IR (neat): 2124, 1932 cm^{-1}; ^{1}H NMR (300 MHz, $CDCl_3$) δ 7.25-7.55 (m, 7H), 7.16 (d, *J* = 7.6 Hz, 2H), 6.48 (m, 1H), 5.41(s, 1H), 5.32 (s, 1H), 2.19 (d, *J* = 2.7 Hz, 3H); ^{13}C NMR (75 MHz, $CDCl_3$) δ 209.8, 147.2, 141.7, 136.7, 128.6, 128.5, 128.4, 128.1, 128.0, 127.9, 126.4, 118.9, 114.4, 106.1, 90.4, 18.0; TOFESMS *m/z* relative intensity 246 (MH^+-N_2 100); HRMS (+ES) Calcd for $C_{18}H_{16}N$: 246.1283, Found: 246.1275.

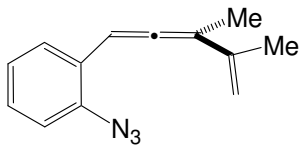

1-(2-Azidophenyl)3-methyl-4-phenylpent-1,2,4-triene (184c).

Following General Procedure 3, acetate **188a** (0.23 g, 1.0 mmol) and isopropenyl magnesium bromide (0.50 M, 6.0 mL) were converted to **184c** (125 mg, 59%). IR (neat): 2124, 1930 cm^{-1}; ^{1}H NMR (300 MHz, $CDCl_3$) δ 7.41 (d, *J* = 7.7 Hz, 1H) 7.28 (t, *J* = 7.9 Hz, 1H), 7.16-7.10 (m, 2H), 6.6 (m, 1H), 5.08 (s, 1H), 5.04 (s, 1H), 2.05 (s, 3H), 2.04 (s, 3H); ^{13}C NMR (75 MHz, $CDCl_3$) δ 208.7, 140.8, 136.7, 128.5, 128.4, 126.7, 125.3, 118.9, 112.0, 107.1, 90.3, 22.0, 16.7; TOFESMS *m/z* relative intensity 184 (MH^+-N_2 100); HRMS (+ES) Calcd for $C_{13}H_{14}N$: 184.1121, Found: 184.1126.

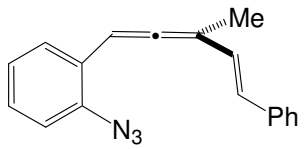

1-(2-Azidophenyl)3-methyl-4-phenylpent-1,2,4-triene (184d).

Following General Procedure 4, acetate **188d** (0.21 g, 0.65 mmol) and methyl magnesium bromide (3.0 M, 2.6 mL) were converted to **184d** (60 mg, 34%). IR (neat): 2122, 1927 cm^{-1}; ^{1}H NMR (300 MHz, $CDCl_3$) δ 7.55-7.10 (m, 9H), 6.82 (d, *J* = 16.1 Hz, 1H), 6.63 (m, 1H), 6.56 (d, *J* = 16.2 Hz, 1H), 2.09 (d, *J* = 2.8 Hz, 3H); ^{13}C NMR (75 MHz, $CDCl_3$) δ 211.6, 137.7, 136.7, 130.5, 129.0, 128.9, 128.8, 128.6, 127.8, 126.9, 126.7, 125.3, 118.9, 104.8, 89.3, 15.7; TOFESMS *m/z* relative intensity 246 (MH^+-N_2 100); HRMS (+ES) Calcd for $C_{18}H_{16}N$: 246.1283, Found: 246.1289.

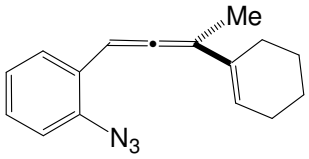

1-(2-Azidophenyl)3-cyclohex-1-enylbut-1,2-diene (184e).

Following General Procedure 4, acetate **188e** (0.30 g, 1.3 mmol) and methyl magnesium bromide (3.0 M, 5.2 mL) were converted converted to **184e** (120 mg, 37%).). IR (neat): 2123, 1928 cm^{-1}; ^{1}H NMR (400 MHz, $CDCl_3$) δ 7.38 (d, *J* = 7.5 Hz, 1H), 7.24 (d, *J* = 7.3 Hz, 1H), 7.16 (d, *J* = 7.0, 1H), 7.09 (t, *J* = 7.5 Hz, 1H), 6.57 (m, 1H), 5.81 (m, 1H), 2.2 (m, 3H), 2.07 (m, 1H), 1.97 (d, *J* = 2.7 Hz, 3H), 1.63-1.68 (m, 4H); ^{13}C NMR (75 MHz, $CDCl_3$) δ 207.6, 136.5, 133.4, 128.4, 128.2, 127.2, 125.2, 123.9, 118.8, 107.1, 90.5, 27.4, 26.4, 23.2, 22.7, 16.3 ; TOFESMS *m/z* relative intensity 224 (MH^+-N_2 100); HRMS (+ES) Calcd for $C_{16}H_{18}N$: 224.1439, Found: 224.1459

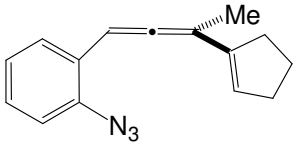

1-(2-Azidophenyl)3-cyclopent-1-enylbut-1,2-diene (184f).

Following General Procedure 4, acetate **188f** (0.30 g, 1.1 mmol) and methyl magnesium bromide (3.0 M, 4.4 mL) converted to **184f** (75 mg, 30%). IR (neat): 2112, 1930 cm^{-1}; ^{1}H NMR (400 MHz, $CDCl_3$) δ 7.38 (dd, *J* = 7.7, 1.5 Hz, 1H), 7.25 (dt, *J* = 7.0, 1.6 Hz, 1H), 7.16 (dd, *J* = 7.9, 1.1 1H), 7.09 (dt, *J* = 7.3, 1.8 Hz, 1H), 6.55 (m, 1H), 5.75 (d, *J* = 1.4 Hz, 1H), 2.50-2.35 (m, 4H), 2.02 (d, *J* = 2.7 Hz, 3H), 1.93 (m, 2H); ^{13}C NMR (100 MHz, $CDCl_3$) δ 208.8, 140.6, 136.6, 128.6, 128.2, 127.1, 127.0, 125.2, 118.8, 103.0,

89.5, 34.1, 33.8, 23.7, 17.0; APCIMS *m/z* relative intensity 210 (MH^+-N_2 100); HRMS (+APMS) Calcd for $C_{15}H_{16}N$: 210.1283, Found: 210.1302.

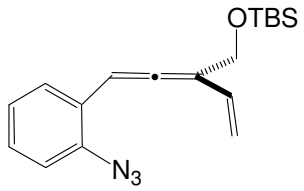

1-*t*-Butyldimethylsilyloxy-2-vinyl-4-(2-azidophenyl)but-2,3-diene (184g).

Following General Procedure 3, acetate **188g** (0.50 g, 1.4 mmol) and vinyl magnesium bromide (1.0 M, 4.2 mL) were converted to **184g** (250 mg, 55%). IR (neat): 2122, 1934 cm^{-1}; ^1H NMR (400 MHz, $CDCl_3$) δ 7.39 (dd, *J* = 7.7, 1.5 Hz, 1H), 7.29 (m, 1H), 7.18-7.09 (m, 2H), 6.10 (m, 1H), 6.38 (dd, *J* = 17.7, 10.1 Hz, 1H), 5.38 (dd, *J* = 17.4, 1.1 Hz, 1H), 5.16 (d, *J* = 10.5, 1.2 Hz, 1H), 4.48 (d, *J* = 2.5 Hz, 2H), 0.9 (s, 9H), 0.09 (s, 3H), 0.08 (s, 3H); ^{13}C NMR (75 MHz, $CDCl_3$) δ 209.0, 136.8, 132.0, 129.0, 128.7, 125.9, 125.2, 118.8, 115.1, 109.8, 91.9, 61.9, 26.2, 18.7, -4.8, -4.9; TOFESMS *m/z* relative intensity 300 (MH^+-N_2 100); HRMS (+ES) Calcd for $C_{18}H_{26}NOSi$: 300.1784, Found: 300.1812.

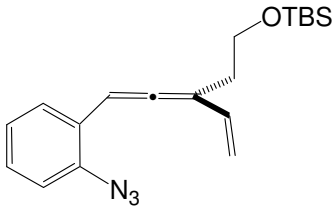

1-*t*-Butyldimethylsilyloxy-3-vinyl-5-(2-azidophenyl)but-3,4-diene (184h).

Following General Procedure 3, acetate **188h** (0.50 g, 1.3 mmol) and vinyl magnesium bromide (1.0 M, 3.9 mL) were converted to **184h** (259 mg, 57%). IR (neat): 2122, 1930 cm^{-1}; ^{1}H NMR (400 MHz, $CDCl_3$) δ 7.36 (d, *J* = 7.9 Hz, 1H), 7.25 (d, *J* = 7.3 Hz, 1H), 7.15 (d, *J* = 8.0 Hz, 1H), 7.08 (t, *J* = 7.5 Hz, 1H), 6.59 (m, 1H), 6.32 (dd, *J* = 17.5, 10.7 Hz, 1H), 5.29 (d, *J* = 17.6 Hz, 1H), 5.13 (d, *J* = 10.7 Hz, 1H), 3.81 (t, *J* = 5.8 Hz, 2H), 2.54-2.49 (m, 2H), 0.89 (s, 9H), 0.06 (s, 3H), 0.04 (s, 3H); ^{13}C NMR (75 MHz, $CDCl_3$) δ 209.8, 136.7, 134.3, 128.8, 128.6, 126.1, 125.2, 118.9, 114.0, 106.2, 90.6, 62.1, 32.1, 26.3, 18.8, -4.8 (2C); TOFESMS *m/z* relative intensity 314 (MH^+-N_2 100); HRMS (+ES) Calcd for $C_{19}H_{28}NOSi$: 314.1940, Found: 314.1919.

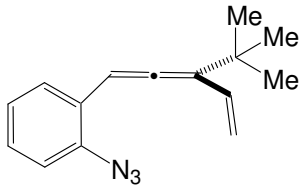

1-(2-Azidophenyl)3-*t*-butylpent-1,2,4-triene (184i).

Following General Procedure 3, acetate **188i** (0.27 g, 1.0 mmol) and vinyl magnesium bromide (1.0 M, 3.0 mL) were converted to **184i** (150 mg, 63%). IR (neat): 2124, 1930 cm^{-1}; ^{1}H NMR (400 MHz, $CDCl_3$) δ 7.43 (dd, *J* = 7.7, 1.4 Hz, 1H), 7.27 (dt, *J* = 8.1, 1.5 Hz, 1H), 7.19 (d, *J* = 7.0 Hz, 1H), 7.12 (t, *J* = 7.6 Hz, 1H), 6.73 (m, 1H), 6.28 (ddd, *J* = 17.0, 10.4, 1.3 Hz, 1H), 5.51 (dd, *J* = 17.1, 0.9 Hz, 1H), 5.26 (dd, *J* = 10.4, 0.9 Hz, 1H), 1.24 (s, 9H); ^{13}C NMR (75 MHz, $CDCl_3$) δ 204.7, 136.6, 130.9, 128.3, 128.0, 126.9, 125.3, 119.0,118.6, 117.2, 92.3, 34.3, 29.9; TOFESMS *m/z* relative intensity 210 (MH^+-N_2 100); HRMS (-ES) Calcd for $C_{15}H_{16}N$: 210.1283, Found: 210.1277.

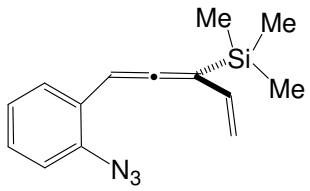

3-(Trimethylsilyl)-1-(2-Azidophenyl)pent-1,2,4-triene (184j).

Following General Procedure 3, acetate **188j** (0.35 g, 1.2 mmol) and vinyl magnesium bromide (1.0 M, 3.6 mL) were converted to **184j** (100 mg, 32%). IR (neat): 2123, 1905 cm^{-1}; ^1H NMR (400 MHz, $CDCl_3$) δ 7.31 (dd, *J* = 7.7, 1.3 Hz, 1H), 7.21 (dd, *J* = 7.1, 1.5 Hz, 1H), 7.16-7.11 (m, 2H), 6.36 (d, *J* = 1.5 Hz, 1H), 6.28 (dddd, *J* = 17.4, 11.5, 10.4, 1.1 Hz, 1H), 5.38 (td, *J* = 17.1, 1.1 Hz, 1H), 5.18 (td, *J* = 10.4, 1.2 Hz, 1H), 0.26 (s, 9H); ^{13}C NMR (75 MHz, $CDCl_3$) δ 211.4, 136.1, 133.1, 127.9, 127.8, 126.7, 125.3, 118.9, 117.1, 103.0, 85.1, -0.3; TOFESMS *m/z* relative intensity 278 (MNa^+ 100); HRMS (+ES) Calcd for $C_{14}H_{17}N_3Si$: 278.1089, Found: 278.1111.

Cyclization Studies of 184a.

Following General Procedure 7, allenylazide **184a** (35 mg, 0.18 mmol) was converted to compounds **185a** (12 mg, 40%) and **189a** (17 mg, 56%).

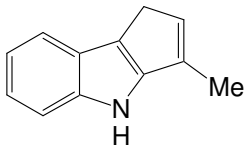

3-Methyl-1,4-dihydrocyclopenta[b]indole (185a).

IR (neat): 3406 cm^{-1}; ^1H NMR (300 MHz, $CDCl_3$) δ 8.03 (bs, 1H), 7.58 (d, *J* = 7.43 Hz, 1H), 7.41 (d, *J* = 7.8 Hz, 1H), 7.09-7.24 (m, 2H), 6.22 (m, 1H), 3.25 (s, 2H),

2.22 (d, *J* = 1.6 Hz, 3H); ^{13}C NMR (75 MHz, $CDCl_3$) δ 148.7, 140.5, 132.7, 131.6, 125.2, 121.0, 120.6, 120.3, 118.5, 112.3, 31.9, 13.5; TOFESMS *m/z* relative intensity 170 (MH^+ 35); HRMS (+ES) Calcd for $C_{12}H_{12}N$:170.0970, Found: 170.0967.

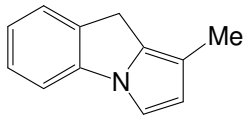

1-Methyl-9H-pyrrolo[1,2-a]indole (189a).

Crystals suitable for X-ray crystallographic analysis were obtained by slow evaporation of an Et_2O solution of **189a** over a period of 48 h at 25 °C. ^{1}H NMR (300 MHz, $CDCl_3$) δ 7.42 (d, *J* = 7.4 Hz, 1H), 7.24-7.33 (m, 2H), 7.10 (t, *J* = 7.3 Hz, 1H), 7.05 (d, *J* = 2.6 Hz, 1H), 6.25 (d, *J* = 2.6 Hz, 1H), 3.77 (s, 2H), 2.18 (s, 3H); ^{13}C NMR (75 MHz, $CDCl_3$) δ 141.8, 135.3, 132.7, 127.7, 126.3, 123.0, 114.8, 111.9, 109.8, 109.6, 28.4, 11.7; TOFESMS *m/z* relative intensity 170 (MH^+ 35); HRMS (+ES) Calcd for $C_{12}H_{12}N$:170.0970, Found: 170.0967.

X-Ray Analysis (189a).

A yellow plate shaped crystal of **189a** ($C_{12}H_{11}N$) with approximate dimensions 0.10 x 0.30 x 0.40 mm, was used for the X-ray crystallographic analysis. The X-ray intensity data were measured at 108(2) K, cooled by Rigaku-MSC X-Stream 2000, on a Bruker SMART APEX CCD area detector system equipped with a graphite monochromator and a MoKα fine-focus sealed tube (λ = 0.71073Å) operated at 1600 watts power (50 kV, 32 mA). The detector was placed at a distance of 5.8 cm from the crystal.

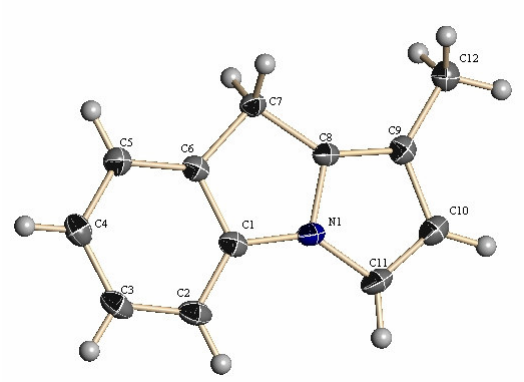

A total of 1850 frames were collected with a scan width of 0.3º in ω and an exposure time of 20 seconds/frame. The total data collection time was about 12 hours. The frames were integrated with the Bruker SAINT software package using a narrow-frame integration algorithm. The integration of the data using a Monoclinic unit cell yielded a total of 5358 reflections to a maximum θ angle of 28.28° (0.90 Å resolution), of which 2066 were independent, completeness = 94.9 %, R_{int} = 0.0178, R_{sig} = 0.0245 and 1729 were greater than 2σ(I). The final cell constants: a = 11.907(4)Å, b = 5.6848(16)Å, c = 12.950(4)Å, α = 90°, β = 92.517(5)°, γ = 90°, volume = 875.7(4)$Å^3$, are based upon the refinement of the XYZ-centroids of 2113 reflections above 20σ(I) with 2.274° <θ <28.242° . Analysis of the data showed negligible decay during data collection. Data were corrected for absorption effects using the multiscan technique (SADABS). The ratio of minimum to maximum apparent transmission was 0.849448.

The structure was solved and refined using the Bruker SHELXTL (Version 6.1) Software Package, using the space group P2(1)/n, with Z = 4 for the formula unit, C12H11N. The final anisotropic full-matrix least-squares refinement on F^2 with 119 variables converged at R1 = 5.17 %, for the observed data and wR2 = 13.90 % for all data. The goodness-of-fit was 1.072. The largest peak on the final difference map was

0.403 $e^-/Å^3$ and the largest hole was -0.249 $e^-/Å^3$. Based on the final model, the calculated density of the crystal is 1.283 g/cm^3 and F(000) amounts to 360 electrons.

Cyclization Studies of 184b.

Following General Procedure 7, allenylazide **184b** (45 mg, 0.16 mmol) was converted to compounds **185b** (16 mg, 40%) and **189b** (12 mg, 30%).

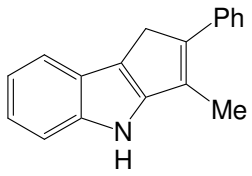

3-Methyl-2-phenyl-1,4-dihydrocyclopenta[b]indole (185b).

IR (neat): 3414 cm^{-1}; ^1H NMR (400 MHz, $CDCl_3$) δ 8.07 (bs, 1H), 7.60 (d, *J* = 7.4 Hz, 1H), 7.52 (m, 2H), 7.45-7.41 (m, 3H), 7.25 (m, 1H), 7.18-7.11 (m, 2H), 3.69 (q, *J* = 1.8 Hz, 2H), 2.39 (t, *J* = 1.7 Hz, 3H); ^{13}C NMR (75 MHz, $CDCl_3$) δ 150.0, 143.5, 140.2, 138.3, 128.9, 128.1, 127.6, 126.6, 125.1, 120.8, 120.6, 118.7, 118.6, 112.3 34.7, 12.9; TOFESMS *m/z* relative intensity 246 (MH^+ 100); HRMS (+ES) Calcd for $C_{18}H_{16}N$: 246.1283, Found: 246.1262.

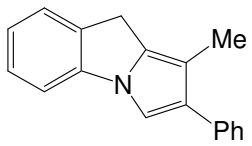

1-Methyl-2-phenyl-9H-pyrrolo[1,2-a]indole (189b).

^1H NMR (300 MHz, $CDCl_3$) δ 7.54-7.52 (m, 2H), 7.45-7.40 (m, 3H), 7.34-7.28 (m, 3H), 7.24 (m, 1H), 7.11 (dt, *J* = 7.2, 1.5 Hz, 1H), 3.85 (s, 2H), 2.3 (s, 3H); ^{13}C NMR (75 MHz, $CDCl_3$) δ 141.6, 137.0, 134.8, 134.0, 130.0, 128.8, 128.2, 127.9, 126.3, 126.1,

123.2, 110.3, 109.9, 107.7, 28.6, 11.4; TOFESMS *m/z* relative intensity 246 (MH^+ 100); HRMS (+ES) Calcd for $C_{18}H_{16}N$: 246.1283, Found: 246.1262.

Cyclization Studies of 184c.

Following General Procedure 7, allenylazide **184c** (35 mg, 0.17 mmol) was converted to compounds **185c** (11 mg, 36%) and **189c** (11 mg, 36%).

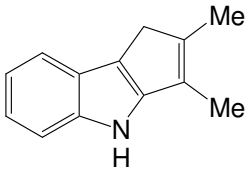

2,3-Dimethyl -1,4-dihydrocyclopenta[b]indole (185c).

IR (neat): 3406 cm^{-1}; ^1H NMR (400 MHz, $CDCl_3$) δ 7.94 (bs, 1H), 7.51 (d, *J* = 7.7 Hz, 1H), 7.38 (d, *J* = 7.8 Hz, 1H), 7.13-7.04 (m, 2H), 3.19 (s, 2H), 2.13 (s, 3H), 2.08 (s, 3H); ^{13}C NMR (75 MHz, $CDCl_3$) δ 149.9, 141.6, 139.7, 125.4, 125.3, 120.3, 119.7, 117.9, 116.9, 112.1, 36.5, 15.0, 10.8; TOFESMS *m/z* relative intensity 183 (MH^+ 100); HRMS (+ES) Calcd for $C_{13}H_{14}N$: 184.1126, Found: 184.1095.

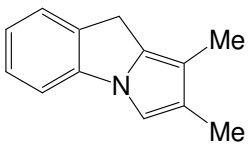

1,1-Dimethyl-9H-pyrrolo[1,2-a]indole (189c).

^1H NMR (300 MHz, $CDCl_3$) δ 7.37 (d, *J* = 7.3 Hz, 1H), 7.27 (t, *J* = 7.6 Hz, 1H), 7.16 (d, *J* = 7.7 Hz, 1H), 7.02 (t, *J* = 7.2 Hz, 1H), 6.88 (s, 1H), 3.75 (s, 2H), 2.14 (s, 3H), 2.08 (s, 3H); ^{13}C NMR (75 MHz, $CDCl_3$) δ 141.9, 134.7, 132.8, 127.7, 126.1, 124.0,

122.4, 111.6, 109.3, 107.6, 28.5, 11.3, 9.8; TOFESMS *m/z* relative intensity 183 (MH^+ 100); HRMS (+ES) Calcd for $C_{13}H_{14}N$: 184.1126, Found: 184.1095.

Cyclization Studies of 184d.

Following General Procedure 7, allenylazide **184d** (35 mg, 0.13 mmol) was converted to compound **186d** (9 mg, 36%).

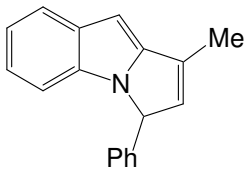

1-Methyl-3-phenyl-3H-pyrrolo[1,2-a]indole (186d).

^{1}H NMR (400 MHz, $CDCl_3$) δ 7.66 (dd, *J* = 6.6, 1.7 Hz, 1H), 7.36-7.30 (m, 3H), 7.21-7.11 (m, 2H), 7.05-7.01 (m, 2H), 6.94 (dd, *J* = 7.7, 1.5 Hz, 1H), 6.34 (s, 1H), 6.17 (m, 1H), 5.70 (s, 1H), 2.21 (s, 3H); ^{13}C NMR (75 MHz, $CDCl_3$) δ 149.0, 138.2, 134.5, 133.9, 133.3, 132.1, 129.3, 128.4, 127.3, 122.0, 121.5, 119.5, 109.8, 90.6, 65.7, 12.9; TOFESMS *m/z* relative intensity 246 (MH^+ 20); HRMS (+ES) Calcd for $C_{18}H_{16}N$: 246.1283, Found: 246.1259.

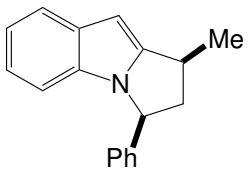

1-Methyl-3-phenyl-2,3-dihydro-1H-pyrrolo[1,2-a]indole (190d).

A deoxygenated solution of compound **186d** (9.0 mg, 0.04 mmol) and 5 mg of 10% Pd on carbon in 5 mL of THF was stirred at room temperature under H_2 at 1 atm for

2 h. The solution was then filtered through Celite and concentrated *in vacuo* to afford a yellow oil. The crude compound was purified over an alumina column using 20% Et_2O in hexanes to give **190d** as a yellow film (6 mg, 54%). Crystals suitable for X-ray crystallographic analysis were obtained by slow evaporation of an Et_2O solution of **190d** over a period of 48 h at 25 °C. mp: 90-95 °C; ^{1}H NMR (400 MHz, $CDCl_3$) δ 7.57 (d, *J* = 7.9 Hz, 1H), 7.38-7.35 (m, 3H), 7.28-7.24 (m, 2H), 7.03 (dt, *J* = 7.1, 0.8 Hz, 1H), 6.90 (dt, *J* = 7.1, 1.0 Hz, 1H), 6.59 (d, *J* = 8.1 Hz, 1H), 6.24 (s, 1H), 5.35 (t, *J* = 8.2 Hz, 1H), 3.45 (m, 1H), 3.18 (m, 1H), 2.13 (m, 1H), 1.49 (d, *J* = 6.8 Hz, 3H); ^{13}C NMR (75 MHz, $CDCl_3$) δ 150.6, 141.4, 133.8, 132.6, 129.2, 128.3, 127.1, 120.8, 120.4, 119.6, 110.8, 92.1, 61.9, 49.1, 32.7, 20.1; TOFESMS *m/z* relative intensity 248 (MH^+ 45); HRMS (+ES) Calcd for $C_{18}H_{18}N$: 248.1439, Found: 248.1445.

X-Ray Analysis (190d).

A yellow needle shaped crystal of **190d** ($C_{36}H_{34}N_2$ dimeric) with approximate dimensions 0.04 x 0.08 x 0.35 mm, was used for the X-ray crystallographic analysis. The X-ray intensity data were measured at 298(2) K, on a Bruker SMART APEX CCD area detector system equipped with a graphite monochromator and a MoKα fine-focus sealed tube (λ = 0.71073Å) operated at 1600 watts power (50 kV, 32 mA). The detector was placed at a distance of 5.8 cm from the crystal.

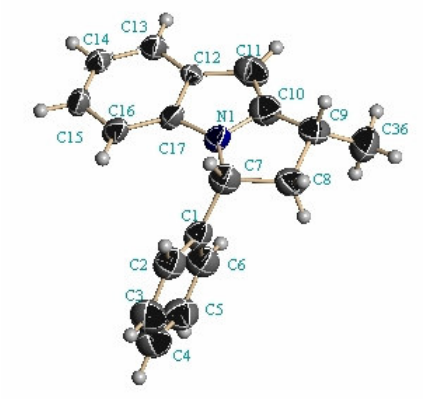

A total of 1850 frames were collected with a scan width of 0.3º in ω and an exposure time of 10 seconds/frame. The total data collection time was about 8 hours. The frames were integrated with the Bruker SAINT software package using a narrow-frame integration algorithm. The integration of the data using a Triclinic unit cell yielded a total of 8236 reflections to a maximum θ angle of 28.27 ° (0.90 Å resolution), of which 6090 were independent, completeness = 89.6 %, R_{int} = 0.0758, R_{sig} = 0.2293 and 1717 were greater than 2σ(I). The final cell constants: α = 5.538(3)Å, β = 9.573(5)Å, γ = 25.815(14)Å, α = 90°, β = 87.270(12)°, γ = 90°, volume = 1367.1(13)$Å^3$, are based upon the refinement of the XYZ-centroids of 715 reflections above 20σ(I) with 2.269° <θ <27.720°. Analysis of the data showed negligible decay during data collection. Data were corrected for absorption effects using the multiscan technique (SADABS). The ratio of minimum to maximum apparent transmission was 0.03821.

The structure was solved and refined using the Bruker SHELXTL (Version 6.1) Software Package, using the space group P-1, with Z = 2 for the formula unit, $C_{36}H_{34}N_2$. The final anisotropic full-matrix least-squares refinement on F^2 with 345 variables converged at R1 = 8.23 %, for the observed data and wR2 = 21.67 % for all data. The

goodness-of-fit was 0.829. The largest peak on the final difference map was 0.233 $e^-/Å^3$ and the largest hole was -0.247 $e^-/Å^3$. Based on the final model, the calculated density of the crystal is 1.202 g/cm^3 and F(000) amounts to 528 electrons.

Cyclization Studies of 184e.

Following General Procedure 7, allenylazide **184e** (31 mg, 0.12 mmol) was converted to compounds **185e** (10 mg, 36%) and **189e** (14 mg, 51%).

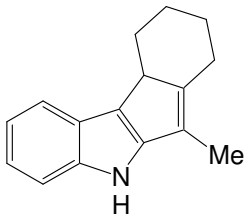

6-Methyl -5,7,8,9-hexahydroindeno[2,1-b]indole (185e).

IR (neat): 3406 cm^{-1}; ^1H NMR (400 MHz, $CDCl_3$) δ 7.95 (bs, 1H), 7.52 (d, *J* = 7.8 Hz, 1H), 7.39 (d, *J* = 8.0 Hz, 1H), 7.10 (t, *J* = 7.1 Hz, 1H), 7.03 (t, *J* = 7.2 Hz, 1H) 3.05 (dd, *J* = 12.5, 5.5 Hz, 1H), 2.8 (m, 1H), 2.68 (m, 1H), 2.27 (m, 1H), 2.08 (s, 3H), 2.6 (m, 1H), 1.85 (m, 1H), 1.28-1.21 (m, 2H), 1.00 (m, 1H); ^{13}C NMR (75 MHz, $CDCl_3$) δ 149.7, 148.8, 136.0, 139.7, 122.3, 121.2, 120.2, 119.6, 117.9, 112.2, 45.2, 33.6, 28.9, 27.3, 26.0, 10.4; TOFESMS *m/z* relative intensity 224 (MH^+ 10); HRMS (+ES) Calcd for $C_{16}H_{18}N$: 214.1422, Found: 224.1439.

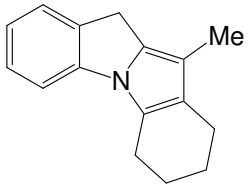

11-Methyl-2,3,4,10-tetrahydro-1H-indolo[1,2-a]indole (189e).

^{1}H NMR (400 MHz, $CDCl_3$) δ 7.37 (d, *J* = 7.4 Hz, 1H), 7.28-7.24 (m, 2H), 7.05 (m, 1H), 3.74 (s, 2H), 2.96(t, *J* = 5.6 Hz, 2H), 2.51(t, *J* = 6.0 Hz, 2H), 2.04 (s, 3H), 1.95-1.85 (m, 2H), 1.85-1.80 (m, 2H); ^{13}C NMR (75 MHz, $CDCl_3$) δ 142.5, 135.2, 130.6, 127.6, 126.2, 122.5, 122.0, 121.6, 110.2, 109.5, 28.1, 23.8, 23.7, 23.2, 22.4, 9.6; TOFESMS *m/z* relative intensity 224 (MH^+ 10); HRMS (+ES) Calcd for $C_{16}H_{18}N$: 214.1422, Found: 224.1439.

Cyclization Studies of 184f.

Following General Procedure 7, allenylazide **184f** (40 mg, 0.17 mmol) was converted to compound **186f** (14 mg, 40%).

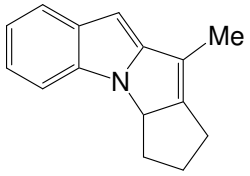

Pyrrolo-indole (186f)

^{1}H NMR (400 MHz, $CDCl_3$) δ 7.59 (d, *J* = 8.2 Hz, 1H), 7.25 (s, 1H), 7.12 (t, *J* = 7.3 Hz, 1H), 7.03 (t, *J* = 7.1 Hz, 1H), 6.11 (s, 1H), 4.8 (t, *J* = 8.5 Hz, 1H), 2.46-2.27 (m, 6H), 2.04 (s, 3H); ^{13}C NMR (75 MHz, $CDCl_3$) δ 154.1, 152.2, 135.2, 132.8, 123.4, 121.7, 121.0, 119.1, 108.9, 89.1, 66.3, 29.7, 27.8, 21.2, 11.2; TOFMSES *m/z* relative intensity 210 (MH^+ 10); HRMS (+MSES) Calcd for $C_{15}H_{16}N$: 210.1283, Found: 210.1274.

Cyclization Studies of 184g.

Following General Procedure 7, allenylazide **184g** (49 mg, 0.15 mmol) was converted to compounds **185g** (10 mg, 40%) and **189g** (13 mg, 56%).

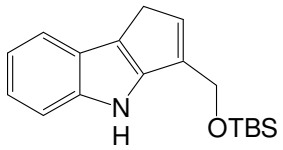

3-(*t*-Butyldimethylsilyloxymethyl)-1,4-dihydrocyclopenta[b]indole (185g).

IR (neat): 3395 cm^{-1}; ^1H NMR (300 MHz, $CDCl_3$) δ 8.23 (bs, 1H), 7.58 (m, 1H), 7.41 (m, 1H), 7.14-7.06 (m, 2H), 6.29 (m, 1H), 4.76 (d, *J* = 1.7 Hz, 2H), 3.29 (d, *J* = 1.6 Hz, 2H), 0.97 (s, 1H), 0.14 (s, 6H); ^{13}C NMR (75 MHz, $CDCl_3$) δ 147.1, 140.4, 137.8, 129.7, 124.8, 121.2, 120.7, 120.2, 118.5, 112.4, 61.1, 32.0, 29.4, 18.8, -4.8 (2C); TOFESMS *m/z* relative intensity 300 (MH^+ 10); HRMS (+ES) Calcd for $C_{36}H_{51}N_2O_2Si_2$: 599.3489, Found: 599.3466.

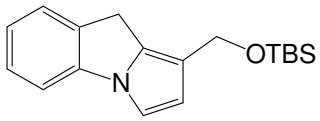

1-(*t*-Butyldimethylsilyloxymethyl)-9H-pyrrolo[1,2-a]indole (189g).

^1H NMR (300 MHz, $CDCl_3$) δ 7.41 (d, *J* = 7.5 Hz, 1H), 7.30-7.24 (m, 2H), 7.09 (t, *J* = 7.3 Hz, 1H), 7.06 (d, *J* = 2.1 Hz, 1H), 6.33 (d, *J* = 2.6 Hz, 1H), 4.73 (s, 2H), 3.85 (s, 2H), 0.96 (s, 9H) 0.13 (s, 6H); ^{13}C NMR (75 MHz, $CDCl_3$) δ 141.5, 135.2, 133.0, 127.7, 126.3, 123.3, 117.1, 112.8, 109.94, 109.92, 59.6, 29.1, 26.5, 18.9, -4.7 (2C); TOFESMS *m/z* relative intensity 300 (MH^+ 10); HRMS (+ES) Calcd for $C_{36}H_{51}N_2O_2Si_2$: 599.3489, Found: 599.3466.

Cyclization Studies of 184h.

Following General Procedure 7, allenylazide **184h** (25 mg, 0.07 mmol) was converted to compounds **185h** (12 mg, 52%) and **189h** (10 mg, 43%).

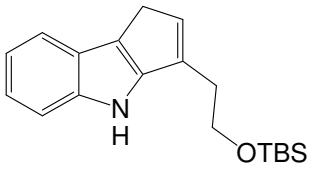

3-(*t*-Butyldimethylsilyloxyethyl)-1,4-dihydrocyclopenta[b]indole (185h).

IR (neat): 3372 cm^{-1}; ^1H NMR (300 MHz, $CDCl_3$) δ 8.8 (bs, 1H), 7.57 (m, 1H), 7.38 (m, 1H), 7.13-7.07 (m, 2H), 6.22 (m, 1H), 3.95 (t, *J* = 5.7 Hz, 2H), 3.25 (s, 2H), 2.82 (t, *J* = 5.6 Hz, 1H), 0.99 (s, 9H), 0.14 (s, 6H); ^{13}C NMR (75 MHz, $CDCl_3$) δ 148.5, 140.1, 136.1 131.9, 125.2, 120.6, 120.4, 120.0, 118.4, 112.2, 63.9, 32.7, 31.8, 26.5, 18.9, -4.9; TOFMSES *m/z* relative intensity 314 (MH^+ 25); HRMS (+MSES) Calcd for $C_{19}H_{28}NOSi$: 314.1940, Found: 314.1929.

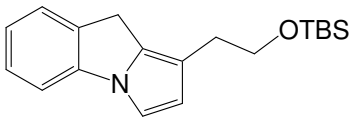

1-(*t*-Butyldimethylsilyloxyethyl)-9H-pyrrolo[1,2-a]indole (189h).

^1H NMR (300 MHz, $CDCl_3$) δ 7.40 (d, *J* = 7.6 Hz, 1H), 7.30 (d, *J* = 7.8 Hz, 1H), 7.24 (d, *J* = 7.7 Hz, 1H), 7.07 (t, *J* = 7.4 Hz, 1H) 7.04 (d, *J* = 2.4 Hz, 1H), 6.25 (d, *J* = 2.6 Hz, 1H), 3.84 (t, *J* = 7.7 Hz, 2H), 3.79 (s, 2H), 2.78 (t, *J* = 7.5 Hz, 2H), 0.93 (s, 9H) 0.07 (s, 6H); ^{13}C NMR (75 MHz, $CDCl_3$) δ 141.7, 135.1, 133.0, 127.8, 126.3, 123.3, 114.2, 113.6, 109.9, 109.7, 64.5, 31.0, 28.7, 26.4, 18.9, -4.8; TOFESMS *m/z* relative intensity 314 (MH^+ 25); HRMS (+ES) Calcd for $C_{19}H_{28}NOSi$: 314.1940, Found: 314.1929.

Cyclization Studies of 184i.

Following General Procedure 7, allenylazide **184i** (60 mg, 0.25 mmol) was converted to compounds **185d** (30 mg, 57%) and **189d** (11 mg, 20%).

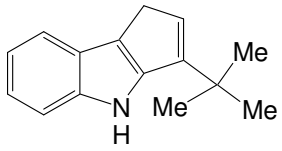

3-*t*-Butyl-1,4-dihydrocyclopenta[b]indole (185i).

IR (neat): 3414 cm^{-1}; ^1H NMR (400 MHz, $CDCl_3$) δ 8.09 (bs, 1H), 7.60 (m, 1H), 7.43 (m, 1H), 7.29-7.13 (m, 2H), 6.19 (t, *J* = 1.6 Hz, 1H), 3.24 (d, *J* = 1.6 Hz, 2H), 1.4 (s, 9H); ^{13}C NMR (75 MHz, $CDCl_3$) δ 147.5, 147.0, 140.5, 127.6, 124.8, 122.1, 120.7, 120.3, 118.5, 112.2, 32.8, 31.2, 30.2; TOFESMS *m/z* relative intensity 212 (MH^+ 100); HRMS (+ES) Calcd for $C_{15}H_{18}N$: 212.1439, Found: 212.1436.

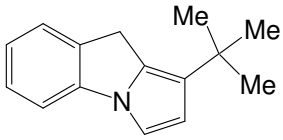

1-*t*-Butyl-9H-pyrrolo[1,2-a]indole (189i).

^1H NMR (400 MHz, $CDCl_3$) δ 7.38 (d, *J* = 7.4 Hz, 1H), 7.28-7.22 (m, 2H), 7.07 (dd, *J* = 7.4, 1.2 Hz, 1H), 7.04 (d, *J* = 2.9 Hz, 1H), 6.32 (d, *J* = 2.8 Hz, 1H), 3.92 (s, 2H), 1.36 (s, 9H); ^{13}C NMR (75 MHz, $CDCl_3$) δ 141.8, 135.2, 130.1, 127.8, 127.7, 126.0, 123.0, 111.7, 109.7, 109.2, 31.7, 31.3, 30.8; TOFESMS *m/z* relative intensity 212 (MH^+ 100); HRMS (+ES) Calcd for $C_{15}H_{18}N$: 212.1439, Found: 212.1436.

Cyclization Studies of 184j.

Following General Procedure 7, allenylazide **184j** (27 mg, 0.16 mmol) gave **192** as the product (14 mg, 72%).

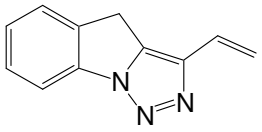

3-Vinyl-4H-[1,2,3]triazolo[1,5-a]indole (192)

^{1}H NMR (400 MHz, $CDCl_3$) δ 7.92 (d, *J* = 7.8 Hz, 1H), 7.58 (d, *J* = 7.6 Hz, 1H), 7.51 (t, *J* = 7.7, Hz, 1H), 7.39 (t, *J* = 7.6 Hz, 1H), 6.93 (dd, *J* = 17.8, 11.2 Hz, 1H), 5.76 (d, *J* = 17.8, Hz, 1H), 5.48 (d, *J* = 11.2 Hz, 1H), 4.01 (s, 2H); ^{13}C NMR (75 MHz, $CDCl_3$) δ 140.2, 137.7, 136.4, 135.5, 129.0, 127.4, 127.2, 126.9, 116.8, 113.2, 27.5; TOFESMS *m/z* relative intensity 184 (MH^+ 100); HRMS (+ES) Calcd for $C_{11}H_{10}N_3$: 184.0875, Found: 184.0870.

6.5 Meloscine Model System Synthesis Studies

6.5.1 General Procedure 8. Addition of Sodium Azide to Vinyl Ketones

To a solution of the indicated vinyl ketone (1.0 equiv) in AcOH and water (1:1v/v) sodium azide (4.0 equiv) was added and the reaction solution was allowed to stir at room temperature. After 24 h, the excess AcOH was quenched carefully with solid sodium carbonate. The solution was extracted three times with Et_2O (300 mL), the combined organic extracts were washed with brine, dried over Na_2SO_4 and the solvent was evaporated. The dark oil was purified by column chromatography using 25% ether in hexanes to give the keto azide.

6.5.2 General Procedure 9. Synthesis of Propargylic Acetates

The keto azide (1.0 equiv) was taken up in THF (0.10 M) and treated with propynyl lithium (1.3 equiv) or 1-propynyl magnesium bromide (1.3 equiv) at room temperature. After 20 min, the dark solution was treated with 15 mL of aqueous NH_4Cl and the mixture was extracted with 50 mL of Et_2O. The combined extracts are washed with brine and dried over Na_2SO_4 to give a viscous oil which was taken to the next step without purification.

The crude alcohol was taken up in CH_2Cl_2 (0.10 M) and treated with DMAP (1.2 equiv) and Ac_2O (1.2 equiv). After complete consumption of the starting material by TLC, the reaction mixture was treated with a saturated solution of $NaHCO_3$, extracted with 50 mL of CH_2Cl_2 and washed with brine. Evaporation of the combined organic

phases gave a dark oil. The crude acetate was purified by column chromatography (30% ether in hexanes).

6.5.3 General Procedure 10. Tetrasubstituted Allenyl Azide Synthesis

To a solution of $ZnCl_2$ (3.0 equiv) in THF (0.10 M) was added vinyl magnesium bromide (1.0 M in THF, 3.0 equiv) and the mixture was stirred at room temperature for 30 min. The reaction mixture then was treated with $Pd(PPh_3)_4$ (5 mol%) in THF and the propargylic acetate (1.0 equiv) in THF was cannulated subsequently. The reaction mixture was stirred at room temperature until the starting material disappeared (TLC). After the addition of 10 mL of aqueous NH_4Cl solution, the organic layer was extracted with Et_2O and the combined extracts were washed with water and finally with brine. Drying this solution over Na_2SO_4 and removal of solvent under reduced pressure resulted in an orange oil. The crude product was purified by SiO_2 column chromatography using 1% ether hexane as the eluent to give the allenes as pale oils.

6.5.4 General Procedure 11. Cyclization of Tetrasubstituted Allenes

A deoxygenated solution of allenylazide in toluene-d_8, (0.1 M) was heated in a sealed tube for 15 min, after which time the reaction mixture was cooled and the solvent was evaporated to give an orange oil. Purification of the crude oil was accomplished by column chromatography using 70-95% ether in hexanes.

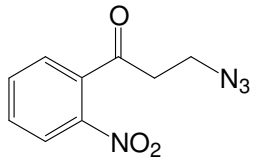

3-Azido-1-(2-nitrophenyl)-propan-1-one (241).

Following General Procedure 8, the nitro vinyl ketone **243** [99] (0.70 g, 4.0 mmol) was coverted to the keto azide **241** (450 mg, 52%). IR (neat): 2105, 1709, 1529 cm^{-1}; ^1H NMR (400 MHz, $CDCl_3$) δ 8.07 (dd, *J* = 8.3, 1.1 Hz, 1H), 7.74 (dt, *J* = 7.5, 1.1 Hz, 1H), 7.62 (dt, *J* = 7.6, 1.5 Hz, 1H), 7.42 (dd, *J* = 7.8, 1.5 Hz, 1H), 3.70 (t, *J* = 6.3 Hz, 2H), 3.05 (t, *J* = 6.4 Hz, 2H); ^{13}C NMR (75 MHz, $CDCl_3$) δ 200.3, 145.9, 137.5, 135.0, 131.4, 127.8, 124.9, 46.3, 42.2; TOFMSES *m/z* relative intensity 192 (MH^+-N_2 100); HRMS (+MSES) Calcd for $C_9H_8N_4O_3Na$: 243.0494, Found: 243.0505.

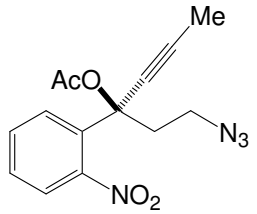

1-Acetoxy-1-(azidoethyl)-1-(nitrophenyl)but-2-yne (244).

Following General Procedure 9, the nitro-ketoazide **241** (0. 44 g, 2.0 mmol) was coverted to the acetate **244** (100 mg, 17%). IR (neat): 2100, 1754, 1537 cm^{-1}; ^1H NMR (400 MHz, $CDCl_3$) δ 7.82 (d, *J* = 7.9 Hz, 1H), 7.53 (dt, *J* = 8.0, 1.7 Hz, 1H), 7.42 (m, 2H), 3.54 (m, 2H), 2.71 (m, 1H), 2.44 (m, 1H), 2.06 (s, 3H), 1.97 (s, 3H); ^{13}C NMR (75 MHz, $CDCl_3$) δ 168.7, 133.8, 133.2, 131.4, 129.5, 129.0, 124.1, 87.1, 76.6, 75.8, 47.8, 41.9, 21.6, 4.2; TOFMSES *m/z* relative intensity 303 (MH^+ 38); HRMS (+MSES) Calcd for $C_{14}H_{15}N_4O_4$: 303.1093, Found: 303.1095.

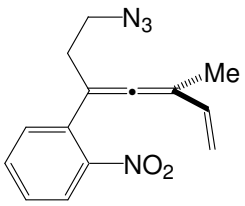

1-(Azidoethyl)-1-(nitrophenyl)-3-methylpent-1,2,4-triene (245).

Following General Procedure 10, the acetate **244** (0.08 g, 0.26 mmol) and vinyl magnesium bromide (1.0 M, 0.78 mL) were coverted to the allene **245** (8 mg, 11%). IR (neat): 2097, 1920 cm^{-1}; ^1H NMR (400 MHz, $CDCl_3$) δ 7.84 (dd, *J* = 8.3, 0.9 Hz, 1H), 7.57 (dt, *J* = 8.1, 1.0 Hz, 1H), 7.43 (d, *J* = 7.8 Hz, 2H), 6.36 (dd, *J* = 17.6, 10.6 Hz, 1H), 5.21 (d, *J* = 17.4 Hz, 1H), 5.13 (d, *J* = 10.6 Hz, 1H), 3.46 (t, *J* = 6.9 Hz, 2H), 2.65 (t, *J* = 6.9 Hz, 2H), 1.87 (d, *J* = 0.8 Hz, 3H); ^{13}C NMR (75 MHz, $CDCl_3$) δ 205.7, 135.4, 132.5, 132.4, 131.2, 129.0, 128.6, 124.7, 115.0, 104.5, 99.6, 49.9, 32.9,14.6.

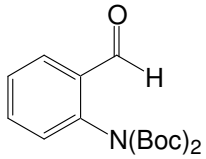

2-Di-*ter*-butoxycarbonylamino benzaldehyde (248).

To a solution of compound **247**[100] (2.7 g, 12 mmol) in toluene (75 mL) was added Boc-anhyride (3.2 g, 15 mmol) and DMAP (1.8 g, 15 mmol) and the reaction mixture was refluxed over a period of 24 h. The reaction mixture was cooled to room temperature and the organic layer was extracted three times with 75 mL of Et_2O, washed with brine and dried over Na_2SO_4. Evaporation of the combined organic extracts resulted in a brown solid which was purified by flash chromatography (30% ether in hexanes) to afford a white solid (3.7 g, 94%): mp 82-86 °C IR (neat): 1796, 1704 cm^{-1}; ^1H NMR (400 MHz,

$CDCl_3$) δ 10.1 (s, 1H), 7.88 (dd, *J* = 7.6, 1.8 Hz, 1H), 7.60 (dt, *J* = 7.6, 1.6 Hz, 1H), 7.48 (t, *J* = 7.6 Hz, 1H), 7.21 (dd, *J* = 7.8, 1.0 Hz, 1H), 1.38 (s, 18H); ^{13}C NMR (75 MHz, $CDCl_3$) δ 190.0, 151.5, 141.1, 134.8, 132.8, 130.6, 130.0, 128.8, 83.8, 28.2. TOFMSES *m/z* relative intensity 344 (MNa^+ 100); HRMS (+MSES) Calcd for $C_{17}H_{23}NO_5Na$: 344.1474, Found: 344.1448.

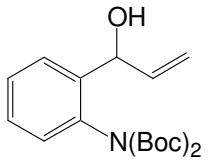

1-(2-Di-*ter*-butoxycarbonylaminophenyl)-prop-2-ene-1-ol (249).

A solution of compound **248** (0.50 g, 1.6 mmol) in THF was cooled to -40 °C and vinyl magnesium bromide (1.0 M in THF, 1.9 mL, 1.9 mmol) was added dropwise under nitrogen. After complete consumption of starting material, the reaction mixture was poured into 100 mL of satd. NH_4Cl solution and the mixture was extracted with 300 mL of Et_2O, washed with water and brine. Drying the combined organic extracts over Na_2SO_4, followed by evaporation of the solvent, gave a pale yellow oil. A small batch was purified over a short column silica gel using 40% ether in hexanes to give the alcohol **249**. IR (neat): 3434, 1732, cm^{-1}; ^1H NMR (400 MHz, $CDCl_3$) δ 7.81 (d, *J* = 8.0 Hz, 1H), 7.35 (m, 2H), 7.28 (bs, 1H), 7.10 (t, *J* = 8.2 Hz, 1H), 6.16 (d, *J* = 5.0 Hz, 1H), 6.07 (m, 1H), 5.33 (d, *J* = 16.8 Hz, 1H), 5.32 (d, *J* = 10.0 Hz, 1H), 1.54 (s, 9H), 1.48 (s, 9H); ^{13}C NMR (75 MHz, $CDCl_3$) δ 153.8, 153.4, 136.8, 135.1, 129.7, 129.3, 128.6, 128.4, 123.9, 117.7, 83.4, 80.7, 76.6, 28.2, 28.2.TOFMSES *m/z* relative intensity 372 (MNa^+ 100); HRMS (+MSES) Calcd for $C_{19}H_{27}NO_5Na$: 372.1787, Found: 372.1791.

The crude alcohol was dissolved in 100 mL of acetone and treated with excess Jones reagent. After checking the completion of the reaction by TLC, the reaction mixture was filtered through a Celite plug. Excess acetone was evaporated and the residue was extracted into 200 mL of CH_2Cl_2, washed with brine and dried over Na_2SO_4. Evaporation of the organic solvent gave the crude vinyl ketone which was carried over crude to the next step. Following General Procedure 8, the vinyl ketone gave amino compound **250** as the exclusive product (vide infra).

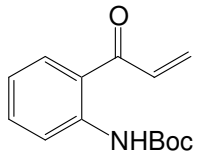

1-(2-*ter*-butoxycarbonylaminophenyl)-prop-2-ene-1-one (251).

A solution of compound **247**[100] (2.1 g, 9.5 mmol) in THF (50 mL) was cooled to -20 °C and vinyl magnesium bromide (1.0 M in THF, 24 mL, 24 mmol) was added dropwise under nitrogen. After complete consumption of starting material (TLC), the reaction mixture was poured into 100 mL of satd. NH_4Cl solution and the mixture was poured into 300 mL of ether. The combined organic extracts were washed with water and then brine. Drying this solution over Na_2SO_4, followed by evaporation of the solvent gave a pale yellow oil.

The crude alcohol was dissolved in 100 mL of acetone and treated with excess Jones reagent. After checking the completion of the reaction by TLC, the reaction mixture was filtered through a Celite plug. Excess acetone was evaporated and the residue was extracted with 200 mL of CH_2Cl_2, which was washed with brine and dried

over Na_2SO_4. Evaporation of the organic solvent gave the crude vinyl ketone which was purified using 30% ether in hexanes to give the vinyl ketone **251** (1.8 g, 75%).IR (neat): 3350, 1729, 1653 cm^{-1}; ^1H NMR (400 MHz, $CDCl_3$) δ 10.7 (bs, 1H), 8.46 (d, *J* = 7.7 Hz, 1H), 7.84 (dd, *J* = 8.0, 1.4 Hz, 1H), 7.54 (dt, *J* = 8.6, 1.5 Hz, 1H), 7.20 (dd, *J* = 17.0, 10.6 Hz, 1H), 7.06 (dt, *J* = 8.1, 1.0 Hz, 1H), 6.43 (dd, *J* = 17.0, 1.6 Hz, 1H), 5.92 (dd, *J* = 10.5, 1.6 Hz, 1H), 1.54 (s, 9H); ^{13}C NMR (75 MHz, $CDCl_3$) δ 194.0, 153.5, 142.5, 135.2, 133.7, 131.5, 130.6, 122.3, 121.4, 119.9, 80.9, 28.7. TOFMSES *m/z* relative intensity 270 (MNa^+ 100); HRMS (+MSES) Calcd for $C_{14}H_{18}NO_3$: 248.1287, Found: 248.1278.

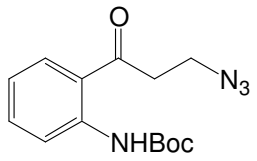

3-Azido-1-(2-*ter*-butoxycarbonylaminophenyl)-propan-1-one (250).

Following General Procedure 8, vinyl ketone **251** (1.7 g, 6.9 mmol) was converted to azide **256** (1.0 g, 50%): mp 68-70 °C; IR (neat): 3380, 2104, 1728, 1656 cm^{-1}; ^1H NMR (400 MHz, $CDCl_3$) δ 10.8 (bs, 1H), 8.5 (d, *J* = 8.6 Hz, 1H), 7.84 (d, *J* = 8.0 Hz, 1H), 7.54 (t, *J* = 8.4 Hz, 1H), 7.04 (t, *J* = 7.8 Hz, 1H), 3.73 (t, *J* = 6.4 Hz, 2H), 3.29 (t, *J* = 6.4 Hz, 2H), 1.54 (s, 9H); ^{13}C NMR (100 MHz, $CDCl_3$) δ 201.1, 153.4, 142.5, 135.7, 131.0, 121.4, 121.1, 119.8, 81.1, 46.6, 39.1, 28.7; TOFMSES *m/z* relative intensity 312 (MNa^+ 100); HRMS (+MSES) Calcd for $C_{14}H_{18}N_4O_3Na$: 313.1277, Found: 313.1280.

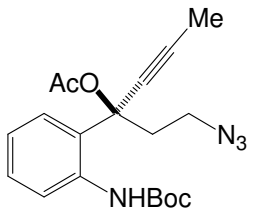

1-Acetoxy-1-(azidoethyl)-1-(2-*ter*-butoxycarbonylaminophenyl)but-2-yne (252).

Following General Procedure 9, ketoazide **250** (1.0 g, 3.5 mmol) was coverted to the acetate **252** (0.61 g, 47%): fuses 128-134°C IR (neat): 3379, 2099, 1731, 1650 cm^{-1}; ^1H NMR (400 MHz, $CDCl_3$) δ 7.97 (d, *J* = 8.0 Hz, 1H), 7.7 (bs, 1H), 7.53 (d, *J* = 8.0 Hz, 1H), 7.29 (t, *J* = 7.4 Hz, 1H), 7.06 (t, *J* = 7.7 Hz, 1H), 3.48 (m, 1H), 3.35 (m, 1H), 2.55 (m, 1H), 2.34 (m, 1H), 2.12 (s, 3H), 2.05 (s, 3H), 1.5 (s, 9H); ^{13}C NMR (75 MHz, $CDCl_3$) δ 168.2, 153.2, 135.9, 129.5, 128.9, 127.3, 123.7, 122.9, 87.4, 80.9, 77.7, 76.8, 47.6, 40.2, 28.7, 21.8, 4.2; TOFMSES *m/z* relative intensity 395 (MNa^+ 60); HRMS (+MSES) Calcd for $C_{19}H_{24}N_4O_4Na$: 395.1695, Found: 395.1684.

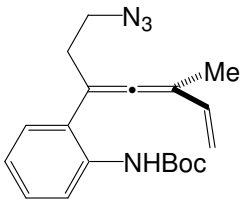

1-(Azidoethyl)-1-(2-*ter*-butoxycarbonylaminophenyl)-3-methylpent-1,2,4-triene (253).

Following General Procedure 10, acetate **252** (0.43 g, 1.2 mmol) and vinyl magnesium bromide (1.0 M, 3.6 mL) were coverted to the allene **253** (0.22 g, 56%). IR (neat): 2098, 1937 cm^{-1}; ^1H NMR (400 MHz, $CDCl_3$) δ 8.07 (d, *J* = 8.2 Hz, 1H), 7.33-

7.16 (m, 3H), 7.06 (t, *J* = 7.5 Hz, 1H), 6.45 (dd, *J* = 17.3, 10.6 Hz, 1H), 5.25 (d, *J* = 17.2 Hz, 1H), 5.17 (d, *J* = 10.6 Hz, 1H), 3.44 (t, *J* = 6.5 Hz, 2H), 2.67 (t, *J* = 6.5 Hz, 2H), 1.98 (s, 3H), 1.55 (s, 9H); ^{13}C NMR (75 MHz, $CDCl_3$) δ 205.9, 153.2, 136.2, 135.0, 128.6, 127.9, 125.7, 123.3, 120.4, 115.0, 103.5, 98.5, 80.7, 49.8, 33.6, 28.7, 15.3; TOFMSES *m/z* relative intensity 363 (MNa^+ 100); HRMS (+MSES) Calcd for $C_{19}H_{24}N_4O_2Na$: 363.1810 Found: 363.1805.

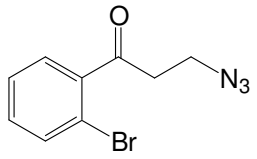

3-Azido-1-(2-bromophenyl)-propan-1-one (257).

Following General Procedure 8, vinyl ketone **256**[100] (16 g, 76 mmol) was coverted to the keto-azide **257** (14.4 g, 74%). IR (neat): 2097, 1694 cm^{-1}; ^{1}H NMR (400 MHz, $CDCl_3$) δ 7.60 (d, *J* = 7.9 Hz, 1H), 7.42 (dd, *J* = 7.7, 1.7 Hz, 1H), 7.36 (dt, *J* = 7.8, 1.8 Hz, 1H), 7.29 (dd, *J* = 7.5, 1.8 Hz, 1H), 3.69 (t, *J* = 6.4 Hz, 2H), 3.20 (t, *J* = 6.4 Hz, 2H); ^{13}C NMR (100 MHz, $CDCl_3$) δ 201.4, 141.1, 134.3, 132.5, 129.2, 128.0, 119.2, 46.5, 42.0; TOFMSES *m/z* relative intensity 253.99 (MH^+ 50); HRMS (+TOFMSAP) Calcd for $C_9H_9N_3OBr$: 253.9929, Found: 253.9937.

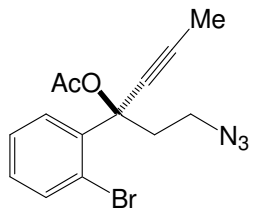

1-Acetoxy-1-(azidoethyl)-1-(2-bromophenyl)but-2-yne (258).

Following General Procedure 9, keto-azide **257** (1.0 g, 3.9 mmol) was coverted to the acetate **258** (0.60 g, 46%). IR (neat): 2099, 1731 cm^{-1}; ^1H NMR (400 MHz, $CDCl_3$) δ 7.99 (dd, *J* = 7.9, 1.6 Hz, 1H), 7.57 (dd, *J* = 8.0, 1.3 Hz, 1H), 7.34 (dt, *J* = 7.9, 1.2 Hz, 1H), 7.15 (dt, *J* = 7.8, 1.6 Hz, 1H), 3.57 (m, 1H), 3.39 (m, 1H), 2.79 (m, 1H), 2.36 (m, 1H), 2.13 (s, 3H), 2.02 (s, 3H); ^{13}C NMR (75 MHz, $CDCl_3$) δ 168.8, 138.5, 135.9, 130.8, 130.0, 127.8, 119.1, 86.7, 78.5, 76.8, 47.9, 39.6, 21.6, 4.3; TOFMSES *m/z* relative intensity 358 (MNa^+ 90); HRMS (+MSES) Calcd for $C_{14}H_{14}N_3O_2BrNa$: 358.0167, Found: 358.0190.

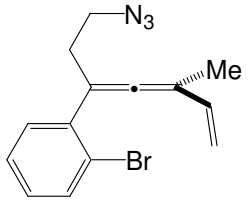

1-(Azidoethyl)-1-(2-bromophenyl)-3-methylpent-1,2,4-triene (259).

Following General Procedure 10, acetate **258** (0.50 g, 1.5 mmol) was coverted to the allene **259** (0.25 g, 55%). IR (neat): 2096, 1946 cm^{-1}; ^1H NMR (400 MHz, $CDCl_3$) δ 7.60 (d, *J* = 7.5 Hz, 1H), 7.31 (m, 1H), 7.30 (m, 1H), 7.14 (m, 1H), 6.48 (dd, *J* = 17.4, 10.6 Hz, 1H), 5.20 (d, *J* = 17.4 Hz, 1H), 5.11 (d, *J* = 10.6 Hz, 1H), 3.41 (t, *J* = 6.9 Hz, 2H), 2.68 (t, *J* = 6.9 Hz, 2H), 1.93 (s, 3H); ^{13}C NMR (75 MHz, $CDCl_3$) δ 206.3, 138.8, 135.4, 133.6, 130.8, 129.2, 127.9, 123.4, 114.1, 103.2, 102.2, 47.8, 33.2, 14.9; TOFMSES *m/z* relative intensity 276 (MH^+ -N_2 100); HRMS (+MSEI) Calcd for $C_{14}H_{14}N_3Br$: 303.0371, Found: 303.0344.

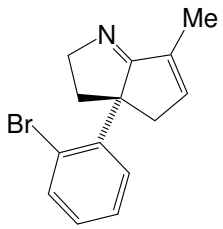

Cyclization of Bromo-Allene 259.

Following General Procedure 11, allenylazide **259** (0.20 g, 0.66 mmol) gave **260** as the product (134 mg, 74%). Crystals suitable for X-ray crystallographic analysis were obtained by slow evaporation of an Et_2O/pentane (1:1) solution of **260** over a period of 48 h at 25 °C. Mp: 100-105 °C; ^{1}H NMR (400 MHz, $CDCl_3$) δ 7.64 (dd, *J* = 7.8, 1.4 Hz, 1H), 7.17 (dt, *J* = 7.5, 1.4 Hz, 1H), 7.11 (dt, *J* = 7.9, 1.9 Hz, 1H), 6.92 (dd, *J* = 7.6, 1.8 Hz, 1H), 6.38 (s, 1H), 4.11 (q, *J* = 7.2 Hz, 1H), 3.70 (m, 1H), 2.88 (dd, *J* = 17.3, 1.7 Hz, 1H), 2.60 (d, *J* = 16.4 Hz, 1H), 2.56 (dd, *J* = 12.7, 4.4 Hz, 1H), 2.10 (m, 1H), 2.06 (d, *J* = 1.7 Hz, 3H); ^{13}C NMR (75 MHz, $CDCl_3$) δ 191.2, 146.1, 143.0, 135.9, 135.0, 128.8, 128.3, 127.3, 124.1, 64.4, 64.1, 43.1, 40.8, 12.3; TOFMSES *m/z* relative intensity 276 ($MH^+ - N_2$ 100); HRMS (+MSEI) Calcd for $C_{14}H_{15}NBr$: 276.0388, Found: 276.0391.

X-Ray Analysis of 260.

A colorless block shaped crystal of **260** ($C_{14}H_{14}BrN$) with approximate dimensions 0.08 x 0.09 x 0.15 mm, was used for the X-ray crystallographic analysis. The X-ray intensity data were measured at 133(2) K, cooled by Rigaku-MSC X-Stream 2000, on a Bruker SMART APEX CCD area detector system equipped with a graphite monochromator and a MoKα fine-focus sealed tube (λ = 0.71073Å) operated at 1600

watts power (50 kV, 32 mA). The detector was placed at a distance of 5.8 cm from the crystal.

A total of 1850 frames were collected with a scan width of 0.3º in ω and an exposure time of 10 seconds/frame. The total data collection time was about 8 hours. The frames were integrated with the Bruker SAINT software package using a narrow-frame integration algorithm. The integration of the data using a Triclinic unit cell yielded a total of 4946 reflections to a maximum θ angle of 28.47° (0.90 Å resolution), of which 3003 were independent, completeness = 96 %, R_{int} = 0.0591, R_{sig} = 0.1088 and 1766 were greater than 2σ(I). The final cell constants: a = 7.433(8)Å, b = 7.991(8)Å, c = 10.455(11)Å, α = 85.140(17)°, β = 79.187(19)°, γ = 78.799(17)°, volume = 597.6(11)$Å^3$, are based upon the refinement of the XYZ-centroids of 2783 reflections above 20σ(I) with 2.843° <θ <28.24°. Analysis of the data showed negligible decay during data collection. Data were corrected for absorption effects using the multiscan technique (SADABS). The ratio of minimum to maximum apparent transmission was 0.0426.

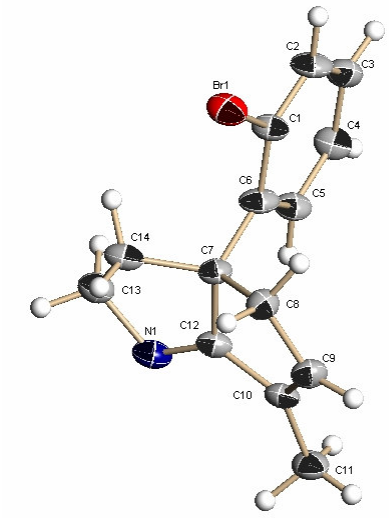

The structure was solved and refined using the Bruker SHELXTL (Version 6.1)

Software Package, using the space group P-1, with Z = 2 for the formula unit, $C_{14}H_{14}BrN$. The final anisotropic full-matrix least-squares refinement on F^2 with 146 variables converged at R1 = 6.93 %, for the observed data and wR2 = 20.91 % for all data. The goodness-of-fit was 0.987. The largest peak on the final difference map was 1.453 $e^-/Å^3$ and the largest hole was -1.009 $e^-/Å^3$. Based on the final model, the calculated density of the crystal is 1.535 g/cm^3 and F(000) amounts to 280 electrons.

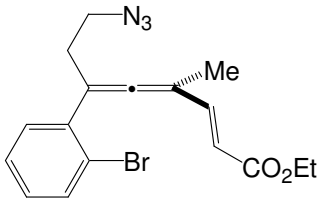

1-(Azidoethyl)-1-(2-bromophenyl)-3-methyl-5-carbethoxypent-1,2,4-triene (261)

To a solution of propargyl acetate **258** (0.20 g, 0.60 mmol) and $Pd(PPh_3)_4$ (69 mg, 0.06, 10 mol%) in 10 mL of THF was added (*Z*)-ethoxycarbonylethenylzinc iodide **179**[76] (2.5 mmol) in 5.0 mL of THF and the mixture was stirred at room temperature for 2 h. after which water was added and the mixture was extracted with 15 mL of Et_2O. The organic layer was dried over Na_2SO_4 and solvent was evaporated in vacuo. The crude product was purified by chromatography using 8% Et_2O in hexane as the eluent to give **261** as a yellow oil (90 mg, 40%). IR (neat): 2098, 1944, 1715 cm^{-1}; ^1H NMR (400 MHz, $CDCl_3$) δ 7.61 (d, *J* = 8.2, 0.9 Hz, 1H), 7.42 (d, *J* = 15.7 Hz, 1H), 7.31 (m, 2H), 7.18 (m, 1H), 5.89 (d, *J* = 15.8 Hz, 1H), 4.23 (q, *J* = 7.1 Hz, 2H), 3.42 (t, *J* = 6.9 Hz, 2H), 2.70 (t, *J* = 7.0 Hz, 2H), 1.93 (s, 3H), 1.32 (t, *J* = 7.1 Hz, 3H); ^{13}C NMR (90 MHz, $CDCl_3$) δ

209.2, 167.0, 143.8, 137.2, 133.3, 130.3, 129.2, 127.6, 123.0 118.5 102.6, 101.9, 60.4, 49.2, 32.7, 14.8, 14.3; TOFMSES *m/z* relative intensity 348 (MH^+ -N_2 50); HRMS (+MSEI) Calcd for $C_{17}H_{19}NBrO_2$: 348.0599, Found: 348.0600.

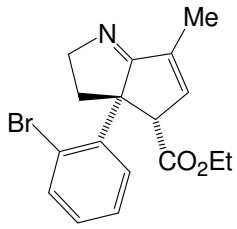

Cyclization of Ester-Allene 261.

Following General Procedure 11, allenylazide **261** (25 mg, 0.06 mmol) gave **262** as the product (12 mg, 52%).^{1}H NMR (400 MHz, $CDCl_3$) δ 7.55 (dd, *J* = 7.8, 1.1 Hz, 1H), 7.21 (dt, *J* = 7.4, 1.1 Hz, 1H), 7.12 (dt, *J* = 7.6, 1.6 Hz, 1H), 6.96 (dd, *J* = 7.5, 1.5 Hz, 1H), 6.30 (s, 1H), 4.08 (dd, *J* = 15.0, 7.0 Hz, 1H), 4.0 (m, 2H), 3.71 (d, *J* = 2.6 Hz, 1H), 3.66 (m, 1H), 3.14 (dd, *J* = 12.5, 4.6 Hz, 1H), 2.20 (dd, *J* = 12.2, 7.3 Hz, 1H), 2.06 (s, 3H), 1.09 (t, *J* = 7.2 Hz, 3H); ^{13}C NMR (75 MHz, $CDCl_3$) δ 189.4, 172.5, 144.1, 139.3, 137.8, 134.6, 130.2, 129.1, 127.4, 125.0, 67.9, 64.2, 61.5, 57.9, 41.5, 14.0, 12.1; TOFMSES *m/z* relative intensity 348 (MH^+ 100); HRMS (+MSEI) Calcd for $C_{17}H_{19}NBrO_2$: 348.0599, Found: 348.0573.

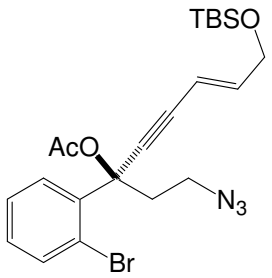

1-(*t*-Butyldimethylsilyloxy)-6-acetoxy-6-(azidoethyl)-6-(2-bromophenyl)-hex-2-ene-4-yne (264).

Following General Procedure 9, the keto-azide **257** (0.66 g, 2.6 mmol) and 1-(*t*-Butyldimethylsilyloxy)pent-2-ene-4-ynyl lithium (2.6 mmol) were coverted to the acetate **264** (0.70 g, 55%). IR (neat): 2097, 1751 cm^{-1}; ^{1}H NMR (400 MHz, $CDCl_3$) δ 7.95 (d, *J* = 7.9 Hz, 1H), 7.59 (d, *J* = 8.0 Hz, 1H), 7.35 (t, *J* = 7.6 Hz, 1H), 7.16 (t, *J* = 7.9 Hz, 1H), 6.35 (td, *J* = 15.8, 3.9 Hz, 1H), 5.94 (td, *J* = 15.8, 2.0 Hz, 1H), 4.29 (dd, *J* = 3.6, 2.2 Hz, 2H), 3.58 (m, 1H), 3.41 (m, 1H), 2.83 (m, 1H), 2.43 (m, 1H), 2.13 (s, 3H), 0.95 (s, 9H), 0.11 (s, 6H); ^{13}C NMR (75 MHz, $CDCl_3$) δ 168.7, 144.9, 138.2, 135.9, 130.8, 130.0, 127.8, 119.1, 107.7, 88.4, 86.3, 78.6, 63.1, 47.8, 39.5, 26.3, 21.6, 18.8, -5.0; TOFMSES *m/z* relative intensity 492 (MH^+ 75); HRMS (+MSES) Calcd for $C_{22}H_{31}N_3O_3SiBr$: 492.1318, Found: 492.1309.

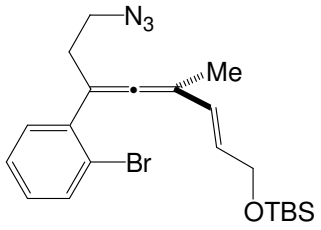

1-(Azidoethyl)-1-(2-bromophenyl)-3-methyl-6-(*te*r-Butyldimethylsilyloxy)-hexa-1,2,4-triene (265).

Following General Procedure 4, acetate **264** (0.73 g, 1.5 mmol) and methyl magnesium bromide (3.0 M, 6.0 mL) were coverted to the allene **265** (0.20 g, 30%). IR (neat): 2097, 1957 cm^{-1}; ^1H NMR (400 MHz, $CDCl_3$) δ 7.59 (d, *J* = 7.7 Hz, 1H), 7.29 (m, 2H), 7.13 (m, 1H), 6.33 (dd, *J* = 15.7, 1.3 Hz, 1H), 5.74 (td, *J* = 15.6, 5.2 Hz, 1H), 4.22 (d, *J* = 5.2 Hz, 2H), 3.40 (t, *J* = 7.0 Hz, 2H), 2.66 (t, *J* = 7.1 Hz, 2H), 1.92 (s, 3H), 0.94 (s, 9H), 0.11 (s, 6H); ^{13}C NMR (75 MHz, $CDCl_3$) δ 206.3, 139.0, 133.6, 130.8, 129.4, 129.1, 128.1, 127.9, 123.4, 102.6, 102.1, 64.3, 49.8, 33.3, 26.4, 18.9, 15.7, -4.7; TOFMSES *m/z* relative intensity 420 (MH^+-N_2 100); HRMS (+MSES) Calcd for $C_{21}H_{31}NOSiBr$: 420.1358, Found: 420.1354.

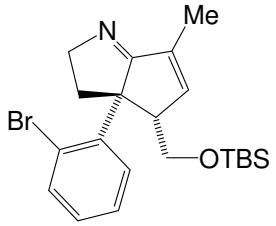

Cyclization of Ene-Allene 265.

Following General Procedure 11, allenylazide **265** (18 mg, 0.04 mmol) gave **266** as the product (10 mg, 59%).^1H NMR (400 MHz, $CDCl_3$) δ 7.60 (dd, *J* = 7.8, 1.2 Hz, 1H), 7.16 (dt, *J* = 7.4, 1.1 Hz, 1H), 7.08 (dt, *J* = 7.3, 1.4 Hz, 1H), 6.89 (m, 1H), 6.60 (s, 1H), 4.43 (m, 1H), 4.02 (dd, *J* = 15.0, 7.0 Hz, 1H), 3.61 (ddd, *J* = 14.6, 14.6, 3.8 Hz, 1H), 3.35 (d, *J* = 11.4 Hz, 1H), 2.88 (m, 2H) 2.12 (s, 3H), 2.00 (ddd, *J* = 18.8, 11.3, 7.1 Hz, 1H), 0.85 (s, 9H), 0.00 (s, 3H), -0.03 (s, 3H); ^{13}C NMR (75 MHz, $CDCl_3$) δ 192.2, 147.9, 139.6, 135.9, 135.5, 131.0, 129.0, 127.7, 124.0, 65.0, 63.8, 63.1, 54.7, 40.8, 26.3, 18.6,

12.1, -4.90, -4.97; TOFMSES *m/z* relative intensity 420 (MH^+ 100); HRMS (+MSES) Calcd for $C_{21}H_{31}NOSiBr$: 420.1358, Found: 420.1352.

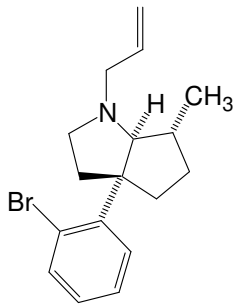

Reductive Allylation of 260.

To a solution of compound **260** (54 mg, 0.20 mmol) in acetonitrile and silver perchlorate (41 mg, 0.20) at 0 °C were added dropwise allyl iodide (22 μL, 0.24 mmol). After addition, the reaction mixture was stirred at room temperature in the dark. After 24 h, $NaBH_4$ (11 mg, 0.30 mmol) was added and the reaction was allowed to stir at 0 °C for 30 min. Excess $NaBH_4$ was then destroyed by the careful addition of water and the reaction mixture was taken up in 10 mL CH_2Cl_2. The organic layer was extracted twice with 5 mL CH_2Cl_2 and the combined extracts were dried over Na_2SO_4. Evaporation of the solvent gave a crude yellow oil as a 3:1 mixture of isomers ascertained by ^1H NMR of the crude oil. This material was purified by column chromatography using 15% ether in hexanes. Purification resulted in isolation of a major isomer **267** (13 mg, 21%). The minor isomer could not be obtained cleanly for complete characterization. ^1H NMR (400 MHz, $CDCl_3$) δ 7.65 (d, *J* = 7.9 Hz, 1H), 7.43 (d, *J* = 7.4 Hz, 1H), 7.26 (t, *J* = 7.4 Hz, 1H), 7.07 (t, *J* = 7.7 Hz, 1H), 6.01 (m, 1H), 5.25 (d, *J* = 17.0 Hz, 1H), 5.15 (d, *J* = 10.0 Hz, 1H), 3.46 (dd, *J* = 13.2, 5.8 Hz, 1H), 3.25 (s, 1H), 3.05 (m, 1H), 2.42 (m, 1H), 2.37-

2.31 (m, 3H), 2.21 (m, 1H), 2.16 (m, 1H), 2.01 (m, 1H), 1.2 (m, 1H), 1.06 (d, *J* = 7.1 Hz, 3H); ^{13}C NMR (75 MHz, $CDCl_3$) δ 147.5, 136.3, 135.4, 128.3, 127.3, 126.3, 124.1, 116.8, 79.5, 60.1, 58.1, 53.9, 40.3 (2C), 38.8, 33.9, 19.1; TOFMSES *m/z* relative intensity 320 (MH^+ 100); HRMS (+MSES) Calcd for $C_{17}H_{23}NBr$: 320.1014, Found: 320.0988.

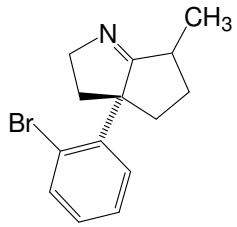

Reduction of Compound 260.

To a solution of compound **260** (20 mg, 0.07 mmol) in THF (5 mL) cooled to -25 °C, succinic acid (10 mg, 0.08 mmol) was added, followed by BH_3-THF complex (80 μL, 0.08 mmol, 1.0 M in THF). The reaction was stirred at -25 °C for 4 h, after which the reaction mixture is treated with satd. $NaHCO_3$ solution. The solution was taken up in ether and the organic layer was extracted twice with 5 mL ether. The combined extracts are dried over Na_2SO_4 and the solvent was evaporated. Purification of the crude oil using prep-plate chromatography resulted in isolation of starting material (8 mg, 40%) and **268** (5 mg, 25%). ^{1}H NMR (400 MHz, $CDCl_3$) δ 7.66 (dd, *J* = 7.9, 1.3 Hz, 1H), 7.21 (dt, *J* = 7.5, 1.4 Hz, 1H), 7.12 (dt, *J* = 7.8, 1.7 Hz, 1H), 6.97 (dd, *J* = 7.6, 1.6 Hz, 1H), 4.04 (dd, *J* = 14.2, 7.4 Hz, 1H), 3.67 (m, 1H), 2.74 (m, 1H), 2.49 (dd, *J* = 12.62, 5.3 Hz, 1H), 2.09 (m, 3H), 1.51 (m, 1H), 1.28 (d, *J* = 6.7 Hz, 3H); ^{13}C NMR (75 MHz, $CDCl_3$) δ 193.3, 143.3, 135.3, 128.6, 127.8, 127.4, 124.0, 64.9, 63.6, 42.2, 35.5, 33.9, 33.4, 16.6;

TOFMSES *m/z* relative intensity 278 (MH^+ 100); HRMS (+MSES) Calcd for $C_{14}H_{17}NBr$: 278.0544, Found: 278.0551.

Bibliography

1. (a) Fischer, E. Untersuchungen űber Depside und Gerbstoffe (Studies on Depsides and Tannins); Springer Verlag: Berlin, **1919**. (b) Freudenberg, K. Chem. Ber. **1919**, *52*, 1238.

2 Schmidt, O. T.; Mayer, W. *Angew. Chem*. **1956**, *68*, 103.

3. (a) Haslam, E.; Cai, Y. *Nat. Prod*. Rep. **1994**, 41. (b) Haslam, E. *In Plant Polyphenols. Synthesis, Properties, Significance*; Hemingway, R. W., Laks, P. E., Eds.; Plenum Press: New York, **1992**; p 169. (c) Haslam, E. Plants polyphenols - Vegetable tannins revisited; Cambridge University Press: Cambridge, **1989**. (d) Haslam, E. *In Natural Products of Woody Plants*; Rowe, J. W.,Ed.; Springer-Verlag: Berlin-Heidelberg-New York, **1989**; Vol.1, p 399. (e) Haslam, E. *J. Chem. Ecol*. **1988**, *14*, 1789. (f) Haslam, E. *Rec. Adv. Phytochem*. **1986**, *20*, 163. (g) Haslam, E*. Prog. Chem. Org. Nat. Prod*. **1982**, *41*, 1.

4. (a) Okuda, T.; Yoshida, T.; Hatano, T. *Phytochemistry* **1993**, *32*, 507. (b) Yoshida, T.; Hatano, T.; Kuwajima, T.; Okuda, T. *Heterocycles* **1992**, *33*, 463. (c) Okuda, T.; Yoshida, T.; Hatano,T. *Heterocycles* **1990**, *30*, 1195. (d) Okuda, T.; Yoshida, T.; Mori, K.; Hatano, T. *Heterocycles* **1981**, *15*, 132.

5. (a) Nonaka, G.-I.; Harada, M.; Nishioka, I. *Chem. Pharm. Bull.* **1980**, *28*, 685. (b) Saijo, R.; Nonaka, G.-I.; Nishioka, I. *Chem.Pharm. Bull.* **1989**, *37*, 2063. (c) Tanaka, T.; Nonaka, G.-I.; Nishioka, I. *J. Chem. Res. (S)* **1985**, 176. (d) Nonaka, G.-I.; Akazawa, M.; Nishioka, I. *Heterocycles* **1992**, *33*, 597. (e) Nonaka, G.-I.; Tanaka, T.; Nita, M.; Nishioka, I. *Chem. Pharm. Bull.* **1982**, *30*, 2255. (f) Tanaka, T.; Kirihara, S.; Nonaka, G.-I.; Nishioka, I. *Chem. Pharm. Bull.* **1993**, *41*, 1708. (g) Lin, J.-H.; Ishimatsu, M.; Takashi, T.; Nonaka, G.-I.; Nishioka, I. *Chem. Pharm. Bull.* **1990**, *38*, 1844. (h) Lin, J.-H.; Tanaka, T.; Nonaka, G.-I.; Nishioka, I.; Chen, I.-S. *Chem. Pharm. Bull.* **1990**, *38*, 2162.

6. (a) Miyamoto, K.; Koshiura, R.; Ikeya, Y.; Taguchi, H. *Chem. Pharm. Bull.* **1985**, *33*, 3977. (b) Miyamoto, K.; Kishi, N.; Koshiura, R. Jpn. *J. Pharmacol*. **1987**, *43*, 187. (c) Miyamato, K.-I.; Nomura, M.; Sasakura, M.; Matsui, E.; Koshiura, R.; Murayama, T.; Furukawa, T.; Hatano, T.; Yoshida, T.; Okuda, T. *Jpn. J. Cancer Res*. **1993**, *84*, 99.(d) Murayama, T.; Kishi, N.; Koshiura, R.; Tagaki, K.; Furukawa,T.; Miyamoto, K.-I. *Anticancer Res*. **1992**, *12*, 1471. (e) Miyamoto,K.-I.; Kishi, N.; Murayama, T.; Furukawa, T.; Koshiura, R. *Cancer Immunol. Immunother.* **1988**, *27*, 59

7. Berlinck, R.G. S.; Hatano, T.; Okuda, T.; Yoshida, T. Hydrolyzable tannins and related polyphenols. In: Herz, W.; Kirby, G. W.; Moore, R.E.; Steglich, W.; Tamm, Ch. (eds.). Progress in the chemistry of organic natural products. Springer-Verlag, New York, p.1 (**1995**)

8. Helm, R.F.; Zhentian, L.; Ranatunga, T. *In Plant Polyphenols 2: Chemistry, Biology, Pharmacology, Ecology* Edited by Gross et al. Kluwer Academic/Plenum Press: New York, **1999**; p 83.

9. (a) Gupta, R. K.; Al-Shafi, S. M. K.; Layden, K.; Haslam, E. *J. Chem. Soc., Perkin Trans. 1* **1982**, 2525.(b) Haddock, E. A.; Gupta, R. K.; Haslam, E. *J. Chem. Soc.,Perkin Trans. 1* **1982**, 2535.

10. Feldman, K. S.; Sahasrabudhe, K.; Quideau, S.; Hunter, K. L.; Lawlor, M. D. *In Plant Polyphenols 2: Chemistry, Biology, Pharmacology, Ecology* Edited by Gross et al. Kluwer Academic/Plenum Press: New York, **1999**; p 101

11. (a) Feldman, K. S.; Quideau, S. *Chem. Rev*. **1996**, *96*, 475. (b) Feldman, K. S.;. *Phytochem*. **2005**, *66*, 1984.

12. (a) Okuda, T.; Hatano, T.; Ogawa, N,; Kira, R.; Matsuda, M. T. *Chem. Pharm. Bull.* **1984**, *32*, 4662. (b) Okuda, T.; Hatano, T.; Yazaki, K.; Ogawa, N. *Chem. Pharm. Bull.* **1982**, *30*, 4230.

13. McDonald, P. D.; Hamilton, G. A. Mechanisms of phenolic oxidative coupling reactions. *In*: Trahanovsky, W.S. (ed.) Oxidation in organic chemistry, v.5. Academic Press, New York, **1973**, p.97

14. Perkin, A. G.; Nierenstein, M. *J. Chem. Soc., Part. 1* **1905**, *87*, 1412.

15. Hathway, D. E. *J. Chem. Soc.* **1957**, 519.

16. Mayer, W.; Hoffman, E. H.; Losch, N.; Wolf.; H.; Wolter, B.; Schilling, G.; *Ann*. **1984**, 929.

17. Grimshaw, J.; Haworth, R. D. *J. Chem. Soc.* **1956**, 4225.

18. Nelson, T. D.; Meyers, A. I. *J. Org. Chem*. **1994**, *59*, 2577.

19. Lipshutz, B. H.; Liu, Z.-P.; Kayser, F. *Tetrahedron Lett*. **1994**, *35*, 5567.

20. Critchlow, A.; Haslam, E.; Haworth, R. D.; Tinker, P. B.; Waldron, N. M. *Tetrahedron*, **1967**, *23*, 2829.

21. (a) Feldman, K. S.; Ensel, S. M. *J. Am. Chem. Soc.* **1993**, *115*, 1162. (b) Feldman, K. S.; Ensel, S. M. *J. Am. Chem. Soc.* **1994**, *116*, 3357.

22. Bubb, W. A.; Sternhell, S. *Tetrahedron Lett*. **1970**, *35*, 4499.

23. Mohamadi, F.; Richards, N. G. J.; Guida, W. C.; Liskamp, R.; Lipton, M.; Caufield, C.; Chang, G.; Hendrickson, T.; Still, W. C. *J. Comput. Chem*. **1990**, *11*, 440.

24. Feldman, K. S.; Hunter, K. L. *Tetrahedron Lett*. **1998**, *39*, 8943.

25. Feldman, K. S.; Ensel, S. M.; Minard, R. M. *J. Am. Chem. Soc.* **1994,** *116,* 1742.

26. Feldman, K. S.; Sahasrabudhe, K. *J. Org. Chem.* **1999,** *63,*

27. Feldman, K. S.; Sambandam, A. *J. Org. Chem.* **1995**, *60, 8171*

28. Feldman, K. S.; Smith, R. S. *J. Org. Chem.* **1996**, *61, 2606.*

29 Khanbabaee, K.; van Ree, T. *Synthesis*, **2001**, 1585.

30. Okuda, T.; Yoshida, T.; Hatano, T. *J. Chem. Soc., Perkin Trans. 1* **1982**, 9.

31. (a) Haddock, E. A.; Gupta, R. K.; Haslam, E. *J. Chem. Soc., Perkin Trans. 1* **1982**, 2535. (b) Hatano, T.; Hattori, S.; Ikeda, Y.; Shingu, T.; Okuda, T. *Chem. Pharm. Bull.* **1990**, *38*, 1902. (c) Self, R.; Eagles, J.; Galletti, G. C.; Mueller-Harvey, I.; Hartley, R. D.; Lea, A. G. H.; Magnolato, D.; Richli, U.; Gujer, R.; Haslam, E. *Biomed. Environ. Mass Spectrom.* **1986**, *13*, 449.

32. (a) Schmidt, O. T.; Schmidt, D. M.; Herok, J. *Liebigs Ann. Chem.* **1954**, *587*, 67. (b) Schmidt, O. T.; Blinn, F.; Lademann, R. *Liebigs Ann. Chem.* **1952**, *576*, 75. (c) Schmidt, O. T.; Schmidt, D. M. *Liebigs Ann. Chem.* **1952**, *578*, 31.

33. Tanaka, T.; Nonaka, G.I.; Nishioka, I.; Miyahara, K.; Kawasaki, T. *J. Chem. Soc., Perkin Trans. 1* **1986**, 369.

34. Zhang, Y.-Jun.; Abe, T.; Tanaka, T.; Yang, Ren.; Kuono, I. *J. Nat. Prod.* **2001**, *64*, 1527.

35. (a) Iversen, T.; Bundle, D. R. *Can. J. Chem.* **1982***, 60*, 299. (b) Reeves, R. E. *J. Am. Chem. Soc.* **1949**, *71*, 2116.

36. Okuda, T.; Yoshida, T.; Hatano, T.; Koga, T.; Toh, N.; Kuriyama, K. *Tetrahedron Lett.* **1982**, *23*, 3937.

37. The directed Monte Carlo algorithm of MacroModel V 6.5 was used to identify low-energy conformers of the species reported. In each case, a 3000- to 10000-step conformational search was utilized, depending upon the number of rotatable bonds involved. All reported minima were located several times.

38. Feldman, K. S.; Iyer, M. R.; Liu, Y. *J. Org. Chem*. **2003**, *68*, 7433.

39. (a) Dowd, P. *Acc. Chem. Res.* **1972**, *5*, 242. (b) Berson, J. A. In *Diradicals*; Borden, W. T., Ed.; Wiley-VCH: New York, **1982**; Chapter 4, p 151. (c) Little, R. D. *Chem. Re*v. **1996**, *96*, 93. (d) Allan, A. K.; Carroll, G. L.; Little, R. D. *Eur. J. Org. Chem.* **1998**, 1.

40. (a) Quast, H.; Weise Ve´lez, C. A. *Angew. Chem., Int. Ed. Engl.* **1978**, *17*,213. (b) Quast, H.; Fuss, A.; Heublein, A. *Angew. Chem., Int. Ed. Engl.* **1980**, *19*, 49. (c) Quast, H.; Meichsner, G. *Chem. Ber.* **1987**, *120*, 1049. (d) Quast, H.; Fuss, A.; Heublein, A.; Jakobi, H.; Seiferling, B. *Chem. Ber.* **1991**, *124*, 2545. For studies on related systems, see: (e) Quast, H.; Bieber, L. *Angew. Chem., Int. Ed. Engl.* **1975**, *14*, 428. (f) Quast, H.; Bieber, L.; Danen, W. C. *J. Am. Chem. Soc.* **1978**, *100*, 1306-1307. (g) Quast, H.; Bieber, L.; Meichsner, G. *Chem. Ber.* **1988**, *121*, 2117. (h) Quast, H.; Fuss, A.; Nűdling, W. *Eur. J. Org. Chem.* **1998**, 317 and references therein.

41. (a) Bleiholder, R. F.; Shechter, H. *J. Am. Chem. Soc.* **1968**, *90*, 2131. (b) Barraclough, D.; Moorhouse, N. P.; Onwuyali, E. I.; Scheinmann, F.; Hursthouse, M. B.; Galas, A. M. R. *J. Chem. Res., Synop* **1984**, 102.

42. (a) Bingham, E. M.; Gilbert, J. C. *J. Org. Chem.* **1975**, *40*, 224. (b) Barker, S. J.; Storr, R. C. *J. Chem. Soc., Perkin Trans. 1* **1990**, 485.

43. Chambers, T. S.; Kistiakowsy, G. B. *J. Am. Chem. Soc.* **1934,** *56,* 399.

44. Gajewski, J. J. *In: Mechanisms of Molecular Migrations,* Vol. 4, B. Thyagarajan, Ed., Wilet, New York, **1971**, p. 1.

45. Dowd, P. *J. Am. Chem. Soc.* **1966**, *88,* 2587.

46. Weiss, F. *Q, Rev. Chem. Soc*., **1970**, *24*, 278.

47. Berson, J. A.; Bushby, R. J.; McBride, J. M.; Tremelling, M. *J. Am. Chem. Soc.* **1971**, *93,* 1544.

48. Closs, G. L. *J. Am. Chem. Soc.* **1971**, *93,* 1546.

49. (a) Platz, M. S.; Berson, J. A. *J. Am. Chem. Soc.* **1976**, *98,* 6743. (b) Platz, M. S.; Berson, J. A. *J. Am. Chem. Soc.* **1980**, *102,* 2358.

50. Crawford, R. J.; Cameron, D. M. *J. Am. Chem. Soc.* **1966**, *88,* 2589.

51. Gajewski, J. J.; Yeshurun, A.; Bair, E. J. *J. Am. Chem. Soc.* **1972**, *94,* 2138.

52. Wentrup, C. *Reactive Molecules*, Wiley: New York **1984**, Chapter 4.

53. Berson, J. A. *Acc. Chem. Res*. **1978**, *11*, 446.

54. Little, R. D.; Losinski-Dang, L.; Venegas, M. G. *Tetrahedron Lett*. **1983**, *24*, 4499.

55. Carpenter, B. K.; Little, R. D.; Berson, J. A. *J. Am. Chem. Soc.* **1976**, *98,* 5723.

56. Little, R. D.; Bukhari, A.; Venegas, M. G. *Tetrahedron Lett*. **1979**, *20*, 305.

57. Little, R. D.; Mueller, G. W. *J. Am. Chem. Soc.* **1979**, *101,* 7129.

58. Van Hijfte, L.; Little, R. D.; Petersen, J. L.; Moeller, K. D. *J. Org. Chem*. **1987**, *52*, 4647.

59. Little, R. D.; Carroll, G L.; Petersen, J. L. *J. Am. Chem. Soc.* **1983**, *105*, 928.

60. Little, R. D.; Higby, R. G.; Moeller, K. D. *J Org Chem.* **1983**, *48*, 3139.

61. Feldman, K. S.; Mareska, D. A. *J. Org. Chem*. **1999**, *64,* 5650.

62. Feldman, K. S.; Iyer, M. R. Unpublished Results.

63. Lee, H.-Y.; Kim, Y. *J. Am. Chem. Soc.* **2003**, *125*, 10156.

64. (a) Wolff, L.. *Ann*. **1912**, *394*, 68. (b) Alder, K.; Stein, G. *Ann*. **1931**, *485*, 211. (c) Scheiner, P.; Vaughan, W. R. *J. Org. Chem*. **1961**, *26*, 1923. (d) Scheiner, P. *J. Org. Chem*. **1965**, *30*, 7.

65. Bottini, A. T.; Olsen, R. E. *J. Am. Chem. Soc.* **1962**, *84*, 195.

66. (a) Taylor, D. R. *Chem. Rev*. **1967**, *67*, 317. (b) Jacobs, T. L.; Illingworth, G. E. *J. Org. Chem*. **1963**, *28*, 2692.

67. (a) Oishi, Y.; Sakamoto, E.; Fujimoto, H.; *Inorg. Chem*. **1996**, *35*, 231. (b) Wojcicki, A. *New. J. Chem*. **1997**, *21*, 733.

68. Bertozzi, C. R.; Bendarski, M. D. *Tetrahedron Lett*. **1992**, *33*, 3109.

69. Mukai, C.; Kobayashi, M.; Kubota, S.; Takahashi, Y.; Kitagaki, S. *J. Org. Chem*. **2004**, *69*, 2128.

70. Boyer, J. H. *J. Am. Chem. Soc.* **1951**, *73*, 5248.

71. Konno, T.; Tanikawa, M.; Ishihara, T.; Yamanaka, H. *Collect. Czech. Chem. Commun.* **2002**, *67*, 1421.

72. (a) Quast, H.; Nahr, U. *Chem. Ber.* **1984**, *117*, 2761. (b) Quast, H.; Fuss, A.; Nahr, U. *Chem. Ber.* **1985**, *118*, 2164. (c) Dunkin, I. R.; Shields, C. J.; Quast, H. *Tetrahedron* **1989**, *45*, 259. (d) Quast, H.; Hergenröther, T. *Chem. Ber.* **1992**, *125*, 2625.

73. (a) Schmidt, R.; Schmidt, H. *Helv. Chim. Acta* **1974**, *57*, 1883. (b) de Kimpe, N.; Palamareva, M.; Verhe, R.; de Buyck, L.; Schamp, N. *J. Chem. Res., Synop* **1986**, 190. (c) Kim, H.; Ziani-Cherif, C.; Oh, J.; Cha, J. K. *J. Org. Chem.* **1995**, *60*, 792. (d) Jin, S.-j.; Choi, J.-R.; Oh, J.; Lee, D.; Cha, J. K. *J. Am. Chem. Soc.* **1995**, *117*, 10914.(e) Kende, A. S.; Huang, H. *Tetrahedron Lett.* **1997**, *38*, 3353. (f) Prie´, G.; Prévost, N.; Twin, H.; Fernandes, S. A.; Hayes, J. F.; Shipman, M. *Angew. Chem., Int. Ed.* **2004**, *43*, 6517.

74. (a) Hrovat, D. A.; Murcko, M. A.; Lahti, P.H.; Borden, W. T. *J. Chem. Soc., Perkin Trans.* 2 **1998**, 1037. (b) Little, R. D.; Brown, L. M.; Masjedizadeh, M. R. *J. Am. Chem. Soc*. **1992**, *114*, 3071. Calculations on the related oxatrimethylenemethane system indicate that the H_2C-C(=O)-CH_2 unit is best represented as a singlet diyl and not a zwitterionic resonance form.

75. Shengming, M.; Zhang, A. *J. Org. Chem*. **2002**, *67,* 2287.

76. Knochel, P.; Rao, C. J. *Tetrahedron*. **1993**, *49*, 29.

77. (a) Davidson, E. R.; Gajewski, J. J.; Shook, C. A.; Cohen, T. *J. Am. Chem. Soc.* **1995**, *33*, 8495. (b) Shook, C. A.; Romberger, M. L.; Jung, S.-H.; Xiao, M.; Sherbine, J. P.; Zhang, B.; Lin, F.-T.; Cohen, T. *J. Am. Chem. Soc.* **1993**, *115*, 10754.

78. Feldman, K. S.; Iyer, M. R. *J. Am. Chem. Soc.* **2005**, *127*, 4590.

79. Regas, D.; Afonso, M. M.; Rodríguez, M. L.; Palenzuela, J. A. *J.Org. Chem.* **2003**, *68*, 7845.

80. Kashulin, I. A.; Nifantev, I. E. *J. Org. Chem.* **2004**, *69*, 5476.

81. Feldman, K. S.; Iyer, M. R.; Hester, D. K. II. *Org. Lett.* **2006**, *8*, 3113.

82. López, C. S.; Feldman, K. S.; Faza, O. N.; Iyer, M. R.; Hester, D. K. II. Unpublished results.

83. (a) Schleyer, P. v. R.; Maerker, C.; Dransfeld, A.; Jiao, H.; Hommes, N. J. R. *J. Am. Chem. Soc.* **1996**, *118*, 6317. (b) Herges, R.; Geuenich, D. *J. Phys. Chem. A.* **2001**, *105*, 3214.

84. (a) Shields, T. C.; Billups, W. E.; Lepley, A. R. *J. Am. Chem. Soc.* **1968**, *90*, 4749. (b) Roth, W. R.; Schmidt, T. *Tetrahedron Lett.* **1971**, 3639. (c) Kende, A.

S.; Riecki, E. E. *J. Am. Chem. Soc.* **1972**, *94*, 1397. (d) Billups, W. E.; Leavell, K. H.; Lewis, E. S.; Vanderpool, S. *J. Am. Chem. Soc.* **1973**, *95*, 8096. (e) Gilbert, J. C.; Higley, D. P. *Tetrahedron Lett.* **1973**, 2075. (f) Pikulin, S.; Berson, J. A. *J. Am. Chem. Soc.* **1985**, *107*, 8274. (g) Direct (IR) detection of triplet-4-methylene-2-pentene-1,5-diyl: Maier, G.; Senger, S. *J. Am. Chem. Soc.* **1997**, *119*, 5852.

85. Bernauer, K.; Englert, G.; Vetter, W.; Weiss, E. *Helv. Chim. Acta*. **1969**, *52*, 1886.

86. Palmisano, G.; Danieli, G.; Lemsa, G.; Riva, R.; Riva, S. *J. Org. Chem.* **1984**, *49*, 4138.

87. (a) Overman, L. E.; Robertson, G. M.; Robichaud, A. J. *J. Org. Chem.* **1989**, *54*, 1236. (b) Overman, L. E.; Robertson, G. M.; Robichaud, A. *J. Am. Chem. Soc.* **1991**, *113*, 2598.

88. Schultz, A. G.; Dai, M. *Tetrahedron Lett*. **1990**, *31*, 4727.

89. (a) Hugel, G.; Lévy, J. J. *J. Org. Chem.* **1984**, *49*, 3275. (b) Hugel, G.; Lévy, J. J. *J. Org. Chem.* **1986**, *51*, 1594.

90. Hugel, G.; Gourdier, B.; Lévy, J. J. *Tetrahedron Lett*. **1974**, *15*, 1597.

91. Andriamialisoa, R. Z.; Diatta, L.; Rasonaivo, P.; Langlois, P.; Potier, P. *Tetrahedron* **1975**, *31*, 2347.

92. Pierron, C.; Garnier, J.; Lévy, J. J.; Le Men, J. *Tetrahedron Lett*. **1971**, *11*, 1007.

93. Manisse, N.; Chuche, J. *Bull. Soc. Chim. Fr*. **1972**, 2422.

94. Peet, N. P.; Cargill, R. L. *J. Org. Chem.* **1973**, *38*, 1215.

95. (a) Overman, L. E.; Sworin, M.; Burk, R. *J. Org. Chem.* **1983**, *48*, 2685. (b)) Overman, L. E.; Sworin, M. *Tetrahedron* **1981**, *37*, 4041.

96. Schultz, A. G.; Wang, A. *J. Am. Chem. Soc.* **1998**, *120*, 8259.

97. Schultz, A. G.; Dai, M.; Khim, S.-K.; Pettus, L.; Thakkar, K. *Tetrahedron Lett*. **1998**, *39*, 4203.

98. Chang, H. S.; Bergmeier, S. C.; Frick, J. A.; Bathe, A.; Rapoport, H. *J. Org. Chem.* **1994**, *59*, 5336.

99. Carrión, M. D.; Camacho, M, E.; León, J.; Escames, G.; Tapias, V.; Acuña-Castroviejo, D.; Gallo, M, A.; Espinosa, A. *Tetrahedron***, 2004,** *60*, 4051**.**

100. Nugent, B. M.; Williams, A. L.; Prabhakaran, E. N.; Johnston, J. N. *Tetrahedron* **2003**, *59*, 8877.

101. (a) Muci A. R.; Buchwald S. L. *Top. Curr. Chem*. **2002**, *219*, 131. (b) Prim, D.; Campagne, J.-M.; Joseph, D.; Andrioletti, B. *Tetrahedron* **2002**, *58*, 2041. (c) Wolfe, J. P.; Buchwald, S. L. *J. Org. Chem.* **2000**, *65*, 1144. (d) Hartwig J. F. *Pure Appl. Chem.* **1999**, *71* 1417. (e) Yang, B. H.; Buchwald, S. L. *J. Organomet. Chem.* **1999**, *576*, 125. (f) Hartwig J. F. *Angew. Chem., Int. Ed.* **1998**, *37*, 2046. (g) Schlummer, B.; Scholz, U. *Adv. Synth. Catal.* **2004**, *346*, 1599. (g) Gold, H.; Ax, A.; Vrang, L.; Samuelsson, B.; Karlen, A.; Hallberg, A.; Larhed, Mats**.** *Tetrahedron* **2006**, *62*, 4671.

102. Muratake, H.; Natsume, M,; Nakai, H.; *Tetrahedron*, **2004**, *60*, 11783.

103. Still, W. C.; Kahn, M.; Mitra, A. *J. Org. Chem.* **1978**, *43*, 2923.

.

VITA

Malliga R. Iyer

Malliga Ramnarayan Iyer was born June 24, 1979 in Mumbai (Bombay) India. She was raised in Dombivli, Mumbai and received her BSc in Chemistry from the University of Mumbai in 1999. Consequently, she joined the Indian Institute of Technology (IIT) Bombay to pursue her Master's degree in chemistry. She gained admission to IIT by topping the All India admissions entrance test. While at IIT, she followed her interest in organic chemistry by working on the synthesis of natural product goniotriol under the direction of Prof. G. K. Trivedi. She also had the privilege to work as a Visiting Student Research Scholar (VSRP) at the Tata Institute of Fundamental Research (TIFR) in the summer of 2000. While at TIFR, she worked under the guidance of Prof K. V. R. Chary, on the isolation, purification and solution-state NMR characterization of Klenow fragment of DNA polymerase. Malliga joined the PhD program in the Chemistry department of Penn State in fall 2001. Under the mentorship of Prof Ken Feldman, she worked on several challenging projects in the area of organic synthesis methodology development and total synthesis of natural products. At Penn State, she was the recipient of the Roberts Fellowship (2001) and the Dalalian Fellowship (2005). Upon completion of her doctoral work, Malliga will continue her research training in organic synthesis.